Universidade de Lisboa
Faculdade de Medicina de Lisboa

THE ROLE OF NOTCH-SIGNALLING IN AVIAN THYMUS AND PARATHYROID GLANDS DEVELOPMENT

Marta Sofia Carvalho Teles de Figueiredo

Orientador | Prof. Doutora Hélia Cristina de Oliveira Neves
Co-orientador | Prof. Doutor António José Saraiva da Cunha Cidadão

Tese especialmente elaborada para obtenção do grau de Doutor em Ciências Biomédicas, especialidade Biologia do Desenvolvimento

2021

Universidade de Lisboa
Faculdade de Medicina de Lisboa

THE ROLE OF NOTCH-SIGNALLING IN AVIAN THYMUS AND PARATHYROID GLANDS DEVELOPMENT

Marta Sofia Carvalho Teles de Figueiredo

Orientador | Prof. Doutora Hélia Cristina de Oliveira Neves
Co-orientador | Prof. Doutor António José Saraiva da Cunha Cidadão

Tese especialmente elaborada para obtenção do grau de Doutor em Ciências Biomédicas, especialidade Biologia do Desenvolvimento

Júri:
Presidente: Doutor José Augusto Gamito Melo Cristino, Professor Catedrático e Presidente do Conselho Científico da Faculdade de Medicina da Universidade de Lisboa
Vogais:
- Doutor António Alfredo Coelho Jacinto, Professor Catedrático Convidado da Faculdade de Ciências Médicas da Universidade Nova de Lisboa
- Doutora Isabel Maria Mestre Marques Palmeirim de Alfarra Esteves, Professor Catedrática da Faculdade de Medicina e Ciências Biomédicas da Universidade do Algarve
- Doutora Solveig Thorsteinsdottir, Professora Associada com Agregação da Faculdade de Ciências da Universidade de Lisboa
- Doutor Edgar Rodrigues Almeida Gomes, Professor Associado da Faculdade de Medicina da Universidade de Lisboa
- Doutor Domingos Manuel Pinto Henrique, Investigador Auxiliar da Faculdade de Medicina da Universidade de Lisboa
- Doutora Hélia Cristina de Oliveira Neves, Professora Auxiliar da Faculdade de Medicina da Universidade de Lisboa (Orientadora)

Fundação para a Ciência e Tecnologia, Bolsa SFRH/BD/86110/2012

2021

A impressão desta tese foi aprovada pelo Conselho Científico da Faculdade de Medicina de Lisboa em reunião de 16 de outubro de 2018.

Published work during this thesis:

Figueiredo, M. *et al*., 2016. Notch and Hedgehog in the thymus/parathyroid common primordium: Crosstalk in organ formation. *Developmental biology*, 418(2), pp.268–282. Available at: http://www.ncbi.nlm.nih.gov/pubmed/27544844.

Figueiredo, M. & Neves, H., 2018. Two-step Approach to Explore Early-and Late-stages of Organ Formation in the Avian Model: The Thymus and Parathyroid Glands Organogenesis Paradigm. *Journal of Visualized Experiments*, (136), e57114. Available at: https://www.jove.com/video/57114/two-step-approach-to-explore-early-late-stages-organ-formation-avian.

Figueiredo, M. & Neves, H., 2019. Isolation of Embryonic Tissues and Formation of Quail-Chicken Chimeric Organs Using The Thymus Example. *Journal of Visualized Experiments*, (144), e58965. Available at: https://www.jove.com/video/58965/isolation-embryonic-tissues-formation-quail-chicken-chimeric-organs.

Agradecimentos

“So much accomplished, so much still to be done.”

O meu primeiro agradecimento vai para a Hélia, que me guiou neste capítulo, muitas vezes árduo, de “fazer ciência”. Viu em mim o potencial de começar e continuar um projeto que ela idealizou e que fomos desbravando juntas. Por todo o apoio, ensinamentos, paciência, amizade, sorrisos partilhados, dedicação, e exigência, um muito muito obrigada. Sem ela, nada disto seria possível.

Quero agradecer a todos que, durante o meu percurso, fizeram parte não só da Unidade de Biologia da Hematopoiese do Instituto de Histologia e Biologia do Desenvolvimento da FMUL, como do João Barata Lab (UBCA), e do Sérgio Dias Lab, do IMM. Um agradecimento especial ao Prof. António Cidadão, à Isabel Alcobia, à Rita Zilhão, e à Isabel Palmeirim e ao seu grupo pelo apoio e discussões enriquecedoras. Obrigada ao Vítor Proa, à Joana Silva e à Sofia Santos (do nosso grupo), à Alice Melão, Nádia Cavaleiro, Rita Silva, Vanda Póvoa, Mariana Oliveira, Rita Fragoso, e ao Daniel (da UBCA), e à Inês Martins e à Ana de Barros (Sérgio Dias Lab) por toda a disponibilidade e ajuda, mas também pela boa disposição, companheirismo, momentos hilariantes, gargalhadas e no fundo, por terem feito com que cada dia valesse ainda mais a pena.

Em especial, levo comigo memórias incríveis e amizades especiais (que guardarei para sempre) com a Joana, a Alice, e a Inês. Melhores almoços de sempre. Um muito muito obrigada por tudo, dentro e fora do laboratório (vocês sabem). Um agradecimento mesmo do coração à minha maior (mas mais pequena) companheira de jornada, Joana, que se aventurou por terras longínquas mais cedo que do que eu gostaria (egoistamente). É das pessoas mais especiais que conheci neste período e, mesmo estando em países diferentes, sei que é daquelas amizades que ficam para a vida. Mesmo não tendo acompanhado “presencialmente” todo o meu doutoramento, sinto que é como se tivesse, e parte deste trabalho é dela também, pelas suas próprias mãos, mas também indiretamente pelo seu apoio incondicional. Mas sem ti Joana, nunca mais foi a mesma coisa.

Agradeço também ao grupo da Leonor Saúde e do Domingos Henrique, tal como à Unidade de BioImaging, por toda a disponibilidade e ajuda durante este longo processo.

Um enorme obrigada a todos os amigos que acompanharam, de perto ou de longe, esta maratona: os “de infância”, os “de Tondela”, os “da FCUL”, os “de Alcobaça”, os “que moraram comigo” e os “do IMM”. São muitos, e dos bons. Sempre lá, com um abraço, um sorriso, uma gargalhada, e a darem aquele empurrão quando mais preciso. Ah, e alguma paciência! Tenho sorte. Mesmo. E espero que todos vocês saibam o vosso papel nesta fase da minha vida.

Um muito obrigada ao Andrei, que entrou na minha vida já eu ia mais ou menos a meio desta corrida. Acreditando mais em mim do que eu própria, ele dá-me força e tranquilidade nos momentos em que elas me faltam. Sem ele, tudo teria sido mais difícil. Obrigada por seres quem és, pelo apoio incondicional, pelo amor, pela amizade, pelo companheirismo, pelo positivismo, pela paciência, pelos sonhos, e pelos sorrisos. Estamos quase a fechar este capítulo.

Por fim, agradeço à minha família, e em especial aos meus pais, que tanto contribuíram para a pessoa sou hoje. Obrigada pelo amor aos livros, à natureza, e aos “porquês” deste mundo. Obrigada por todo o apoio e amor incondicional, pela paciência, e por acreditarem que consigo sempre ir mais longe. Obrigada por estarem sempre lá.

Demorou, mas foi.

Abstract

The thymus generates central immune tolerance by producing self-restricted and self-tolerant T-cells, while the parathyroid glands regulate extracellular calcium homeostasis through the production of the parathyroid hormone (Pth). Despite their functional differences, they share a common endodermal origin in the pharyngeal region, which in avian corresponds to the endoderm of the 3rd and 4th pharyngeal pouches (3/4 PP).

The involvement of several transcription factors and signalling pathways (including the Hedgehog pathway) during the early stages of thymus and parathyroid glands (T/PT) development has been reported over the years. However, the molecular mechanisms and interactions between major signalling pathways regulating their early development are still poorly understood. Namely, the potential contribution of Notch signalling – one of the major pathways involved in cell-fate determination and boundary formation – at these early stages remains unknown. Recently, and using the avian model, we observed the expression of Notch-related molecules in the presumptive territories of T/PT. In addition, during my master's thesis I showed that the pharmacological inhibition of Notch signalling at these stages of T/PT development blocked *Gcm2* (parathyroid marker) and altered *Foxn1* (thymic marker) expressions, detected through *in situ* hybridization. These data suggest a potential role of Notch signalling during thymus and parathyroid glands early development. In addition, Notch and Hedgehog pathways have been shown to interact in several biological contexts.

In this thesis, we investigated the role of Notch signalling at the early stages of T/PT development, and its possible interaction with Hedgehog in this context. Using the quail-chick developmental model and pharmacological inhibitors *in vitro* and *in vivo*, we show, for the first time, that Notch is crucial for T/PT common primordium development and for parathyroid formation. Notch signalling was found to be required (within a 48h time-window) for the normal expression of *Foxn1* and *Gcm2* at early stages of development. Moreover, Notch signals within this time-window were found to be crucial for parathyroid glands formation. We also show that Hedgehog acts upstream of Notch during T/PT early development. Hedgehog positively regulates the median domains of the pouch endoderm – the *Gata3*$^{+}$/*Gcm2*$^{+}$ anterior domain and the *Lfng*$^{+}$ posterior domain – which seem to be more Hedgehog-responsive than the pouch tips, namely the dorsal tip

where the thymus is formed. In addition, we provide evidence that the *Lfng*-expression domain is involved in the definition of the dorsal/posterior boundary of *Foxn1*/thymic rudiment.

To clarify the tissue-specific role of Notch signalling at the early stages of T/PT development, isolated quail 3/4PP endoderm was electroporated with a *Tol2*-mediated gene transfer and tetracycline-dependent conditional expression system of vectors generated during my master thesis to induce loss- and gain-of-function of Notch signalling. A new loss-of-function construct (pT2K-NLS-Cherry-DNMAML1-eGFP) was also developed. However, the results obtained using the tested conditions were inconclusive, limiting the analysis of tissue-specific roles of Notch signalling in T/PT development during this thesis.

This work provides new insights into the role of Notch signalling in T/PT early development, and into the interactions between major signalling pathways that regulate this development. However, which tissue – the endoderm or the surrounding mesenchyme – is the main driver of these Notch effects remains unanswered.

Keywords: Notch signalling; Hedgehog signalling; thymus; parathyroid glands; early-organogenesis.

Resumo

O timo é um órgão linfoide primário, responsável pela geração de um reportório funcional de linfócitos T auto-restritos e auto-tolerantes que atuam como parte da resposta imune adaptativa. Este complexo processo de amadurecimento dos linfócitos T é dependente de interações das suas células precursoras, os timócitos, com as células especializadas do nicho tímico, as células epiteliais tímicas (CETs). O desenvolvimento do timo é acompanhado de perto pelo desenvolvimento das glândulas paratiroides, responsáveis pela regulação da homeostase do cálcio extracelular. As suas células epiteliais sintetizam e secretam a hormona paratiroide (Pth) em resposta a alterações nos níveis de cálcio no sangue, de forma a repor o equilíbrio.

Apesar de terem funções completamente distintas, estes dois órgãos partilham a mesma origem embrionária: a endoderme da 3ª bolsa faríngica (BF) no ratinho e no humano (com a particularidade de no humano as paratiroides provirem também da 4ª BF) e a endoderme da 3ª e 4ª BF (3/4BF) nas aves. Localizadas na região faríngea, as bolsas faríngeas são estruturas bilaterais transitórias geradas pela evaginação da endoderme lateral do intestino anterior primordial em direção à ectoderme. Os domínios presuntivos do timo e das glândulas paratiroides no primórdio comum são identificados pela expressão dos marcadores moleculares *Foxn1* (Forkhead box N1) e *Gcm2* (Glial cells missing 2), respetivamente.

Experiências pioneiras realizadas por Le Douarin e Jotereau através do modelo de quimeras codorniz-galinha mostraram pela primeira vez a origem endodérmica das CETs, assim como a importância das interações epitélio-mesenquimais na sua especificação. Algumas destas interações ao nível molecular têm vindo a ser reveladas. Recentemente, H. Neves (enquanto estudante em pós-Doutoramento no laboratório de Le Douarin) e colaboradores, demonstraram que a expressão sequencial de dois fatores de crescimento – *Bmp4* e o *Fgf10* – no mesênquima e na endoderme é fundamental para a especificação da endoderme da 3/4BF nos epitélios do timo e das glândulas paratiroides.

Para além de BMP e FGF, outras vias de sinalização têm sido identificadas como participantes no desenvolvimento do timo e das paratiroides, incluindo a via parácrina Hedgehog. No entanto, as suas interações na regulação das fases iniciais do desenvolvimento destes órgãos são ainda pouco compreendidas. Adicionalmente, apesar do conhecido envolvimento da sinalização Notch nas fases mais tardias da organogénese

do timo – na diferenciação não só dos linfócitos-T, mas também das CETs – existem poucas evidências do seu potencial papel no início da organogénese do timo e das paratiroides.

A sinalização Notch é uma importante via envolvida em processos de decisão do destino celular, proliferação, sobrevivência e diferenciação celular, tanto no desenvolvimento embrionário como no adulto. A sua ativação depende da interação de um ligando transmembranar (Delta ou Serrate) de uma célula com o recetor transmembranar (Notch) de uma célula vizinha. Esta ligação promove a clivagem proteolítica do recetor pela enzima γ-secretase, libertando o domínio intracelular de Notch (ICN) da membrana. O fragmento ICN é transportado para o núcleo, onde forma um complexo de ativação de transcrição dos genes alvo com várias proteínas, incluindo o co-ativador Mastermind-like 1 (MAML1). Os genes alvo melhor caracterizados são os genes *Hes* (Hairy and Enhancer of Split).

Recentemente, o nosso grupo observou que os genes envolvidos na sinalização Notch (recetores, ligandos e genes alvo) são diferencialmente expressos na endoderme da 3/4BF – inclusivamente nos territórios presuntivos do timo e das glândulas paratiroides – e no mesênquima circundante, em embriões de galinha. Durante a minha tese de mestrado, desenvolvemos um sistema organotípico de cultura *in vitro* da zona faríngica (explante contendo a 3/4BF) de embriões de galinha que mimetiza os acontecimentos precoces do desenvolvimento embrionário destes rudimentos. Através desse sistema, e de hibridação *in situ* desses explantes, pude observar que o bloqueio farmacológico da sinalização Notch *in vitro* nas fases iniciais do desenvolvimento do timo e das paratiroides inibe a expressão de *Gcm2* (marcador das glândulas paratiroides) e altera a expressão de *Foxn1* (marcador do epitélio tímico) na endoderme das bolsas faríngicas. Estes dados sugerem que a sinalização Notch está envolvida na fase inicial do desenvolvimento destes dois órgãos. Para além disso, sabe-se que as sinalizações Notch e Hedgehog interagem em inúmeros contextos biológicos.

O principal objetivo desta tese foi estudar o papel da sinalização Notch durante as fases iniciais de desenvolvimento do timo e das glândulas paratiroides, e a sua potencial interação com a via Hedgehog, utilizando embriões de galinha e codorniz como modelos experimentais.

Através da inibição farmacológica de Notch (com dois inibidores da γ-secretase) *in vitro* e *in vivo* na zona faríngea nas fases iniciais do desenvolvimento destes órgãos, provamos, pela primeira vez, que a sinalização Notch é crucial para o desenvolvimento do primórdio comum do timo e das paratiroides. Mostramos que o bloqueio da ativação de Notch numa janela de 48h reduz significativamente a expressão de *Foxn1*, *Gcm2*, e *Pth*, e que a sua influência é potencialmente exercida pelos genes alvo *Hey1* e *Gata3*. De forma a avaliar se este efeito negativo na expressão dos marcadores nas fases iniciais do desenvolvimento teria consequências a longo prazo na organogénese dos órgãos, transplantámos os tecidos que cresceram *in vitro* na presença do inibidor de Notch na membrana corioalantóide de embriões de galinha e deixou-se desenvolver *in ovo* por 10 dias. Este ensaio *in vivo*, que permite avaliar a capacidade dos tecidos transplantados de formar órgãos, mostrou que a ausência de sinais Notch na janela inicial do desenvolvimento do primórdio comum compromete de forma irreversível o futuro desenvolvimento das paratiroides, mas não do timo. Verificou-se que, durante o desenvolvimento *in ovo* (sem inibidor) desses tecidos, a expressão de *Foxn1* e de *Hes5.1* (gene alvo de Notch) é recuperada, permitindo a posterior formação do timo.

Verificou-se ainda que os sinais da via Notch nos domínios centrais da endoderme da bolsa são regulados positivamente pela sinalização Hedgehog. A inibição farmacológica de Hedgehog *in vitro* e *in vivo* na zona faríngea compromete a expressão de *Gata3* e *Gcm2* no domínio anterior da endoderme das bolsas e de *Lfng* – um modulador da via Notch – no domínio posterior. Esta ausência de *Lfng* no domínio posterior da bolsa leva à invasão deste domínio pelo território tímico adjacente (*Foxn1*$^{+}$), sugerindo que o domínio *Lfng*$^{+}$ está envolvido na definição da fronteira dorsal/posterior do rudimento tímico.

Apesar de mostrarmos que o bloqueio farmacológico da via Notch na zona faríngea tem consequências especificamente a nível da endoderme das bolsas faríngeas que dão origem ao timo e às paratiroides, os restantes tecidos da zona faríngea – o mesênquima circundante e a ectoderme exterior – estão também expostos a esse bloqueio. Permanece, portanto, em aberto qual/quais dos tecidos fornece os sinais Notch responsáveis pela sua influência nesta fase do desenvolvimento. De forma a avaliar o papel da sinalização Notch especificamente na endoderme das bolsas faríngeas, desenvolvemos uma estratégia genética de perda e de ganho de função da via Notch especifica de tecido. Para isso, a endoderme foi isolada, manipulada geneticamente, e

associada a um mesenquima numa combinação heteroespecífica de tecidos. Foi usado um sistema de vetores que combina a transferência génica mediada por *Tol2* e a expressão condicional dependente de tetraciclina, onde foram integrados vetores que permitem a perda e ganho de função de Notch. Na minha tese de mestrado, gerou-se um vetor que expressa uma forma dominante-negativa do co-ativador MAML1 (DNMAML1) que se sabe bloquear a via de sinalização (perda de função) e um que expressa o ICN, que tem a capacidade de ativar constitutivamente a sinalização Notch, independente da ligação a um ligando de Notch (ganho de função). Durante esta tese, um segundo vetor para perda de função foi construído com o objetivo de aumentar a estabilidade da proteína DNMAML1 (que tem apenas 205 pares de bases) e a sua eficiência, através da adição de uma sequência com um sinal de localização nuclear que a direciona para o núcleo. A endoderme da 3/4BF isolada de embriões de codorniz foi eletroporada com este sistema e associada a um mesênquima de galinha permissivo ao seu desenvolvimento. No entanto, a aplicação desta estratégia genética nas condições testadas produziu, durante esta tese, resultados inconclusivos, impedindo assim a clarificação do papel específico de tecido da sinalização Notch no desenvolvimento inicial do timo e das paratiroides.

Este trabalho revela pela primeira vez o envolvimento da sinalização Notch nas fases iniciais do desenvolvimento do timo e das glândulas paratiroides, e contribui para o conhecimento das interações entre as vias de sinalização que regulam estes processos. Este tipo de conhecimento é essencial para a compreensão dos eventos responsáveis pela manutenção de um órgão saudável ao longo da vida e pela reparação da sua função em situações patológicas. Fica, no entanto, em aberto o papel específico de cada tecido na regulação da sinalização Notch neste contexto multi-tecidual.

Palavras-chave: Sinalização Notch; sinalização Hedgehog; timo; glândulas paratiroides; organogénese inicial.

Abbreviations

3D – Three dimensional

aa – Amino acid

Actb – Beta-actin

ADAM – A disintegrin and metalloprotease

bHLH – Basic Helix Loop Helix

BMP – Bone Morphogenetic Protein

bp – Base pairs

c – Chicken

cm – Centimetre

C. elegans – *Caenorhabditis elegans*

cDNA – Complementary DNA

CAM – chorioallantoic membrane

CBF-1 - C promoter-binding factor 1

Cyc – Cyclopamine

CSL – CBF1/Suppressor of Hairless/Lag-1

D. melanogaster – *Drosophila melanogaster*

DAPI – 4',6-diamidino-2-phenylindole

DAPT – N-[N-(3,5-Difluorophenacetyl-L-alanyl)]-S-phenylglycine t-Butyl Ester

DBZ – Dibenzazepine

DIG – Digoxigenin

DMEM – Dulbecco's Modified Eagle Medium

DMSO – Dimethyl sulfoxide

DN – Dominant Negative

DNA – Deoxyribonucleic Acid

Dox – Doxycycline

E – Embryonic day

EDTA – Ethylenediaminetetraacetic Acid

E. coli – *Escherichia coli*

Eya1 – Eyes absent homolog 1

FBS – Fetal Bovine Serum

Foxn1 – Forkhead box protein N1

FGF – Fibroblast Growth Factor

GATA3 – GATA Binding Protein 3

Gcm2 – Glial cells missing homologue 2

GFP – Green Fluorescence Protein

Gli – Glioma-associated oncogene

h – Hour

Hes – Hairy Enhancer of Split

Hey – Hes-related with YRPW motif

HH – Hamburguer and Hamilton stage

Hh – Hedgehog

Hoxa3 – Homeobox protein A3

HPRT – Hypoxanthine phosphoribosyltransferase 1

ICN – Intracellular domain of Notch

IRES – Internal ribosome entry site

Jag – Jagged

kb – Kilobase

L – Litre

LB – Luria Bertani

Lfng – Lunatic Fringe

Ly – LY-411.575

m – Mouse

MAML – Mastermind-like

mg – Milligram

min – Minute

mm – Millimetre

mM – Millimolar

mRNA – Messenger RNA

ms – Millisecond

m/v – Mass/volume

NCCs – Neural crest cells

ng/mL – Nanogram/millilitre

nM – Nanomolar

NLS – Nuclear Localization Sequence

o.n. – Overnight

PA – Pharyngeal Arch

PAR– Pharyngeal Arch Region

Pax – Paired box protein

PBS – Phosphate Buffered Saline

PCR – Polymerase Chain Reaction PEST

Pen/Strep – Penicillin/Streptomycin

PFA – Paraformaldehyde

poly(A) – Polyadenylation signal

PP – Pharyngeal Pouch

q – Quail

qRT-PCR – Quantitative reverse transcriptase PCR

RA – Retinoic Acid

RBPJ-κ – Kappa J region recombining binding protein suppressor of hairless

RNA – Ribonucleic Acid

rpm – Revolutions per minute

RT – Room temperature

rtTA – Reverse tetracycline transactivator

sec – Second

Shh – Sonic hedgehog

Six – Sine oculis homeobox

ss – Somite stage

Su(H)- Suppressor of Hairless

TAE – Tris-acetate-EDTA buffer

Tbx1 – T-box 1

tTA – Tetracycline controllable transactivator

U – Unit of activity

UTP – Uridine triphosphate

UV – Ultraviolet

V – Volt

Vis – Vismodegib

v/v – Volume/volume

Wnt – Wingless/Integrated

µg – Microgram

µL – Microlitre

Index

Index of Figures

CHAPTER I

CHAPTER II

CHAPTER III

CHAPTER IV

CHAPTER V

CHAPTER VI

Index of Tables

CHAPTER I

CHAPTER II

CHAPTER V

CHAPTER I

General Introduction

CHAPTER I - GENERAL INTRODUCTION

This thesis aims to shed light on the molecular mechanisms involved in the early stages of thymus and parathyroid glands development, in particular on the role of Notch signalling and its interaction with the Hedgehog pathway. The thymus regulates T-lymphocyte differentiation, whereas the parathyroid glands are responsible for calcium homeostasis. Despite their distinct functions, they share a common endodermal origin in the pharyngeal region, which will be detailed further on.

I.1 Thymus

The thymus is an essential component of the adaptive immune system conserved in all vertebrates (Boehm *et al.*, 2012). It is a specialized primary lymphoid organ that supports T-cell (and natural killer cell) development and maturation, and its absence (athymia) results in severe or complete immunodeficiency (Flanagan, 1966; Kirkpatrick and DiGeorge, 1968; Auricchio *et al.*, 2005). Histologically, the thymus is an encapsulated and vascularized lobular organ that can be divided in distinguishable subcapsular, cortical, cortico-medullary junction, and medullary regions.

Although its existence was known for centuries, thymic immunological functions were only discovered in 1961 by Jacques Miller. Mice thymectomized immediately after birth showed a deficit in a specific type of lymphocytes, that were later called T-lymphocytes (Miller, 1961). It took, however, two decades more for the immunological properties of central tolerance – the production of self-restricted and self-tolerant T-cells, by eliminating self-reactive T-cells before their export into the periphery, where they could potentially cause harm – to be attributed to the thymus (Ohki *et al.*, 1987).

Paradoxically, the thymus is one of the first organs to degenerate in healthy individuals, through a gradual age-associated process known as thymic involution (Steinmann, Klaus and Müller-Hermelink, 1985; Chinn *et al.*, 2012). Thymic involution is initiated around the onset of puberty and is a major cause of the age-related decline in immune system function. It is associated with a decline in the production of naïve T-cells, which impairs the immune response to novel challenges (reviewed in Lynch *et al*. 2009).

I.1.1 T-cell development

The undifferentiated lymphoid progenitor cells (LPCs) circulating in the blood enter the thymus in the cortico-medullary junction and initiate a journey through different thymic compartments (cortex and medulla), which result in lymphoblast differentiation into naïve T-cells, and their exit from the thymus (Fig. 1) (reviewed in Petrie 2003).

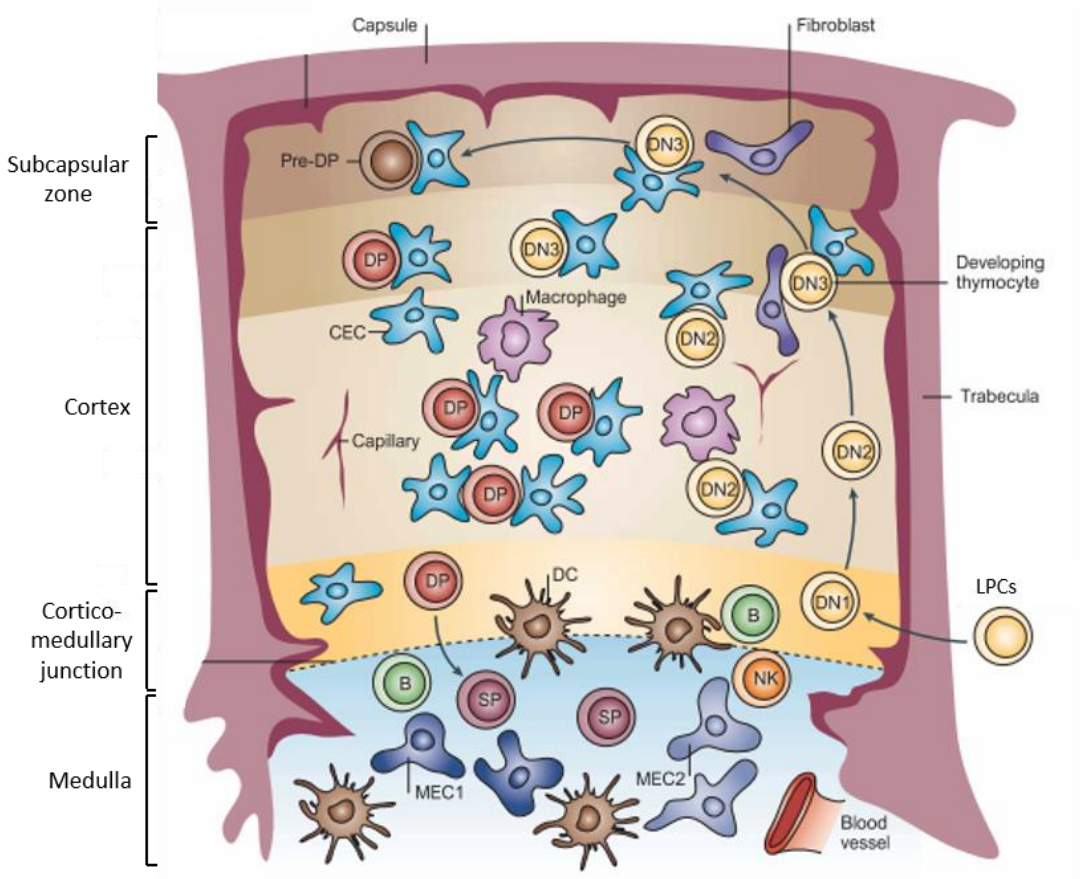

Figure 1. Thymus structure and T-cell differentiation. The thymus can be divided into subcapsular, cortical, cortico-medullary junction, and medullary regions, each containing unique stromal cells that provide the essential signals needed for T-cell differentiation. Undifferentiated LPCs – $CD4^{-}CD8^{-}$ double-negative (DN) – enter the thymus in the cortico-medullary junction and migrate through the cortex to the subcapsular zone, where they acquire both $CD4^{+}CD8^{+}$ co-receptors (DP). DP cells then migrate back towards the cortico-medullary junction and differentiate into either $CD4^{+}$ or $CD8^{+}$ single-positive (SP) cells, before moving into the medulla, where negative selection occurs. SP cells that survive negative selection in the medulla exit the thymus to the periphery. CEC, cortical epithelial cell; DC, dendritic cell; MEC, medullary epithelial cell. Adapted from Blackburn & Manley, 2004.

Cortical T-cell differentiation occurs in three maturational stages that can be identified based on the expression of co-receptors CD4 and CD8: 1st stage - $CD4^{-}CD8^{-}$ double negative (DN), 2nd stage - $CD4^{+}CD8^{+}$ double positive (DP), and 3rd stage - either $CD4^{+}$ or $CD8^{+}$ single positive (SP) (Lind *et al.*, 2001; Carpenter and Bosselut, 2010). The 1st stage is the most immature stage, that comprises LPCs that had entered the thymus and migrate through the cortex to the subcapsular zone. This stage involves several phenotypical and biological events that will lead to pre-T-cell receptor (TCR)-mediated selection, and acquisition of both $CD4^{+}CD8^{+}$ co-receptors (DP) (2nd stage). Then, as DP thymocytes migrate back towards the cortico-medullary junction (3rd stage), positive selection takes place as well as maturation into $CD4^{+}$ (helper) and $CD8^{+}$ (cytotoxic) SP T-cells. Finally, SP thymocytes with the correct avidity to recognize self-major histocompatibility complex (MHC) move on to the medulla where negative selection occurs, deleting self-reactive thymocytes (Fig. 1) (reviewed in Anderson *et al*. 2007; Petrie & Zúñiga-Pflücker 2007). This rigorous selection process ensures that the T-cell repertoire is self-MHC restricted and self-tolerant, with only 3-5% of incoming LPCs surviving and exiting the thymus as naïve T-cells (Merkenschlager *et al.*, 1997).

Many studies have been focused on the unique microenvironment of this organ that allows the selection of a functional and self-tolerant T-cell repertoire (Gordon and Manley, 2011; Miller, 2011; Klein *et al.*, 2014).

I.1.2 Thymic microenvironment

In young individuals, the thymus contains large numbers of developing T-cell precursors embedded in a network of epithelia known as the thymic stroma (Gordon and Manley, 2011). Each area is comprised of unique stromal cells, which provide the essential signals needed for the stringent T-cell developmental program (Anderson, Lane and Jenkinson, 2007). This multi-component stroma is organized in a three-dimensional (3D) cellular network, comprised of thymic epithelial cells (TECs), dendritic cells, endothelial cells, macrophages and fibroblasts (Nowell, Farley and Blackburn, 2007).

TECs are the major component of the thymic stroma, structurally and functionally. They form a complex intricate 3D network of endodermal-derived cells that allows close proximity between the developing LPCs and subsets of TECs that provide distinct

microenvironmental niches, essential for proper thymocyte differentiation (Fig. 1) (Alves *et al.*, 2009; Manley *et al.*, 2011). The cortical and medullary subsets of TECs (cTEC and mTEC, respectively) exhibit different morphology, gene expression profiles, and lymphopoietic functions (Alves *et al.*, 2009). cTECs are required for commitment, expansion and positive selection of thymocytes to recognize self-MHC (Cosgrove *et al.*, 1992), whereas mTECs support negative selection, that eliminates potentially autoreactive T-cells, thus inducing self-tolerance (Gotter *et al.* 2004; reviewed in Klein *et al*. 2014). In addition, TECs also provide migratory cues (through the expression of several chemokines) to LPCs and developing lymphoblasts to the process of homing and migration through the distinct thymic compartments, respectively (reviewed in Takahama 2006). Interestingly, the crosstalk between epithelial cells and developing LPCs works in a bidirectional manner, as it is as essential to T-cell development as to TECs maturation (van Ewijk, Shores and Singer, 1994; Klug *et al.*, 1998; van Ewijk *et al.*, 2000; Anderson *et al.*, 2006).

The thymic capsule is composed of mesenchymal cells that are also interspersed throughout the organ, and are neural crest-derived (Le Douarin and Jotereau, 1975). Pivotal experiments performed in the mid-70s by Le Douarin and Jotereau using quail-chick chimeras were the first to demonstrate their origin. Transplanted quail neural crest cells (NCCs) into the corresponding location of a chicken host generated the thymic capsule (Le Douarin and Jotereau, 1975). Furthermore, studies in the mouse showed these NC-derived cells persist in the adult thymus, and are a source of pericytes and smooth muscle cells that contribute to the structural support of thymic vasculature (Foster *et al.*, 2008; Muller *et al.*, 2008). Several studies have also shown the requirement of NCCs to thymus development, as discussed further in Section I.3.1.3.

I.2 Parathyroid glands

The parathyroid glands were the last major organ to be recognized in humans (Modarai, Sawyer and Ellis, 2004). These glands are responsible for the production of the parathyroid hormone (Pth), which is an 84-amino acid peptide essential to regulate calcium and phosphate homeostasis.

Serum calcium is important to many functions, including synaptic activity, muscle contraction, blood coagulation, and bone mineralization (Okabe and Graham, 2004). Parathyroid glands detect changes in calcium levels in the blood via the membrane-bound calcium-sensing receptor (CaSR), that regulates Pth secretion. When calcium levels are low, Pth promotes calcium release from bone to the circulating blood and enhances calcium reabsorption in the kidney, stabilizing calcium levels (Potts, 2005; Chen *et al.*, 2013; Neves and Zilhão, 2014).

Histologically, the parathyroid glands are round to ovoid structures limited by a thin fibrous capsule that overlies a network of adipose tissue, blood vessels and glandular parenchyma (Krstic, 1991; Chen *et al.*, 2013).

The parathyroid epithelium is composed of chief and oxyphil cells (parenchymal cells), usually arranged in nests and cords and nourished by a rich capillary network. Chief cells comprise the major cell type of the parathyroid glands and play a key role in calcium homeostasis by sensing extracellular calcium changes and releasing the appropriate amount of Pth. Oxyphil cells are derived from chief cells and retain the ability to release Pth, but their functional significance is still unclear. These cells are usually found either individually or in small groups intermingled among chief cells, and they are absent in many lower vertebrates such as rat and chicken (Krstic 1991; reviewed in Christakis & Palazzo 2014; Arrangoiz *et al*. 2017). The capsule of connective tissue is of neural crest origin (Graham, Okabe and Quinlan, 2005; Johansson *et al.*, 2015) and extends into the parenchyma delineating the gland into multiple lobules. The stroma is formed by fibrous connective tissue septa with capillaries, and adipose cells (which increase in number with age) (Krstic 1991; reviewed in Christakis & Palazzo 2014; Arrangoiz *et al.* 2017).

I.3 Early stages of thymus and parathyroid glands formation

The adult thymus and parathyroids have very distinct anatomic locations. In mammals, the thymus is a bilobed organ located in the central compartment of the thoracic cavity, anterior to the heart and behind the sternum. In birds, two thymi exist, located bilaterally along the neck near the jugular vein, and are divided in seven lobes each, which are subdivided in lobules (Fig. 2A) (Lillie, 1952; Neves *et al.*, 2012). On the

other hand, the parathyroid glands were named due to their anatomical proximity to the thyroid, and they vary in number among vertebrates. Humans and birds have two pairs of parathyroids, while mice have only one pair (reviewed in Neves and Zilhão, 2014; Manley, 2015). In birds, the parathyroids are specifically located under the thyroid gland (Fig. 2A) (Neves *et al.*, 2012; Neves and Zilhão, 2014). Despite their distinct anatomic location, these organs share the same embryological origin.

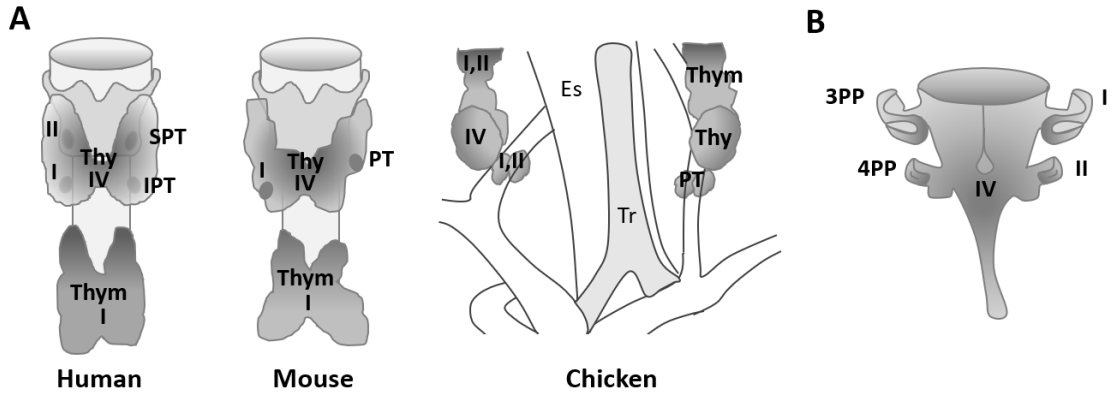

Figure 2. Adult location and corresponding embryological origin of pharyngeal endoderm-derived organs. Schematic representation of the adult location of several pharyngeal endoderm-derived organs in distinct animal models: human, mouse and chicken (A). 3D illustration of the posterior pouches of the foregut endoderm, from the 3rd PP to the 4th PP (B). Roman numbers correlate the adult location (A) to the embryological origin (B) of the various organs among different species. Es, oesophagus; IPT, inferior parathyroid glands; PP, pharyngeal pouch; PT, parathyroid glands; SPT, superior parathyroid glands; Thy, thyroid gland; Thym, thymus; Tr, trachea. Adapted from Neves & Zilhão, 2014.

I.3.1 Morphogenesis in the pharyngeal region

Thymus and parathyroid glands (T/PT) derive from a common endodermal primordium in the pharyngeal region. The pharyngeal region comprises 5 pairs of pharyngeal arches (PA) (1, 2, 3, 4 and 6) on the cranial lateral side of the embryo, which are formed in a sequential rostral to caudal manner. The pharyngeal arches are composed of a mesodermal core enclosed by NC-derived mesenchyme, an outer ectodermal cover, and an inner endodermal lining. Bilateral transient outpocketings of pharyngeal endoderm form the pharyngeal pouches (PP). The contact of the PP endoderm with the ectoderm invaginations, the pharyngeal clefts, separates the different arches (reviewed in Grevellec & Tucker 2010).

In mammals, the thymic epithelium derives from the 3rd PP (3PP) endoderm (Gordon *et al.*, 2001), whereas the parathyroid epithelium derives from the 3PP and 3rd and 4th PP (3/4PP) in mouse and human, respectively (Fig. 2A and B) (Okabe and Graham, 2004). Interestingly, in birds, both thymic and parathyroid glands epithelia originate from a common endodermal primordium that develops from the 3/4PP (Fig. 2A and B) (Neves *et al.*, 2012).

Worth noting, thymic epithelium origin was under debate for many decades, but a single endoderm origin of the thymic epithelium was demonstrated by Le Douarin & Jotereau, through the quail-chick chimera system (Le Douarin and Jotereau, 1975). Isolated endoderm of the 3/4PP from early quail embryos was able to form a fully functional thymus when transplanted to an ectopic location (Le Douarin and Jotereau, 1975).

Following pouch formation, the pouch becomes subdivided into complementary and distinct parathyroid and thymic prospective domains, which can be discriminated by the expression of the organ-specific genes, glial cells missing homologue 2 (*Gcm2*) and forkhead box protein N1 (*Foxn1*), respectively (Gordon *et al.*, 2001). The T/PT common primordium begins to form and grow, lined by NC-derived connective tissues (Le Douarin and Jotereau, 1975; Manley and Condie, 2010), with a subsequent detachment from the pharynx by apoptotic cell death (Gordon *et al.*, 2004), separation of the thymic and parathyroid rudiments, and migration to their final anatomical locations (Le Douarin and Jotereau, 1975; Gordon and Manley, 2011). The contribution of NCCs to these events is discussed in greater detail below in Section I.3.1.3.

In the mouse, the dorsal part of the 3PP endoderm expresses *Gcm2* as early as mouse (m) embryonic (E) day 9.5 and gives rise to the parathyroid glands, whereas the ventral part expresses *Foxn1* from mE11.25 and gives rise to the thymus (Fig. 3A and C) (Gordon *et al.*, 2001). Notably, *Foxn1* transcripts were detected as early as mE10.5 by RT-PCR (Fig. 3C) (Balciunaite *et al.*, 2002). The T/PT common primordium starts to detach from the pharynx at mE11.5, and thymus and parathyroid glands become separated between mE12-12.5 (Gordon and Manley, 2011).

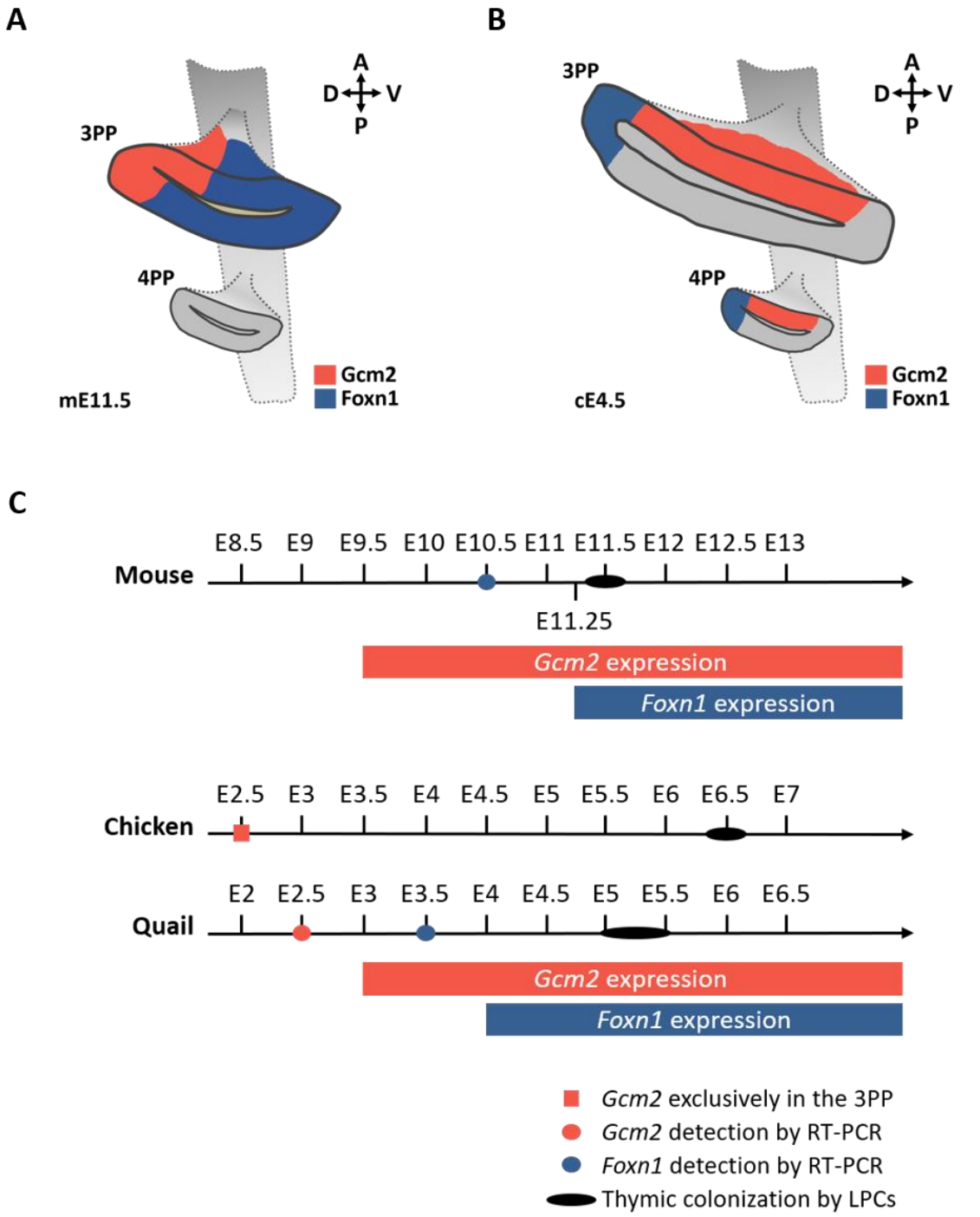

Figure 3. *Foxn1* and *Gcm2* expression during thymus and parathyroid glands development in the mouse and the avian models. Schematic representations of *Foxn1* and *Gcm2* expression domains in the 3/4PP endoderm of mouse embryos at mE11.5 (A) and of chicken embryos at cE4.5 (B). Timeline of *Gcm2* and *Foxn1* expression, as well as the first appearance of LPCs in the mouse, chicken, and quail models (C). A, anterior; D, dorsal; c, chicken; LPCs, lymphoid progenitor cells; m, mouse; P, posterior; PP, pharyngeal pouch; RT-PCR, reverse transcription-PCR; V, ventral.

Similarly, avian embryos also express *Gcm2* and *Foxn1* in the endodermal rudiments of the parathyroid glands and thymus, respectively. Interestingly, these domains occupy inverted positions along the dorsal-ventral axis compared to mammals, with *Gcm2* expression domain being located in a more ventral position (Okabe and Graham, 2004; Neves *et al.*, 2012), and *Foxn1* expression in the dorsal tip of the 3/4PP endoderm (Fig. 3B) (Neves *et al.*, 2012). *In situ* expression of *Gcm2* in the 3/4PP endoderm begins at E3 in quail (qE3) (Neves *et al.*, 2012) and at E3.5 in chicken (cE3.5) or Hamburger and Hamilton stage (HH) 22 (Fig. 3C) (Okabe and Graham, 2004). The *Foxn1* domain of expression is detected in avian embryos at qE4 and cE4.5 (HH25) (Fig. 3C) (Neves *et al.*, 2012). These species exhibit an asynchronous developmental time-window of 8-12h between them (Fig. 3C) due to the faster development of quail embryos, which fully develop in 16/17 days, whereas chicken embryos take 21 days (Sellier *et al.* 2006).

Interestingly, *Gcm2* expression was firstly observed in the 3PP at cE2.5 (HH18) and in both 3/4PP by cE3.5 (Okabe and Graham, 2004) in chicken embryos, following the natural chronological formation of the pouches. In addition, *Gcm2* and *Foxn1* were shown to be expressed earlier than detected by *in situ* hybridization (Nehls *et al.*, 1994; Balciunaite *et al.*, 2002; Neves *et al.*, 2012). In quail, *Gcm2* and *Foxn1* expression was detected by RT-PCR at qE2.5 (25–30 somite-stage) and qE3.5, respectively (half a day before *in situ* detection) (Fig. 3C) (Neves *et al.*, 2012).

In chicken, the T/PT common primordium begins to develop at cE4.5 (Neves *et al.*, 2012), thymic and parathyroids organ rudiments separate from the pharynx at cE4.5-5 (HH25), the thymic epithelium starts to be colonized by LPCs at cE6.5 (HH29-30), and becomes surrounded by a capsule of NCCs at around cE7 (HH31) (Le Douarin and Jotereau, 1975).

Gcm2 expression is initiated before the formation of the T/PT common primordium, which may illustrate the evolutionary legacy, but also the need to define the parathyroid domain within the pouch to protect it from a thymus fate (Liu, Yu and Manley, 2007). The expression of *Gcm2* and *Foxn1* is maintained throughout parathyroids and thymus development until adult stages, both in mammals and birds (Nehls *et al.*, 1996; Gordon *et al.*, 2001; Neves *et al.*, 2012).

I.3.1.1 Thymic epithelial marker – *Foxn1*

Foxn1 gene, originally named *winged helix nude* (Whn) (Nehls *et al.*, 1994), belongs to the family of winged helix/forkhead transcription factors. It binds to specific DNA sequences via the evolutionarily conserved forkhead box domain, activating its target genes. *Foxn1* gene is mutated in the mouse mutant *nude*, whose phenotype is characterized by the lack of hair and congenital athymia, resulting in severe immunodeficiency (Nehls *et al.*, 1994, 1996). The name "nude" comes from the mutant's first description in 1966, as these mice exhibited a lack of fur development since birth, distinct from previously described "hairless" mutants (Flanagan, 1966). Although *Foxn1*-deficient mice lack a functional thymus, a thymic primordium is formed and migrates to its final position (Nehls *et al.*, 1996). However, TECs remain in an early progenitor state and fail to attract T-cell precursors, which remain in the surrounding perithymic mesenchyme (Nehls *et al.*, 1994, 1996; Itoi *et al.*, 2001; Bleul *et al.*, 2006). As a consequence, the thymus does not develop its characteristic 3D organization and eventually degenerates into cysts (Vroegindeweij *et al.*, 2010). Interestingly, isolated mouse pharyngeal endoderm at mE9.0 (when no functionally relevant levels of *Foxn1* are expressed) was able to give rise to a functional thymus when grafted ectopically (Gordon *et al.*, 2004). This evidence supported previous data (Blackburn *et al.*, 1996) suggesting that *Foxn1* is required cell-autonomously for TECs differentiation and thymus colonization, rather than being responsible for thymus specification (Nehls *et al.*, 1994, 1996; Bleul *et al.*, 2006). Other factors, upstream of *Foxn1*, must regulate thymus-cell fate decision.

I.3.1.2 Parathyroid epithelial markers – *Gcm2* and *Pth*

Gcm2 encodes a transcription factor homologous of the *Drosophila* gene *Gcm* (Akiyama *et al.*, 1996). It is the earliest known marker of the parathyroid glands in all higher vertebrates (except for fish, which do not have parathyroids). *Gcm2* deletion in mice results in the lack of parathyroid glands, showing its key importance in parathyroids development (Günther *et al.*, 2000). However, *Gcm2* does not specify parathyroid cell fate, as other parathyroid-specific markers, including *CCL21* and *CaSR*, are initiated in *Gcm2*-deficient mice (Liu, Yu and Manley, 2007). Although *Gcm2*$^{-/-}$ embryos develop a

parathyroid-specific domain, they are unable to maintain *CCL21* and *CaSR* expression and to express *Pth*, and the primordium undergoes rapid and coordinated apoptosis by mE12.5 (Liu, Yu and Manley, 2007). These data highlight *Gcm2* as a major regulator of the differentiation and survival of parathyroid precursor cells, but not of parathyroids specification (Liu, Yu and Manley, 2007).

The earliest *Pth* expression is detected in the parathyroid-specific domain at mE11.5 in mice (Günther *et al.*, 2000) and at cE5 (HH25) in chicken (Pinheiro, 2011), and is maintained throughout parathyroid epithelium differentiation (Okabe and Graham, 2004; Liu, Yu and Manley, 2007; Pinheiro, 2011). The absence of *Pth* in the parathyroid domain of *Gcm2* knockout mice supports that *Pth* is downstream of *Gcm2* in parathyroids development (Günther *et al.*, 2000; Liu, Yu and Manley, 2007).

I.3.1.3 NCCs contribution

The pharyngeal region becomes colonized by NCCs early in development, and the interaction between the developing epithelia and these mesenchymal cells will contribute to T/PT development (Le Douarin and Jotereau, 1975; Graham, Okabe and Quinlan, 2005). NCCs are a transient population formed between the neural tube and the surface ectoderm that migrate to several locations in the embryo giving rise to many different cell types including neurons, cartilage, melanocytes, and smooth muscle (reviewed in Krispin, Nitzan and Kalcheim, 2010).

Robert Auerbach was the first to demonstrate the importance of cellular interactions between the thymic epithelium and NC-derived mesenchymal cells (Auerbach, 1960). Mouse fetal thymic lobes striped of the mesenchymal capsule were unable to further develop, while those supplemented with various sources of mesenchyme grew and achieved lobulation *in vitro* to varying degrees, depending on the source of the supplemented mesenchyme (Auerbach, 1960). The ablation of cardiac NCCs in chick embryos resulted in impaired T/PT development and in ectopic locations of these organs (Bockman and Kirby, 1984), strongly suggesting a crucial role of cardiac NCCs in their morphogenesis. However, other studies using the quail-chick chimera system have shown that isolated pharyngeal endoderm is able to form normal thymus and parathyroid glands when transplanted, prior to NCCs migration, to an ectopic site (Le Lièvre and Le Douarin,

1975). These studies suggest that the initial organ formation is NCC-independent, and the epithelium can recruit heterologous mesenchyme to participate in a functional organ. Furthermore, quail-chick chimeras experiments also highlighted the fact that not all mesenchyme is "permissive" to T/PT development (Le Douarin, 1967; Le Douarin, Bussonnet and Chaumont, 1968). Thus, although the role of NCCs in this context can be mimicked by non-NC-derived mesenchymal cells, there are still properties of NCCs we do not fully comprehend.

Even though NCCs seem to be dispensable for initial organ patterning, they play an important role at later stages of T/PT development. The involvement of NCCs in boundary formation between thymic and parathyroid domains was shown in *Pax3*-knockout mice (Splotch) that are largely deficient of migratory NCCs. Splotch mice display an enhanced thymic domain and subsequent larger thymus, at the expense of the parathyroid glands, which become correspondingly smaller (Griffith *et al.*, 2009). Other studies using mouse mutants have also pointed to NCCs' involvement in the detachment of T/PT from the pharynx by promoting endodermal apoptosis (Griffith *et al.*, 2009; Chen *et al.*, 2010; Chojnowski *et al.*, 2014), and in thymus-parathyroids separation process by intercalating between the rudiments (Chojnowski *et al.*, 2016). NCCs were also shown to drive thymus migration in an active way, whereas the parathyroids seem to be "dragged" along in the process until separation occurs (Foster *et al.*, 2010).

I.4 Molecular regulation of thymus and parathyroid glands early-organogenesis

Organogenesis comprises distinct stages regulated by a network of interacting signalling molecules and transcription factors that ensure correct organ formation. While most of the data on the molecular regulators of early stages of T/PT development have come from mouse mutants, several studies in the avian and zebrafish models have also added relevant knowledge to this domain (reviewed in O'Neill *et al.*, 2013; Neves and Zilhão, 2014). The role and expression patterns of the main potential regulators in thymus and parathyroids formation are briefly discussed below and summarized in Table 1 and Fig. 4.

Table 1. Relevant expression pattern and potential role of key signalling molecules and transcription factors implicated in T/PT early development.

Gene	Relevant Expression Pattern	Relevant Role	Reference
RA	Mesenchyme surrounding the pharyngeal endoderm	Posterior PP segmentation and formation	Wendling *et al.*, 2000; Quinlan *et al.*, 2002; Blentic, Gale and Maden, 2003; Niederreither *et al.*, 2003; Kopinke *et al.*, 2006
Tbx1	Surface ectoderm, pharyngeal endoderm and non-NC-derived mesenchyme; later in the presumptive PT domain, excluded from the T domain	Pharyngeal region segmentation, PP formation; later possibly involved in promoting PT fate/suppressing T fate	Garg *et al.*, 2001; Jerome and Papaioannou, 2001; Lindsay *et al.*, 2001; Vitelli *et al.*, 2002; Xu, Cerrato and Baldini, 2005; Liu, Yu and Manley, 2007; Choe and Crump, 2014
Fgf8	Surface ectoderm, pharyngeal endoderm and non-NC-derived mesoderm; later restricted to PP endoderm and clefts	PP formation, possible role in guiding pouch epithelial outpocketing; later in PP patterning	Crossley and Martin, 1995; Abu-Issa *et al.*, 2002; Frank *et al.*, 2002; Macatee, Hammond and Arenkiel, 2003; Gardiner *et al.*, 2012; Choe and Crump, 2014
Hoxa3	PP endoderm and NC-derived mesenchyme	PP specification, early T/PT formation and survival	Manley and Capecchi, 1995, 1998; Su *et al.*, 2001; Diman *et al.*, 2011; Chojnowski *et al.*, 2014
Eya1	Surface ectoderm, PP endoderm, NC-derived mesenchyme	PP patterning and outgrowth	Xu *et al.*, 2002; Zou *et al.*, 2006
Six1/4	Surface ectoderm, PP endoderm, NC-derived mesenchyme	Early T/PT formation and survival	Zou *et al.*, 2006

Pax1	PP endoderm	Early T/PT development, possible regulation of Foxn1 expression	Neubüser, Koseki and Balling, 1995; Wallin *et al.*, 1996; Su *et al.*, 2001; Kelly, 2012
Pax9	PP endoderm	PP development, possible regulation of Foxn1 expression, early T/PT formation and separation from the pharynx	Neubüser, Koseki and Balling, 1995; Peters *et al.*, 1998; Hetzer-Egger *et al.*, 2002; Kelly, 2012
Gata3	PP endoderm; first in T domain, later in PT domain	Possible role in PP patterning and survival; later in PT differentiation and survival	Grigorieva and Mirczuk, 2010; Wei and Condie, 2011
Bmp4	NC-derived mesenchyme, surface ectoderm, presumptive T domain prior to *Foxn1* expression	Epithelial-mesenchymal interactions involved in PP patterning, early T/PT development, separation and migration, formation of functional thymus; regulation of *Foxn1* expression	Ohnemus *et al.*, 2002; Bleul and Boehm, 2005; Patel *et al.*, 2006; Soza-Ried *et al.*, 2008; Gordon *et al.*, 2010; Neves *et al.*, 2012; Swann *et al.*, 2017
Noggin	Mesenchyme and PT domain	PP patterning, opposing Bmp signalling	Patel *et al.*, 2006; Neves *et al.*, 2012
Wnt4	PP endoderm and surrounding mesenchyme	Possible regulation of *Foxn1* expression	Balciunaite *et al.*, 2002
Shh	Pharyngeal endoderm, but excluded from PP endoderm	PP patterning and early PT development	Moore-Scott and Manley, 2005; Grevellec, Graham and Tucker, 2011; Bain *et al.*, 2016
Gcm2	PT domain	PT differentiation	Günther *et al.*, 2000; Gordon *et al.*, 2001; Okabe and Graham, 2004; Liu, Yu and Manley, 2007; Pinheiro, 2011
Foxn1	T domain	TEC differentiation	Nehls *et al.*, 1994; Blackburn *et al.*, 1996; Gordon *et al.*, 2001; Itoi *et al.*, 2001

NC, neural crest; PP, pharyngeal pouch; PT, parathyroid glands; T, thymus; TEC, thymic epithelial cell.

I.4.1 Morphogenesis of the pouch

I.4.1.1 Retinoic acid

Retinoic acid (RA), the biologically active derivative of vitamin A, was shown to be one of the diffusible mesodermal signals that pattern the posterior pharyngeal endoderm in mice (Wendling *et al.,* 2000), quail (Quinlan *et al.*, 2002), and zebrafish (Kopinke *et al.,* 2006) (Fig. 4A). Reduced RA signalling through pharmacologic compounds (Wendling *et al.,* 2000; Kopinke *et al.,* 2006), genetic manipulation (Niederreither *et al.,* 2003), or retinoid-deficient diet (Quinlan *et al.,* 2002) results in the complete absence of the most posterior PP (3-6PP). Moreover, RA was found to positively regulate the expression of early PP-endoderm markers – such as *Fgf8, Pax1*, and *Pax9* – and other important factors in pouch formation and development – such as *Tbx1* and *Hoxa3*, respectively (Wendling *et al.,* 2000; Quinlan *et al.,* 2002; Niederreither *et al.,* 2003; Roberts *et al.,* 2005; Diman *et al.,* 2011). Interestingly, blocking RA signalling during pouch formation in zebrafish embryos did not impair pouch specification, but affected the morphogenesis and segmentation of the pouches in a time-dependent manner (Kopinke *et al.,* 2006). The loss of RA signalling was also found to result in NCCs defects, but several studies have shown that RA influence in neural crest outgrowth is secondary to its role in patterning the pharyngeal endoderm (Dupé *et al.*, 1999; Wendling *et al.*, 2000; Niederreither *et al.*, 2003). Taken together, the data suggest that RA is a major regulator in posterior pouch segmentation and formation, that subsequently supports NCCs migration.

I.4.1.2 T-box 1 and fibroblast growth factor 8

T-box 1 (*Tbx1*) belongs to the evolutionary conserved family of T-box transcription factors, that is defined by a common DNA-binding domain – designated T-box – and the capacity to interact with other transcriptional factors to regulate target genes expression (Naiche *et al.*, 2005). During pouch formation, *Tbx1* is expressed in the surface ectoderm overlying the pharynx, the pharyngeal endoderm and non-NC-derived mesenchyme (Fig. 4A), later becoming restricted to the PPs endoderm and mesodermal core of the PAs (Garg *et al.*, 2001; Vitelli *et al.*, 2002; Zhang *et al.*, 2005). With the use

of a *Tbx1*-lacZ reporter gene, it was also shown that *Tbx1* displays both anterior/posterior and medial/lateral gradients in the developing pharyngeal region (Vitelli *et al.*, 2002). *Tbx1* is one of the responsible genes for the malformations found in DiGeorge syndrome (the most common genetic deletion in humans), that include cardiovascular defects, abnormal facial features, and hypoplasia or aplasia of T/PT (Jerome and Papaioannou, 2001; Lindsay *et al.*, 2001; Vitelli *et al.*, 2002; and reviewed in Baldini, 2005). *Tbx1*$^{-/-}$ mouse mutants display a hypoplastic pharyngeal cavity, with abnormal patterning of the 1st PA, hypoplasia of the 2PA, aplasia of the caudal PAs (3-6PAs), and impaired formation of the 2-4PP, that ultimately results in T/PT aplasia (Jerome and Papaioannou, 2001; Lindsay *et al.*, 2001; Vitelli *et al.*, 2002). The non-segmented caudal pharyngeal apparatus of *Tbx1*$^{-/-}$ mice suggests that *Tbx1* has an important role in pharyngeal region segmentation, but recent evidence from the zebrafish model revealed that the endoderm of the *Tbx1* mutant retains, to some extent, segmental characteristics (Choe and Crump, 2014).

Moreover, *Tbx1* was shown to be required for pouch formation in both mouse (Xu, Cerrato and Baldini, 2005) and zebrafish models (Choe and Crump, 2014). *Tbx1*'s role may be associated with the regulation of cell proliferation, as *Tbx1*$^{-/-}$ mice mutants have a downregulation of the proliferative activity of endodermal cells (Xu, Cerrato and Baldini, 2005). Whether *Tbx1* influence in PP formation is exerted exclusively through the endoderm or with the contribution of the mesenchyme, as well the role of *Tbx1* in each compartment, are not completely understood. Deletion of *Tbx1* exclusively in the pharyngeal endoderm (Arnold *et al.*, 2006; Jackson *et al.*, 2014) or non-NC-derived mesoderm (Zhang, Huynh and Baldini, 2006) of mice recapitulated most of the developmental defects of *Tbx1*$^{-/-}$ embryos, suggesting that *Tbx1* is required in both tissues, and that epithelial-mesenchymal interactions may be relevant in this process.

Increasing evidence has pointed to fibroblast growth factor 8 (*Fgf8*) as a potential downstream effector of *Tbx1* role in PP formation. Fgf8 is an important member of the FGFs family, which comprises small proteins generally secreted that bind to transmembrane tyrosine kinase receptors (FGFRs) and are involved in cell proliferation, differentiation and survival (reviewed in Dorey and Amaya, 2010). *Fgf8* is expressed in the pharyngeal endoderm, overlying ectoderm, and non-NC-derived mesenchyme prior to pouch formation (Fig. 4A), becoming restricted to the PPs endoderm and their respective ectodermal clefts upon their formation (Crossley and Martin, 1995). While

Fgf8 null mice die at mE8.5 (Meyers, Lewandoski and Martin, 1998), *Fgf8* hypomorphic mutants display hypoplasia/aplasia of the 3/4PA and PP (and consequently, of T/PT), suggesting a role in 3/4PP formation (Abu-Issa *et al.*, 2002; Frank *et al.*, 2002). These hypomorphic mice display defects in NCCs (Abu-Issa *et al.*, 2002; Frank *et al.*, 2002) that resemble the NCCs-ablation phenotype (Bockman and Kirby, 1984), suggesting a role in NCCs regulation. In agreement, *Fgf8* deletion solely in the pharyngeal endoderm resulted in normal segmentation of the pharyngeal region (Jackson *et al.*, 2014).

Fgf8 expression was shown to be reduced in *Tbx1*-deleted tissues (Arnold *et al.*, 2006; Zhang, Huynh and Baldini, 2006; Jackson *et al.*, 2014), and loss of *Fgf8* downregulates mitotic activity in both pharyngeal endoderm and mesenchyme (Park *et al.*, 2006), suggesting that *Tbx1* may be regulating proliferation in the pharyngeal region through *Fgf8*. In addition, time-lapse imaging data in *Tbx1*$^{-/-}$ zebrafish embryos exposed a morphogenetic role of mesenchymal *Tbx1* in pouch formation, whereby it induces the mesenchymal expression of *Fgf8*, which is responsible for guiding pouch epithelial outpocketing (Choe and Crump, 2014). The authors hypothesized that *Tbx1* may act primarily in the mesenchyme for pouch morphogenesis, and subsequently in the endoderm for other aspects of pouch cell biology, such as their proliferative expansion (Choe and Crump, 2014).

I.4.2 The 3/4PP endoderm patterning and early T/PT development

I.4.2.1 Hox-Eya-Six-Pax regulatory network

There is growing evidence that a *Hox-Eya-Six-Pax* regulatory network of transcription factors is operating during T/PT common primordium specification and differentiation. These genes are expressed at least initially in the 3/4PP endoderm (Fig. 4), and the null mutants for each of them have normal pouch formation, but then fail to form or have hypoplastic T/PT (Manley and Capecchi, 1995; Peters *et al.*, 1998; Su *et al.*, 2001; Hetzer-Egger *et al.*, 2002; Xu *et al.*, 2002; Zou *et al.*, 2006). However, it is difficult to pinpoint the role of these transcription factors at the cellular level, and how they co-regulate the development of the 3/4PP. Changes in this cascade have been occurring throughout the years, and it remains possible that *Hoxa3* regulates *Pax1* and *Pax9* independently of *Eya1* and *Six1*.

Hoxa3 expression is unaltered in *Eya1*$^{-/-}$, *Six1*$^{-/-}$, *Pax1*$^{-/-}$, and *Pax9*$^{-/-}$ single mice mutants, as well as in *Eya1*$^{-/-}$*Six1*$^{-/-}$, *Six1*$^{-/-}$*Six4*$^{-/-}$, and *Pax1*$^{-/-}$*Pax9*$^{-/-}$ double homozygous embryos (Zou *et al.*, 2006), suggesting that *Hoxa3* is upstream of the remaining genes. While *Eya1*$^{-/-}$ mice show a strong reduction of *Six1* expression but no changes in *Pax1/9* expression, *Eya1*$^{-/-}$*Six1*$^{-/-}$ embryos were reported to have undetectable *Pax1* expression (but unchanged *Pax9* expression) in the pouches at mE10.5 (Zou *et al.*, 2006). Considering these data, and the fact that *Eya1* and *Six1* expression is unaltered in *Pax1*/*Pax9* single and double homozygous mutants (Zou *et al.*, 2006), it is plausible that *Eya1* and *Six* genes are upstream of *Pax1/9*. However, it is also possible that they are acting in parallel pathways, both regulated by *Hoxa3*.

I.4.2.1.1 Homeobox protein A3

Homeobox protein A3 (*Hoxa3*) belongs to the homeobox family of transcription factors that are known to play an important role in patterning the anterior-posterior axis of bilaterian embryos (Krumlauf, 1994; Alexander, Nolte and Krumlauf, 2009). In the mouse, *Hoxa3* is expressed in the 3/4PP endoderm and in the surrounding NCCs from mE8.5 and mE9.5, respectively (Fig. 4B) (Manley and Capecchi, 1998; Diman *et al.*, 2011). *Hoxa3*$^{-/-}$ mice form normal 3/4PP but fail to develop thymus and parathyroids, resulting in their aplasia (Chojnowski *et al.*, 2014). The specific deletion of the *Hoxa3* gene in the endoderm or in NCCs results in small ectopic T/PT, whereas the simultaneous deletion in both tissues mimics the null phenotype, indicating that expression of *Hoxa3* in either cell type is sufficient for these organs formation (Chojnowski *et al.*, 2014). Although for many years the *Hoxa3*$^{-/-}$ phenotype was thought to be due to a failure in the specification of the common primordium into thymic and parathyroid domains (Manley and Capecchi, 1995; Su *et al.*, 2001; Manley and Condie, 2010), recent work performed in the Manley lab have shown that T/PT specification and differentiation initiate (Chojnowski *et al.*, 2014). *Foxn1* and *Gcm2* initiate their expression, but the primordium undergoes coordinated apoptosis shortly after (Chojnowski *et al.*, 2014). Although this work revealed that *Hoxa3* does not establish 3/4PP identity, it clearly showed that *Hoxa3* modulates, but is not required for, thymus and parathyroids-specific gene expression, and that it protects T/PT rudiments from cell death (Chojnowski *et al.*, 2014).

I.4.2.1.2 Eyes absent 1 and sine oculis homeobox 1 and 4

Eyes absent homolog 1 (*Eya1*) is a member of the eyes absent gene family, homolog of the *Drosophila* eyes absent (*Eya*) gene (Bonini, Leiserson and Benzer, 1993), and encodes a transcription co-activator that is expressed in the pharyngeal endoderm, NC-derived mesenchyme, and ectoderm from mE9.5 (Fig. 4B) (Xu *et al.*, 2002). *Eya1*$^{-/-}$ mice lack thymus and parathyroid glands, and the expression of *Foxn1* and *Gcm2* was not detected at mE9.5-11.5, suggesting that *Eya1* is necessary for early initiation of T/PT organogenesis (Xu *et al.*, 2002). In addition, *Eya1* was proven to be a canonical activator of sine oculis homeobox 1 (*Six1*) (Li *et al.*, 2003), a member of the *Six* gene family of transcription factors homologous to *Drosophila* sine oculis (*so*) gene (Serikaku and O'Tousa, 1994). *Eya1* acts synergistically with *Six1* to regulate proliferation and survival of organ-specific precursors (Li *et al.*, 2003). In the pharyngeal region, *Six1* is co-expressed with *Eya1* (Fig. 4B) and its expression is *Eya1*-dependent (Xu *et al.*, 2002). *Six1* knockout mice display a phenotype with strong similarities to *Hoxa3*$^{-/-}$ mice, as the expression of *Gcm2* and *Foxn1* initiates, but the primordium undergoes apoptosis, leading to the complete disappearance of these glands by mE12.5 (Zou *et al.*, 2006; Chojnowski *et al.*, 2014). The fact that the expression of organ-specific genes initiates in *Six1*$^{-/-}$ mice, but not in *Eya1*$^{-/-}$ mutants, also supports the notion that *Eya1* acts upstream of *Six1* (Zou *et al.*, 2006). In addition, the double knockout of *Six1* and *Six4* (a closely related family member, co-expressed with *Six1* in the pharyngeal endoderm) shows a complete absence of *Gcm2* and *Foxn1* expression, indicating that both genes act synergistically and downstream of *Eya1* to regulate organ primordium-specific gene expression during early T/PT formation (Zou *et al.*, 2006).

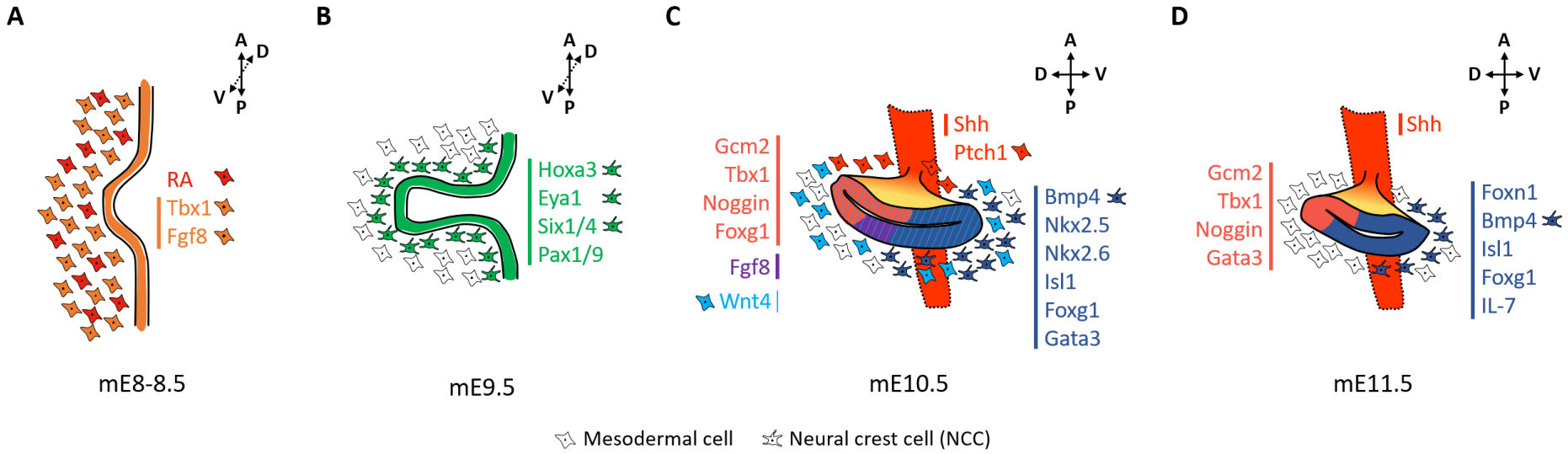

Figure 4. Molecular regulation of early thymus and parathyroid glands organogenesis through time and space. Schematic representation of the expression patterns of the potential regulators at different phases of early thymus and parathyroid glands development in the mouse model. Pouch formation is mainly dependent on RA, Tbx1 and Fgf8 signalling (A). After the pouch is formed, it is surrounded by mesenchymal cells of mesodermal and neural crest origin and its development is also dependent on the presence of the transcription factors *Hoxa3*, *Eya1*, *Six1/4*, and *Pax1/9* (green) (B). The pharyngeal pouch then becomes patterned into two distinct domains likely through Shh/Noggin and Bmp4 signallings, which are also involved in the development of the parathyroid glands and the thymus, respectively. *Fgf8* expression in the posterior domain (purple) may also have a role in pouch patterning. The dorsal domain of the pouch starts to express *Gcm2* (the main regulator of parathyroids differentiation), along with *Tbx1*, *Noggin*, and *Foxg1* (pink), while the prospective thymic domain in the ventral region may be regulated by *Bmp4*, *Nkx2.5*, *Nkx2.6*, *Isl1*, *Foxg1*, and *Gata3* (blue). The pharyngeal endoderm also expresses *Wnt4*, which was suggested to regulate *Foxn1* expression. (C). When the two domains are completely established, the differentiation of the parathyroid glands is also dependent on *Gata3*, and the thymic domain expresses *Bmp4*, *Isl1*, *Foxg1*, and *IL7*, in addition to *Foxn1* (the main regulator of thymus differentiation) (D). Gene expression in the pharyngeal endoderm and surrounding mesenchyme is indicated by vertical bars and cell cartoons, respectively. Many of these genes are also expressed in the pharyngeal ectoderm, as described in the text. A, anterior; D, dorsal; m, mouse; P, posterior; V, ventral. Adapted from O'Neill *et al.*,2013, and Neves and Zilhão, 2014**.**

I.4.2.1.3 Paired box protein 1 and 9

Pax1 and *Pax9* are closely related members of the paired box (*Pax*) family of transcription factors (Dahl, Koseki and Balling, 1997). Distinct from the other players of the *Hox-Eya-Six-Pax* cascade, their expression is restricted to the pharyngeal endoderm. *Pax1* and *Pax9* are expressed in the pharyngeal endoderm from mE8.5, in the pharyngeal pouches by mE9.5 (Fig. 4B), and in TECs further in development (Neubüser, Koseki and Balling, 1995; Wallin *et al.*, 1996). Although these highly homologous genes exhibit overlapping patterns of expression in the pharyngeal region, *Pax9* mRNA levels were observed to be distinctly lower than those of *Pax1* (Neubüser, Koseki and Balling, 1995). *Pax1*$^{-/-}$ mice display thymic and parathyroid glands hypoplasia, along with mild defects in T-cell development (Wallin *et al.*, 1996). A much more drastic phenotype is observed in *Pax9*$^{-/-}$ mutants, as the T/PT common primordium fails to detach from the pharynx and develops ectopically as a polyp-like structure within the laryngeal cavity (Hetzer-Egger *et al.*, 2002). Although the mutant thymic primordium expresses *Foxn1* and is colonized by LPCs, it is severely hypoplastic, T-cell development is greatly impaired, and the thymic lobes gradually become filled with apoptotic cells, resulting in highly disorganized rudiments (Hetzer-Egger *et al.*, 2002).

Worth noting, *Pax1/9* expression initiates in *Hoxa3*$^{-/-}$ mice, but fails to be maintained (Manley and Capecchi, 1995), which mimics what is observed for *Gcm2* expression in these mice (Chojnowski *et al.*, 2014). This points to a potential regulatory network between *Hoxa3*, *Pax1/9*, and *Gcm2*. While *Pax1*$^{-/-}$ mice show a reduction in *Gcm2* levels, resulting in hypoplastic parathyroids, the compound mutants *Hoxa3*$^{+/-}$*Pax1*$^{-/-}$ display an inability in maintaining *Gcm2* expression, and the hypoplastic parathyroid rudiment observed at formation eventually disappears (Su *et al.*, 2001). This evidence suggests a *Hoxa3-Pax1-Gcm2* regulatory cascade, although the presence of parathyroids in *Pax1* single mutants indicates the existence of other players under the control of *Hoxa3* in parathyroids differentiation.

A potential candidate is *Pax9*, as both *Pax1* and *Pax9* binding sites were found to be present in the promotor of *Gcm2* gene (Maret *et al.*, 2008). Interestingly, functional redundancy between *Pax1* and *Pax9* was reported during vertebral column development in a gene dosage-dependent manner (Peters *et al.*, 1999). The fact that *Hoxa3*$^{+/-}$*Pax1*$^{-/-}$ hypoplastic thymi are also ectopic, a feature not observed in *Pax1*$^{-/-}$ mutants but

characteristic of *Pax9*$^{-/-}$ mice, also suggests functional redundancy between *Pax1/9* in thymus development. Analysis of several *Pax1/9* compound mutants have provided further evidence suggesting a gene-dose cooperation between the two genes in this context (Kelly, 2012). Location, size, and structure of the thymus were affected in a gene dosage-dependent manner, and *Pax1*$^{-/-}$*Pax9*$^{-/-}$ mutants displayed an hypoplastic thymic rudiment, ectopically located in the larynx, and with deficits in TECs and T-cell development (Kelly, 2012). While this phenotype resembles that of *Pax9* single mutants, it lacks *Foxn1* expression. Interestingly, *Pax*$^{-/-}$*Pax9*$^{+/-}$ mice exhibited a 2-fold decrease in *Foxn1* expression, indicating that *Foxn1* expression was also reduced in a gene dosage-dependent manner (Kelly, 2012). These data suggested, for the first time, that *Pax1/9* are required for the initiation of *Foxn1* expression, in a cooperative way (Kelly, 2012).

I.4.2.2 *Nkx2-5, Nkx2-6, Isl1, Foxg1,* and *IL7*

Several candidate regulators of thymic specification have been proposed based on their expression in the presumptive thymic domain, prior to the activation of *Foxn1* (mE11.25) (Wei and Condie, 2011). The endodermal expression of the homeobox proteins Islet1 (*Isl1*), *Nkx2-5*, and *Nkx2-6* is restricted to the presumptive thymic domain at mE10.5 (Fig. 4C) (Wei and Condie, 2011). *Foxg1*, a member of the forkhead family of transcription factors, is expressed in regions that include both parathyroids and thymic presumptive domains at mE10.5, and one day later it becomes restricted to the thymic domain (Fig. 4C and D) (Wei and Condie, 2011). *Isl1* and *Foxg1* continue to be expressed in TECs throughout thymus development, suggesting these factors may have a continuous role in TEC differentiation (Wei and Condie, 2011). Interleukin 7 (*IL7*), a cytokine required for thymocyte differentiation and survival (von Freeden-Jeffry *et al.*, 1995), is also one of the earliest markers of thymus-fated cells (Zamisch *et al.*, 2005). *IL7* expression is initiated between mE10.5 and mE11.5, when it is exclusively expressed in the thymic domain (Fig. 4D) (Zamisch *et al.*, 2005). Worth noting, both *Foxg1* and *IL7* were shown to be expressed in the thymic rudiment of *nude* mice (Zamisch *et al.*, 2005; Wei and Condie, 2011). In conclusion, *Nkx2-5*, *Nkx2-6*, *Isl1*, *Foxg1,* and *IL7* are *Foxn1*-independent specific early markers of thymus-fated cells (Zamisch *et al.*, 2005; Wei and Condie, 2011). However, whether they are involved in the activation of *Foxn1* expression, in its maintenance, and/or in *Foxn1*-independent aspects of thymus development remains

unclear (Wei and Condie, 2011). Also, the potential associations between the known regulators of T/PT early development and these factors are still uncertain, but several studies have revealed examples of such interactions in other developmental contexts (Reifers *et al.*, 2000; Park *et al.*, 2006; Liao *et al.*, 2008; Quaranta *et al.*, 2018; Hettige and Ernst, 2019).

I.4.2.3 Major signalling pathways

The major challenge nowadays when studying organ development is to achieve a comprehensive view of the regulatory actions of the major signalling pathways. Besides the number of transcriptional factors described so far, signalling pathways like bone morphogenetic protein (BMP) (Bleul and Boehm, 2005; Patel *et al.*, 2006; Soza-Ried *et al.*, 2008; Gordon *et al.*, 2010; Neves *et al.*, 2012; Swann *et al.*, 2017), fibroblast growth factor (FGF) (Revest *et al.*, 2001; Abu-Issa *et al.*, 2002; Frank *et al.*, 2002; Jenkinson, Jenkinson and Anderson, 2003; Macatee, Hammond and Arenkiel, 2003; Dooley *et al.*, 2007; Gardiner *et al.*, 2012), Wingless-int (Wnt) (Balciunaite *et al.*, 2002), Notch (Grigorieva and Mirczuk, 2010; Kameda *et al.*, 2013), and Hedgehog (Shah *et al.*, 2004; Moore-Scott and Manley, 2005; Grevellec, Graham and Tucker, 2011; Bain *et al.*, 2016), were also shown to be involved in 3/4PP patterning and early phases of T/PT development.

I.4.2.3.1 BMP, FGF, and Wnt pathways

BMPs are a group of secreted morphogenetic growth factors that belong to the transforming growth factor-b (TGF-b) family. They are involved in embryonic patterning and development, and regulate tissue homeostasis and regeneration (Wang *et al.*, 2014). Their paracrine signalling is made through transmembrane serine/threonine kinase receptors. Similar to other developmental pathways, BMP signalling activity is regulated by opposing effects of activators and inhibitors of the pathway. These signals were suggested to be involved in the definition of thymic and parathyroids boundaries during the patterning of the 3PP endoderm in the mouse (Patel *et al.*, 2006). *Bmp4* is expressed in the presumptive domain of the thymus before the settlement of high levels of *Foxn1* expression, while its antagonist, *Noggin*, is expressed in the *Gcm2*$^{+}$ domain, the

complementary territory of the pouch (Fig. 4C and D) (Patel *et al.*, 2006). In addition to the endodermal expression, *Bmp4* is also expressed in the surrounding mesenchyme, including NCC-derived cells, and in the ectodermal compartment (Fig. 4C and D) (Patel *et al.*, 2006).

Work from our lab using the avian model revealed the involvement of BMP- and FGF-related molecules in the endodermal-mesenchymal interactions that are essential for T/PT early development (Neves *et al.*, 2012). The results showed that the early endoderm, that expresses *Bmp receptor 1b and 2* in the pouches, signals the adjacent mesenchyme (possibly by Fgf8). This induces *Bmp4* transcription in the mesenchyme, which in turn promotes the specification of the thymus fate. A sequential expression of *Bmp4* and *Fgf10* in the mesenchyme was found to be crucial for the formation of a *Foxn1*$^{+}$ thymic rudiment. Interestingly, *Bmp4* signals are only required through a short period of time (between qE2.5-3 or cE3-3.5), after which *Fgf10* expression takes over, sustaining the later development of the endoderm into a *Foxn1*$^{+}$ thymic rudiment. Coincidently to the disappearance of *Bmp4* and initiation of *Fgf10* in the mesenchymal compartment, *Bmp4* starts being expressed by the pouch endoderm. Mesenchymal *Bmp4* was also shown to regulate the maintenance of *Gcm2* expression in the parathyroid domain (Neves *et al.*, 2012). The simultaneous presence of transcripts of BMP receptors in the endoderm and *Bmp4* ligand in the adjacent mesenchyme strongly suggests that mesenchymal-derived *Bmp4* signals regulate the pouch patterning process (Neves *et al.*, 2012). Moreover, studies in mice genetically modified to have *Noggin* expression under the *Foxn1* promotor showed that Bmp4 signalling in the endoderm is also necessary for the maintenance of *Foxn1* expression (Soza-Ried *et al.*, 2008; Swann *et al.*, 2017). This supported previous data showing that Bmp4 treatment upregulated *Foxn1* transcripts in fetal thymic organ cultures (FTOC) (Tsai, Lee and Wu, 2003).

Besides the potential role of FGF signalling (through *Fgf8*) in pouch formation described early in this Chapter, the analysis of mice with a hypomorphic or null allele of *Fgf8* (Frank *et al.*, 2002) and mice with specific deletion of *Fgf8* in both the endoderm and ectoderm (Macatee, Hammond and Arenkiel, 2003) have confirmed *Fgf8* involvement in T/PT development. More recently, FGF-related molecules, including *Fgf8*, were shown to be expressed in the posterior region of the 3PP and in the surrounding mesenchyme at mE10.5, when *Gcm2* is already expressed, but *Foxn1* is not (Fig. 4C) (Gardiner *et al.*, 2012). The deletion of two members of the Sprouty (*Spry*) class of FGF

antagonists – *Spry1 and 2* – led to a delay in *Foxn1* expression and a reduction of the *Gcm2*$^{+}$ domain, which later resulted in T/PT hypoplasia (Gardiner *et al.*, 2012). Interestingly, *Bmp4* expression was also downregulated in the thymic domain of the mutants, supporting the notion that FGF signalling in the posterior domain of the pouch may regulate the initiation of the patterning events of the 3PP in the mouse (Gardiner *et al.*, 2012). These alterations, caused by enhanced expression of FGF targets, were shown to be partially suppressed by genetic reduction of *Fgf8* (Gardiner *et al.*, 2012).

The Wnt family of secreted glycolipoproteins controls several cellular processes during development and in adult homeostasis, such as cell proliferation, polarity, and fate specification. In the mouse, *Wnt4* expression was found in the 3PP endoderm and surrounding mesenchyme before the appearance of *Foxn1* (Fig. 4C), and overexpression of *Wnt4* in TEC lines induced *Foxn1* transcription, highlighting its potential role in *Foxn1* regulation (Balciunaite *et al.*, 2002).

Further evidence on the regulation of *Foxn1* expression by BMP and Wnt pathways came from the hair follicle development in mice. Overexpression of *Noggin* in the skin reduced *Foxn1* mRNA levels in hair follicles (Kulessa, Turk and Hogan, 2000), while Wnt5a treatment in cultured mouse skin induced *Foxn1* expression (Hu *et al.*, 2010). Worth noting, *Wnt5b*, a paralog of *Wnt5a*, is expressed in the 3PP of mouse embryos prior to strong *Foxn1* expression (Balciunaite *et al.*, 2002). However, *Wnt5b*'s precise domain of expression in the pouch and its potential link with *Foxn1* remain unexplored.

I.4.2.3.2 Notch signalling

Notch signalling (described in more detail in Section I.6.1) is a major pathway involved in multiple cellular events like fate decision, proliferation, survival, and differentiation, during development and in the adult life. Notch effects are highly dependent on dose, timing, and context (reviewed in Lai, 2004; Bray, 2006; Hurlbut *et al.*, 2007; Hori, Sen and Artavanis-Tsakonas, 2013; Shida *et al.*, 2015). In brief, Notch signalling is activated through the binding of a Notch ligand (from the Delta or Serrate/Jagged families) in a cell with a Notch receptor in a neighbouring cell (trans-activation). This binding promotes a proteolytic cleavage of the receptor by the γ-

secretase complex, and the resulting intracellular domain of Notch moves to the nucleus and binds to several proteins, namely the DNA-binding protein CSL, to activate the transcription of Notch target genes (reviewed in Andersson, Sandberg and Lendahl, 2011; Henrique and Schweisguth, 2019).

The most well-known involvement of Notch signalling related to thymus is, undeniably, in T-cell lineage commitment and maturation. Numerous studies have shown that Notch is required for the late stages of thymus development, not only in the cross-talk between TECs and LPCs (reviewed in Abramson and Anderson, 2017), but also throughout T-cell development (reviewed in Maillard, Fang and Pear, 2005; Radtke, Fasnacht and Macdonald, 2010; Shah and Zuniga-Pflucker, 2014). Namely, Notch was found to be involved in T-cell commitment (Jaleco *et al.*, 2001), in the choice between αβ and γδ TCR (Washburn *et al.*, 1997), and in the CD4 versus CD8 lineage decision (Robey *et al.*, 1996). Despite all the knowledge gathered over the years concerning the role of Notch signalling in the late stages of thymus development and T-cell development, evidence of a role in the early phases of thymus (as well as of parathyroid glands) development is scarce.

Most of what is known regarding Notch in those early stages involves the Notch target *Hes1*, which was found to be downstream of *Tbx1* in the development of the pharyngeal structures (van Bueren *et al.*, 2010) and to be required for the migration of T/PT to their final destination (Kameda *et al.*, 2013). In our lab, *Hes1* expression was observed in the 3/4PP endoderm in chicken embryos at cE3 and cE4 (unpublished data). Additionally, the transcriptional factor *Gata3*, a known Notch target in different stages of T-cell development, with CSL-binding sites in its upstream promotor (Hoflinger *et al.*, 2004; Fang *et al.*, 2007), was also shown to be required for the development of the T/PT common primordium and to directly bind to the *Gcm2* promotor region and upregulate its expression in the mouse (Grigorieva and Mirczuk, 2010). *Gata3* is found in the presumptive territory of the thymus between mE9.5-10.5, but by mE11.5 it becomes restricted to the $Gcm2^{+}$ parathyroid domain (Grigorieva and Mirczuk, 2010; Wei and Condie, 2011). $Gata3^{-/-}$ mice embryos lack *Gcm2* expression as well as T/PT primordia, while $Gata3^{+/-}$ heterozygotes display smaller T/PT primordia with fewer *Gcm2*-expressing cells (Grigorieva and Mirczuk, 2010). It is thus possible that *Gata3* has distinct roles at different time-windows of the early development of the common primordium, but further studies are needed to clarify this. Since there are no reports of *Gata3* transcripts

in the presumptive domain of the parathyroid glands before or at the time of *Gcm2* initiation, it likely regulates the differentiation and survival of parathyroid progenitor cells by maintaining *Gcm2* expression, rather than parathyroids specification.

In addition, previous data from our lab revealed that other Notch signalling-related genes are expressed in T/PT presumptive territories and in the surrounding mesenchyme in chicken embryos (Figueiredo, 2011). At cE3, before the observation of *Gcm2* and *Foxn1* expression, *Notch1* receptor and target genes *Hes5.1* and *Hes6.1* are expressed in the surrounding mesenchyme of the 3/4PP. *Hes6.1* mRNA is also detected in the posterior domain of the 3PP endoderm and the ventral region of the 4PP. By cE4, when *Gcm2* is already being expressed, but *Foxn1* is not, *Notch1* and *Hes5.1* are expressed in the anterior domain of the 3/4PP, and interestingly, *Hes6.1* transcripts become restricted to the posterior domain of both pouches (Figueiredo, 2011). Moreover, we have developed an *in vitro* system where dissected pharyngeal region explants from chicken embryos were cultured for 48h in the presence or absence of a pharmacological inhibitor of Notch signalling (γ-secretase inhibitor, DAPT). *In situ* hybridization of pharyngeal explants grown in the presence of DAPT showed a block of *Gcm2* expression (in 87.5% of explants), while *Foxn1* transcript levels were either down- or upregulated (Figueiredo, 2011). Our preliminary data suggest that Notch signalling is involved in the early development of these glands.

I.4.2.3.3 Hedgehog signalling

The Hedgehog (Hh) pathway (described in greater detail in Section I.6.2) is a major paracrine regulator of many fundamental processes in development including cell proliferation, survival, and differentiation, cell fate, stem cell maintenance and tissue polarity. Hh ligands act as morphogens, signalling both at short range and over many cell diameters (creating gradients). Briefly, Hh activation depends on the binding of a Hh ligand to the receptor Patched1 (Ptch1) in a receiving cell, which releases Smoothened (Smo), another membrane receptor, from Ptch1 repression. The free Smo moves to a specialized cellular structure called primary cilium to induce the downstream signalling cascade, involving the activation of zinc-finger transcription factors – Ci in *Drosophila*, and glioma-associated oncogene (Gli) proteins in vertebrates –, which promote the

transcription of Hh target genes (reviewed in Varjosalo and Taipale, 2008; Lee, Zhao and Ingham, 2016).

Hh signalling was shown to be involved in cranio-facial and neck morphogenesis (reviewed in Grevellec and Tucker, 2010) and to regulate T/PT common primordium development (Moore-Scott and Manley, 2005). The pharyngeal expression of Hh ligand sonic hedgehog (*Shh*) and *Ptch1* is mainly restricted to the anterior pouches' region in chicken and mouse embryos (Moore-Scott and Manley, 2005; Grevellec, Graham and Tucker, 2011). By the time *Gcm2* starts being expressed, *Shh* is present throughout the pharyngeal endoderm, with the exception of the pharyngeal pouches (Moore-Scott and Manley, 2005; Grevellec, Graham and Tucker, 2011). *Ptch1* transcripts co-localize with those of *Shh* and are also present in mesenchymal cells surrounding *Shh*-expressing endoderm. By mE10.5, the strongest signals of *Ptch1* in the posterior pouches' region are detected in the mesenchyme surrounding the *Shh*$^{+}$-pharyngeal endoderm. Intriguingly, while *Shh* and *Ptch1* mRNAs were detected in the 1PP and 2PP of mouse embryos between mE10.5 and mE11.5, no *Shh* expression and low to no expression of *Ptch1* was observed in the 3/4PP endoderm (Moore-Scott and Manley, 2005; Grevellec, Graham and Tucker, 2011; Bain *et al*., 2016). *Shh* null mice display loss of *Noggin*/*Gcm2* expression domain in the 3PP, while *Bmp4*$^{+}$ and *Foxn1*$^{+}$ domains expanded (Moore-Scott and Manley, 2005). This abnormal patterning of the common primordium results in the lack of parathyroid glands (Moore-Scott and Manley, 2005) and in thymic functional defects (Shah *et al*., 2004). Similar changes were observed in chicken embryos treated with a pharmacological inhibitor of Hh signalling (Smo inhibitor, cyclopamine) at HH14-16 (cE2-2.5) (Grevellec, Graham and Tucker, 2011). However, Shh inhibition at a later stage (HH21, cE3.5) resulted in unchanged *Gcm2* transcription in the 3PP, and ectopic expression of *Gcm2* and *CasR* in the anterior pharyngeal region (Grevellec, Graham and Tucker, 2011). The current data suggest that, at early stages of development, Shh-Bmp4 opposing gradients may be regulating the patterning of thymic and parathyroid domains, in which Shh and Bmp4 promote parathyroid and thymus development, respectively. At later stages, Shh signalling may have a suppressive role, restricting the development of the parathyroid glands to the caudal pharyngeal pouches (Grevellec, Graham and Tucker, 2011). Worth noting, the genetic deletion of *Smo* in the endoderm or in the adjacent NCCs of mouse embryos did not prevent *Gcm2* expression, suggesting that each tissue alone is sufficient to promote parathyroids development (Bain *et al.*, 2016).

A decade ago, a *Shh-Tbx1-Gcm2* regulatory network was proposed by the Manley lab (Liu, Yu and Manley, 2007). It was based on the fact that: Shh signalling regulates *Tbx1* expression in the pharyngeal region of mouse and chicken embryos (Garg *et al.*, 2001; Yamagishi *et al.*, 2003); *Tbx1* expression in the 3PP becomes restricted to the parathyroids-fated domain by mE10.5, prior to *Foxn1* appearance (Vitelli *et al.*, 2002; Manley *et al.*, 2004; Liu, Yu and Manley, 2007); *Gcm2* is one of the downregulated genes in the pharyngeal region of *Tbx1*$^{-/-}$ mice (Ivins *et al.*, 2005); and *Tbx1* is not altered in *Gcm2* knockout mice (Liu, Yu and Manley, 2007). Moreover, the exclusion of *Tbx1* expression from the presumptive thymic domain also suggested that its absence may be required for thymus fate specification. Tbx1's suppressive role was later confirmed after its ectopic expression in the thymus-fated domain (under the *Foxn1* promotor) of mouse embryos was shown to inhibit *Foxn1* expression (Reeh *et al.*, 2014). However, *Tbx1* ectopic expression was not sufficient to induce *Gcm2* expression in that domain (Reeh *et al.*, 2014). Similar results were obtained with the constitutive activation of Hh signalling in the endoderm of mice, in which an expanded *Tbx1*$^{+}$ domain partially suppressed *Foxn1* expression, but did not promote an expansion of the *Gcm2*$^{+}$ domain (Bain *et al.*, 2016). The data thus confirmed *Tbx1* as a target of Shh signalling in the patterning of the 3PP, and Shh and Tbx1 as negative regulators of thymus development. It also suggested that other players, independent of Shh, must be involved in parathyroids fate specification. The precise mechanisms behind Hh regulation of pouch patterning in the apparently Hh-negative T/PT presumptive tissues remain yet to be clarified.

Altogether, these data suggest complex interactions between signalling pathways and transcription factors in the induction or maintenance of T/PT specific markers. For most of these molecular players, it remains uncertain whether they are directly involved in cell fate specification. Since *Foxn1* and *Gcm2* are exclusively required for the differentiation, rather than the specification, of their respective organs (Blackburn *et al.*, 1996; Zamisch *et al.*, 2005; Liu, Yu and Manley, 2007), increasing efforts are being made to identify the molecular players that specify these fates.

I.5 Notch and Hedgehog interactions during embryonic development

Cell specification, as well as the formation and development of distinct tissues, often depend on interactions between signalling pathways, which can act sequentially, in parallel, or even modulating canonical components of another pathway. Hh and Notch pathways have been shown to interact in several ways and in many biological contexts. For instance, Hh and Notch were shown to cooperate in the regulation of epithelial-mesenchymal transition of hepatic cells (Xie *et al.*, 2013), and Notch was shown to increase neural progenitors' response to Shh by modulating the expression or the position of *Ptch1*, *Smo*, and *Gli3* in the primary cilia (Kong *et al.*, 2015; Stasiulewicz *et al.*, 2015). In addition, Hh effector proteins Gli2 and Gli3 were found to be direct targets of Notch transcriptional complex in neural stem cells (Li *et al.*, 2012). Worth noting, many of the known interactions between the two pathways place Hh upstream of Notch. This is the case in arterial differentiation (Lawson, Vogel and Weinstein, 2002), gut development (Kim *et al.*, 2011), the neural plate (Kong *et al.*, 2015; Stasiulewicz *et al.*, 2015), and limb development (McGlinn *et al.*, 2005). In the latter, Shh was shown to induce the activation of *Jagged1* expression through Gli3. Moreover, during retina development, Shh is able to induce Notch-independent *Hes1* expression through the binding of Gli2 to the *Hes1* promotor (Wall *et al.*, 2009). It is thus possible that these pathways are also interacting during the development of T/PT common primordium.

I.6 Procedures to manipulate signalling pathways

In this thesis, we aimed to unravel the role of Notch signalling in the early stages of thymus and parathyroid glands development, as well as to define whether Notch and Hh were interacting in this context. For that, we designed pharmacological and genetic approaches to modulate Notch signalling and pharmacological strategies to suppress Hedgehog signalling. These signalling pathways will be described in detail in the next sections, along with the respective modulation strategies.

I.6.1 Notch signalling

The Notch pathway comprises a complex family of type I transmembrane proteins that are conserved throughout evolution: Notch receptors (Notch 1-4 in mammals; Notch 1-2 in avian), and ligands of the DSL (*D. melanogaster* Delta and Serrate, and *C. elegans* Lag-2) family (Delta-like 1-3 and Jagged 1-2 in mammals; Delta-like 1,3,4 and Serrate 1-2 in avian) (Fig. 5) (reviewed in D'Souza, Meloty-Kapella and Weinmaster, 2010; Kovall and Blacklow, 2010). Ligand-receptor interaction leads to a conformational change of the Notch receptor that will allow access to two proteolytic cleavage sites. The first cleavage is performed by a member of the disintegrin and metalloprotease (ADAM) family at the S2 cleavage site to release the extracellular fragment, and the second by the γ-secretase multiprotein enzyme complex at the S3 site to fully release the intracellular Notch (ICN; active form) into the cytosol (Fig. 5). ICN undergoes nuclear translocation and binds to the DNA-binding protein CSL (an acronym for CBF-1/RBPJ-κ in mammals, Su(H) in *D. melanogaster*, and Lag-1 in *C. elegans*), which in the absence of a Notch ligand, is part of a transcriptional repressor complex. The ICN-CSL complex recruits transcriptional co-activators of the mastermind-like family (MAML), which work as a scaffold for the assembly of a large multiprotein transcription activation complex. A variety of other co-activators, including histone acetyltransferases p300/CBP, are also involved in the transcriptional activation of Notch target gene expression. The transcriptional activation complex is then able to induce target gene expression (Fig. 5) (reviewed in Kopan and Ilagan, 2009; Musse, Meloty-Kapella and Weinmaster, 2012; Hori, Sen and Artavanis-Tsakonas, 2013; Carrieri and Dale, 2017; Henrique and Schweisguth, 2019).

Although there are several CSL binding sites throughout the genome, the best characterized Notch targets belong to the Enhancer of Split (E(spl)) complex in *Drosophila*, and the Hairy/Enhancer of Split (Hes) and Hes-related (Hey or Hrt) family of genes in vertebrates. They encode basic helix-loop-helix (bHLH) transcriptional repressors that control many secondary targets, including their own genes. Hes and Hey proteins regulate negatively their target genes by forming homodimers or heterodimers between members of the same family or of distinct families. The heterodimers between Hes and Hey family proteins seem to be even more stable and more efficient than the homodimers. The fast degradation of ICN to prevent further transcription, and the self-

repression of the target genes, along with their short-lived mRNAs and proteins, contribute to the characteristically fast and burst-like activation of Notch signalling (reviewed in Fior and Henrique, 2009; Bray and Bernard, 2010; Kobayashi and Kageyama, 2014).

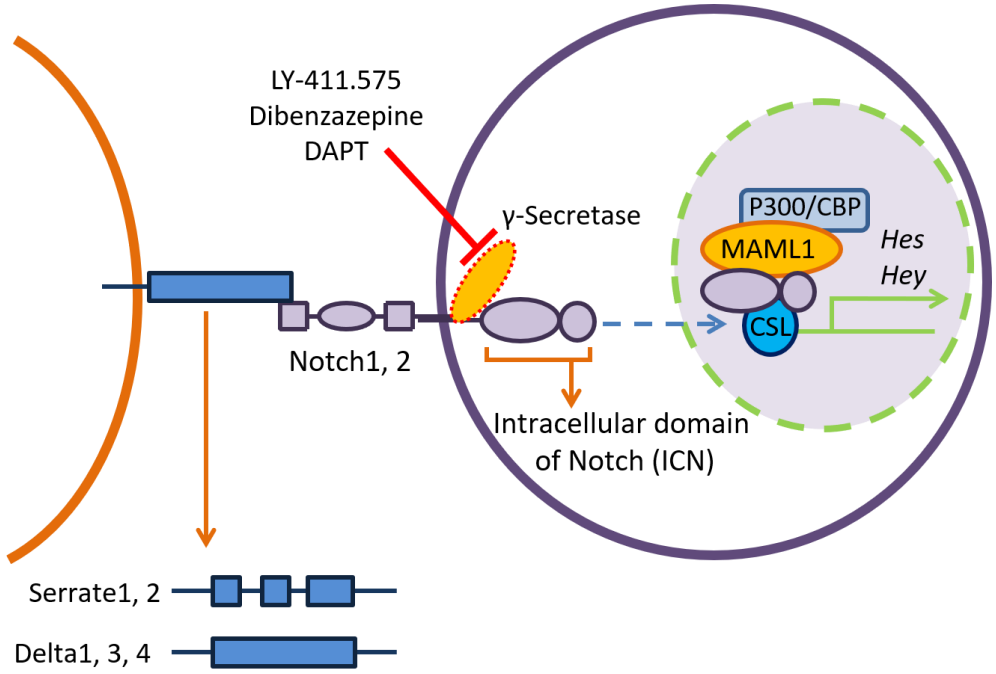

Figure 5. Notch signalling pathway in avian. The binding of a Notch ligand (Serrate 1,2 or Delta-like 1,3,4) in a cell to the Notch receptor (Notch 1,2) of a neighbouring cell leads to a series of proteolytic cleavages of the receptor, the last one being catalysed by the γ-secretase complex, producing the free intracellular domain of Notch (ICN). ICN translocates to the nucleus and binds to the DNA-binding protein CSL and several transcription co-activators, such as MAML1 and P300/CBP, inducing the transcription of Notch target genes. Pharmacologic inhibitors of Notch signalling such as LY-411.575, Dibenzazepine, and DAPT, act through the suppression of the γ-secretase complex.

Despite the apparent simplistic molecular design of the Notch signalling, its functional diversity suggests the existence of additional levels of signalling regulation. Several complex regulatory mechanisms such as regulation of expression patterns, post-translational modifications, trafficking of the Notch ligands and receptors, feedback loops, and nuclear modulation were shown to affect the availability and activity of Notch receptors and ligands at the cell surface, as well as the activation of downstream targets (Henrique and Schweisguth, 2019). For instance, ICN is known to repress Delta (Shimojo, Ohtsuka and Kageyama, 2011), while it usually activates Jagged (Manderfield *et al.*, 2012). Besides the trans-interaction between Notch ligands and receptors on

neighbouring cells, ligand-receptor interactions can occur within the same cell in a cell-autonomous way, resulting in functionally neutralized Notch receptors (cis-inhibition) (reviewed in Del Álamo, Rouault and Schweisguth, 2011). This mechanism also defines the Notch state of a cell. If a cell has more Notch receptors than ligands there will still be some receptors left to receive signals after cis-inhibition and the cell will be a "receiver" (rich in Notch receptors, with high levels of Notch activity), whereas the opposite proportions lead to a "sender" cell state (rich in Notch ligands, with low levels of Notch activity) (Sprinzak *et al.*, 2010). One of the best characterized post-translational modification is the glycosylation of Notch receptors by the Fringe family of glycosyltransferases (Lunatic Fringe, Manic Fringe, and Radical Fringe). Fringe proteins, through glycosylation, modulate the affinity of Notch to its ligands (reviewed in Bray, 2006; Andersson, Sandberg and Lendahl, 2011; de Celis, 2013). While Lunatic and Manic Fringe promote Notch-Delta interactions (both trans- and cis-) while reducing Notch responsiveness to Jagged/Serrate ligands, Radical Fringe enhances signalling from both ligands (Hicks *et al.*, 2000; Yang, 2005). Another factor likely contributing to the pleiotropic nature of Notch pathway is the less understood non-canonical signalling. Non-canonical ligands, independence of Notch cleavage, or CLS-independent signalling are among those mechanisms, which may reflect interactions with other signalling pathways. The most well studied effect of non-canonical Notch is the negative regulation of Wnt/β-catenin signalling, as opposed to the synergetic interactions between the two pathways (reviewed in D'Souza, Meloty-Kapella and Weinmaster, 2010; Heitzler, 2010; Andersen *et al.*, 2012).

The modes of action of Notch signalling may be roughly divided into three main categories: lateral inhibition, binary cell fate decisions, and lateral induction (Fig. 6) (reviewed in Bray, 1998, 2006; Lai, 2004).

Lateral inhibition allows one cell from a homogenous progenitor population to adopt a cell fate and prevent their neighbours from undergoing the same specification (Fig. 6A). In this process, Notch signalling amplifies small or weak differences within a population of cells that initially express equal amounts of Notch ligands and receptors. A subtle change in Notch activity in one cell is amplified by inducing a negative feedback loop in the neighbouring cells, leading to clear signalling differences between them. The classic example is neuroblast differentiation, where stochastic variation in gene expression leads to high levels of proneural genes in the presumptive neuroblast cell,

upregulating Delta. High amounts of Delta will activate Notch in the neighbouring cells, where the production of Hes proteins will inhibit proneural gene expression, decreasing Delta. These cells become "receivers" and adopt an epidermal fate, whereas the presumptive neuroblast becomes a "sender" and later on, a neuroblast (Fig. 6A) (reviewed in Lai, 2004; Kageyama *et al.*, 2008).

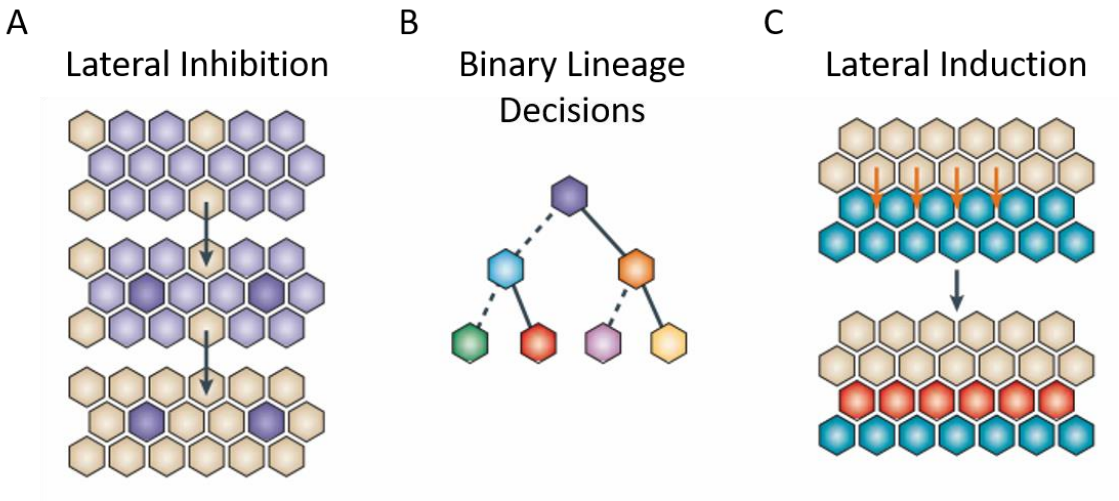

Figure 6. Notch signalling patterning mechanisms. Lateral inhibition (A). From a homogeneous group of cells (light purple), an imbalance in Notch signalling activity occurs. Through signalling feedback, this imbalance is amplified over time, leading to the generation of one cell in each group (dark purple) with high levels of Notch ligands (low Notch activity), and the surrounding cells to have an abundance of Notch receptors (high Notch activity), resulting in a different cell fate (yellow). Binary lineage decisions (B). A single precursor cells gives rise to two unique daughter cells. Notch signalling is activated in one daughter cell (solid line) but not in the other daughter cell (dashed line). The different colours represent various cell types that can be generated from a single cell. Lateral induction (C). Inductive signalling to establish boundaries between cell populations. One population of cells (yellow) signals to a neighbouring group of cells (green) and a new cell population (red) is created at the boundary. Notch signalling is elevated in these boundary cells, which become an organizing centre, coordinating growth in the adjacent populations. Adapted from Haines & Irvine, 2003.

Binary fate decisions are a result of asymmetric cell divisions (Fig. 6B). Distinct cell fates are determined by asymmetric distribution of Notch regulators, such as the cytoplasmic Notch inhibitor Numb, that promotes Notch degradation, into the two daughter cells. In neural development, frequently one daughter cell is maintained as a progenitor (elevated Notch activity) as the other adopts neuronal or glial fate (reduced Notch activity) (Fig. 6B) (reviewed in Knoblich, 2008).

Lateral induction, or inductive signalling, is the least described mechanism of Notch action. It promotes the development of a specific cell type or body region, often through the establishment of boundaries between developmental territories. In lateral induction, Notch signalling is activated in cells at the boundary between two populations of cells, which can establish an organizing centre that coordinates growth and patterning of the adjacent populations and/or separate them (Fig. 6C). A classic example is the *Drosophila* wing development, where Notch signalling is activated in a zone between the dorsal and ventral halves of the wing imaginal disc – called the wing margin. The dorsal half of the wing disc expresses *Notch*, *Delta*, *Serrate*, and *Fringe* (*Drosophila* has only one fringe protein), while the ventral domain expresses *Notch* and *Delta*. In *Drosophila*, Fringe increases the affinity of Notch receptor to Delta ligands, decreasing Notch affinity to Serrate/Jagged. Low levels of Notch signalling are thought to occur within the domains, probably due to cis-inhibition, with dorsal cells in a "sender" state with free Serrate to signal, and ventral "receiver" cells, with free Notch in their membranes. With Fringe being expressed on the dorsal side, Serrate is only able to activate Notch signalling in the adjacent ventral cells. This activation induces an increase in Delta ligands, making the cell switch from a "receiver" to a "sender" state, and activate Notch signalling in the adjacent dorsal cells (LeBon *et al.*, 2014). These interactions with positive feedback create a new population of cells with high levels of Notch signalling at the boundary, which will express specific factors for the regulation of wing development (Fig. 6C) (reviewed in Bray, 1998; Haines and Irvine, 2003; Lai, 2004). A different way by which Notch creates boundaries to determine cell fate is through oscillations. The best-known example comes from somitogenesis, which was found to be regulated by a molecular oscillator, the segmentation clock (Palmeirim *et al.*, 1997). Notch components, such as *Hes1*, *Hes7*, and Lunatic Fringe (*Lfng*) are among the "clock" genes expressed in a cyclic way to regulate the time-controlled somite formation. Notch signalling has been shown to be required for the expression of all "clock" genes, synchronization of the oscillations in neighbouring cells, and the regulation of the period of the segmentation clock (reviewed in Kageyama *et al.*, 2010; Carrieri and Dale, 2017; Liao and Oates, 2017).

To modulate Notch signalling, we developed pharmacological and genetic strategies. The pharmacological approach consisted of suppressing the pathway *in vitro* and *in vivo* using two pharmacological inhibitors of the γ-secretase complex, LY-411.575

and Dibenzazepine, known to inhibit the Notch pathway more potently than DAPT (Fig. 5) (Groth *et al.*, 2010; Rothenaigner *et al.*, 2011; Wolfe, 2012; Zheng *et al.*, 2013).

The genetic approach was developed using a combined system of *Tol2*-mediated gene transfer and tetracycline-dependent conditional expression, known to allow a stable and conditional genetic modulation in avian (Sato *et al.*, 2007; Watanabe *et al.*, 2007). This method has two versions, the Tet-On (Fig. 7A) and the Tet-Off (Fig. 7B) systems (Watanabe *et al.*, 2007). Both are composed by three vectors: pCAGGS-T2TP, a transposase that allows the stable integration of the two following plasmids; pT2K-BI-TREeGFP, a plasmid containing a cassette in which *GFP* and a gene of choice can be bidirectionally transcribed under the control of a tetracycline-responsive element (TRE); and pT2K-CAGGS-rtTA-M2 (Tet-On) or pT2K-CAGGS-tTA (Tet-Off), that constitutively express transcriptional activators that act on the TRE promotor. The reverse Tet-controlled transcriptional activator (rtTA) only binds to TRE (activating transcription of the TRE-driven gene) in the presence of doxycycline (an analogue of tetracycline; Dox) (Tet-On; Fig. 7A). Tet-controlled transcriptional activator (tTA) binds to TRE and activates transcription in a constitutive way in the absence of Dox, and Dox addition induces the release of tTA from TRE and the shutdown of TRE-driven gene transcription (Tet-Off; Fig. 7B). Thus, both systems allow stable integration of transgenes in the avian genome, which can be expressed in specific time-points of development, and cells expressing the transgene identified by *GFP* expression.

The forced expression of the intracellular domain of Notch1 (*ICN1*) was shown to promote constitutive activation of Notch signalling in a ligand-independent manner (Weinmaster, 1997). On the other hand, *in vitro* and *in vivo* studies have shown that the production of truncated MAML1 proteins consisting of only the N-terminal ICN-binding domain profoundly block Notch signalling, presumably due to their inability to recruit other components of the Notch transcriptional activation complex (Fryer *et al.*, 2002; Weng *et al.*, 2003; Maillard *et al.*, 2004). Thus, to genetically modulate Notch signalling in avian embryonic tissues we induced a constitutive expression of the dominant-negative (DN) form of MAML1 protein (*DNMAML1*) (loss-of-function) and of the *ICN1* (gain-of-function), through the Tet-Off system.

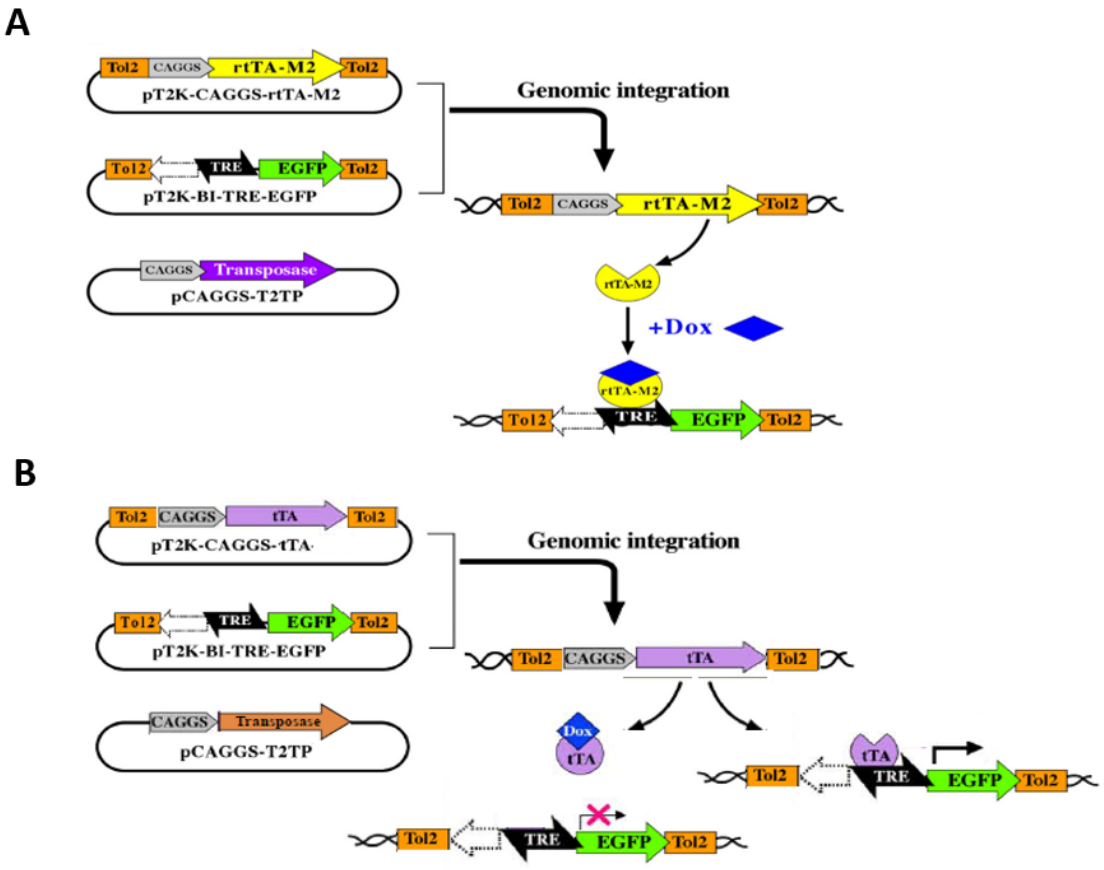

Figure 7. *Tol2*-mediated gene transfer system and tetracycline-dependent conditional expression combined system – Tet-On (A) and Tet-Off (B) Systems. Transient activity of transposase (pCAGGS-T2TP) will induce the transposon construct containing either TRE-eGFP (pT2K-BI-TREeGFP) or rtTA (pT2K-CAGGS-rtTA-M2) (A) or tTA (pT2K-CAGGS-tTA) (B) to be integrated into the host genome. Upon integration, the Tet-On system (A) activates the transcription of TRE-driven genes only in the presence of Dox, while the Tet-Off system (B) constitutively activates TRE-driven genes transcription (in the absence of Dox), which is inactivated by the addition of Dox. Adapted from Sato *et al.*, 2007 and Watanabe *et al.*, 2007.

I.6.2 Hedgehog signalling

Vertebrates have three Hh gene homologs: *Shh*, Indian hedgehog (*Ihh*), and Desert hedgehog (*Dhh*). Shh is the most potent of the Hh ligands and the most broadly expressed in mammals. Hh signalling proteins undergo several post-translational modifications in their path to the cell membrane before gaining full activity. Evidence from several studies support the release of unlipidated and lipidated active forms of Hh that may result in different signalling ranges. Dispatched (Disp), a transmembrane transporter protein, has been implicated in the secretion of Hh, but also in Hh endocytosis by secreting cells,

facilitating the packaging of Hh into exosomes that are associated with long-range signalling activity (reviewed in Varjosalo and Taipale, 2008; Lee, Zhao and Ingham, 2016). In vertebrates, primary cilia (microtubule-based organelles) were found to serve as signalling hubs for the Hh pathway, as the transport machinery within the cilium is essential for Hh signal transduction (Fig. 8) (Huangfu *et al.*, 2003).

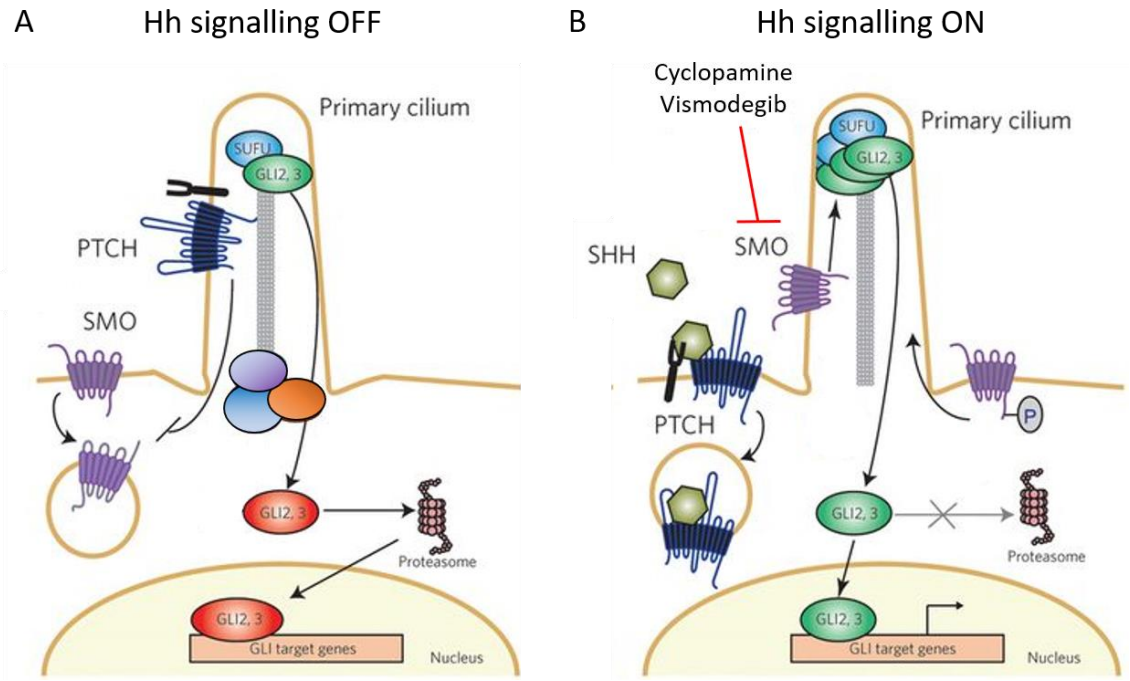

Figure 8. Hedgehog signalling pathway in vertebrates. Vertebrate Hedgehog signalling occurs in a cellular projection known as the primary cilium. Hedgehog signalling in the absence of ligand (A). Ptch is localized to the cilium and suppresses the activity of Smo, preventing its accumulation in the cilium through an undetermined mechanism. Sufu inhibits the transcription factors Gli2 and Gli3 through a direct interaction and leads to the generation of their repressor forms (GLI2,3R) by the proteasome. Hedgehog signalling in the presence of ligand (B). Hedgehog ligands bind to Ptch and promote its downregulation and removal from the cilium. Smo accumulates in the primary cilium, where it is activated and can signal to downstream components. This results in the translocation of Sufu–Gli complexes to ciliary tips. Dissociation of these complexes results in translocation of active Gli2 and Gli3 into the nucleus, promoting Hedgehog target gene transcription. Pharmacologic inhibitors of Hedgehog signalling, such as Cyclopamine and Vismodegib, bind to Smo, suppressing its activity. Adapted from Sharpe *et al.*, 2015.

Vertebrates also have a *Ptch1* homologue – *Ptch2* – which is now starting to be more characterized. Although it was shown to be dispensable for embryogenesis (distinct from Ptch1), recent studies found that it co-operates with Ptch1 and plays a compensatory

role in signal transduction (Alfaro *et al.*, 2014; Zhulyn *et al.*, 2015). In the absence of Hh, Ptch1 is localized in the cilium, where it inhibits the activity and accumulation of Smo, another transmembrane protein (Fig. 8A). Hh binding leads to the dissipation of Ptch1 and the relief of Smo inhibition, allowing Smo to move into the primary cilium and transduce the Hh signal to the nucleus (Fig. 8A). This process is regulated by numerous cytoplasmic proteins that interact with each other in complex ways. Hh signal transmission is dependent on changes in the balance between activator and repressor forms of the Gli transcription factors. Suppressor of fused (Sufu) is one of the regulators of Gli proteins, being involved in their production, trafficking, and function. Upon Hh binding, Gli factors are transported, attached to Sufu, to the tip of the primary cilium, where the Gli-Sufu complex is dissociated, allowing Gli proteins to exert their actions (Fig. 8B) (reviewed in Hooper and Scott, 2005; Lee, Zhao and Ingham, 2016).

Gli proteins are the terminal effectors of Hh signalling, and vertebrates possess three of them (Gli1-3). *Gli1* is itself a direct Hh-target gene and works as a transcriptional activator. Although it was shown that Gli2 and Gli3 can be processed to function as transcriptional activators or repressors, Gli2 acts mainly as an activator, an Gli3 as a repressor (Ruiz i Altaba, 1997). Like *Gli1*, *Ptch1/2* and Hh interacting protein (*Hhip*) – an antagonist receptor with high affinity to the three Hh ligands, preventing their interaction with Ptch1 and inhibiting Hh signalling – are also direct targets of Hh signalling. *Gli1* is part of a positive feedback loop, while *Ptch1/2* and *Hhip* are part of a negative regulatory feedback loop (Rahnama *et al.*, 2006). Since the expression of *Gli1* and *Ptch1* is highly dependent on active Hh signalling, their transcription is often used as a readout of pathway activation (Hooper and Scott, 2005). The different cellular responses to these morphogenic Hh proteins depend on the type of receiving cell, the Hh dose and the time of exposure (reviewed in Varjosalo and Taipale, 2008). In addition, several studies have suggested that Hh proteins can also exert their effects independently of Gli factors. These so called "non-canonical" pathways include a Smo-dependent and transcription-independent type, and a Ptch1-regulated pathway that is independent of Smo (reviewed in Brennan *et al.*, 2012; Lee, Zhao and Ingham, 2016).

To analyse the effects of Hh inhibition in the early stages of T/PT development *in vitro* and *in vivo*, we used two pharmacological inhibitors of Smo, Cyclopamine and Vismodegib, which target and suppress Smo activity (Chen *et al.*, 2002; Singh *et al.*, 2011; Lin and Matsui, 2012).

I.7 Avian embryos as a model system

The chicken embryo has been a classic model in developmental biology since the time of comparative and experimental embryology. In the last 50 years, the chicken embryo has contributed to some of the most important general concepts in vertebrate developmental biology. Several features of the avian embryos make them a powerful model to study developmental biology. Among them are the availability and low cost of fertilized eggs that can be incubated to specific, well characterized, stages of development; the ease of tissue accessibility from pre-gastrulation throughout all developmental stages; the fact that the avian model is the one that most resembles other higher vertebrates while still permitting experimental intervention *in ovo*; and the fact that chicken share more than a half of its genes with human (Bourikas and Stoeckli, 2003; Stern, 2004, 2005; Bronner-Fraser, 2008).

The quail-chick chimera system, developed by Le Douarin in the 1970s, combines the power of stable and specific genetic labelling of cell populations (taking advantage of their difference in heterochromatin structure) with the ease of access/manipulation presented by the avian embryo (Le Douarin, 1973). The use of quail-chick chimeras allowed the selective labelling of define groups of cells and the analysis of their pathways of migration, along with the identification of their interactions during morphogenesis and organogenesis. As a result, it significantly contributed to some of the most important findings in developmental biology's, concerning fate mapping, patterning, cell lineage, and differentiation (Dieterlen-Lièvre and Le Douarin, 2004; Le Douarin and Dieterlen-Lièvre, 2013).

In the past 20 years, the *in ovo* electroporation technique in the chicken model was developed and optimized in order to facilitate loss- and gain-of-function experiments, allowing the definition of gene function during early embryonic development (Nakamura *et al.*, 2004; Nakamura and Funahashi, 2013). In addition, the possibility to combine those experiments with the chimeric technique, offering more precision in the analysis of the developmental events under study, reinforced the usefulness of the quail/chick model (Creuzet *et al.*, 2002).

I.8 Aim and outline of this thesis

While numerous studies have identified specific genes and pathways involved in thymus and parathyroids early stages of development, the contribution of Notch signalling – a pathway known to be involved in cell fate decisions and boundary formation – is still unclear. In addition, the molecular interactions between major signalling pathways in the regulation of these events remain poorly understood. Notch signalling related-genes are expressed in T/PT presumptive domains and surrounding tissues at early stages of development, and Notch and Hedgehog pathways have been shown to interact in several biological contexts. This work aims to unravel the role of Notch signalling in T/PT common primordium development, and its possible interaction with Hedgehog in this context.

In **Chapter II** the experimental procedures used during these studies are described.

Chapter III describes in detail the methodology of our two step-approach to study early and late stages of organogenesis in the avian model.

In **Chapter IV** we provide the very first evidence of a role of Notch signalling in thymus and parathyroid glands early development. Using *in vitro*, *in vivo*, and *in ovo* approaches to modulate Notch and Hedgehog pathways with pharmacological agents, we show that Notch is crucial for T/PT common primordium development and for parathyroid formation, in a Hedgehog-dependent manner.

Chapter V describes in detail the methodology of the isolation of embryonic tissues, such as the 3/4PP pharyngeal endoderm and somatopleural mesenchyme, that can be combined to form *ex vivo* chimeric organs and study tissue-specific contributions during early and late stages of organ formation in the avian model.

In **Chapter VI** the genetic approach developed to clarify the tissue-specific role of Notch signalling during early development of the thymus and parathyroids is presented. Notch signals were aimed to be specifically modulated in the 3/4PP endoderm by combining the *Tol2* transposon and tetracycline-dependent conditional expression systems with the quail-chick chimera model. The loss- and gain-of-function studies were inconclusive, which limited the analysis of tissue-specific roles of Notch signalling in T/PT development.

Finally, **Chapter VII** provides a general discussion of the results obtained in the previous chapters. Moreover, suggestions of future experiments to further investigate the role of Notch activity in this context and clarify its interaction with Hedgehog (and others) are also presented.

CHAPTER II

Materials and Methods

CHAPTER II - MATERIALS AND METHODS

II.1 Molecular biology procedures

II.1.1 Preparation of chemically competent *E. coli* bacteria

The DH5α strain of *E. coli* was used for all transformations performed in this study. Before transformation, these cells need to become competent to take up exogenous DNA and stably maintain it. For that, non-competent bacterial cells from frozen glycerol stock were streak out onto LB plates, grown overnight at 37ºC. Single colonies were selected for the starter culture with 3mL of fresh LB without antibiotics and grown o.n. in a 37°C shaker (225rpm). The next day 2mL from the starter culture were diluted into 200mL of fresh LB without antibiotics and incubated in a 37ºC shaker (225rpm) for 3h (until it reaches optical density at 600nm (OD600) of 0.4–0.6). From that point on, all steps were performed on ice, refrigerated centrifuges, and using cold solutions. The cells were harvested through centrifugation at 4000rpm for 5min at 4ºC and the supernatant discarded. After adding half of the initial bacterial volume of cold MgCl2 0.1M, cells were centrifuged again, and the supernatant removed. Half of the initial bacterial volume of cold CaCl2 0.1M was then added and incubated on ice for 30min. The cells were harvested again, the supernatant discarded, and the pellet was carefully resuspended in CaCl2 0.1M/15% Glycerol to 1/15 of the original/initial volume. The final volume suspension was distributed in aliquots of 500µL into 1.5mL sterile cryotubes and stored at -80ºC.

II.1.2 Transformation of chemically competent *E. coli* bacteria

Frozen aliquots of 100-200µL of competent bacteria (DH5α) were thawed on ice and incubated with 100-500ng of circular plasmid DNA for 20min on ice. This mix was then exposed to a heat shock at 42ºC for 2min followed by cooling on ice for 10min. Next, 1mL of LB medium was added to the mix, and incubated in a 37°C shaker (225rpm) for 45min. Bacteria were plated (20-300µL) on solid LB Agar medium containing ampicillin (100µg/mL) (Sigma) and incubated o.n. at 37ºC to select the transformed bacteria.

II.1.3 Plasmid DNA purification and cell banks

Single colonies of transformed DH5α were collected and inoculated to 5mL of LB medium supplemented with 5µL of ampicillin (100µg/mL) in a 50mL falcon. For small scale preparation of plasmid DNA, cells were grown overnight in a 37ºC shaker (225rpm) and the purification of plasmid DNA was carried out using QIAprep®Spin Miniprep Kit (QIAGEN) according to the manufacturer's instruction. For large scale preparation of plasmid DNA, cells were incubated for 7-8h (37ºC, 225rpm). Then, 1mL of this pre-culture was added to 50 or 100mL (high- or low-copy plasmids, respectively) of LB medium supplemented with ampicillin (100µg/mL) in a 250 or 500mL Erlenmeyer flask, respectively. Cultures were grown overnight at 37ºC at 225rpm. The plasmid DNA purification was performed using QIAfilter Plasmid Midi Kit (QIAGEN) according to the recommended protocol. DNA purification of digested plasmids/fragments during the generation of new plasmids was carried out using QIAquick PCR Purification Kit (QIAGEN), according to the manufacturer's instructions. DNA concentration and purity were determined using NanoDrop® ND-1000 Spectrophotometer (Thermo Scientific) and samples were stored at -20ºC.

For each new plasmid, a working cell bank was performed by adding 150µL of the pre-culture to 850µL of glycerol 100% in a sterile 2mL eppendorf and storing at -80ºC.

II.1.4 DNA and RNA quantification

The concentration and purity of nuclear acids was determined by spectrophotometry using the NanoDrop® ND-1000 Spectrophotometer (Thermo Scientific). One A_{260} unit corresponds to 50µg/ml of double-stranded DNA and to 40µg/ml of single-stranded RNA. Samples purity was evaluated based on A_{260}/A_{280} ratio (pure preparations of DNA and RNA, i.e., without significant amounts of proteins or phenol contaminants, show ratio values of 1.8 and 2.0, respectively).

II.1.5 Restriction digestions

Enzymatic restriction of DNA was performed for approximately 1h30-3h at 37ºC using 5-10U of commercially available restriction enzymes and respective buffers (Promega, New England Biolabs). The volume of enzyme used in each reaction never exceeded 10% of the total reaction volume.

II.1.6 Polymerase Chain Reaction (PCR)

To produce inserts for cloning in several DNA vectors, PCR primers were designed for the specific target sequences. PCR reactions were performed with 10ng of the template DNA in 25µL PCR reaction using PhusionTM Master Mix with HF Buffer (Finnzymes) and 0.5µM final concentration of primers, according to manufacturer's instructions. The cycling conditions were: 1 cycle of initial denaturation at 98ºC for 30sec; 30 cycles of denaturation at 98ºC for 10sec, annealing at 65ºC for 30sec, and extension at 72ºC for 15sec/Kb (761bp product for mCherrryNLS); a final extension cycle at 72ºC for 10min. The annealing temperature was adjusted for each primer and template set. All PCR reactions were performed in a MyCyclerTM Thermal Cycler (Bio-Rad).

II.1.7 TOPO II PCR cloning

PCR products were cloned in pCR®II-TOPO® vector using TOPO TA Cloning® Kit (Invitrogen) according to the manufacturer's instructions. To add single 3' adenine overhangs to the PCR products, PCR products were previously incubated at 72ºC for 10min with 0.25µL of Go-Taq Polymerase (5U/µL, Promega). TOPO® Cloning reactions were transformed into One Shot® MAX Efficiency® DH5α-T1R Chemically competent *E. coli* cells (Invitrogen) according to the manufacturer's instructions.

II.1.8 Dephosphorylation

Before ligation of the inserts to the vector backbone, the vector was dephosphorylated to prevent auto-ligation, by adding 1X Calf Intestinal Phosphatase (Promega), 1X of the appropriate buffer, and incubated for 3h at 37ºC.

II.1.9 Generation of blunt ends with Klenow

To fill-in 5' overhangs produced after restriction digestions the DNA Polymerase I, Large (Klenow) Fragment was used. 1µg of purified insert was incubated with 50µM dNTPs (Invitrogen), 5U Klenow (NEB), and the appropriate buffer, in a final reaction volume of 30µL, for 30min at room temperature (RT). Then, enzyme inactivation was performed at 75ºC for 10min.

II.1.10 DNA ligation

Ligations were performed overnight at room temperature (RT), using 1µL of T4 DNA Ligase (NEB 400U/µL) and the correspondent ligation buffer in a final volume of 20µL. The correlation between backbone vector and the insert to be cloned was: ng of insert = ((ng of vector x Kb size of insert)/Kb size of vector) x 10. Half the ligation volume was then used to transform DH5α cells as described above.

II.1.11 Analysis and isolation of DNA/RNA by agarose gel electrophoresis

Analysis of RNA and DNA integrity, purification of specific DNA fragments and confirmation of PCR amplification products as well as digestion results were performed using agarose gel electrophoresis. UltraPureTM Agarose (Invitrogen) was dissolved by heating in 1X TAE buffer (40mM Tris, 1mM EDTA, 0.35% glacial acetic acid) to a final concentration of 0.8-1.5% (according to the required resolution for DNA size: 0.8% (w/v) for fragments sizes of 1Kb-10Kb and 1.5% (w/v) for fragments sizes < 0.5Kb). GelRedTM Nucleic Acid Gel Stain, 10,000X in DMSO (Biotium) was used as intercalating agent and added to the gel at 1:10,000. Samples were mixed with 6X Loading Dye Solution (Fermentas) in 6:1 proportion, loaded into the gel. The size of the fragments was estimated by comparison with DNA ladders (FastRuler™ Low Range DNA Ladder, FastRuler™ Middle Range DNA Ladder or O'GeneRuler™ 1kb DNA Ladder – Fermentas) ran along with DNA samples. Electrophoresis was run in 1X TAE at 5-10V/cm of gel length, results were seen on a UV transilluminator and images were acquired with ChemiDocTM XRS+ (Bio-Rad) and Image Lab 4.1 software. When DNA was extracted from the gels, the region of the gel containing the DNA fragment of interest

was excised under ultraviolet light at 365nm and purified using QIAquick Gel Extraction Kit (QIAGEN), according to the manufacturer's instructions.

II.1.12 DNA constructs

II.1.12.1 DNA constructs already available

pCAGGS-STOP-IRES-GFP – kindly provided by Domingos Henrique, this vector contains a combination of a CMV enhancer and the chick β-actin promoter, and an additional internal ribosomal entry site (IRES) followed by a nuclear enhanced green fluorescent protein (EGFP) downstream of the polylinker, which are then followed by a stop codon in each frame, allowing coupled expression of the proteins of interest with EGFP.

pCAG-CherryNLS – kindly provided by Filipe Vilas-Boas, this pCAGGs vector contains a *mCherry* sequence fused to a nuclear localization signal (*Cherry-NLS*) (Vilas-Boas *et al.*, 2011).

pT2K-DNMAML1eGFP – previously generated and used in our laboratory in preliminary studies (Figueiredo, 2011), this pT2K-BI-TREeGFP vector contains the DNMAML1 sequence (205bp).

pT2K-ICN1eGFP – previously generated and used in our laboratory in preliminary studies (Figueiredo, 2011), this pT2K-BI-TREeGFP vector contains the ICN1 sequence (2417 bp).

pT2K-BI-TREeGFP – from the combined system of *Tol2*-mediated gene transfer and tetracycline-dependent conditional expression, kindly provided by Yoshiko Takahashi (Sato *et al.*, 2007).

pT2K-CAGGS-tTA – from the combined system of *Tol2*-mediated gene transfer and tetracycline-dependent conditional expression, kindly provided by Yoshiko Takahashi (Sato *et al.*, 2007).

II.1.12.2 New DNA constructs generated for Notch modulation studies

Two new DNA constructs were generated through the insertion of a fused sequence of DNMAML1 and CherryNLS into two different plasmids: pT2K-BI-TREeGFP and pCAGGS-STOP-IRES-GFP. Both plasmids were generated to induce a Notch signalling loss-of-function through electroporation. Each new plasmid was verified by 3 independent restriction digestions and analysis on agarose gel electrophoresis.

pT2K-NLS-Cherry-DNMAML1eGFP (in collaboration with Joana Silva)

A MAML1 peptide containing only the N-terminal ICN-binding domain of MAML1 (13-74aa) has been shown to have potent dominant negative effects in Notch signalling (Weng *et al.*, 2003; Maillard *et al.*, 2004). mCherry is a red fluorophore with high photostability and rare fluorescence-intensity fluctuations (Seefeldt *et al.*, 2008) and its fused version with a nuclear localization signal was used as a tag for DNMAML1 in this work. mCherry-nuclear localization signal (*CherryNLS*) was cloned in fusion with DNMAML1 sequence in pT2K-DNMAML1eGFP, generating pT2K-NLS-Cherry-DNMAML1eGFP plasmid. *CherryNLS* (761bp) was amplified from the pCAG-CherryNLS plasmid (Vilas-Boas *et al.*, 2011) by PCR using modified primers to introduce an EcoRV restriction site (capital and bold letters) and allow direct cloning in fusion with DNMAML1 sequence. The final primers used were: forward 5'**GATATC**atggtgagcaagggcgaggag 3' and reverse 5'**GATATC**tgtacaatcaggggtcttctacc 3'. The PCR product was cloned into a pCR®II-TOPO® vector. Next, both TOPO-CherryNLS and pT2K-DNMAML1eGFP were digested with EcoRV. The extracted and purified CherryNLS fragment from TOPO-CherryNLS was ligated with the dephosphorylated and purified pT2K-DNMAML1eGFP.

pCAGGS-NLS-Cherry-DNMAML1-GFP

NLS-Cherry-DNMAML1 fragment (966pb) was extracted from pT2K-NLS-Cherry-DNMAML1eGFP with NheI/XbaI, and the overhangs were blunted with Klenow. The pCAGGS-STOP-IRES-GFP plasmid was digested with EcoRV, dephosphorylated, and ligated with the previously prepared NLS-Cherry-DNMAML1 fragment.

II.1.13 RNA isolation and reverse transcription (in collaboration with Joana Silva)

All steps of RNA extraction and cDNA synthesis were performed in a laminar flow hood to avoid contamination. Concentration and purity of both the RNA and cDNA samples were determined using the NanoDrop® ND-1000 Spectrophotometer (Thermo Scientific).

II.1.13.1 RNA isolation from samples for qRT-PCR calibration curves

Quail E9 embryos were dissected and thymi and parathyroid glands were separately isolated. Chicken E18 embryos were as well dissected to isolate thyroid glands. An OP9 cell line carrying a plasmid to express GFP (OP9-GFP; Schmitt, 2002) was also subjected to RNA isolation. Total RNA from chicken or quail organs (thymus, parathyroid and thyroid) and OP9-GFP cell line was extracted using High Pure RNA Isolation Kit (Roche), according to the manufacturer's instructions. Samples were DNase digested for 40min and RNA was eluted in 50µL of Elution Buffer.

II.1.13.2 RNA isolation from organotypic assays

Total RNA from the samples was extracted using a combination of TRIzol reagent (Invitrogen) and RNeasy Mini Kit (QIAGEN) manufacturer's instructions. RNA samples were obtained from freshly isolated 3/4PAR from qE3 (3/4PAR-0h) and from 3/4PAR grown *in vitro* for 48h (3/4PAR-48h). Triplicates of 7 explants/ sample were analysed for each culture condition (0h and 48h). To each sample, 1mL of Trizol was added and they were then maintained at -80ºC until RNA extraction. After thawing at RT, 200µL of chloroform were added. Tubes were vigorously shaken for 15sec, allowed to stand 10min at RT and centrifuged at 13000rpm for 15min at RT. Aqueous (colourless) phase, avoiding organic phase, was withdrawn to a clean eppendorf and ethanol precipitation of RNA was performed as described on the RNeasy Mini Kit protocol. DNase digestion was carried out for 15min and RNA was eluted in 50µL of RNase-free water. All RNA samples were stored at -80ºC.

II.1.13.3 Reverse transcription

First-strand cDNA synthesis was performed in a total volume of 20µL, by reverse transcription of 1µg of total RNA using the SuperScriptTM III Reverse Transcriptase kit and Oligo (dT)12-18 Primer (Invitrogen), according to the manufacturer's instructions. Synthesized cDNAs were stored at -20ºC.

II.1.14 Quantitative Real-Time PCR (qRT-PCR) (in collaboration with Joana Silva)

Specie-, organ- and construct-specific primers were designed and tested, and qRT-PCR assays were optimized. Primers were designed either by using Primer3 software or manually (list in Table 1). DNMAML, ICN1, and GFP primer pairs were designed to be intron-spanning (to exclude amplification of genomic DNA) and near 3'poly-A. qRT-PCR assays were run in a ViiA7TM Fast Real-Time PCR System (Applied Biosystems) in MicroAmp® Optical 384-Well Reaction Plate (Applied Biosystems). Plate preparation was performed in a laminar flow hood to avoid contamination, and reactions were performed in 10µL final volume using 5µL of Power SYBR® Green PCR Master Mix (Applied Biosystems), 0.4µM final concentration of primers and 1mL (up to 1mg) of cDNA. Thermocycling conditions were composed by an initial denaturation at 50°C for 20sec and 95°C for 10min, followed by 40 cycles at 95°C for 15sec and at 60°C for 1min. To control primers specificity, at the end of each experiment a melting curve was generated. Relative quantification of gene expression was determined by the ΔΔCt method (Livak and Schmittgen, 2001) using beta-actin (*Actb*) and hypoxanthine-guanine phosphoribosyltransferase (*Hprt*) as endogenous genes. Three biological replicates were always used for each condition.

Table 1. List of primers used in qRT-PCR assays.

Primer	Forward primer (5'-3')	Reverse primer (5'-3')	Product size (bp)
Actb	TGGCACCTAGCACAATGAAA	GCCAGGATAGAGCCTCCAAT	82
Hprt	ACGCCCTCGACTACAATGAA	CAACTGTGCTTTCATGCTTTG	98
Foxn1	CGACATCGATGCTCTGAATC	AGGCTGTCATCCTTCAGCTC	81
Gcm2	TCAGAATTCCCAGAAAAAGAGA	GAGGGCAGATTTTGCATGTT	93
Pth	CTGATGGAAGACCAATGATGAA	AAGCCAGTCCTGTCTCTCCA	98
Gata3	CTGTAATGCCTGTGGGCTCT	CATTTTTCGGTTTCTGGTCTG	94
Pax1	GGGAAGTCACGGACAGAAAA	GGATCGAGAGTCCGTGGAT	81
Fgf8	GCATGAACAAGAAGGGGAAA	AGCGCCGTGTAGTTGTTCTC	97
Hey1	ACCGTGGATCACCTGAAGAT	CGGTAGTCCATAGCCAAAGC	80
Hes5.1	CCGACATCCTGGAGATGACT	AGGCATACCCTTCGCAGTAA	99
Hes6.1	GGAGGTGCTGGAGCTGAC	GCATGCACTGGATGTAGCC	122
Patched1	GGAAGCCACTGAGAATCCTG	TGCAATCTGGGACTTGACTG	81
Shh	CGGCTTCGACTGGGTCTACT	ATTTCGCTGCCACTGAGTTT	80
Gli1	AAGGATGACGGCAAGCTG	GTCACTGCTGCACGATGACT	86
Gli3	TGGAATGCTTCCAAGACTGA	CTGCAGCTGCTGTTTGATTG	96
DNMAML1	CTGGAGCGCCAGCAAACCTT	TCATCAGTGCTTGCCGGCCC	78
ICN1	TAGTCAGCTGACGCGTGCTA	TTGCTCGACTCCGTCACTTTG	106
GFP	CGACAACCACTACCTGAGCA	GAACTCCAGCAGGACCATGT	82

II.1.15 Anti-sense RNA probe synthesis

In this work, several RNA antisense probes were used for *in situ* hybridization of chicken and quail tissues/embryos. Digoxigenin (DIG) RNA anti-sense probes were synthesized by T3, T7 or Sp6 polymerase, from plasmid templates containing the cDNAs of several genes (Table 2), according to the following steps.

II.1.16 DNA template preparation

Plasmid templates were linearized with the appropriate restriction enzyme (see Table 2). The digestion reaction was performed in a total volume of 150µL containing 20µg of DNA, 15µL of 10X enzyme buffer, 5µL of restriction enzyme (6U-20U/µL) and RNase-free water. After digestion, linearized plasmid DNA was subjected to a phenol-chloroform extraction and ethanol precipitation. In short 150µL of phenol: chloroform 1:1 (v/v) (Ambion) were added per sample and the lower phase (chloroform) removed by pipetting with thin tips. After centrifuging at 11000rpm for 5min at 4ºC, the lower phase was removed again. 150µL of chloroform were added per sample, centrifuged at 11000rpm for 10 min at 4ºC and then the lower phase removed. To precipitate DNA 15µL

of sodium acetate (NaAC) 3M and 450µL of absolute ethanol were added per sample and incubated at -80ºC for 30min. The mix was centrifuged at 13000rpm for 30min at 4ºC, the supernatant was removed and the pellet dried and resuspended in 10µL of RNase-free water.

Table 2. Linearization site and RNA Polymerase for each probe used.

Probe	Linearization site	RNA polymerase	References
Delta1	EcoRV	T3	(Henrique *et al.*, 1995)
Fgf8	EcoRI	T7	(Crossley and Martin, 1995)
Foxn1	NotI	SP6	(Neves *et al.*, 2012)
Gata3	SpeI	T7	(Lilleväli *et al.*, 2007), kindly provided by Domingos Henrique
Gcm2	NotI	SP6	(Neves *et al.*, 2012)
Gli1	HindIII	T3	(Valeria Marigo *et al.*, 1996)
Gli3	EcoRV	T3	(Valeria Marigo *et al.*, 1996)
Hey1	EcoRI	T3	(Leimeister *et al.*, 2000), kindly provided by Isabel Palmeirim
Hes5.1	NotI	T3	(Fior and Henrique, 2005)
Jagged1	HindIII	T7	(Myat *et al.*, 1996)
Lfng	StuI	T3	(Aulehla and Johnson, 1999)
Notch1	HindIII	T3	(Myat *et al.*, 1996)
Shh	HindIII	T3	(Riddle *et al.*, 1993)
Patched1	SalI	T3	(V Marigo *et al.*, 1996)
Pax1	XbaI	T3	(Wallin *et al.*, 1996)

II.1.17 Probe synthesis

The synthesis of antisense DIG-labelled RNA probes was carried out by *in vitro* transcription using standard procedures. The reaction contained 8µL of Transcription Optimized 5X Buffer (Promega), 4µL of 0.1M DTT (Promega), 2µL of each rGTP, rATP, rCTP (10mM) (Roche), 1,3µL of rUTP (10mM) (Roche), 0,7µL of Digoxigenin-11-UTP (10mM) (Roche), 2µL of RNasin® Ribonuclease Inhibitor (Promega), 2µL of the appropriate RNA polymerase (see Table 2) and 14µL of RNAse free water. Then 2µL (2µg) of the linearized templates were added, and the mix incubated at 37ºC for 2h.

Samples were treated with 6µL of DNase I recombinant RNase-free (10U/µL) (Roche) at 37°C for 15min. Purification of the probe was performed using illustra MicroSpin G-50 Columns (GE Healthcare) according to manufacturer's instructions. Probe quality and success of transcription reaction were analysed by agarose gel electrophoresis (see Section II.1.11).

II.2 Developmental biology procedures

II.2.1 Embryo manipulation

Fertilised Japanese quail (*Coturnix coturnix japonica*) and chicken (*Gallus gallus*) eggs were stored at 16ºC and incubated at 38ºC in a humidified incubator to initiate development. Embryos were staged according to the Hamburger and Hamilton (HH) development table (Hamburger and Hamilton, 1951) in the chicken, and to corresponding HH-stages in the quail. At specific stages of development, embryos were either directly dissected from the eggs, or after *in vivo* manipulated through electroporation, bead implantation, drug injection, or to serve as a recipient of grafted explants growth. Dissected embryos had their extra-embryonic membranes removed on 2% agar-coated petri dishes containing phosphate buffer solution (PBS), and were further processed differently depending on the subsequently used method: isolation of RNA, whole mount *in situ* hybridization or organotypic *in vitro* culture.

II.2.1.1 Dissection of embryonic pharyngeal regions

The third and fourth pharyngeal arches region (3/4PAR) was dissected from quail embryos at E3 (HH21) on PBS (3/4PAR-0h) and kept on ice until used for RNA extraction (see Section II.1.13.1) and qRT-PCR (see Section II.1.14) or developed *in vitro* in organotypic cultures (see Section II.2.2.2). The 3/4PAR included the 3/4PP and foregut endoderm and the ventral mesenchymal- and ectodermal-neighbouring cells. The dorsal structures like notochord, somites, and neural tube were removed (Fig. 1A–F).

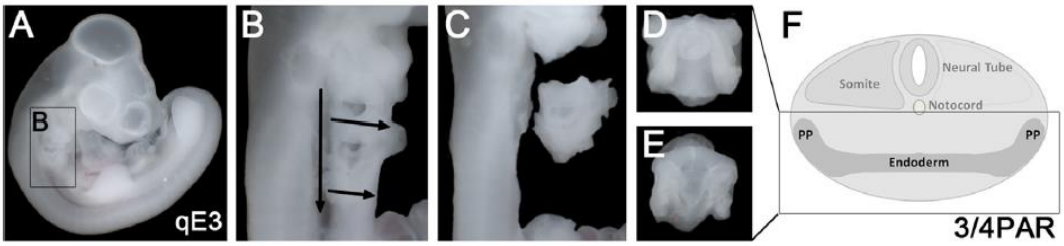

Figure 1. Isolation of the 3/4PAR. Sequential mechanical isolation steps of the 3/4PAR (A-C). Ventral (D) and Dorsal (E) views of the isolated 3/4PAR. Schematic representations of the transversal section of the embryo at the region of interest (F) and of the experimental design (G). PAR, pharyngeal arch region.

II.2.1.2 Isolation of quail and chicken embryonic tissues

The 3/4PAR was dissected from qE3 embryos (as described in the previous section) and treated with a solution of pancreatin (25g/L, Sigma) for 60-90min on ice to allow further enzymatic and mechanical separation of the endoderm from both the pharyngeal mesenchyme and ectoderm. The posterior region of E2.5 chick embryos (HH17) at the level of somites 19 to 24 was dissected, and treated with pancreatin solution (25g/L, Sigma) for 10-20min on ice to allow the dissociation of somatopleural mesenchyme from endodermal and ectodermal tissues. The procedures of tissue isolation are further detailed in Chapter V. Isolated pharyngeal endoderm was further electroporated (see next Section) and combined with isolated somatopleural mesenchyme in heterospecific organotypic cultures (see Section II.2.2.1). Chicken pharyngeal endoderm was isolated at E3.5 and E4.5 (HH24-25) similarly to qE3, and *in situ* hybridized with *Shh* probe as previously described (Neves *et al*., 2012).

II.2.1.3 Electroporation of isolated pharyngeal endoderm

Isolated quail 3/4PP endoderm was genetically modified by electroporation using the The Gene Pulser Xcell™ system (BIO-RAD). Isolated endoderms were transferred to a Gene Pulser® Electroporation Cuvette (BIO-RAD, 0.4cm electrode gap) and mixed gently, ensuring no air bubbles were introduced. Cells were electroporated at 250V, 500µF in PBS, with distinct combinations of the Tet-Off system of vectors (detailed in Chapter I Figure 6B) and Notch constructs; 15µg of pT2K-CAGGS-tTA (transactivator) and 30µg of either pT2K-BI-TREeGFP (vector control condition), pT2K-DNMAML1eGFP (1st loss-of-function condition), pT2K-NLS-Cherry-

DNMAML1eGFP (2nd loss-of-function condition), or pT2K-ICN1eGFP (gain-of-function condition). These experiments were performed without the transposase plasmid, using the transient effect of the vectors, due to the short period of culture. In addition, two other experimental conditions were performed, using 15µg of the transient pCAAGS-NLS-Cherry-DNMAML1-IRES-STOP-eGFP (3rd loss-of-function condition), or 15µg of pCAGGS-eGFP as a control condition. After electroporation, the endodermal tissues were kept in 100% FBS (Invitrogen) for 5-10min, on ice, and further used to generate heterospecific cultures (see Section II.2.2.1).

II.2.2 *In vitro* organotypic assays

II.2.2.1 Heterospecific cultures

For each electroporation condition, 4-5 isolated and electroporated endoderms were associated with 4-5 isolated mesenchymes on Nucleopore membrane filters (Millipore) supported by fine meshed metal grids (Goodfellows), placed in culture dishes and in contact with culture medium – RPMI-1640 Medium (Sigma) supplemented with 10% Fetal Bovine Serum (FBS) (Invitrogen), 1x Pen/Strep (Invitrogen) – for 48h in a humidified incubator at 37ºC with 5% CO_2. The procedures of tissue isolation are further detailed in Chapter V. After 48h, cultured tissues were washed in PBS, RNA extracted (see Section II.1.13.1) and qRT-PCR analysed (see Section II.1.14).

II.2.2.2 Embryonic 3/4PAR cultures

Dissected 3/4PAR were placed on a 24mm Transwells with 0.4mm Pore Polycarbonate Membrane Insert (Corning Product #3412). Seven regions per well were placed with the ventral side up and the dorsal side in contact with the membrane (Fig. 2G). The tissues were grown partially immersed in culture medium – RPMI-1640 Medium (Sigma) supplemented with 10% FBS (Invitrogen), 1x Pen/Strep (Invitrogen) – in a humidified incubator at 37°C with 5% CO2, for 48h (3/4PAR-48h). This procedure is further detailed in Chapter III. To inhibit Notch signalling, culture medium was supplemented with LY-411.575 (Ly, Stemgent - Stemolecule™) at 50nM (Ly-50), 100nM (Ly-100), or 200nM (Ly-200), or with Dibenzazepine (DBZ, Selleckchem) at 5µM (DBZ-5), 10µM (DBZ-10), or 15µM (DBZ-15). In Hh signalling inhibition assays,

culture medium was supplemented with 20μM of Cyclopamine (Cyc, Sigma) or with 10μM of Vismodegib (Vis, Selleckchem). In parallel, 3/4PARs were grown with culture medium supplemented with the drug solvent, DMSO, at similar concentrations as those present in the medium of experimental conditions [Control-50 (Ly) - 0.0005% DMSO; Control-100 (Ly) - 0.001% DMSO; Control-200 (Ly) - 0.002% DMSO; Control-5 (DBZ) - 0.05%; Control-10 (DBZ) - 0.10%; Control-15 (DBZ) - 0.15%; Control (Cyc) - 0.16%; Control (Vis) - 0.2%] (control conditions). Following the incubation period, cultured explants were either used for RNA isolation and qRT-PCR (see Section II.1.13.1 and II.1.14) or grafted onto chorioallantoic membrane (CAM) at cE8 (see Section II.2.3.2).

II.2.3 *In vivo* assays

II.2.3.1 Short-term *in ovo* development

II.2.3.1.1 *In ovo* electroporation of neural tube

The neural tube of E2 chicken embryos (HH13) was injected with two different combinations of plasmids that included Tet-Off system vectors (Sato *et al.*, 2007) (Fig. 6B in Chapter I) and electroporated (Fig. 2). The experimental condition involved a mix of pT2K-CAGGS-tTA and pT2K-NLS-Cherry-DNMAML1eGFP vectors, while the control condition consisted of pT2K-CAGGS-tTA and pT2K-BI-TREeGFP. Plasmids pT2K-NLS-Cherry-DNMAML1eGFP, and pT2K-BI-TREeGFP were at around 2μg/μL; pT2K-CAGGS-tTA and pT2K-NLS-Cherry-DNMAML1eGFP/pT2K-BI-TREeGFP were at 1:2 proportion as recommended by Watanabe and collaborators (Watanabe *et al.*, 2007). pCAG-CherryNLS plasmid was used as a control vector to assess the electroporation efficiency (except in the pT2K-NLS-Cherry-DNMAML1eGFP condition) at a concentration of 0,1μg/μL. Fast Green was used for contrast in the plasmid mix in a 1:10 proportion, enabling the visualization of the injection site and its further distribution within the neural tube.

DNA mix was injected into the lumen of the neural tube of E2 chicken embryos with a microinjection capillary glass (Harvard Apparatus), using the Inject + Matic Microinjector (Inject + Matic) (Fig. 2A). Platinum electrodes (Nepagene), distanced 4mm apart were placed parallel to the neural tube on the surface of the embryo, along the anteroposterior axis (Fig. 2A), and some drops of PBS with 1x Pen/Strep were added to

the surface of the embryo. Using an ElectroSquare Porator ECM830 (BTX), 4 pulses of 25V for 50ms, spaced by 100ms were applied twice. The side of the neural tube closer to the positive electrode was the experimental side (having directional entry of DNA into those cells), while the other was the control side (Fig. 2B). Embryo viability, *CherryNLS* and *GFP* expression were evaluated at 24h after electroporation, using Leica MZ10F Fluorescence stereomicroscope equipped with an Evolution™ MP 5.0 Mega-pixel Camera Kit (Media Cybernetics). Viable electroporated embryos were harvested, fixed, and *Hes5.1* expression analysed.

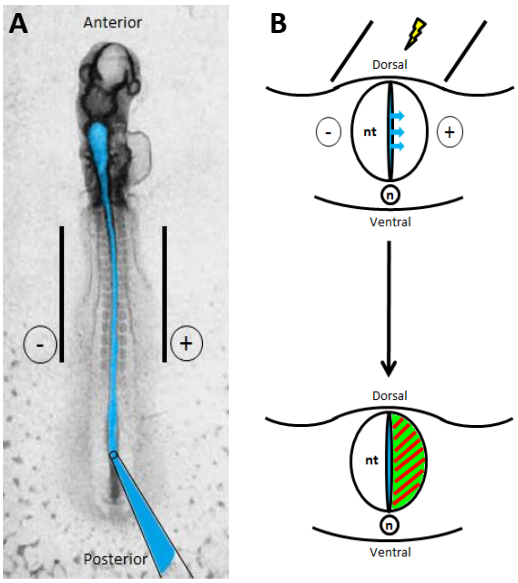

Figure 2. *In ovo* electroporation of the neural tube of chick embryos. Schematic representation of an HH13 embryo (E2) (adapted from Hamburger & Hamilton, 1951) injected with DNA solution into the neural tube's lumen prior to electroporation (A). Electrodes position and polarity are shown by bars and by minus (-) and plus (+) signs, respectively. Schematic representation of the electroporation of a neural tube injected with DNA solution (blue) (B). GFP (green) and CherryNLS (red) expression is expected in the right side of the neural tube, according to electrodes position. nt, neural tube; n, notochord.

II.2.3.1.2 Cyclopamine beads implantation in the pharyngeal region – Hh signalling inhibition

Heparin acrylic beads (Sigma) were rinsed in PBS and soaked overnight at 4°C in a solution of 6mM of Cyclopamine (Cyc; Sigma). A window in the shell of cE2.5 eggs (HH17) was opened, and qE3 eggs (HH21) were opened and transferred to 30 mm petri-dishes containing 2mL of PBS. After local removal of extra-embryonic membranes, Cyc- and PBS-beads were inserted in the embryos' pharynx lumen through the second/third clefts and placed at the level of the 3/4PP (Cyc and Control-PBS, respectively). To increase Hh inhibition effects multiple beads (around 20 in chicken and 40 in quail) were placed per embryo. Embryos were allowed to develop for 20-24h – chicken embryos (after closure of the egg shell with tape) in a humidified incubator at 38°C, and quail

embryos in petri dishes in a humidified incubator with 5% CO_2 at 37°C – before further fixing.

II.2.3.1.3 LY-411.575 administration – Notch signalling inhibition

A window in the shell of cE2.5 and cE3.5 eggs was opened, extra-embryonic membranes were locally removed, and 20–40µL of 5µM, 10µM or 20µM of Ly were injected on the right side of the embryo near the region of the heart and pharyngeal arches. In parallel, control embryos were injected with 20–40µl of DMSO at a similar concentration as the one present in the medium of experimental conditions (0.05%, 0.1% and 0.2%, respectively). After closure of the eggshell with tape, chicken embryos were left to develop *in ovo* for 20–24h in a humidified incubator at 38°, before further fixing.

II.2.3.2 Long-term *in ovo* development – organ formation assay

The 3/4PAR explants grown *in vitro* for 48h were grafted on the CAM of chicken embryos at cE8 (detailed procedure in Chapter III). This classic technique supports the three-dimensional growth of grafted tissues using the CAM as a vascular supplier of nutrients and gas exchanges. Transplanted tissues were allowed to develop *in ovo* for 10 days in a humidified incubator at 38°C, as previously described (Neves *et al*., 2012). For Notch inhibition assays, the 3/4PAR-48h explants derived from Ly-200 (3/4PAR Ly-200) were grafted and developed in CAM (Graft-Ly) (experimental condition). For the control conditions, 3/4PAR-48h explants derived from Control-200 (3/4PAR Control-200) were grafted and developed in CAM (Control-Ly). For both conditions, transplanted tissues further developed *in ovo* for 3 and 10 days in a humidified incubator at 38°C. *Hes5.1* and *Foxn1* expression, and survival and organ formation were evaluated in CAM-derived explants grown *in ovo* for 3 and 10 days, respectively.

II.3 Sample collection, processing, and analysis

Quail and chicken embryos, *in vitro* explants and CAM-derived explants were collected and fixed overnight in 4% paraformaldehyde/PBS at 4°C. Samples were then processed for whole-mount *in situ* hybridization and immunohistochemistry.

II.3.1 *In situ* hybridization

Chicken and quail embryos, *in ovo* electroporated chicken embryos, isolated chicken pharyngeal endoderm, and quail explants grown in CAM for 10 days were collected and fixed overnight with 4% paraformaldehyde at 4°C. Whole-mount *in situ* hybridizations (WM-ISH) were performed as previously described (Henrique *et al.*, 1995; Etchevers *et al.*, 2001), using DIG-labelled antisense RNA probes. Staining reaction was performed using NBT/BCIP (Roche).

II.3.2 Immunohistochemistry

Paraffin sections of *in ovo* electroporated chicken embryos post-WM-ISH for *Hes5.1* were processed for immunocytochemistry with the GFP antibody according to manufacture instructions and as described (Neves *et al.*, 2012). Paraffin sections of explants developed *in ovo* for 10 days were analysed by haematoxylin-eosin staining (H&E) to determine the number, size and morphology of thymic lobes and parathyroid glands formed. Sections of CAM-explants were further treated for immunocytochemistry with the anti-pan [Lu-5] Cytokeratin antibody (Pan CK) (Abcam; for labelling epithelial cells), according to manufacture instructions and as described (Neves *et al.*, 2012).

II.4 Microscopy

In situ hybridization, H&E, and immunohistochemistry images of paraffin sections were collected using Software Leica Firewire and Leica DM2500 microscope with Leica DFC420 camera. WM-ISH pictures were taken under a Leica Z6 APO equipped with a Leica DFC490 camera.

II.5 Statistical analysis

Means and standard deviations were determined with Microsoft Excel/GraphPad Prism® (version 6.01) software. Two-tailed Student's t-tests and Mann-Whitney non-parametric tests were used for the analysis of *in vitro* and *in ovo* assays, respectively. Results were considered significantly different when the P value was less than 0.05 ($P < 0.05$).

CHAPTER III

Two-step Approach to Explore Early- and Late-stages of Organ Formation in the Avian Model: The Thymus and Parathyroid Glands Organogenesis Paradigm.

Marta Figueiredo & Hélia Neves

Instituto de Histologia e Biologia do Desenvolvimento, Faculdade de Medicina
da Universidade de Lisboa, Edifício Egas Moniz, Piso 3, Ala C,
Av. Prof. Egas Moniz, 1649-028 Lisboa, Portugal

In Journal of Visualized Experiments 2018, 136, e57114

Invitation by Indrani Mukherjee, JoVE's Senior Science Editor

CHAPTER III - TWO-STEP APPROACH TO EXPLORE EARLY- AND LATE-STAGES OF ORGAN FORMATION IN THE AVIAN MODEL: THE THYMUS AND PARATHYROID GLANDS ORGANOGENESIS PARADIGM.

III.1 Abstract

The avian embryo, as an experimental model, has been of utmost importance for seminal discoveries in developmental biology. Among several approaches, the formation of quail-chicken chimeras and the use of the chorioallantoic membrane (CAM) to sustain the development of ectopic tissues date back to the last century. Nowadays, the combination of these classical techniques with recent *in vitro* methodologies offers novel prospects to further explore organ formation.

Here we describe a two step-approach to study early-and late-stages of organogenesis. Briefly, the embryonic region containing the presumptive territory of the organ is isolated from quail embryos and grown *in vitro* in an organotypic system (up to 48 h). Cultured tissues are subsequently grafted onto the CAM of a chicken embryo. After 10 days of *in ovo* development, fully formed organs are obtained from grafted tissues. This method also allows the modulation of signalling pathways by the regular administration of pharmacological agents and tissue genetic manipulation throughout in vitro and *in ovo* development steps. Additionally, developing tissues can be collected at any time-window to analyse their gene-expression profile (using quantitative PCR (qPCR), microarrays, etc.) and morphology (assessed with conventional histology and immunochemistry).

The described experimental procedure can be used as a tool to follow organ formation outside the avian embryo, from the early stages of organogenesis to fully formed and functional organs.

III.2 Introduction

Avian embryos have been widely used in seminal developmental biology studies. The main advantages of the avian model include the possibility to open the egg, the relatively easy access to the embryo, and the ability to perform micromanipulation. Some examples comprise the classic quail-chicken chimera system for studying cell fate (Le Douarin, 2005), application of specific growth factors to the embryo (Chuong *et al.*, 2005), and the growth of ectopic cellular structures in the CAM (Le Douarin, 2005; Davey and Tickle, 2007; Nowak-Sliwinska, Segura and Iruela-Arispe, 2014).

To get new insights into distinct stages of organ formation, we have recently developed a method which combines grafting techniques with in vitro manipulation of embryonic tissues (Figueiredo *et al.*, 2016). The two-step approach enables the discrimination and exploration of both early- and late-stages of organogenesis, which are often limited due to highly dynamic and complex tissue interactions (Chuong *et al.*, 2005). Moreover, the lack of suitable tissue-specific markers frequently limits the use of genetically modified animal models (National Research Council., 2000). This novel method of the two-step approach largely overcomes such limitations.

To study early-stages of organ formation, in the first step, the quail embryonic territory comprising the prospective organ rudiment is isolated and grown in an *in vitro* organotypic system for 48 h. During this period, pharmacological modulation of specific signalling pathways can be performed by adding drugs to the culture medium (Moura *et al.*, 2011; Figueiredo *et al.*, 2016). Additionally, cultured tissues can be collected at any stage of *in vitro* growth and probed for gene-expression (using methods as qPCR, microarrays, etc.).

In the second step, 48 h-cultured tissues are then grafted onto the CAM of a chicken (c) embryo at embryonic day (E) 8 (Hamburger and Hamilton (HH)-stages 33–35) (Hamburger and Hamilton, 1951). The CAM behaves as a vascular supplier of nutrients and allows gas exchanges (Le Douarin, 2005; Davey and Tickle, 2007; Figueiredo *et al.*, 2016) to grafted tissues enabling its development *in ovo* for longer periods of time. This experimental step is especially well suited to study late-stages of organogenesis, as fully formed organs can be obtained after 10 days of *in ovo* development (Takahashi, Bontoux and Le Douarin, 1991; Maeda and Noda, 2003;

Figueiredo *et al.*, 2016; Ishida and Mitsui, 2016). Morphological analysis is easily performed by conventional histology to confirm proper organ formation and donor origin of cells can be identified by immunohistochemistry using species-specific antibodies (*i.e,* MAb Quail PeriNuclear (QCPN)). During the CAM incubation period, grafts can also be grown in the presence of pharmacological agents and collected at any stage of development to evaluate the progression of organogenesis.

The two-step approach, described here in depth, has already been employed in Figueiredo *et al.* (Figueiredo *et al.*, 2016) to explore the avian parathyroid/thymus common primordium development. Accordingly, the inherent particularities of the embryonic territories and stages of development involved in the organogenesis of the thymus and parathyroid glands will be presented below.

The thymus and parathyroid glands epithelia, though functionally distinct, both derive from the endoderm of the pharyngeal pouches (PP) (Le Douarin and Jotereau, 1975). In avian, the epithelia of these organs originate from the third and fourth PP endoderm (3/4PP) (Le Douarin and Jotereau, 1975), while in mammals the thymic epithelium derives from the 3PP and the epithelium of parathyroid glands derives from the 3PP and 3/4PP in mouse and human, respectively (Gordon *et al.*, 2001; Farley *et al.*, 2013).

One of the earliest stages in the formation of these organs is the emergence of discrete thymus and parathyroid domains in the common primordium. In chicken, these domains can be identified by *in situ* hybridization, with specific molecular markers, at E4.5 (Neves *et al.*, 2012). As development proceeds, these organ rudiments individualize and separate from the pharynx, while a thin mesenchymal capsule, formed by neural crest-derived cells, surrounds them (at E5; HH-stage 27). Later on, the thymic epithelium is colonized by hematopoietic progenitor cells (at E6.5; HH-stage 30) (Le Douarin and Jotereau, 1975).

As in classical quail-chicken studies (Le Douarin and Jotereau, 1975; Le Douarin, 2005), the two-step approach is particularly useful to study the formation of hematopoietic/lymphoid organs, namely the thymus (Figueiredo *et al.*, 2016). As the quail explant, with the organ rudiment, is grafted in the chicken embryo prior to hematopoietic progenitor cell colonization, a chimeric thymus is formed with chicken blood-borne progenitor cells infiltrating a quail thymic epithelial counterpart. This method is,

therefore, a useful tool to explore the contribution of hematopoietic cells in the development of the avian hemato/lymphoid system.

III.3 Protocol

All these experiments follow the animal care and ethical guidelines of the Centro Académico de Medicina de Lisboa.

1. Incubation of Fertilized Quail and Chicken Eggs

1.1) Incubate Japanese quail (*Coturnix coturnix japonica*) and chicken (*Gallus gallus*) fertilized eggs for 3 and 8 days, respectively.

1.1.1) Place the eggs with the air chamber (egg blunt end) facing up in a humidified incubator at 38°C.

1.1.2) Use around 20 quail eggs and 40 chicken eggs to perform this experiment.

Note: These numbers should be doubled when establishing this procedure for the first time.

2. Isolation of Quail Embryonic Region Containing the Presumptive Territory of Thymic and Parathyroid Rudiments

Note: Perform egg manipulation procedures in sterile conditions using a horizontal laminar flow hood and sterilized instruments and materials.

2.1) Prepare a large borosilicate glass bowl about 3/4 filled with cold phosphate-buffered saline (PBS) solution.

2.2) Open a quail egg after 3 days of incubation by tapping the shell and cutting a circular opening on the opposite side of its blunt end with curved scissors. Carefully remove pieces of shell and transfer the embryo to the glass bowl filled with cold PBS.

2.3) Hold the quail (q) embryo at E3 (qE3) (the quail stage corresponding to the HH-stage 21 of the chicken) with the help of thin forceps. Make a cut into the vitelline membrane

enveloping the yolk using curved scissors. Continue to cut around and externally to the circumference of extra-embryonic vessels.

2.4) Transfer the embryo to a small bowl about 3/4 filled with cold PBS with the help of thin forceps. Thoroughly wash the embryo from the remaining attached yolk.

2.5) Use a skimmer to transfer the embryo to a 100mm glass Petri dish with black base (see Table of Materials in Appendix I) containing 10mL of cold PBS.

2.6) Place the Petri dish under a stereomicroscope.

Note: From this point forward, perform the microsurgery procedures under a stereomicroscope for progressive magnification. As an illumination source, it is advised to use LED lights incorporated in the stereomicroscope or in the optic fibers, considering the limited heat load.

2.7) Hold the embryo to the bottom of the plate with thin insect pins. Place four pins forming a square shape in the extra-embryonic region.

2.8) Remove the extraembryonic membranes of the cephalic region with the help of thin forceps and place a fifth pin there.

Note: If the embryo is correctly positioned, then the otic vesicle, the heart tube, and the 1st, 2nd, and 3rd pharyngeal arches (PAs) should be visible.

2.9) Dissect the embryonic region of interest, *i.e.*, the 3rd and 4th pharyngeal arch region (3/4PAR), using Wecker eye scissors.

2.9.1) Start cutting longitudinally and parallel to the embryo axis, between the somite/neural tube area and the PAs.

2.9.2) Remove the ventrally positioned heart tube by cutting it. Keeping the scissors in the same position, rotate the Petri dish to reposition the embryo according to the direction of the cut.

2.9.3) Cut between the 2nd and 3rd PAs and below the 4th PA.

2.9.4) Detach the remaining membranes from the 3/4PAR with the help of thin forceps.

2.10) Aspirate the isolated tissues (the 3/4PAR) and transfer them to a glass dish 3/4 filled with cold PBS using a 2mL sterile plastic pipette.

Note: Hereafter, tissues can be grown *in vitro* up to 48h or be immediately grafted onto the CAM of a chicken embryo at E8.

2.11) Keep the glass dish containing the isolated 3/4PAR on ice during the preparation of the *in vitro* assay.

3. *In Vitro* Organotypic Assay: Culture of the Embryonic Region Containing the Presumptive Territory of Thymic and Parathyroid Rudiments

3.1) Prepare the culture medium with RPMI-1640 Medium supplemented with 10% FBS and 1% penicillin/streptomycin.

Note: Soluble pharmacological reagents can be added to the medium (for example, LY-411.575 (Ly) and Dibenzazepine or Cyclopamine and Vismodegib, to inhibit Notch and Hedgehog (Hh) signaling pathways, respectively. For this assay, use 50–200nM of Ly or 5–15µM of Dibenzazepine to inhibit Notch signaling in the 3/4PAR. Use 20µM of cyclopamine or with 10µM of Vismodegib to inhibit Hh signaling in the 3/4PAR (Figueiredo *et al.*, 2016).

3.2) Prepare the *in vitro* culture of the 3/4PP explant in a 6-well plate.

3.2.1) Fill one well from the 6-well plate with 5mL of culture medium. Place a 24mm Polycarbonate Membrane Insert (see Table of Materials) on the well with the help of thin forceps.

3.2.2) Under the stereomicroscope, transfer the 3/4PAR explant from the glass dish to the

membrane surface by gently sliding with the help of a transplantation spoon (or spatula) and thin forceps. Place the explants with the ventral side up and the dorsal side in contact with the membrane. Add up to seven explants per membrane insert. Proceed to step 3.4.

3.3) Alternatively, culture explants in floating membrane filters.

3.3.1) Prepare a 35mm Petri dish with 5mL of culture medium. With the help of thin forceps, float a membrane filter (see Table of Materials) and keep a dry surface in contact with air.

3.3.2) Under the stereomicroscope, transfer the 3/4PAR explant from the glass dish to the membrane filter by gentle sliding with the help of a transplantation spoon (or spatula) and thin forceps. Place the explants with the ventral side up and the dorsal side in contact with the membrane. Add up to 8 explants per membrane filter.

3.4) Carefully place the explants prepared in steps 3.2 and 3.3 in a humidified incubator at 37°C with 5% CO_2.

3.5) After a 48h incubation period, remove the 6-well plate and the 35mm Petri dish from the incubator.

3.5.1) Collect the cultured explants from the membrane insert of the 6-well plate.

3.5.1.1) Add PBS at room temperature (RT) to the membrane insert.

3.5.1.2) Detach the explants from the membrane by vigorous flushing using a 2mL sterile plastic pipette.

3.5.1.3) With the help of the spatula and thin forceps, transfer the cultured explants to a glass dish 3/4 filled with PBS at RT.

3.5.2) Similarly, collect the cultured explants from the floating membrane filter in the 35mm Petri dish.

3.5.2.1) Transfer the membrane filter with thin forceps to a new 35mm Petri dish filled with PBS at RT.

3.5.2.2) Detach the explants from the membrane filter by vigorous pipetting using a 2mL sterile plastic pipette.

3.5.2.3) With the help of thin forceps, discharge the explant-free membrane filter after confirming that no explants remained attached to it.

3.5.2.4) With a spatula and thin forceps, transfer the explants to a glass dish filled with PBS at RT.

3.6) Transfer the cultured explants with a spatula to 1mL of a reagent for total RNA isolation and use for gene-expression studies.

CAUTION: Exposure to this reagent (see Table of Materials) can be a serious health hazard. Wear appropriate protective eyewear, clothing, and gloves. Follow the handling instructions and read the safety data sheets provided by the manufacturer.

3.7) Alternatively, graft the cultured tissues onto CAM of chicken embryos at E8. Follow to step 4.

4. Preparation of the CAM

4.1) Remove the chicken eggs with 8 days of embryonic development from the incubator.

Note: Eggs were incubated with air chamber facing upwards at 38°C in a humidified incubator.

4.2) Cover the blunt end of the egg with clear plastic tape to prevent pieces of the shell from falling into the air chamber. Tap the shell and cut a circular opening in the egg with curved scissors. The air chamber should be visible.

4.3) Remove with caution the white membrane of the air chamber with thin forceps. CAM

is then visible and accessible for ectopic tissue transplantation.

Note: Do not use PBS to hydrate the CAM, before or after transplantation, since PBS promotes sliding and misplacement of the explants. If the membrane dries out, discard the egg.

5. Grafting of Cultured Explants onto the CAM

5.1) Create small vascular lesions/wounds in the smaller vessels of the CAM with a microscalpel in a holder.

Note: Use the tip of a Pasteur pipette to remove blood by capillarity in the case of excess bleeding.

5.2) Use a spatula and thin forceps to transfer the cultured explant to the wounded area of the CAM.

5.3) Cut a piece of a filter paper slightly larger than the explant and place it on the top of the explant.

Note: The filter paper helps tracking the explant location after its development in the CAM. Also, it allows daily drug delivery to the explant during *in ovo* development, if necessary (described in step 5.6).

5.4) Seal the egg window with clear plastic tape and identify it using a charcoal pencil.

Note: The plastic tape protects the embryo from dehydration during the incubation period.

5.5) Incubate the manipulated egg for 10 days in a humidified incubator at 38°C. Follow to step 6.

5.6) Optional Step: Daily drug administration during incubation period

5.6.1) To access the filter, partially lift the plastic tape. Add 100µL of drug solution, drop

by drop, on top of the paper. Re-seal the window and place the egg back in the humidified incubator at 38°C.

Note: For this assay, the dose of 20µM of cyclopamine will inhibit Hh signaling during *in ovo* development[5].

6. Ectopic Organ Formation in the CAM After 10 Days of *In Ovo* Development

6.1) After 10 days of incubation, remove the egg from the incubator and carefully withdraw the plastic tape.

6.2) Cut the CAM around the filter region using curved scissors and transfer the CAM-derived explant with filter paper to a small glass bowl about 3/4 filled with cold PBS.

6.3) With the help of thin forceps transfer the CAM-derived explant to a 100 mm Petri dish with black base containing 10 mL of PBS. Gently remove the filter paper and the excess of membrane using Wecker eye scissors and thin forceps.

6.4) Transfer the CAM-explant to fixative solution (3.7% PFA in PBS) with a skimmer. Euthanize the chicken embryos without removing them from the egg by making a precise cut in the neck region of the embryo with the help of large scissors.

6.5) Assess the organ formation in paraffin sections of the CAM-derived explants by conventional histology and immunohistochemistry.

III.4 Results

The above described protocol details a method that allows the investigation of both early- and late-stages of organogenesis, often limited by complex cellular and molecular interactions. This method was previously employed in Figueiredo *et al.* (Figueiredo *et al.*, 2016) to unravel the role of Notch and Hedgehog (Hh) signalling in avian thymus/parathyroid common primordium development.

Herein, new results are showed in Figure 1 and 2, using the same model of organogenesis. In Figure 1A is depicted the experimental design used to explore the early-stages of thymus and parathyroids formation. The quail embryonic territory comprising the prospective organ rudiments (3/4PAR) was isolated and grown *in vitro* for 48h in an organotypic system.

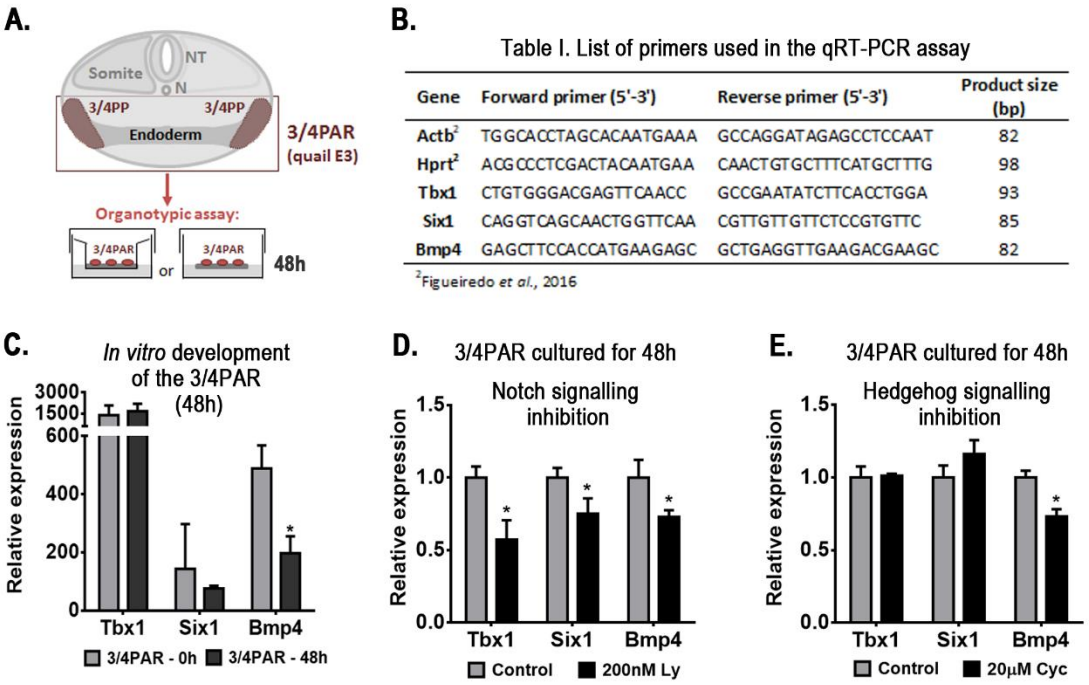

Figure 1. Representative results obtained with the organotypic culture assay: gene-expression analysis of the embryonic region containing the presumptive territories of the thymus and parathyroids (3/4PAR) developed *in vitro* for 48 h. Schematic representation of the transversal section of the embryo at the region of interest and the experimental design (A). Briefly, the 3/4PAR at qE3 was mechanically isolated and grown *in vitro* for 48 h. The expression of the 3/4PAR-related genes, *Tbx1*, *Six1*, and *Bmp4* was examined by qRT-PCR using the primers in the table (B). The expression of *Tbx1*, *Six1*, and *Bmp4* was analyzed in freshly isolated (3/4PAR-0 h) and cultured (3/4PAR-48 h) tissues (C). The expression of PAR-related genes was analyzed in tissues grown *in vitro* for 48 h in the presence of 200 nM

Ly411575 (D) and 20 µM Cyclopamine (E), which are pharmacological inhibitors of Notch and Hedgehog signaling pathways, respectively. Expression of each transcript was measured as a ratio against the mean of the *β-actin* and *Hprt* transcript expression levels and expressed in arbitrary units (each transcript in the control = 1). Means and standard deviations were determined with a software for biostatistics analysis and scientific graphic design. Error bars represent standard deviations of the mean. Two-tailed unpaired Student's *t*-test was used and results were considered significantly different when the *p*-value was less than 0.05 ($p < 0.05$). β-actin, Actb; Cyclopamine, Cyc; Hprt; Hypoxanthine-guaninephosphoribosyltransferase; LY-411.575, Ly; N, Notocord; NT, Neural Tube; PAR, pharyngeal arch region; PP, pharyngeal pouch.

The expression of genes known to be involved in the formation of PAR structures (PAR-related genes), *i.e.*, *Tbx1* (Jerome and Papaioannou, 2001; Nie *et al.*, 2011), *Six1* (Zou *et al.*, 2006), and *Bmp4* (Jerome and Papaioannou, 2001; Neves *et al.*, 2012), was evaluated during the normal development. Quantitative real time PCR (qRT-PCR) was performed as previously described (Figueiredo *et al.*, 2016) (primers are listed in Fig. 1B). Transcripts of the three genes were detected in freshly isolated (3/4PAR-0 h) and in 48 h-cultured tissues (3/4PAR-48 h) (Fig. 1C). Only *Bmp4* expression levels were significantly decreased after 48 h of culture.

To evaluate the role of Notch and Hh signaling pathways in the early-stages of thymus and parathyroid development, pharmacological inhibitors were added to the culture medium during *in vitro* development. Inhibitor doses are described in Figueiredo *et al.* (Figueiredo *et al.*, 2016). The expression levels of the three genes analyzed were significantly reduced in the 3/4PAR grown in the presence of Notch inhibitor, when compared to control conditions (without drug) (Fig. 1D). Conversely, only *Bmp4* transcripts were significantly reduced in the 48 h-cultured tissues when Hh signaling was blocked (Fig. 1E). To study late-stages of thymus and parathyroid glands organogenesis, cultured tissues were then grafted onto CAMs and allowed to further develop for 10 days (see experimental design in Fig. 2A).

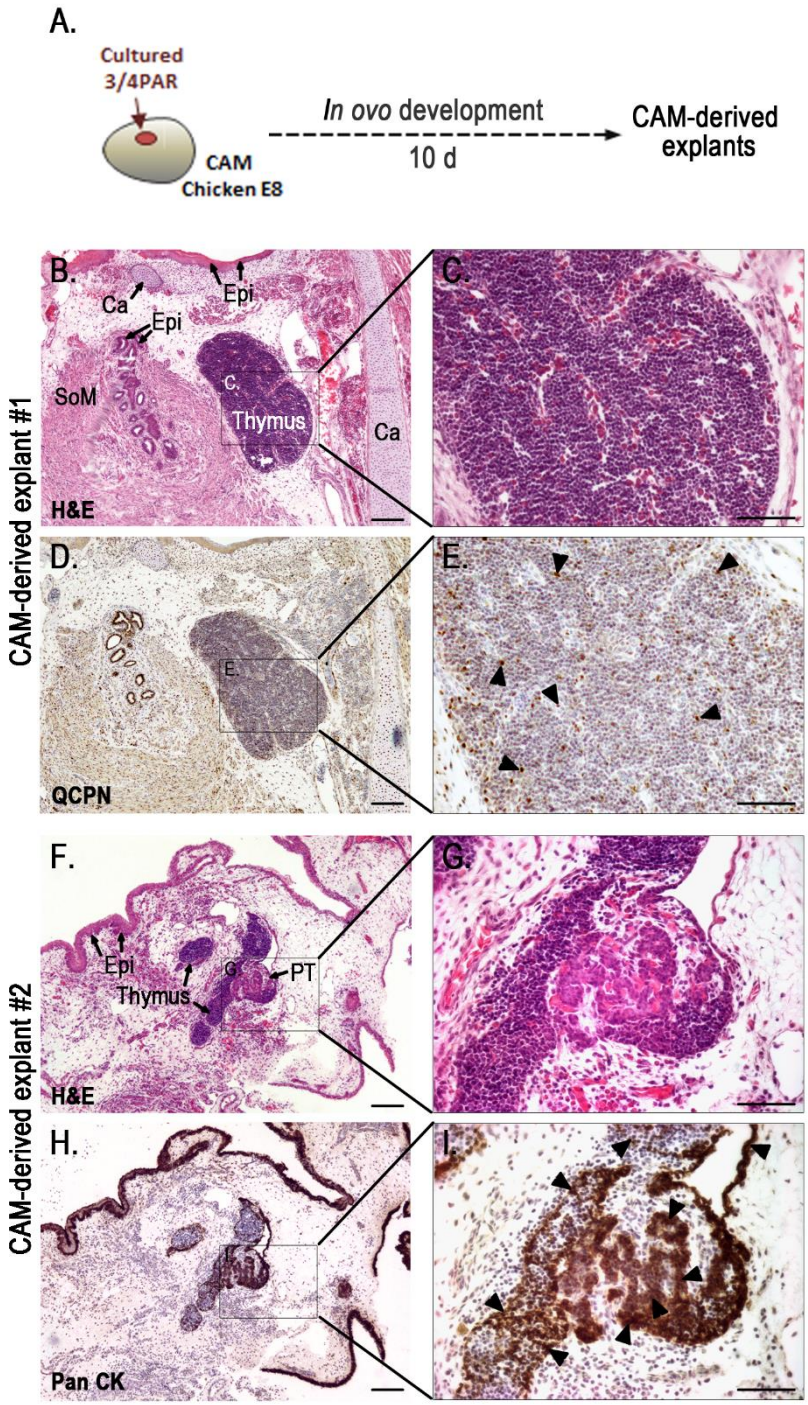

Figure 2. Representative results obtained with the *in ovo* assay: morphological analysis of the grafts grown for 10 days in the chorioallantoic membrane. Schematic representation of 48 h-cultured PAR grafted onto the CAM and developed for a further 10 days (**A**). Serial sections of CAM-derived explants (**B–I**) slides stained with H&E (**B**, **C**, **F**, and **G**) and immunodetected with QCPN (**D** and **E**) and anti-Pan CK (**H** and **I**) antibodies and counterstained with Gill's hematoxylin. Black arrow heads indicate strong immunostaining for QCPN (**E**) and Pan CK (**I**). A transverse section of a chimeric thymus with lymphoid cells of host origin and quail-derived thymic epithelial cells with strong QCPN^{+} signals (black arrowheads) (**E**). Strong pan-CK^{+} signals (black arrowheads) in the epithelia of the thymus and parathyroid glands (**I**). Images were collected using imaging software and a microscope with a camera

(see **Table of Materials**). Ca, cartilage; CAM, chorioallantoic membrane; Epi, epithelium; PAR, pharyngeal arch region; PT, parathyroid glands; SoM, smooth muscle; 10 d, ten days. Scale bars, 50 µm (**B**, **D**, **F**, and **H**) and 100 µm (**C**, **E**, **G**, and **I**).

Morphological analysis of organs developing on CAM-derived explants was performed by conventional histology and immunohistochemistry (Fig. 2B–I), as previously described (Figueiredo *et al.*, 2016). CAM-derived explants showed fully formed chimeric thymus (Fig. 2B–E) with quail-derived ($QCPN^+$) thymic epithelium colonized by lymphoid progenitor cells of donor origin (chicken) (Fig. 2D and E). Serial sections of CAM-derived explants further processed for immunocytochemistry with anti-pan cytokeratin (anti-pan CK) antibody (an epithelial cell marker), showed thymic and parathyroid epithelia with normal morphological features (Fig. 2H and I). The thymic epithelial cells displayed a reticular architecture while parathyroid parenchymal cells were globular, arranged in clusters and encircled by numerous capillaries. Additionally, other PAR-derived structures from the respiratory apparatus could be observed in the grafts. Cartilage, respiratory epithelium, and smooth muscle associated to the mucosa were easily distinguished in Figure 2B.

III.5 Discussion

A crucial aspect for the success of this method is the quality of both the chicken and quail eggs. Considering the long incubation periods, particularly during the *in ovo* assay, a good quality of chicken eggs improves viability rates (up to 90%) by the end of the procedure. To achieve this, test eggs from different suppliers. Incubate unmanipulated eggs for long periods (up to 16–17 days) and check their development. To be considered a good quality batch, more than 80% of the embryos should present normal development. It is also important to ensure that each incubation step provides reproducible synchronous developmental stages to guarantee reliable and truly representative results at the end. Due to egg shell porosity, maintain a humidified atmosphere in the incubator for all egg incubation steps. To avoid environmental contamination, antibiotics can be added to the PBS solutions in the procedure (optional step).

This method starts by isolating quail organ rudiments and growing them in an organotypic system for 48 h. This first step, already used to study thymus and parathyroid early-development (Figueiredo *et al.*, 2016), can also be applied to other organs if the assay limitations are taken into account. Small explants of organ rudiments (less than 3 mm) and short periods of *in vitro* incubation (up to 48 h) are advised to prevent inefficient diffusion of nutrients and drying of the tissues, which usually occurs when explants reach larger dimensions.

This method also allows the modulation of signaling pathways, which bypasses complex genetic manipulation by the use of soluble reagents, such as pharmacological inhibitors (Moura *et al.*, 2011; Figueiredo *et al.*, 2016). For this procedure, increasing doses of the drug should be tested to identify the physiological/toxic culture conditions. The inhibitory actions can be measured by gene expression analysis of the signaling pathway target-genes.

In step two of this procedure, cultured tissues are grafted onto the CAM to study the late-stages of organ formation. The CAM assay has been used in other contexts of organogenesis like skeletal development and feather formation by direct grafting of the organ rudiments onto CAM (Takahashi, Bontoux and Le Douarin, 1991; Maeda and Noda, 2003; Ishida and Mitsui, 2016). Additionally, CAM engraftment was also successfully applied in mice-into-chicken xenografts to study testes maturation (Uematsu

et al., 2014). Although the CAM assay is a powerful research tool to study late-stages of organ formation, it is important to be aware of its limitations. One of the most critical steps of the protocol is the CAM preparation for grafting. It is important to target only the smaller vessels for vascular lesions. However, if only a few of those are lesioned, the subsequent angiogenic response may not be sufficient to promote invasion of grafted tissues by new vessels originating from the CAM. Consequently, the transplanted tissues will not have enough nutrients or gas exchanges to sustain growth. On the other hand, if the integrity of large vessels is compromised when preparing the wounded area, the embryo has to be discarded.

An important limitation of *in ovo* development using the CAM is the anatomical displacement of formed organs, due to three-dimensional constraint of growing explants. This often results in the incomplete separation of thymus and parathyroid glands (Fig. 2F–I), and in inadequate thymic segmentation, with reduction of the normal number of organs formed (Figueiredo *et al.*, 2016).

Another constraint of the CAM system may be a sub-optimal accessibility of pharmacological reagents (Figueiredo *et al.*, 2016), even with daily drug administration, thus limiting the analysis of explant late-stage development. As an example, previous studies showed that Cyclopamine successfully inhibited Hh signaling *in ovo*, while Notch signaling inhibitor, LY-411.575, showed no inhibitory properties *in ovo* (Figueiredo *et al.*, 2016).

Beyond these limitations, this method provides important experimental approaches to investigate the early- and late-stages of organ formation using the avian model. In addition, developing tissues can be manipulated and harvested at any time-window of the *in vitro* and *in ovo* development making the method also suitable for longitudinal studies in organogenesis.

CHAPTER IV

Notch and Hedgehog in the thymus/parathyroid common primordium: crosstalk in organ formation.

Marta Figueiredo[a,b,1], Joana Clara Silva[a,1], Ana Sofia Santos[a], Vitor Proa[a], Isabel Alcobia[a,b], Rita Zilhão[c], António Cidadão[a], and Hélia Neves[a,b]

[a]Instituto de Histologia e Biologia do Desenvolvimento, Faculdade de Medicina da Universidade de Lisboa, Edifício Egas Moniz, Piso 3, Ala C, Av. Prof. Egas Moniz, 1649-028 Lisboa, Portugal;
[b]Instituto de Medicina Molecular, Faculdade de Medicina da Universidade de Lisboa, Av. Prof. Egas Moniz, 1649-028 Lisboa, Portugal;
[c]Departamento de Biologia Vegetal, Faculdade de Ciências da Universidade de Lisboa. Campo Grande C2, 1749-016 Lisboa, Portugal.

[1]Co-authors, these authors contributed equally to this work.

In Developmental Biology 2016; 418 (2): 268–282

CHAPTER IV - NOTCH AND HEDGEHOG IN THE THYMUS/PARATHYROID COMMON PRIMORDIUM: CROSSTALK IN ORGAN FORMATION.

IV.1 Abstract

The avian thymus and parathyroids (T/PT) common primordium derives from the endoderm of the third and fourth pharyngeal pouches (3/4PP). The molecular mechanisms that govern T/PT development are not fully understood. Here we study the effects of Notch and Hedgehog (Hh) signalling modulation during common primordium development using *in vitro*, *in vivo*, and *in ovo* approaches. The impairment of Notch activity reduced *Foxn1*/thymus-fated and *Gcm2*/*Pth*/parathyroid-fated domains in the 3/4PP and further compromised the development of the parathyroid glands. When Hh signalling was abolished, we observed a reduction in the *Gata3*/*Gcm2*- and *Lfng*-expression domains at the median/anterior and median/posterior territories of the pouches, respectively. In contrast, the *Foxn1*-expression domain at the dorsal tip of the pouches expanded ventrally into the *Lfng*-expression domain. This study offers novel evidence on the role of Notch signalling in T/PT common primordium development, in an Hh-dependent manner.

IV.2 Introduction

The parathyroid glands and the thymus are organs with distinct functions, carried out mainly by epithelial cells which have a common embryological origin, that is, the endoderm of the pharyngeal pouches (PP). The epithelia of these organs in the avian model originate from the third and fourth PP (3/4PP) endoderm. It is worth noting, that in mammals the thymic epithelium derives from the 3PP endoderm (Farley *et al*., 2013; Gordon *et al*., 2001) and in mouse and human the epithelium of parathyroids derives from the 3PP and 3/4PP, respectively. The main function of the parathyroid endocrine epithelium is to secrete a peptidic hormone, the parathyroid hormone (Pth), essential for the regulation of calcium and phosphate homeostasis (Potts, 2005). In the thymus, the epithelial cells establish complex interactions with the developing lymphocytes to produce self-restricted and self-tolerant T-cells, which generate central immune tolerance.

Parathyroid and thymic organogenesis starts with the budding off and outgrowth of rudiments from pouches of the foregut endoderm (Manley and Condie, 2010), accompanied by the lining of neural crest-derived connective tissues (Grevellec and Tucker, 2010). These early steps involve pouch patterning and the establishment of a common primordium (Manley and Condie, 2010) in which the distinct parathyroid and thymic prospective domains, can be distinguished by the expression of the organ-specific genes, Gcm2 (Glial cells missing 2) and Foxn1, respectively.

In avian embryos, *Gcm2* transcripts were first detected by RT-PCR in isolated quail (q) endoderm at embryonic day (E) 2.5 (25-30 somite-stage) (Neves *et al*., 2012). However, in situ expression of *Gcm2* has only been observed in the anterior domain of the 3PP and 4PP at Hamburger and Hamilton Stage 18 (HH18) and HH22, respectively (Okabe and Graham, 2004). This temporal sequence of *Gcm2* expression follows the chronological formation of the pouches. As development proceeds, *Pth* is upregulated in the developing glands. In avian, *Pth* expression was first observed *in situ* at chicken (c) E5.5 (HH28) (Grevellec, Graham and Tucker, 2011). In *Gcm2* homozygous null mutant mice, the expression of *Pth* is not initiated and no parathyroid glands are formed (Günther *et al.*, 2000; Liu, Yu and Manley, 2007).

The transcription factor of the winged helix/forkhead class, *Foxn1*, is the earliest known marker of the thymic rudiment. *Foxn1* transcripts were detected in isolated quail

endoderm 24 hours after *Gcm2* expression. At cE4.5, *Foxn1* expression was observed in situ in the dorsal tip of the 3/4PP and transcription endures until birth (Neves *et al*., 2012). The gene is mutated in the nude mouse strain, which displays abnormal hair growth and failure of thymus development, leading to immunodeficiency (Blackburn *et al.*, 1996; Nehls *et al.*, 1996; Bleul *et al.*, 2006).

As in other developmental processes, the activation of the correct transcriptional programs during parathyroid (Neves and Zilhão, 2014) and thymic (Manley and Condie, 2010) organogenesis depends on the crosstalk of several signalling pathways which respond to extracellular signals.

Notch signalling is a major pathway during development that acts in a juxtacrine fashion and is responsible for cell-fate decisions (Lewis, 1998; Lai, 2004). In the last fifteen years, several reports have shown that Notch is fundamental during epithelial-lymphoid cell interactions at late-stages of thymus formation (Rodewald, 2008). Notably, perinatal mutant mice with loss of Notch ligand *Jag2* exhibit aberrant thymic morphology with smaller medullar compartments (Jiang *et al.*, 1998). Notch activity is also required for the commitment of lymphoid progenitor cells to the T-cell lineage (Pui *et al.*, 1999; Radtke *et al.*, 1999), in a ligand dependent manner (Jaleco *et al.*, 2001; Dorsch *et al.*, 2002). Whilst largely unknown, there is some evidence for the role of Notch signalling in the early-development of these organs. In mice, the loss of Notch-target *Hes1* promotes a spectrum of malformations of pharyngeal endoderm-derived organs, including parathyroid glands aplasia/hypoplasia (Kameda *et al.*, 2013) and abnormal thymic formation (Tomita *et al.*, 1999; van Bueren *et al.*, 2010; Kameda *et al.*, 2013).

Paracrine Hedgehog (Hh) signalling is also involved in craniofacial and neck morphogenesis (Grevellec and Tucker, 2010), and regulates T/PT common primordium development (Moore-Scott and Manley, 2005). In *Sonic Hh* (Shh) homozygous null mutants the rudiment boundaries are compromised, displaying an expanded domain of the prospective thymic territory at the expense of the *Gcm2*/parathyroid-fated domain (Moore-Scott and Manley, 2005). This mutant fails to form parathyroid glands (Moore-Scott and Manley, 2005) and displays functional defects in the thymus (Shah *et al.*, 2004). At later stages of development, Shh and Indian Hh, other Hh signalling molecules, are known to regulate thymocyte differentiation after thymic epithelium colonization by lymphoid progenitor cells (Outram *et al.*, 2009).

Hh and Notch pathways interact in multiple biological scenarios (Lawson, Vogel and Weinstein, 2002; McGlinn *et al.*, 2005; Stasiulewicz *et al.*, 2015). In distinct developmental contexts, Notch signalling is known to control morphological boundary formation by the mechanism of lateral inhibition (Lewis, 1998; Lai, 2004; Kiernan, 2013). In light of this evidence, we hypothesized that similar mechanisms could operate in the development of T/PT common primordium. In order to test this hypothesis, Notch and Hh signals were inhibited *in vitro* and *in vivo* in the presumptive territories of thymus and parathyroids by ectopic administration of the respective pharmacological inhibitors. Briefly, our results show a positive regulatory effect of Notch signalling in T/PT common primordium development and parathyroid gland formation. Hh positively regulates the *Gata3*/*Gcm2*/parathyroid-fated domain. Furthermore, Hh establishes the dorsal/posterior boundary of *Foxn1*/thymic rudiment by positively regulating *Lfng*/Notch signals at the posterior/median territory of the developing 3/4PP endoderm.

IV.3 Results

IV.3.1 Notch-target genes *Hey1*, *Hes5.1* and *Gata3* are involved in the 3rd and 4th pharyngeal pouches endoderm development.

To investigate the role of Notch signalling during the development of thymus and parathyroids (T/PT) common primordium we analysed the expression of Notch-target genes, *Hey1*, *Hes5.1*, *Hes6.1* and *Gata3* (Fang *et al.*, 2007; Naito *et al.*, 2011), within the presumptive territories of these organs (3/4PAR) (Figure 1).

Notch-target gene expression was evaluated during normal development of the 3/4PAR. qE3 3/4PAR was isolated (3/4PAR-0h) and grown *in vitro* for 48h (3/4PAR-48h) (Figure 1A). As depicted in Figure 1B, high levels of *Hey1* and *Gata3* transcripts were detected in freshly isolated tissues and significantly decreased after 48h of culture. A similar trend was observed in in the lowly-expressed transcripts, *Hes5.1* and *Hes6.1*. The reduction of *Hey1* and *Gata3* transcript levels was further supported by *in vivo* gene-expression evaluation at similar developmental time-windows, i.e. qE3 and qE4. *Hey1* transcripts were broadly detected along the endoderm, mesenchyme and ectoderm of the 3/4PAR (Figure 1C and D) whereas *Gata3* expression was restricted to the endoderm of the pouches. At qE3, the strongest *Gata3* hybridization signals were observed in the tips and anterior domain of the 3PP endoderm (Figure 1E), the T/PT common primordium territory. After 24h of development, *Gata3*-expression domain was confined to a more median/anterior position (Figure 1F), at the parathyroid rudiment territory (Neves *et al*., 2012). *Gata3* expression was maintained later in the developing parathyroids (Suppl. Fig. 1A). Interestingly, Gata3 has been previously shown to be involved in parathyroid formation (Grigorieva and Mirczuk, 2010).

Notch signalling was then modulated during common primordium formation (Figure 1A and G-L). 3/4PAR was grown *in vitro* in the presence of three doses of the Notch inhibitor LY-411.575 (Ly), at 50nM, 100nM and 200nM (Figure 1G). A strong and significant reduction of *Hey1* (67%, 77% and 74%) and *Hes5.1* expression (98%, 74% and 92%) was observed in the pharyngeal tissues treated with Ly (Ly-50, Ly-100 and Ly-200, respectively), when compared to control conditions. *Gata3* transcript levels were also diminished (45%, 31% and 29% in Ly-50, Ly-100 and Ly-200, respectively) while no changes were observed for *Hes6.1* expression in either condition. This Notch-

target gene belongs to the Hes6 family previously reported to be transcriptionally repressed by *Hes5* genes (Fior and Henrique, 2005).

To validate the specificity of Notch signalling inhibition effects, similar *in vitro* assays were performed using three doses (5μM, 10μM and 15μM) of a different Notch inhibitor, Dibenzazepine (DBZ) (Figure 1H). As expected, a strong decrease of *Hey1* (72%, 71% and 66%) and *Hes5.1* (93%, 93% and 98%) transcript levels was accompanied with a less impressive reduction in *Gata3* expression (46%, 38% and 26%) in explants cultured with increasing doses of DBZ. Likewise, the expression levels of *Hes6.1* in DBZ-treated explants were similar to control conditions.

The capacity to inhibit Notch was further confirmed by an *in vivo* approach with the injection of Ly (5-20μM) on the right side of the pharyngeal region of developing embryos. Ly administration was performed at cE2.5, the developmental stage prior to the formation of T/PT common primordium and to the *in situ* detection of *Gcm2* (Okabe and Graham, 2004). Injected embryos were allowed to develop for 20-24h and then *in situ* analysed for *Hey1* and *Gata3* expression (Figure 1I-L). These genes were selected because of their high expression during *in vitro* development (Figure 1B). Chicken embryos were used in these experiments as some of the probes were inefficient for WM-ISH in quail embryos. In Ly-injected embryos, *Hey1* expression was abolished in all tissues of the pharyngeal region (Figure 1J, n=3/3), while *Gata3* expression was downregulated in the dorsal/tip and anterior domains of common primordium (Figure 1L, n=9/11).

Taken together, our data show that Notch-target genes *Hey1* and *Gata3* may act as positive mediators of Notch activity during the development of the T/PT common primordium.

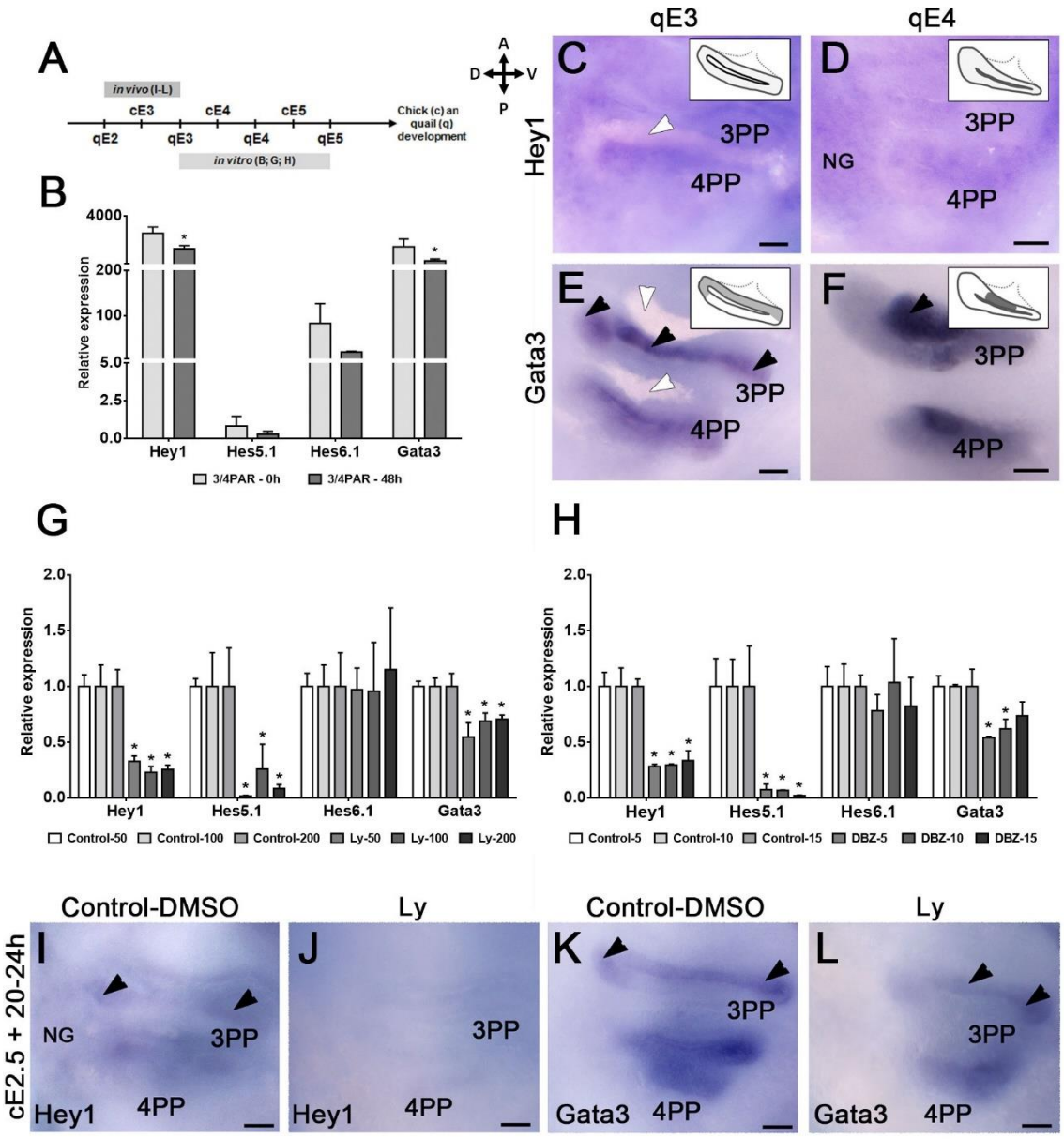

Figure 1. Notch-target genes are involved in T/PT common primordium formation. Timeline of *in vitro* and *in vivo* assays in chicken and quail development (A). *In vitro* (B) and *in vivo* (C-F) expression of Notch-target genes in the 3/4PAR. Isolated 3/4PAR at qE3 was grown *in vitro* for 48h. The expression levels of Notch-target genes of freshly isolated (3/4PAR-0h) and cultured (3/4PAR-48h) tissues were examined by qRT-PCR (B). In parallel, the expression of *Hey1* (C and D) and *Gata3* (E and F) was observed in the endoderm of the 3/4PP at qE3 (C and E, respectively) and qE4 (D and F, respectively) by WM-ISH. Schematic drawings in the top/right panels depict the gene-expression domains in the 3PP, the well-defined pouch. *In vitro* (G and H) and *in vivo* (I-L) expression of Notch-target genes in the 3/4PAR with Notch signalling inhibition. Isolated 3/4PAR at qE3 was grown *in vitro* for 48h with three doses of Ly, 50nM (Ly-50), 100nM (Ly-100) and 200nM (Ly-200) (G) or three doses of DBZ, 5μM (DBZ-5), 10μM (DBZ-10) and 15μM (DBZ-15) (H). The expression levels of Notch-target genes were measured in the cultured tissues by qRT-PCR (each transcript in control=1). With the purpose of inhibiting Notch signalling *in vivo*, the right side of cE2.5 embryos were injected in the pharyngeal region with either DMSO (I and K) or Ly (J

and L) and allowed to develop *in ovo* for 20-24h. The expression of Notch-target genes, *Hey1* (I and J) and *Gata3* (K and L) was detected by WM-ISH. For qRT-PCR, expression of each transcript was measured as a ratio against the mean of the *Actb* and *Hprt* transcript expression levels and expressed in arbitrary units. Black arrowheads point to the strong hybridization signals in the 3PP endoderm and white arrowheads point to the pharyngeal arches. A, anterior; cE, chicken embryonic day; D, dorsal; DBZ, Dibenzazepine; Ly, LY-411.575; NG, nodose ganglion; P, posterior; PP, pharyngeal pouch; qE, quail embryonic day; V, ventral. Scale bars, 50μm.

IV.3.2 Notch signalling inhibition promotes the reduction of Foxn1 and Gcm2/Pth expression in the endoderm of the 3rd and 4th pharyngeal pouches.

To investigate the effects of Notch signalling inhibition during common primordium stages, we analysed the transcript levels of the T- and PT-related markers, *Foxn1* (Neves *et al*., 2012) and *Gcm2/Pth* (Neves *et al*., 2012; Grevellec *et al*., 2011) genes, respectively (Figure 2). The expression analysis was expanded to transcription factors known to be involved in the morphogenesis of the pouches and formation of these organs, the *Pax1* and *Fgf8* genes (Dietrich and Gruss, 1995; Wallin *et al.,* 1996; Su *et al.*, 2001; Frank *et al.,* 2002; Guo *et al.,* 2011). *In vitro* and *in vivo* assays were performed as described in the previous section (schematic representation, Figure 2A).

We began by examining the *in vitro* development of pharyngeal tissues (Figure 2B). Predictably, *Foxn1* transcripts were almost undetectable in 3/4PAR-0h but increased 35-fold during 48h culture, confirming thymic epithelium specification during this developmental time-window (Neves *et al*., 2012). Conversely, the transcription factor *Gcm2* was already strongly expressed in freshly isolated tissues and increased 4-fold in 3/4PAR-48h. In parallel, we observed a striking augmentation of *Pth* expression (986-fold), an indication of parathyroid epithelium differentiation (Günther *et al.,* 2000). Minor changes were globally detected in the expression of *Pax1,* while *Fgf8* transcripts were significantly reduced. A similar trend was observed in the gene expression patterns of *Pax1* and *Fgf8 in situ* at similar developmental time-windows (qE3 and qE4; Figure 2C-F). High levels of *Pax1* expression were observed in the 3/4PP endoderm. The stronger hybridization signals were confined to the dorsal tip of the pouches (Figure 2C and D), the presumptive territory of the thymic rudiment (Neves *et al*., 2012). The expression of *Pax1* was maintained in the thymic epithelium at later stages of development (Suppl. Fig.

1C), as has been observed in mice (Wallin *et al*, 1996). Faint hybridization signals of *Fgf8* were observed in the posterior/median domain of the 3/4PP endoderm at qE3 (Figure 2E) and almost disappeared at qE4 (Figure 2F). In short, our *in vitro* system reproduced the normal dynamic of *Foxn1*, *Gcm2*, *Pth*, *Pax1* and *Fgf8* expression in the developing endoderm of the 3/4PP. The *in situ* study also confirmed the restricted expression of *Pax1* and *Fgf8* in the endodermal pouch compartment at these stages of development.

To analyse the effects of Notch inhibition, pharyngeal tissues were treated with Ly (Figure 2G), as described above. When compared to control conditions, a significant reduction of *Foxn1* expression was observed in Ly-derived explants (35%, 56% and 49% in Ly-50, Ly-100 and Ly-200, respectively), suggesting that the abolishment of Notch activity compromises thymic epithelium specification. A significant decrease of *Pax1* expression (46%, 55% and 65%) was also consistently observed with increasing doses of Ly. In addition, Ly-treated tissues showed a reduction of *Gcm2* transcript levels (around 80%), alongside the almost total lack of *Pth* expression (more than 90% reduction), revealing the requirement of Notch signalling activity in the early-stages of parathyroid epithelium differentiation. No significant changes in *Fgf8* expression levels were detected during *in vitro* development.

Similar results were obtained when Notch signalling was abrogated using DBZ (Figure 2H). *Foxn1*, *Gcm2*, *Pth* and *Pax1* transcript levels were significantly reduced in DBZ-treated explants. The expression levels of *Fgf8* were similar in the DBZ and control conditions.

The *in vivo* results (Figure 2A and I-L) supported the *in vitro* effects, as described above. Ly was injected in the 3/4PAR at cE3.5, the corresponding stage to qE3, and allowed to develop for further 20-24h. As previously reported (Neves *et al*., 2012), *Foxn1*- and *Gcm2*-expression domains were localized in the dorsal-tip (n=4/4; Figure 2I) and median/anterior (n=5/5; Figure 2K) region of the 3/4PP, respectively, in control embryos (Control-DMSO). The expression of *Foxn1* (n=4/4; Figure 2J) and *Gcm2* (n= 5/5; Figure 2L) was strongly diminished in the pouches of Ly-injected embryos. The decrease of *Gcm2* expression was only observed in embryos injected with the highest concentration of Ly (20μM), whereas *Foxn1* expression was reduced even with the lowest dose (5μM). Concordantly, only transcripts of *Gcm2*, and not *Foxn1*, were clearly detected in freshly isolated tissues at qE3 (Figure 2B), the developmental stage similar to the moment of embryo injection.

These data provide evidence that Notch signalling has positive regulatory effects during the development of the T/PT common primordium.

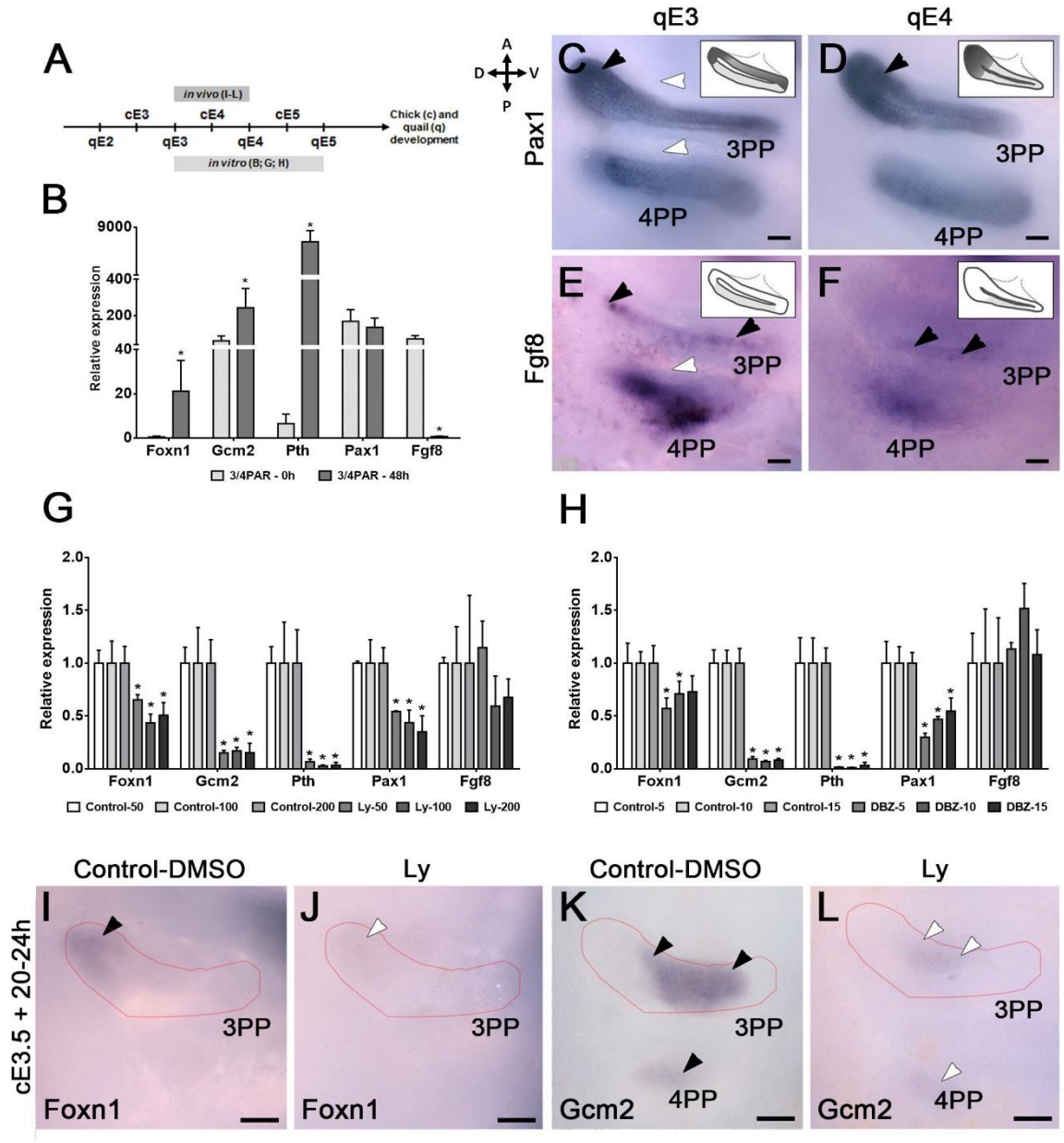

Figure 2. The effects of Notch signalling modulation during T/PT common primordium formation. Timeline of *in vitro* and *in vivo* assays in chicken and quail development (A). *In vitro* (B) and *in vivo* (C-F) expression of thymic, parathyroid and PP endodermal markers in the 3/4PAR. The 3/4PAR at qE3 was mechanically isolated and grown *in vitro* for 48h. Gene-expression levels of freshly isolated (3/4PAR-0h) and cultured (3/4PAR-48h) tissues were examined by qRT-PCR (B). In parallel, *Pax1* (C and D) and *Fgf8* (E and F) expression was detected by WM-ISH in the developing endoderm of the 3/4PP at qE3 (C and E) and qE4 (D and F). Schematic drawings in the top/right panels depict the gene-expression domains in the 3PP, the well-defined pouch. *In vitro* (G and H) and *in vivo* (I-L) expression of thymic, parathyroid and PP endodermal markers in the 3/4PAR with Notch signalling inhibition. Isolated 3/4PAR at qE3 was grown *in vitro* for 48h with three doses of Ly, 50nM (Ly-50), 100nM (Ly-100) and 200nM (Ly-200) (G) or three

doses of DBZ, 5μM (DBZ-5), 10μM (DBZ-10) and 15μM (DBZ-15) (H). For the Notch signalling *in vivo* assay, the expression of *Foxn1* (I and J) and *Gcm2* (K and L) was observed by WM-ISH in the 3/4PAR of cE3.5 embryos developed for 20-24h after Ly (J and L) or DMSO (I and K) injection. For qRT-PCR, expression of each transcript was measured as a ratio against the mean of *Actb* and *Hprt* transcript expression levels and expressed in arbitrary units. The faint red line delimits the 3PP endoderm. Black arrowheads point to the strong hybridization signals and white arrowheads point to pharyngeal arches (C and E) or to weak/absent hybridization signals in the 3/4PP endoderm (J and L). A, anterior; cE, chicken embryonic day; D, dorsal; DBZ, Dibenzazepine; Ly, LY-411.575; P, posterior; PAR, pharyngeal arch region; PP, pharyngeal pouch; qE, quail embryonic day; V, ventral. Scale bars, 50μm.

IV.3.3 Notch signalling inhibition during early-development of the 3rd and 4th pharyngeal arch region impairs the subsequent formation of parathyroid glands.

We then asked if Notch signalling was required at the T/PT common primordium stage for the respective organ formation. To address this question, Ly-treated tissues were grafted onto CAM and allowed to develop *in ovo* for 10 days (Figure 3A).

We have previously used *in ovo* assays to evaluate the capacity of explants to form organs when grafted onto CAM (Neves *et al.*, 2012). Distinct pharyngeal derived organs displaying normal tissue-tissue interactions were formed in CAM-derived DMSO-free explants (3/4PAR-48h) (Suppl. Fig. 1D-J). These organs were, however, anatomically displaced due to physical constrains during the ectopic growth in CAM. Briefly, chimeric thymus was formed as a result of quail thymic epithelial colonization by lymphoid progenitor cells of donor origin (chicken) (Suppl. Fig. 1F). Thymic lobes showed normal morphological characteristics with discrete cortical and medullary compartments (Suppl. Fig. 1E). Only one third of the lobes were formed per explant (4, n=6), compared with the usual bilateral segmentation of up to 7 thymic lobes per embryo. Regarding the parathyroid glands, each explant showed similar size and number of organs formed (1.7, n=6) when compared to normal embryogenesis (2 parathyroids per embryo). The glands showed normal morphological features with parenchymal cells arranged in clusters, encircled by numerous capillaries and surrounded by a dense and irregular connective tissue capsule (Suppl. Fig. 1H and I).

The ability of the pharyngeal tissues treated with Ly (3/4PAR Ly-200) to form organs when grafted onto CAM was then assessed (Graft-Ly) (Figure 3B-M). The number of thymic lobes formed in Graft-Ly was slightly higher than in control conditions, but with similar sizes (Figure 3B) and normal morphology (Figure 3D and F). These results demonstrated that absence of Notch signals at the common primordium stage was not sufficient to block thymus formation. Moreover, the subsequent development of the thymic rudiment may have been caused, at least partly, by the reactivation of Notch activity in the drug-free CAM environment. When Ly-derived explants were analysed 3 days post-grafting onto CAM strong *Hes5.1* expression was observed, confirming the reactivation of Notch signalling (Figure 3H, n=3/4). Likewise, *Foxn1* expression was detected in thymic rudiments derived from Graft-Ly (Figure 3H´) and Graft-Control (Figure 3G´, n=3/3). Altogether, the data indicate that early-absence of Notch signalling may delay thymic epithelium specification from the T/PT common primordium without blocking it. To further explore the role of Notch signalling at later stages of thymus development, explants were grown in CAM with daily administration of 200nM of Ly. Under these conditions, Notch signalling blocking was not achieved, as assessed by Notch-target gene-expression analysis (data not shown). This was probably due to the inaccessibility and/or inappropriate concentration of Ly. The number, size and morphology of the thymuses formed were similar in CAM-derived explants irrespectively of *in ovo* daily administration of Notch inhibitor (data not shown).

The capacity of *in vitro* Ly-treated pharyngeal tissues to form parathyroids was then evaluated (Figure 3I-M). We observed both fewer and significantly small sized parathyroid glands in Graft-Ly explants (40% less than control) (Figure 3I). These glands also showed poorly developed parenchymal cells clusters (Figure 3K and M). These results demonstrate that Notch signalling inhibition at the T/PT common primordium stage is sufficient to prevent normal parathyroid epithelium differentiation and to irreversibly compromise long-term organ formation.

Having shown parathyroids aplasia/hypoplasia in cultured explants deprived of Notch signals, we asked if Notch regulates cell-proliferation and/or cell-death during common primordium stages. 3/4PAR grown *in vitro* with 200nM of Ly was fixed and analysed *in situ*. Apoptotic and mitotic cells were identified by the presence of Casp3 (Suppl. Fig. 2A and B) and Phos-H3 (Suppl. Fig. 2C and D), at 24h and 48h of development, respectively. The number of $Casp3^{+}$ $E\text{-}Cad^{+}$ cells was similar in 24h-

cultured tissues, regardless of the drug treatment (1133±431 and 958±183 apoptotic cells/mm^2 of endodermal tissue in Control- and Ly-derived explants, respectively) (Suppl. Fig. 2A and B). When tissues were analysed after 48h in culture, no differences were observed in the number of Phos-H3 positive nuclei in experimental and control conditions (229±40 and 250±53 mitoses/mm^2 of endodermal tissue in Control- and Ly-derived explants, respectively). Moreover, almost no apoptotic features, characterized by pyknosis, were observed with DAPI staining (Suppl. Fig. 2C and D). Accordingly, similar survival rates were observed in CAM-derived explants [75% (n=6/8) in Graft-Control and 88% (n=8/9) in Graft-Ly], suggesting no involvement of Notch signalling in proliferation/cell death during 3/4PP endoderm development.

Altogether the results indicate that blocking Notch signalling activity during the common primordium stage impairs parathyroid gland formation, possibly by preventing normal epithelium differentiation, without affecting thymus development.

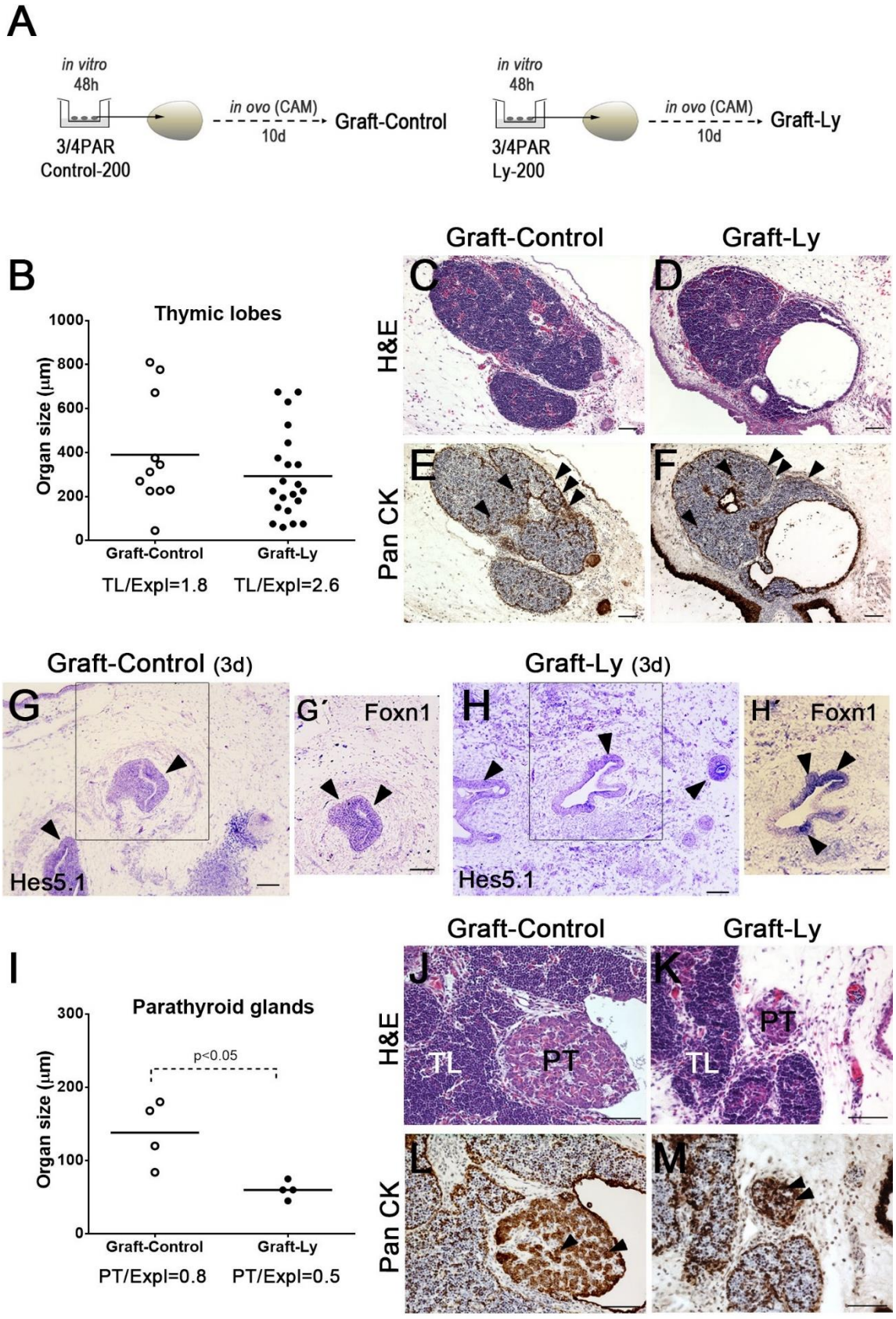

Figure 3. The effect of early-Notch signalling inhibition in the subsequent formation of the thymus and parathyroid glands. Schematic representation of the 3/4PAR grown *in vitro* for 48h in the absence (3/4PAR Control-200) or presence of 200nM of Ly (3/4PAR Ly-200) and then grafted in the CAM of a

cE8 embryo. Explants were allowed to develop *in ovo* for 10 days: Graft-Control, explants grown *in vitro* with DMSO; Graft-Ly, explants grown *in vitro* with Ly (A). The size of thymic lobes (B) and parathyroid glands (I) formed in CAM-derived explants. Serial sections of Graft-Control (C and E; J and L) and Graft-Ly (D and F; K and M) slides were H&E stained (C, D, J and K) and immunodetected with anti-Pan CK antibody and counterstained with Gill's hematoxylin (E, F, L and M). The expression of *Hes5.1* (G and H) and *Foxn1* (G´ and H´) was detected by ISH in serial sections of 3d Graft-Control (G and G´) and Graft-Ly (H and H´) slides. Black arrowheads point to immunoreactive positive cells (E, F, L and M) and to strong hybridization signals in the endoderm (G-H´). CAM, chorioallantoic membrane; Expl, explants; PAR, pharyngeal arch region; PT, parathyroid glands; TL, thymic lobe; 10d, ten days; 3d, three days. Scale bars, 50μm.

IV.3.4 Hedgehog modulates Notch signalling in the developing endoderm of the 3rd and 4th pharyngeal pouches.

Given the role of Notch as a modulator of Hh signalling in the dorso-ventral patterning of the neural tube (Stasiulewicz *et al*., 2015), we further investigated if Hh signalling could be modulated by Notch during T/PT common primordium formation.

We started by studying the expression of distinct Hh-related genes in pharyngeal tissues (Figure 4A-G). The expression of *Patched1* (Hh receptor), *Shh* (Hh ligand), *Gli1* and *Gli3* (Hh-target genes) was analysed during *in vitro* (Figure 4A) and *in vivo* (Figure 4B-G) development, as described above. *Shh* was the most highly expressed Hh-related gene in the developing 3/4PAR (Figure 4A). Its expression was confined to the endodermal territory of the central pharynx, excluding the 3/4PP (data not shown). The transcript levels of *Patched1* were maintained during 48h of culture and its hybridization signals were faint in all pharyngeal tissues (Figure 4B and E). Interestingly, *Gli1* and *Gli3* transcripts were significantly reduced during *in vitro* development. The *in situ* analysis of these genes revealed hybridization signals of *Gli1* (Figure 4C and F) and *Gli3* (Figure 4D and G) along the endoderm, mesenchyme and ectoderm of the 3/4PAR. However, *Gli3* expression was more evident in the anterior/dorsal tip- (Figure 4D) and posterior/dorsal tip-domains (Figure 4G) of the 3PP endoderm, at qE3 and qE4, respectively.

Having demonstrated which genes are involved in the activation of Hh in the 3/4PAR, we asked if blocking Notch activity could interfere with Hh signalling. The expression of Hh-related genes was quantified in 3/4PAR grown *in vitro* for 48h in the

presence of either Notch inhibitor. When compared to control conditions, no differences were observed in the transcript levels of the four genes in Ly- or DBZ-treated tissues (Figure 4H and I). These *in vitro* effects were confirmed by a Hh-related gene-expression analysis of embryos that had Notch signals blocked at similar developmental-time windows. No obvious changes in *Patched1*, *Gli1* and *Gli3* expression were observed in Ly-injected embryos, when compared to control embryos (Suppl. Fig. 3).

To clarify the interactions between the Notch and Hh pathways, we then questioned if Hh activity could modulate Notch signalling during common primordium formation. Pharyngeal tissues were treated with Cyclopamine (Cyc), a well-described teratogen known to inhibit Hh signal transduction by binding to the heptahelical bundle of Smoothened (Chen *et al*., 2002). In parallel, another Hh inhibitor Vismodegib (Vis) was used to validate the *in vitro* Hh inhibitory effects. The expression of Notch-target genes was then analysed in explants grown in the presence of these inhibitors to evaluate the capacity of Hh activity to modulate Notch during common primordium formation (Figure 4J and K). Explants grown in the presence of Cyc or Vis showed a significant reduction of *Hey1* (63% and 29%, respectively) and *Hes5.1* (79% and 60%, respectively) transcript levels, suggesting Notch signalling modulation by Hh during this developmental time-window. Concordantly, no changes were observed in the expression of *Hes6.1* and *Gata3*.

The block of Hh signalling was confirmed by the strong reduction of *Patched1* expression (80%) in tissues grown with either Hh inhibitor (Figure 4K), as previously described (Grevellec *et al*., 2011; Cordero *et al*., 2004). A significant reduction of *Shh* transcripts was also detected in Cyc-treated explants, as has been reported in other developmental contexts (Cordero *et al*., 2004). The expression levels of *Gli1* and *Gli3* were unchanged in both experimental conditions.

Finally, functional readouts of *in vitro* Hh inhibition with Cyc were evaluated (Suppl. Fig. 4). Consistent with results reported in the $Shh^{-/-}$ mice phenotype (Moore-Scott and Manley, 2005), a significant increase in *Foxn1* expression was accompanied with a reduction of the parathyroid-markers, *Gcm2* and *Pth*, in Cyc-treated explants (Suppl. Fig. 4A). The moderate reduction of *Gcm2* transcripts, in contrast with its absence in the mutant mice, is in accordance with a less responsive *Gcm2*-expression domain to Hh at these stages of development (Grevellec *et al*., 2011). Moreover, pharyngeal tissues with compromised Hh activity showed massive apoptosis, disruption of epithelial

integrity (Suppl. Fig. 4B´and C´) and low survival rates when grafted onto the CAM, resulting in thymic hypoplasia and abnormal parathyroid formation (Suppl. Fig. 4E-I´). The results are consistent with previous reports describing the role of Hh in the formation of pharyngeal endoderm-derived organs (Shah *et al.*, 2004; Moore-Scott and Manley, 2005; Outram *et al.*, 2009; Grevellec, Graham and Tucker, 2011).

Together, the data suggest a fine-tuning modulation of Notch and Hh pathways during T/PT common primordium formation. Importantly, Hh signalling may regulate Notch activity during this developmental time-window.

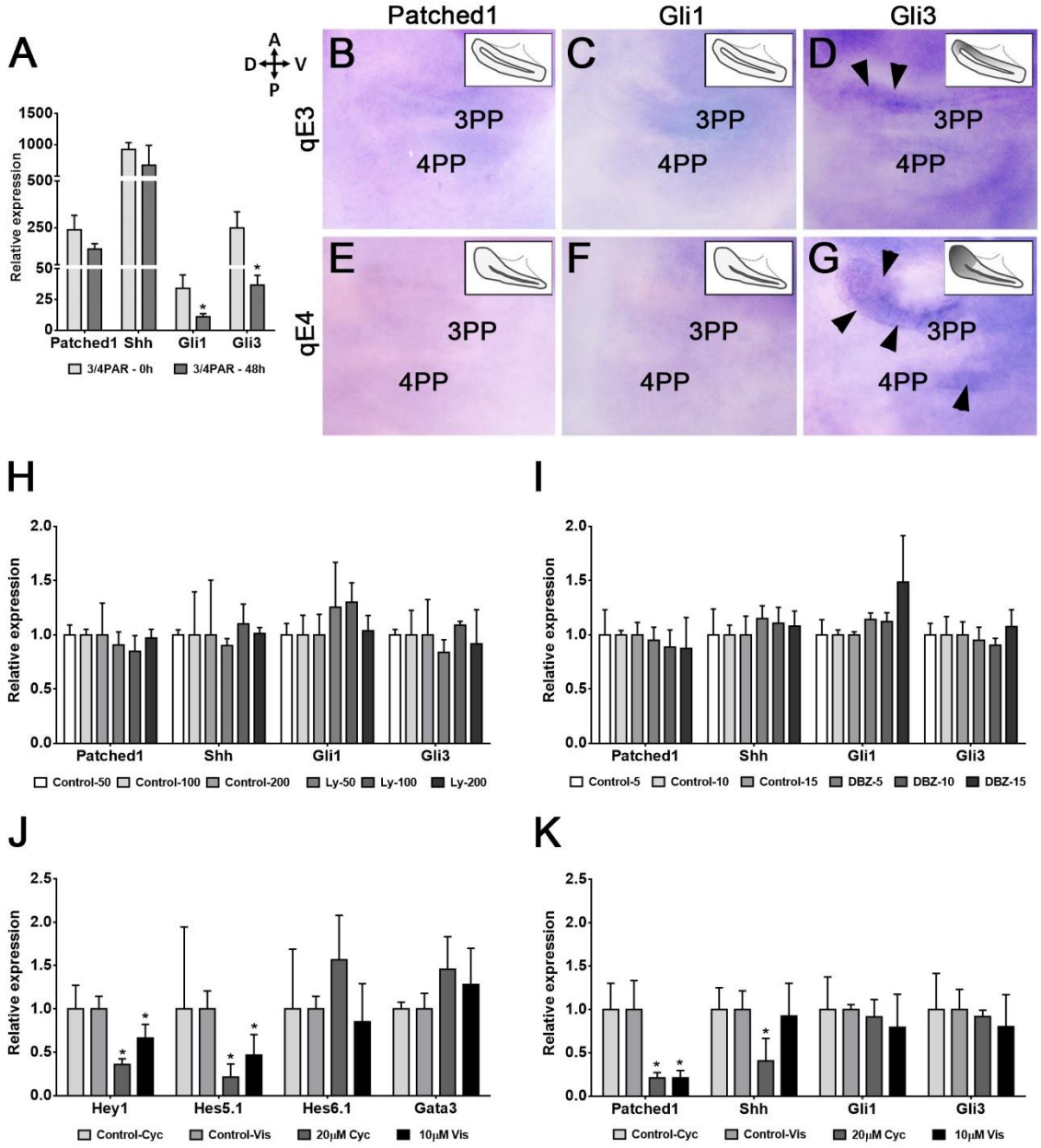

Figure 4. Crosstalk of Notch and Hh signalling pathways during T/PT common primordium formation. *In vitro* (A) and *in vivo* (B-G) expression of Hh-related genes in the 3/4PAR. The 3/4PAR at qE3 was mechanically isolated and grown *in vitro* for 48h. Gene-expression levels of freshly isolated (3/4PAR-0h) and cultured (3/4PAR-48h) tissues were examined by qRT-PCR (A). In parallel, *Patched1* (B and E), *Gli1* (C and F) and *Gli3* (D and G) expression was observed in the developing endoderm of the 3/4PP at qE3 (B-D) and qE4 (E-G). Schematic drawings in the top/right panels depict the gene-expression domains in the 3PP, the well-defined pouch. Notch (H and I) and Hh (J and K) inhibition *in vitro* assays. Expression levels of Hh-related (H, I and K) and Notch-related (J) genes in 3/4PAR grown *in vitro* for 48h in the presence of Ly (H), DBZ (I), Cyc and Vis (J and K) were examined by qRT-PCR. Expression of each transcript was measured as a ratio against the mean of the *Actb* and *Hprt* transcript expression levels and expressed in arbitrary units (each transcript in control=1). Black arrowheads point to the hybridization signals in the 3/4PP endoderm (D and G). A, anterior; Cyc, Cyclopamine; D, dorsal; DBZ, Dibenzazepine; Ly, LY-411.575; P, posterior; PAR, pharyngeal arch region; PP, pharyngeal pouch; qE, quail embryonic day; V, ventral; Vis, Vismodegib. Scale bars, 50μm.

IV.3.5 Hedgehog modulates Notch signalling in distinct domains of the developing endoderm of the 3rd and 4th pharyngeal pouches.

As shown above, Hh regulates the expression of Notch-target genes in cultured tissues. We therefore carried out *in vivo* modulation of Hh activity during the development of T/PT common primordium. Beads soaked with Cyc (6mM) were placed in the lumen of the pharynx through the second cleft and sited near the 3/4PP at cE2.5 and qE3. After 20-24h of development, embryos were fixed and analysed by WM-ISH for Notch-target genes and organ epithelial markers (Figure 5).

Embryos developed with low Hh activity in the pharyngeal region showed a reduction in *Gata3* expression in the anterior/median territory of the 3PP endoderm (Figure 5E, n=4/5), when compared with control embryos (Figure 5A, n=5/5). In the same pouch region, we observed the loss of *Gcm2* expression (Figure 5F, n=4/5), an expected result considering that $Shh^{-/-}$ mice have no *Gcm2* expression in the presumptive territory of the parathyroids (Moore-Scott and Manley, 2005). These results suggested that Hh activity positively regulates Gata3/Notch signals in the Gcm2/parathyroid-fated domain of the 3/4PP endoderm. However, embryos with Cyc-soaked beads (Cyc-beads) showed the maintenance of *Gata3* expression in the dorsal tip of the 3PP, the presumptive thymic domain (Figure 5E). At later stages, low Hh activity in the pharyngeal region led to a

decrease of *Gata3* expression in the 4PP endoderm of qE3 (a similar stage to cE3.5, Figure 5J) embryos (Figure 5G, n=3/3). This effect recapitulates the one observed in the 3PP at an earlier stage of development (cE2.5). This dynamic spatial and temporal action of Hh signalling has already been described for the modulation of *Gcm2* expression during PP development (Grevellec *et al.*, 2011).

To further investigate downstream targets of Hh signalling in the presumptive thymic rudiment, we screened for the expression of other Notch-related genes in 3/4PP endoderm. Several genes were studied, and their expression patterns were unaltered or inconsistently modified when Hh signalling was impaired (Suppl. Fig. 5A-F). Only *Lfng*, a Notch modulator, showed robust modified expression in these conditions. *Lfng* is normally expressed in the posterior/median territory of the 3PP endoderm (Figure 5D, n=4/4), the territory excluded from the T/PT common primordium, and in mesenchymal cells. In the absence of Hh signals, its expression was downregulated in the pouch and in some neighbouring cells (Figure 5H, n=4/4). Lfng is known to inhibit Jag1-mediated signalling and to potentiate Notch1 activation via the Delta1 ligand (Hicks *et al.*, 2000). In cE3, faint expression of *Notch1* (Figure 5I) and *Delta1* (Figure 5K) was observed in the endoderm and neighbouring cells of the 3PP. The expression of *Jag1* (Figure 5L) appeared more restricted to the anterior/median domain of the 3PP. The data indicate a preferential activation of Notch via Lfng/Delta1 in the posterior/median domain of the pouches.

Having in mind that the posterior boundary of Foxn1/thymus-fated domain is the *Lfng*-expression domain, we questioned if the territory of the former could be altered when Hh signalling was abolished. When compared to controls (Figure 5M, n=7/7), qE3 embryos with Cyc-beads presented an enlarged *Foxn1*-expression domain with stronger hybridization signals (Figure 5N, n=4/6). The expansion of the Foxn1/thymus-fated domain was from the dorsal tip to a more posterior/median region of the pouch. This territory partially overlapped with the *Lfng*-expression domain, which in turn was prevented in the absence of Hh. These results thus suggest that Lfng/Notch activity defines the posterior boundary of the Foxn1/thymus-fated domain, in an Hh-dependent manner.

Notably, an enriched expression of *Foxn1* was observed in the 2PP endoderm (Figure 5N), suggesting that Hh signalling prevents the Foxn1/thymus-fated domain in

the most anterior pouches. Similar ectopic and abnormal *Gcm2* expression in the 2PP was previously reported as a result of Hh inhibition (Grevellec *et al*., 2011).

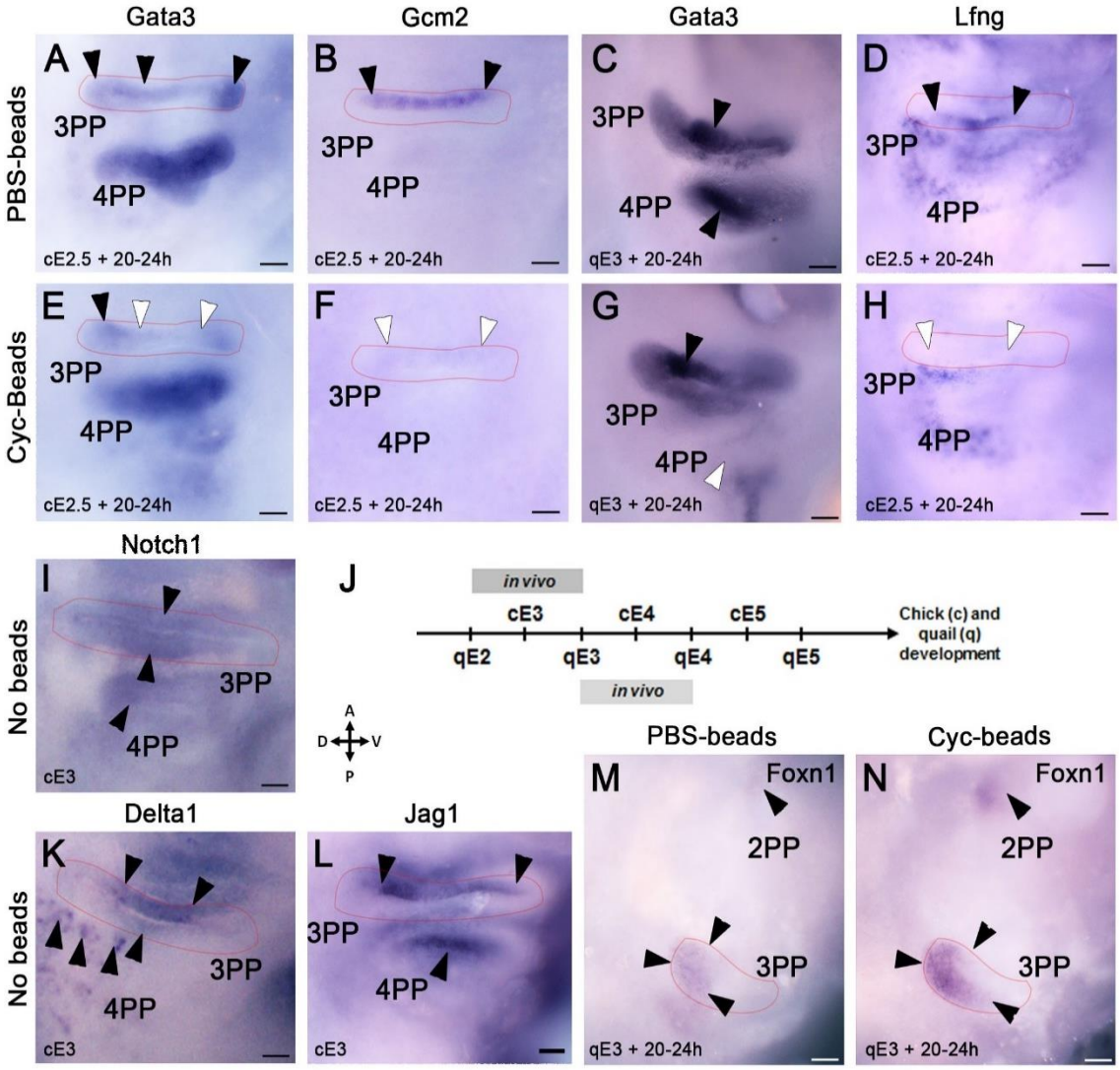

Figure 5. The effect of *in vivo* Hh signalling inhibition during T/PT common primordium formation. PBS-beads (A-D and M) and Cyc-beads (E-H and N) were implanted in the pharyngeal region of cE2.5 (A, B, D-F and H) and qE3 (C, G, M and N) and embryos allowed to develop for 20-24h. Expression of *Gata3* (A, C, E and G), *Gcm2* (B and F), *Lfng* (D and H) and *Foxn1* (M and N) was observed by WM-ISH. In parallel, the expression of *Notch1* (I), *Delta1* (K) and *Jag1* (L) was examined in the pharyngeal region of cE3. Timeline of *in vivo* assays in chicken and quail development (J). Faint red line delimits the 3PP endoderm. Black and white arrowheads point to strong and weak/absent hybridization signals in the PP endoderm, respectively. A, anterior; cE, chicken embryonic day; Cyc, cyclopamine; D, dorsal; P, posterior; PP, pharyngeal pouch; qE, quail embryonic day; V, ventral. Scale bars, 50μm.

IV.4 Discussion

In avian, as in mammals, the thymus and parathyroids epithelia derive from a common endodermal primordium of the pharyngeal pouches. This process involves the patterning of the pouches followed by rudiment specification. In this study, we propose that the temporal and spatial dynamics of the pharyngeal morphogenesis are regulated by Notch and Hh signals during the development of the T/PT common primordium and the formation of thymic and parathyroid rudiments.

IV.4.1 Thymus and parathyroids common primordium

In avian, as opposed to mice, the thymus and parathyroid epithelia derive not from one (3PP) but from two sequentially developing pharyngeal pouches, the 3PP and 4PP. Consistent with the temporal gap of 12h to 24h between the formation of the two pouches, a delay in the expression of several transcriptional regulators known to be involved in PP patterning and early-formation of these organs has also been observed (Manley and Condie, 2010). For example, *Gcm2* expression in the anterior domain of the 3PP was first reported at HH18 (cE3; qE2.5), prior to the formation of the 4PP. Only at HH22 (cE3.5; qE3) was the expression of *Gcm2* observed in the 4PP (Okabe and Graham, 2004). To overcome this complexity we opted to perform the *in vitro* studies at qE3 stage when both pouches are already formed.

We observed a consistent impairment in the development of the T/PT common primordium when Notch signalling was *in vitro* and *in vivo* inhibited (schematic representation in Figure 6A). The expression of thymic and parathyroid markers (*Foxn1* and *Gcm2/Pth*) was strikingly decreased. These effects were accompanied with the reduction of *Gata3*, suggesting that this Notch-target is a downstream mediator of Notch activity during common primordium development. In agreement, heterozygous mice mutants for Gata3 have smaller T/PT common primordium with fewer cells expressing *Gcm2* (Grigorieva *et al*., 2010).

When Hes1, another Notch-target, was deleted in neural crest cells, there was aplasia/hypoplasia of these organs, stressing the importance of driving specific Notch signals into distinct tissues during early stages of thymic and parathyroid formation (Kameda *et al.*, 2013). We have previously developed an *in vitro* experimental system

with the heterospecific association of quail and chicken tissues, which has allowed us to study epithelial-mesenchymal interactions during thymus and parathyroid organogenesis (Neves *et al.*, 2012). Insufficient information on quail and chicken genetic sequences has been a limiting step for discriminating tissues of different origin by qRT-PCR assays. As a consequence, the complete distinction of the endodermal and mesenchymal specific functions during organ formation, particularly important in a cell-cell contact signalling activation like in the Notch pathway, could not be fully addressed in this study.

We identified a new domain in the 3PP at qE3 (cE3.5), excluded from the common primordium, in which the Notch-modulator *Lfng*, and also *Fgf8* were expressed. The reduction of *Lfng* and *Fgf8* (Suppl. Fig. 4A) in the absence of Hh suggests that this domain may be involved in the regulation of T/PT common primordium development, in an Hh-dependent manner. These data, though limited, suggest a putative Shh-Fgf8-Lfng network, involving distinct signalling centres located in the endoderm of the pharynx and within the pouches. In other biological contexts, Lfng is known to respond to Fgf8 signals (Shifley *et al.*, 2008). On the other hand, Fgf8 has been shown to respond to Shh produced by the pharyngeal endoderm during arch patterning (Haworth *et al.*, 2007). And in the developing 3PP, a hyper-responsiveness to Fgf8 alters, at least in part, the initiation of parathyroid- and thymus-fated markers (Gardiner *et al.*, 2012).

The endoderm of the pharynx is indeed the main source of Hh signals, via Shh secretion, during the development of the T/PT common primordium (Figure 6B). The median/anterior and median/posterior territories of the developing pouches are closer to the source of Hh, as opposed to the tips, which will grow apart to more dorsal and ventral positions. At qE3, expression of various Notch-related genes is distributed along the pouches. The median/anterior region and tips of the pouch originate a *Gata3*-expression domain while the median/posterior territory gives rise to the *Lfng*-expression domain. The restricted median/anterior domain of *Gata3* also co-expresses *Gcm2*. As development proceeds, the *Gata3*/*Gcm2* domain starts to express *Pth* and becomes more restricted to a smaller central territory of the anterior/median region of the pouch (Figure 6A), originating the parathyroid rudiment at qE4 (Neves *et al*., 2012).

When Hh signals were abolished in the pharynx, downregulation of *Gata3*/*Gcm2* and *Lfng* expression was observed, indicating that the median domains of the pouches are positively regulated by Hh signalling. In contrast, the expression of *Gata3* was maintained at the tips of the pouches, suggesting that there are Gata3/Notch signals in the common

primordium that respond differently to Hh (schematic representations in Figure 6C). It is therefore conceivable that during the specification of the rudiments, the parathyroid-fated domain is more sensitive to Hh signalling, while the thymus-fated domain is unresponsive to Hh.

Overtime, the source of Shh gets further away and overall the pouches become less sensitive to Hh. In fact, the upregulation of *Gcm2* was reported to correlate with the loss of Hh receptor *Patched1* during 3PP development in mice (Grevellec *et al*., 2011).

IV.4.2 Parathyroid rudiment

The specification of the parathyroid rudiment is known to be dependent on *Gcm2* transcriptional activation. Deficiency of *Gcm2* in mice leads to the absence of parathyroid glands without affecting thymus formation (Liu *et al*., 2007). Notch-target *Gata3* (Fang *et al.*, 2007; Naito *et al.*, 2011) is one of the upstream regulators of *Gcm2*, as *Gata3*$^{-/-}$ mice showed no *Gcm2* expression and no gland formation (Grigorieva *et al.*, 2010). In this investigation, the decreased expression of *Gata3* was accompanied by a sharp reduction of *Gcm2* in the absence of Notch, demonstrating a Notch signalling activation requirement, via Gata3, for parathyroid epithelium differentiation. Evidence supporting this hypothesis was the loss of *Pth* expression and abnormal parathyroid formation, when common primordium was grown in the absence of Notch activity. It has been recently shown in mice that Gata3 cooperates with Gcm2 to activate *Pth* expression (Han, Tsunekage and Kataoka, 2015).

Apart from a possible role in epithelium differentiation, *Gata3*/Notch signals may also regulate cell survival in the parathyroid rudiment. The impairment of *Gcm2*/*Gata3*-Notch signals results in the reduced number and size of the parathyroids, in accordance with the mouse model where parathyroid precursors undergo rapid apoptosis in the absence of *Gcm2* (Lui *et al*., 2007). Although no differences were detected in the number of proliferating or apoptotic cells in the developing pharyngeal endoderm treated with Ly, we cannot exclude the role of Notch in these biological processes. *In situ* analysis showed small clusters of apoptotic cells on the endoderm grown *in vitro* for 24h (not shown). This suggests well-defined domains with a tight regulation of cell numbers that may correspond to organ rudiments, that is, the parathyroid glands. We also postulate that these untraced apoptotic events may occur even earlier during *in vitro* development.

During the course of our study we further attempted to identify the Notch ligands involved in PT rudiment formation. Only *Jag1* was confined to the median/anterior territory of the pouches at cE3, overlapping with the *Gcm2*/parathyroid-fated domain. The capacity of *Jag1*-expressing cells to define boundaries by lateral inhibition has been reported in other developmental processes (Kiernan, 2013). In this study, the *Jag1*-expression domain, as opposed to the *Gata3*/*Gcm2*/parathyroid-fated domain, was not altered when the pharyngeal source of Hh was abolished (Suppl. Fig. 5B), suggesting that Jag1 defines the boundary of the rudiment independent of Hh. It may be that parathyroid cell-fate specification, accompanied by the definition of the boundary of the rudiments, occurs earlier in development. In agreement with this, the location of the parathyroid dorsal boundary appears to be unchanged when *Gcm2*/*Pth* expression is lost.

Nevertheless, the theory that there is positive regulation of Hh in settling the *Gata3*/*Gcm2*/parathyroid-fated domain is supported by the abnormal morphology and size of the glands in the absence of Hh signalling.

IV.4.3 Thymic rudiment

The individual thymic rudiment was previously identified by the *Foxn1*-expression domain in the dorsal tip of the pouches at qE4 (Neves *et al*., 2012). In this work we show that *Foxn1* expression was strongly reduced when Notch signalling was impaired. The early downregulation of *Foxn1* could however be reversed by subsequent restitution of Notch signalling activity in the thymic rudiment.

Notch signalling is known to play a unique function in the control of hair follicle differentiation by modulation of *Foxn1* (Hu *et al.*, 2010). Although hair is an epidermal appendage that arose after the last shared common ancestor between mammals and birds, embryonic chicken feathers and nails also express *Foxn1*, demonstrating the conservation of these developmental processes during evolution (Darnell *et al.*, 2014). In addition, nude mice (*Foxn1*$^{-/-}$) have two major defects, abnormal hair growth and defective development of the thymic epithelium (Blackburn *et al.*, 1996; Nehls *et al.*, 1996; Bleul *et al.*, 2006), suggesting a common Notch-Foxn1 pathway in both developmental processes.

The Notch-target gene *Gata3* may be one of the upstream regulators of *Foxn1*, since *Gata3* is expressed in the dorsal tip of the 3/4PP endoderm during T/PT common primordium formation. At this developmental stage, *Gata3* in the prospective thymic rudiment is modulated by Notch (schematic representation in Figure 6C).

When Hh signalling was blocked, we observed an expansion of the *Foxn1*/thymus-fated domain to a more median/posterior region, at the expense of the loss of *Lfng*–expression domain (Figure 6C). The capacity of the thymic rudiment to expand posteriorly suggests some degree of cell-fate plasticity of endodermal cells in the posterior/median domain of the pouch. Together with *Lfng*, the only Notch ligand faintly expressed in the median/posterior territory of the pouches was *Delta1*. Lfng typically enhances Notch activation by ligands belonging to the Delta family and reduces Notch activation by Jagged family ligands (reviewed in (Stanley and Okajima, 2010)). This suggests that the posterior thymic boundary is determined by a lateral inhibition mechanism via Delta1. In the absence of Hh signals in the pharyngeal region, the disappearance of the *Lfng*-expression domain may result in reduced Delta1 activity and boundary displacement. Specifically, a reduction of the Delta1 signalling strength gradient may result in an augmentation of the posterior thymic rudiment territory. Here, we report the previously unreported regulation of the posterior boundary of thymic rudiment by Notch signalling via Lfng, in an Hh-dependent manner (Figure 6C).

Another Notch-target gene, *Hey1,* was markedly reduced when Notch activity was blocked in the pharyngeal tissues. Although *Hey1* expression was not restricted to the endoderm of the pouches, our data suggest its involvement in the primordium development. In agreement, a recent report showed *Hey1* expression in the thymic epithelium of mice (Subhan *et al.*, 2013).

The transcription factor Pax1, important for thymus (Dietrich and Gruss, 1995; Wallin *et al*., 1996) and parathyroids (Su *et al*, 2001) formation, was also downregulated when Notch signalling was inhibited, suggesting that Notch may act upstream of Pax1 during T/PT common primordium development. Taking into account that *Pax1* is expressed very early in pouch formation (not shown) and during thymic epithelium differentiation; it is therefore conceivable that distinct mechanisms may positively regulate *Pax1*, from pharyngeal pouch morphogenesis to thymus organogenesis. A biphasic role in these distinct windows of development was recently described for the activity of another transcription factor, the *Tbx1* gene (Reeh *et al.*, 2014).

In conclusion, our work shows that Notch signalling is crucial for T/PT common primordium development and parathyroid formation, in an Hh-dependent manner. Finally, we conclude that, despite the evolutionary distance, the regulatory mechanisms controlling the formation of these organs appear to be conserved in avian and mammals.

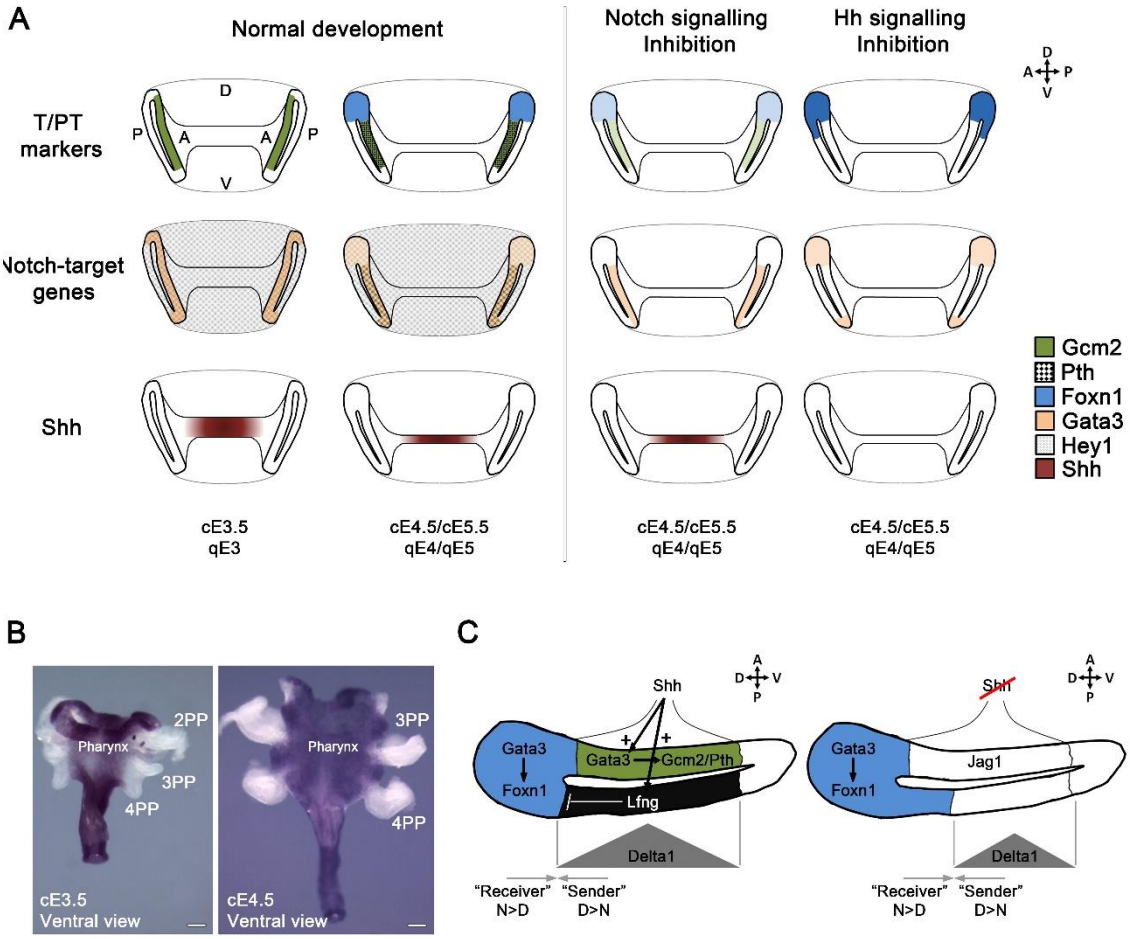

Figure 6. Model of Hh and Notch signalling modulation during thymic and parathyroid rudiment formation. Schematic representation of the results obtained during *in vivo* and *in vitro* assays (A). Cross sections of the most ventral region of the embryo and expression of T/PT markers, Notch-target genes and Shh in 3PP endoderm during normal development and when Notch and Hh signalling is inhibited (A). Expression of *Shh* in isolated pharyngeal endoderm examined by WM-ISH at cE3.5 and cE4.5 (B). Schematic model of Notch and Hh signalling crosstalk during T/PT common primordium formation during normal development and in the absence of Hh signalling (C). In detail is depicted a proposed model for the lateral inhibition mechanism involved in the median/posterior thymic boundary definition. In this case, the relative levels of Notch and Delta determine the cell's signalling state. The cell with more Notch than Delta becomes a 'receiver' and cells with more Delta than Notch become 'sender' cells. In the absence of Hh, reduction of the Delta1 signalling gradient shifts the boundary to a more median position within the pouch. Arrows indicate putative signalling crosstalk (see Discussion for details). A, anterior; cE, chicken embryonic day; D, dorsal; D>N, Delta>Notch; N>D, Notch>Delta; P, posterior; PP, pharyngeal pouch; qE, quail embryonic day; V, ventral. Scale bars, 100μm.

IV.5 Supplementary Data

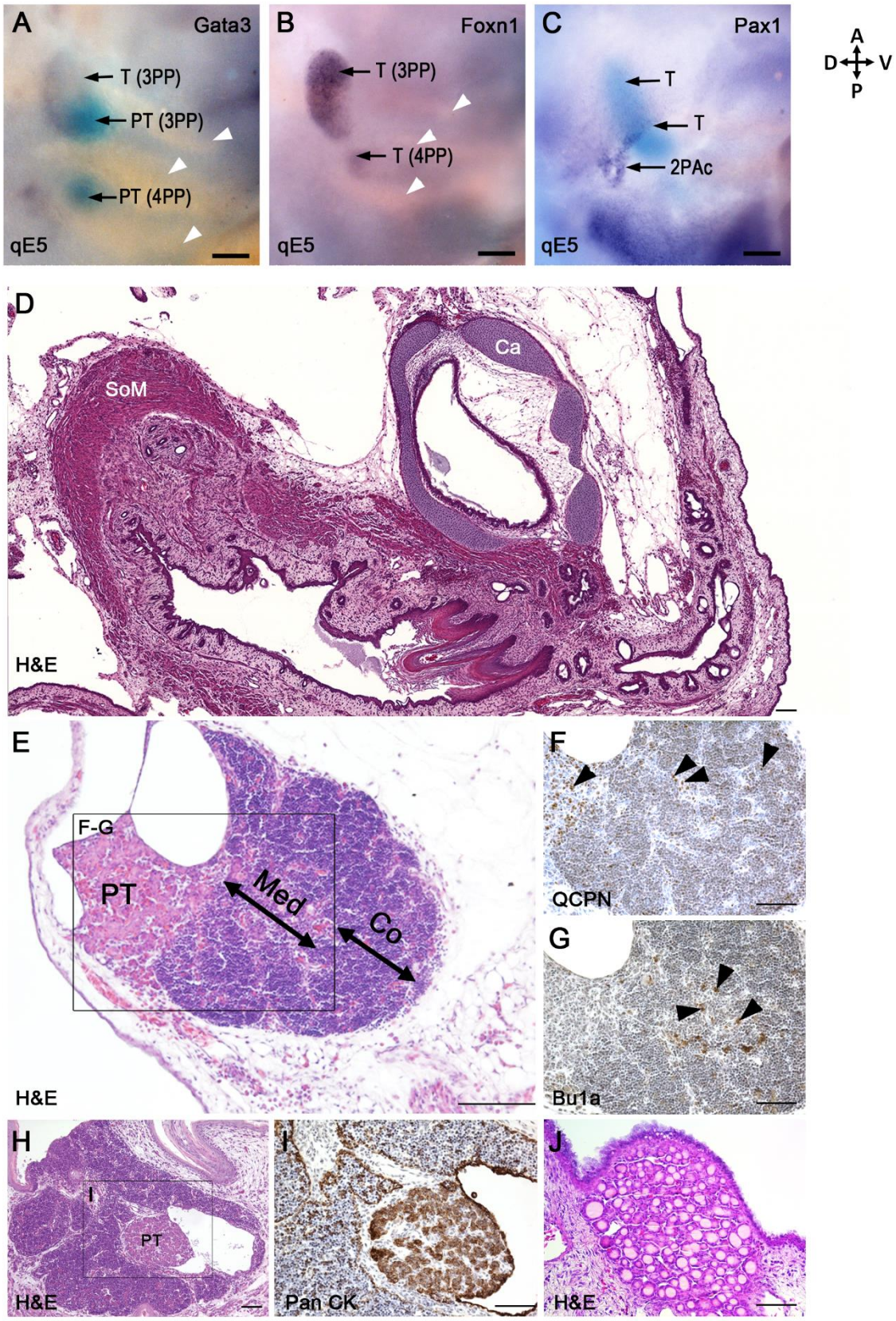

Figure S1. Gene expression in the pharyngeal arch region and organ formation in CAM. Expression of *Gata3* (A), *Foxn1* (B) and *Pax1* (C) in quail embryos at E5 detected by WM-ISH. BM purple detection

allowed discrimination between more internal (light blue) (parathyroid rudiment in A) and superficial (purple) hybridization signals (thymic rudiment in A). Formation of organs from explants grafted onto CAM and developed *in ovo* for 10 days (D-J). Sections of quail 3/4 PAR explants grown for 48h *in vitro* followed by 10 days *in ovo* development. Single (D and J) and serial sections (E-G and H-I) were processed for H&E staining (D, E, H and J) and immunodetected with anti-QCPN (Developmental Studies Hybridoma Bank; for labelling of quail cells) (F), anti-Bu1a (SouthernBiotech; for labelling B-cells) (G) and anti-Pan CK (I) antibodies counterstained with Gill's hematoxylin (blue staining). Transverse section of distinct "organ-like structures": respiratory mucosa involved by cartilage; gut mucosa, with single and stratified epithelium surrounded by arranged layers of smooth muscle (D). Transverse section of chimeric thymus, with clear discrimination between cortical and medullary compartments (E) and with quail-derived thymic epithelial cells ($QCPN^+$- brown staining) and lymphoid cells of host origin (F). Rare B-cell population in thymic medullary and cortical compartments (G). Transverse section of parathyroid gland (H), with parenchymal cells arranged in clusters (Pan CK^+- brown staining), encircled by capillaries and surrounded by a connective tissue capsule (I). Transverse section of thyroid gland with multiple follicles filled with luminal colloid (J). Black and white arrowheads indicate immunoreactive positive cells and pharyngeal arches, respectively. A, anterior; Ca, cartilage; Co, cortex of the thymus; D, dorsal; Med, medulla of the thymus; P, posterior; PAc, pharyngeal arch closure; PT, parathyroid glands; qE, quail embryonic day; SoM, smooth muscle; T, thymus; V, ventral. Scale bars, 50μm (A-C) and 100μm (D-J).

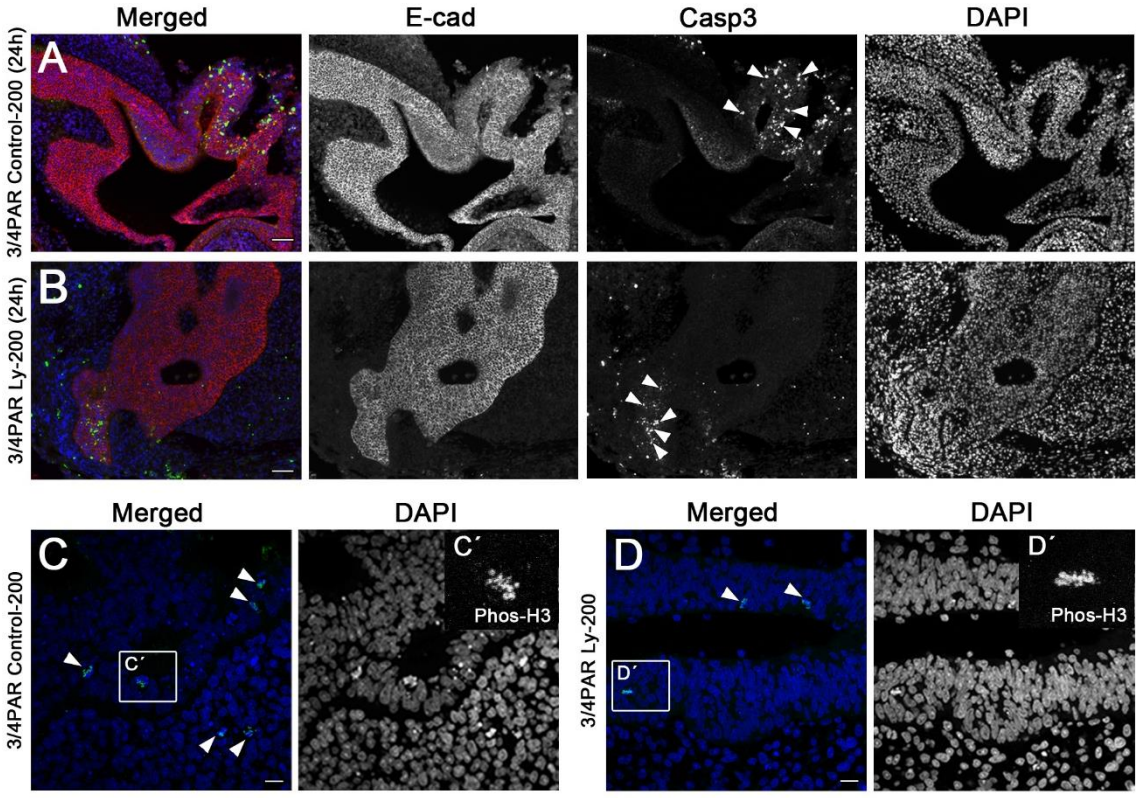

Figure S2. Proliferation and apoptosis of developing 3/4PAR in the absence of Notch signalling. Sections of 3/4PAR grown *in vitro* for 24h (A and B) and 48h (C and D) with DMSO (A and C) and Ly (B and D) were immunostained with anti-E-Cad/anti-Casp3 (A and B) and anti-Phospho-H3 (C and D) counterstained with DAPI. Detail of Phospho-H3 positive cells (C´ and D´). Paraffin sections of 24h-explants were treated for immunofluorescence with the anti-Caspase 3 (Casp3) antibody [anti-cleaved caspase-3 (Asp175) from Cell Signaling, for apoptotic cells] and anti-E-cadherin (E-cad) antibody (BD-610181 from BD Biosciences, for epithelial cells) and counterstained with DAPI, according to the manufacture instructions. Paraffin sections of 48h-explants were treated for immunofluorescence with the Anti-phospho-Histone H3 (Phos-H3) antibody (Anti-phospho-Histone H3 [pSer^{10}], H0412 from Sigma, for mitotic cells) and counterstained with DAPI, according to the manufacture instructions and as described (Neves *et al*., 2012). Three randomly distributed slides with eight pieces per slide were selected from each explant sample. Three explant samples were analysed per culture condition. In each sample image, a Z-pile of 7.6µm (0.4µm sections) was collected using the Metamorph Software (Version 7.7.9.0) and Zeiss Axiovert 200M microscope with Roper Scientific HQ CoolSnap camera. Image J Software (version 1.49T) was used for apoptosis/µm^2 and mitoses/µm^2 counting. Immunofluorescence images were acquired with Zeiss LSM 510 META confocal microscope using LSM510 (version 4.0SP2) software. Scale bars, 50µm (A and B) and 10µm (C and D).

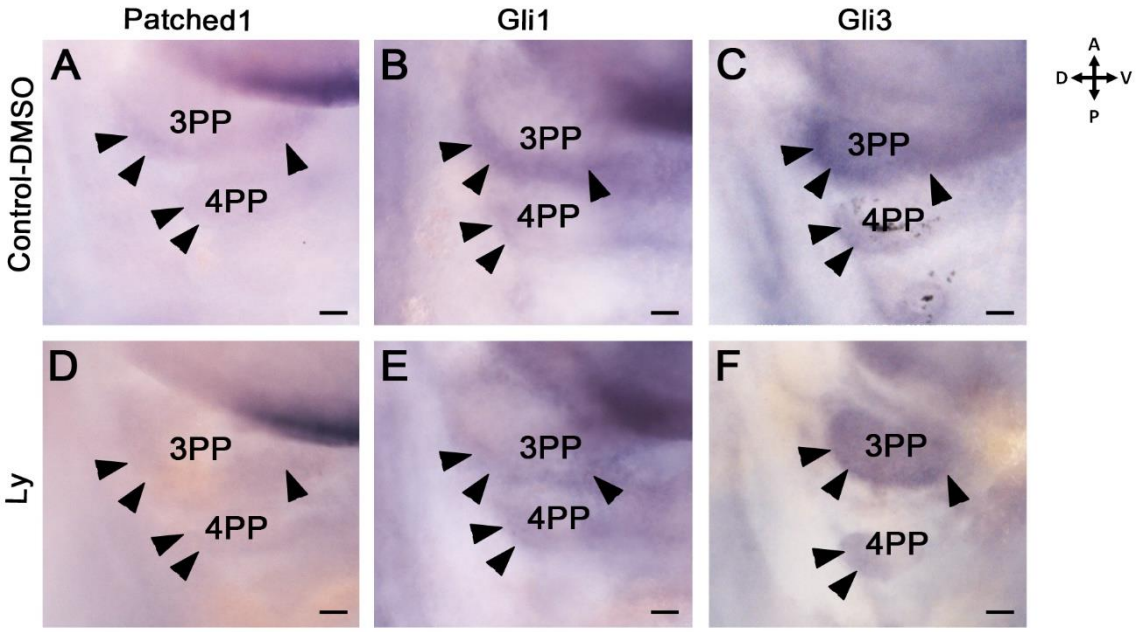

Figure S3. Modulation of Hh-related genes expression in the absence of Notch signalling during T/PT common primordium formation. Expression of *Patched1* (A and D), *Gli1* (B and E) and *Gli3* (C and F) detected by WM-ISH in the 3/4PAR of cE3.5 embryos developed for 20-24h after Ly (D-F) or DMSO (A-C) injection. Black arrowheads point to hybridization signals in the 3/4PP endoderm. A, anterior; D, dorsal; Ly, LY-411.575; P, posterior; PP, pharyngeal pouch; V, ventral. Scale bars, 50µm.

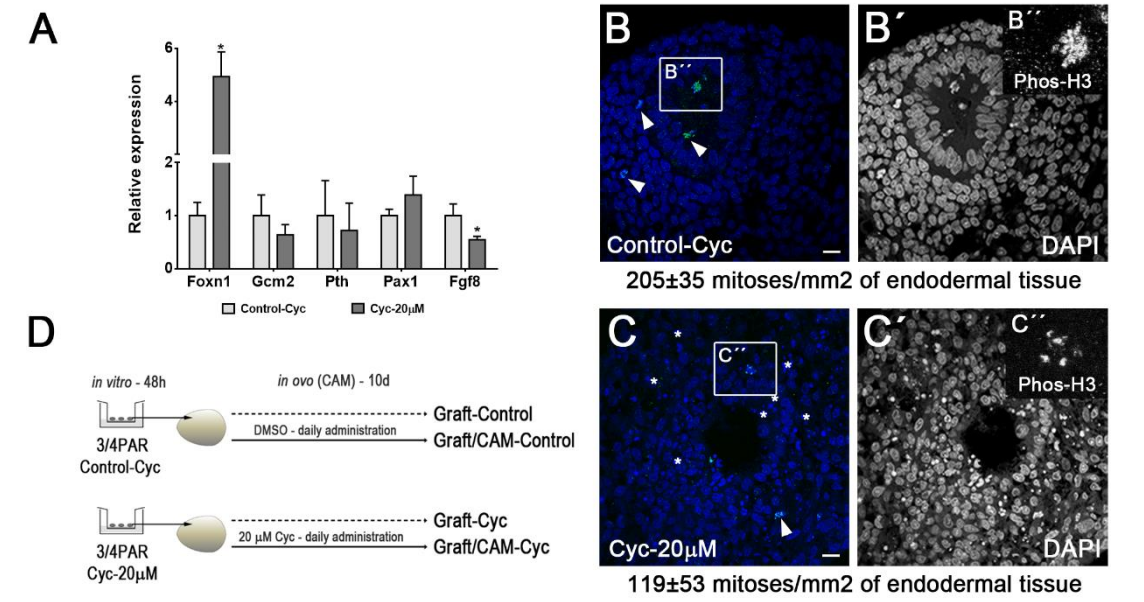

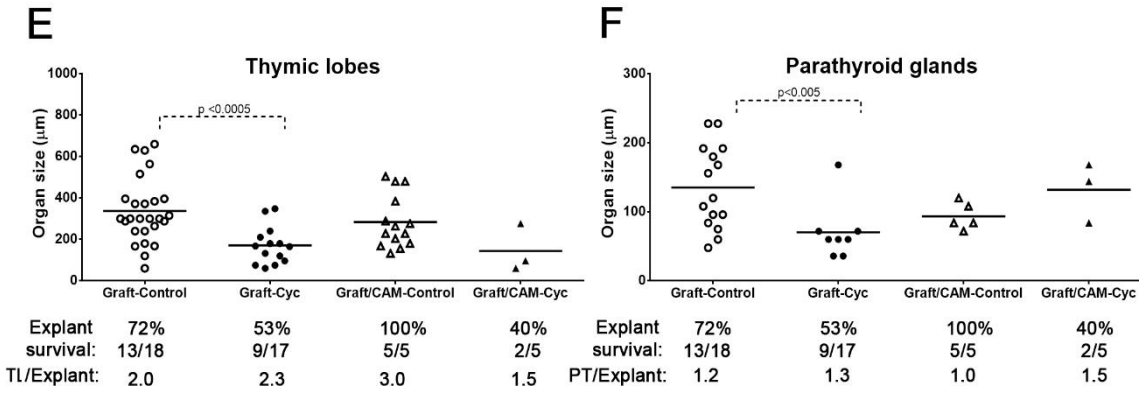

Explant survival:	72% 13/18	53% 9/17	100% 5/5	40% 2/5
TL/Explant:	2.0	2.3	3.0	1.5

Explant survival:	72% 13/18	53% 9/17	100% 5/5	40% 2/5
PT/Explant:	1.2	1.3	1.0	1.5

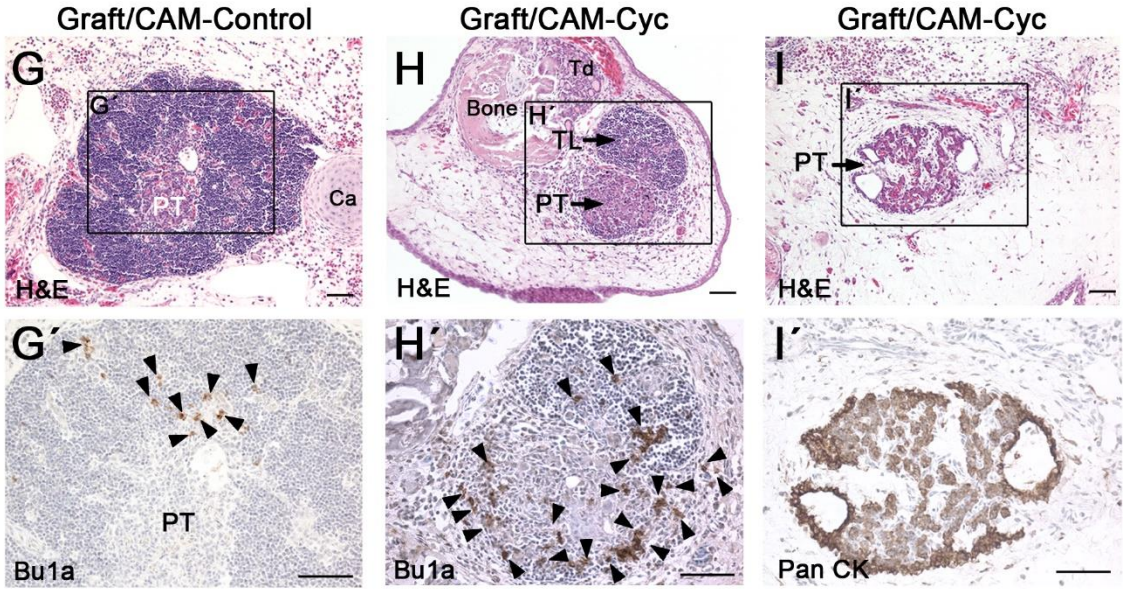

Figure S4. The effect of Hh signalling inhibition in the formation of the thymus and parathyroid glands. For Hh inhibition *in vitro* assay, pharyngeal tissues were grown with 20μM of Cyc and the expression levels of thymic, parathyroid and PP endoderm markers were assessed in cultured tissues by qRT-PCR (each transcript in control=1) (A). Sections of tissues cultured for 48h with DMSO (B and B´) and with 20μM Cyc (C and C´) were immunostained with anti-Phospho H3 antibody counterstained with DAPI. Detail of Phospho-H3 positive cells (B´´ and C´´). Schematic representation of the 3/4PAR grown *in vitro* for 48h in the absence (3/4PAR Control-Cyc) or presence of 20μM Cyc (3/4PAR Cyc-20μM) and further grafted onto CAM of a chicken embryo at E8. Explants were allowed to develop *in ovo* for further 10 days: Graft-Control, explants grown *in vitro* with DMSO; Graft-Cyc, explants grown *in vitro* with Cyc; Graft/CAM-Control, explants grown *in vitro* and *in ovo* with DMSO; Graft/CAM-Cyc, explants grown *in vitro* and *in ovo* with Cyc (D). The sizes of thymic lobes (E) and parathyroid glands (F) formed in CAM-derived explants. Serial sections of Graft/CAM-Control (G and G´) and Graft/CAM-Cyc (H and H´, I and I´) slides were H&E stained (G-I) and immunodetected with anti-Bu1a antibody (G´ and H´) and anti-Pan CK antibody (I´) counterstained with Gill's hematoxylin. Briefly, Graft/CAM-Cyc explants showed a reduction in the number and sizes of thymic lobes along with an augmentation of B-cells (H´). A slight increase in the number and size of parathyroid glands was observed. However, gland hyperplasia was due to expanded mesenchymal spaces along with abnormal epithelial morphology and irregular encapsulation (I´). Expression of each transcript was measured as a ratio against the *Actb* and *Hprt* transcripts mean and expressed in arbitrary units (each transcript in control=1). Ca, cartilage; CAM, chorioallantoic membrane; PAR, pharyngeal arch region; PT, parathyroid glands; TL, thymic lobes; 10d, ten days. White (B and C) and black (G´and H´) arrowheads point immunoreactive positive cells. White asterisks highlight some apoptotic cells (C). Black and white scale bars represent 50μm and 10μm, respectively.

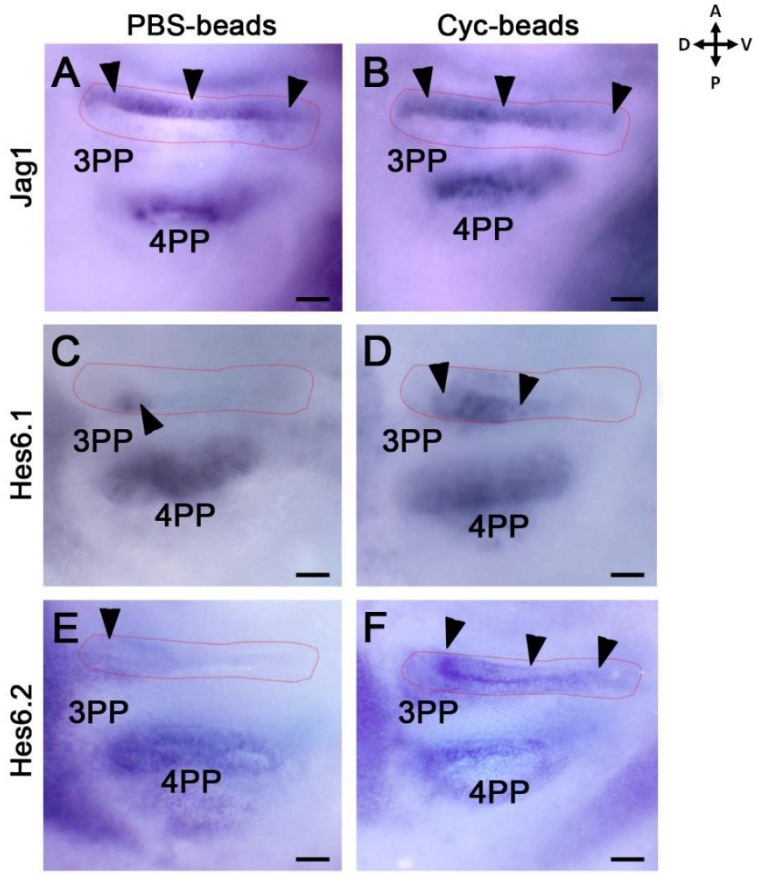

Figure S5. The effect of *in vivo* inhibition of Hh signalling during T/PT common primordium formation. PBS-beads (A, C and E) and Cyc-beads (B, D and F) were implanted in the pharyngeal region of cE2.5 and embryos allowed to develop for further 20-24h. Expression of *Jag1* (A and B), *Hes6.1* (C and D) and *Hes6.2* (E and F) was detected by WM-ISH. Faint red line delimits the 3PP endoderm. Black arrowheads point to strong hybridization signals. A, anterior; cE, chicken embryonic day; Cyc; cyclopamine; D, dorsal; P, posterior; PP, pharyngeal pouch; V, ventral. Scale bars, 50µm.

CHAPTER V

Isolation of Embryonic Tissues and Formation of Quail-Chicken Chimeric Organs Using The Thymus Example

Marta Figueiredo & Hélia Neves

Instituto de Histologia e Biologia do Desenvolvimento, Faculdade de Medicina da Universidade de Lisboa, Edifício Egas Moniz, Piso 3, Ala C, Av. Prof. Egas Moniz, 1649-028 Lisboa, Portugal

In Journal of Visualized Experiments 2019, 144, e58965

Invitation by Indrani Mukherjee, JoVE's Senior Science Editor

CHAPTER V - ISOLATION OF EMBRYONIC TISSUES AND FORMATION OF QUAIL-CHICKEN CHIMERIC ORGANS: THE THYMUS EXAMPLE.

V.1 Short Abstract

This article provides a method to isolate pure embryonic tissues from quail and chicken embryos that can be combined to form ex vivo chimeric organs.

V.2 Long Abstract

The capacity to isolate embryonic tissues was an essential step for establishing the quail-chicken chimera system, which in turn has provided undisputed contributions to unveiling key processes in developmental biology.

Herein is described an optimized method to isolate embryonic tissues from quail and chickens by microsurgery and enzymatic digestion while preserving its biological properties. After isolation, tissues from both species are associated in an *in vitro* organotypic assay for 48h. Quail and chicken tissues can be discriminated by distinct nuclear features and molecular markers allowing the study of the cellular cross-talk between heterospecific association of tissues. This approach is, therefore, a useful tool for studying complex tissue interactions in developmental processes with highly dynamic spatial modifications, such as those occurring during pharyngeal morphogenesis and the formation of the foregut endoderm-derived organs. This experimental approach was first developed to study the epithelial-mesenchymal interactions during early-stages of thymus formation. In this, the endoderm-derived prospective thymic rudiment and mesoderm-derived mesenchyme were isolated from quail and chicken embryos, respectively.

The capacity of the associated tissues to generate organs can be further tested by grafting them onto the chorioallantoic membrane (CAM) of a chicken embryo. The CAM provides nutrients and allows gas exchanges to the explanted tissues. After 10 days of *in ovo* development, the chimeric organs can be analysed in the harvested explants by conventional morphological methods. This procedure also allows studying tissue-specific contributions during organ formation, from its initial development (*in vitro* development) to the final stages of organogenesis (*in ovo* development).

Finally, the improved isolation method also provides three-dimensionally (3D) preserved embryonic tissues, that can also be used for high-resolution topographical analysis of tissue-specific gene-expression patterns.

V.3 Introduction

In the early 1970s, an elegant quail-chicken chimera system was developed by Le Douarin, opening new avenues to understand the role of cell migration and cellular interactions during development, (Le Douarin and Teillet, 1973; Le Douarin, 2005). The model was devised on the premise that cell exchange between the two species would not significantly disturb embryogenesis, later confirmed when used to study numerous developmental processes, including the formation of the nervous and the hematopoietic systems (Le Douarin, 2005). Taking the latter as an example, the cyclic waves of hematopoietic progenitors colonizing the thymic epithelial rudiment was first observed using the quail-chicken chimera system (Le Douarin and Jotereau, 1975). For that, the prospective territory of the thymus, the endoderm of the third and fourth pharyngeal pouches (3/4PP), was mechanically and enzymatically isolated from quail (q) embryos at 15 to 30-somite stage [embryonic day (E) 1.5- E2.5]. These stages correspond to chicken Hamburger and Hamilton (HH) - stages 12-17 (Hamburger and Hamilton, 1951). The isolation procedures started with the use of trypsin to enzymatically dissociate the endoderm from the attached mesenchyme. The isolated endoderm was grafted into the somatopleura region of a host chicken (c) embryo at E3-E3.5 (HH-stages 20-21). This heterologous mesenchyme was considered "permissive" to thymic epithelium development contributing also to the organ formation (Le Douarin and Jotereau, 1975). Afterward, successive waves of chicken host blood-borne progenitor cells infiltrated the quail donor thymic epithelial counterpart contributing to thymus formation in the host embryo (Le Douarin and Jotereau, 1975).

More recently, a modified version of this approach was also proven to be important for studying epithelial-mesenchymal interactions during early-stages of thymus formation (Neves *et al.*, 2012). In this respect, the tissues involved in the formation of the ectopic thymus in chimeric embryos (Le Douarin and Jotereau, 1975) were isolated, both from donor and host embryos, and associated *ex vivo*. An improved protocol was used to isolate the quail 3/4PP endoderm (E2.5-E3) and the chicken somatopleura mesoderm (E2.5-E3). Briefly, embryonic tissues were isolated by microsurgery and subject to *in vitro* pancreatin digestion. Also, the conditions of enzymatic digestion, temperature and time of incubation were optimized according to tissue-type and developmental stage (Table 1).

Table 1. Conditions of enzymatic digestion during embryonic tissues isolation.

Isolated tissue	Stage of development	Concentration	Temperature	Incubation period
Pharynx endoderm	qE2-E2.5	8mg/mL	On ice	45-60min
	cE2.5-E3			
	qE3	8mg/mL	On ice	60-90min
	cE3.5			
	qE4	8mg/mL	On ice	90min
	cE4.5			
Somatopleura mesoderm	qE2-E2.5	8mg/mL	On ice	30-50min
	cE2.5-E3			

c, chicken; E, Embryonic day; q, quail.

Next, the isolated tissues were associated in an organotypic *in vitro* system for 48h, as previously reported (Takahashi, Bontoux and Le Douarin, 1991; Neves *et al.*, 2012). The *in vitro* association of tissues mimics the local cellular interactions in the embryo, overcoming some restrictions of the *in vivo* manipulation. This system is particularly useful to study cellular interactions in complex morphogenic events, such as the development of the pharyngeal apparatus.

The contribution of each tissue in thymus histogenesis, as well as the ability of the heterospecific association to generate a thymus can be further explored using the CAM methodology, previously detailed (Neves *et al.*, 2012; Figueiredo *et al.*, 2016; Figueiredo and Neves, 2018). Succinctly, the cultured tissues were grafted onto the CAM of cE8 embryo and allowed to develop *in ovo* for 10 days. Then, thymus formation was evaluated by morphological analysis in the harvested explants. As in the classical quail-chicken studies (Le Douarin and Jotereau, 1975), the quail thymic epithelium was colonized by hematopoietic progenitor cells (HPCs) derived from the chicken embryo, which was later shown to contribute to organ development (Blackburn *et al.*, 1996; Nehls *et al.*, 1996). The HPCs migrate from the embryo to the ectopic chimeric thymus through the highly vascularized CAM (Neves *et al.*, 2012; Figueiredo *et al.*, 2016; Figueiredo and Neves, 2018). Quail derived thymic epithelium can be identified by immunohistochemistry using species-specific antibodies (*i.e*, QCPN- MAb Quail PeriNuclear), overcoming the need for tissue-specific molecular markers.

This experimental method, as the two-step approach reported in previous publication (Figueiredo and Neves, 2018), allows the modulation of signalling pathways by regular administration of pharmacological agents during *in vitro* and *in ovo* development. Also, explants can be harvested at any time-point of the course of the experiment (Figueiredo and Neves, 2018).

Lastly, the isolation protocol here detailed allows the preservation of the natural properties and 3D-architecture of embryonic tissues, particularly useful for detailing *in situ* gene-expression patterns of embryonic territories otherwise inaccessible by conventional methods. In addition, transcriptome analysis approaches, including RNA-seq or microarrays, can also be applied in isolated tissues without requiring genetic markers while providing a tissue-specific high throughput "omics" analysis.

V.4 Protocol

(Table of Materials in Appendix II)

All these experiments follow the animal care and ethical guidelines of the Centro Académico de Medicina de Lisboa.

1. Fertilized quail and chicken egg incubation

1.1) Place fertilized eggs of Japanese quail (*Coturnix coturnix japonica*) in a 38°C humidified incubator for 3 days. Incubate the eggs (egg blunt end) facing up in the air chamber.

Note: The humidified environment is achieved by placing a water container at the bottom of the incubator.

1.2) Incubate fertilized eggs of chicken (*Gallus gallus*) for 2.5 days in a 38°C humidified incubator. Incubate the eggs in a horizontal position and mark the upper side using a piece of charcoal to identify the embryo location.

Note: Start with 40 quail eggs and 60 chicken eggs when establishing this experiment.

2. Isolation of quail endoderm containing the prospective domain of the thymic rudiment

Note: Use a horizontal laminar flow hood and sterilized instruments and materials for egg manipulation procedures in sterile conditions.

2.1) Remove the embryonic region containing the presumptive territory of thymic rudiment, the pharyngeal arch region containing the 3rd and 4th arches (3/4PAR), as described (Figueiredo *et al.,* 2016; Figueiredo and Neves, 2018).

2.1.1) Fill a large borosilicate glass bowl (100mm x 50mm; 100cm^3) with 60mL of cold phosphate-buffered saline solution (PBS).

2.1.2) With the help of curved scissors, tap and cut a circular hole in the shell of a quail egg that has been incubated for 3 days. Make the hole on the opposite side of the egg blunt and transfer the yolk (with the embryo) to the bowl with cold PBS.

2.1.3) Remove the embryo from the yolk by cutting the vitelline membrane externally to extra-embryonic vessels using curved scissors.

2.1.4) With the help of thin forceps, transfer the embryo to a small bowl (60mm x 30mm; 15cm^3) filled with 10mL of cold PBS.

2.1.5) With a skimmer, move the embryo to a 100mm Petri dish with a black base (see Table of Materials) containing 10mL of cold PBS and place it under a stereomicroscope.

2.1.6) Dissect the 3/4PAR, as previously described (Figueiredo and Neves, 2018).

2.1.7) Aspirate the 3/4PAR and transfer to a glass dish three-quarters filled with cold PBS using a 2mL sterile Pasteur pipette.

2.2) Isolate the endoderm containing the presumptive territory of thymic rudiment (the 3/4PP endoderm) by enzymatic digestion with pancreatin.

2.2.1) With the help of spatula and thin forceps, transfer the 3/4PAR to a glass dish three-quarters filled with cold pancreatin (8mg/mL; 1:3 dilution 25mg/mL with cold PBS).

2.2.2) Incubate for 1h on ice for enzymatic digestion.

Note: The time of enzymatic digestion depends of the stage of development (**Table 1**).

2.2.3) Place the glass dish under the stereomicroscope (40x-60x magnification) to isolate the endoderm from the 3/4PAR.

Note: Keep all surfaces and solutions cold during this procedure. Change to a new cold pancreatin solution if taking a long time to dissect the tissues (>15min). As an

illumination source, use LED lights incorporated in the stereomicroscope or in the optic fibres, considering the limited heat load.

2.2.4) To isolate the endoderm from the surrounding tissues use stainless steel microscalpels in pin holders.

Note: Use microscalpels with a diameter between 0.1mm and 0.2mm and nickel pin holders with a jaw opening diameter of 0mm to 1mm.

2.2.4.1) First remove the neural tube and mesoderm attached to the dorsal surface of the pharyngeal endoderm.

2.2.4.2) With the dorsal side up, carefully detach and remove the mesenchyme between the pharyngeal arches and expose the pharyngeal pouches. Perform this procedure on both sides of the 3/4PAR.

2.2.4.3) Remove the heart tube and the mesenchyme surrounding the anterior pouches.

2.2.4.4) With the ventral side up, cut the ectoderm of the 2nd and 3rd pharyngeal arches and carefully remove the mesenchyme attached to the pouches. Repeat this procedure on the other side of the 3/4PAR. At this stage the thyroid rudiment should be visible.

2.2.4.5) Remove any remaining mesenchymal cells attached to the pharyngeal endoderm with the two microscalpels.

2.2.4.6) Make a transversal cut between the 2nd and 3rd PP, dissociating the pharyngeal endoderm containing the 3rd and 4th pouches from the anterior part of the endoderm having the thyroid rudiment and 2nd pharyngeal pouch.

2.2.4.7) With the help of spatula and thin forceps, transfer the isolated 3/4PP endoderm to a glass dish three-quarters filled with 100% cold fetal bovine serum (FBS).

2.3) Keep the glass dish with the isolated tissues on ice during the preparation of *in vitro* assay. Alternatively, the isolated tissues can be three-dimensionally preserved and *in situ* analysed for gene-expression.

3. Isolation of chicken somatopleura mesoderm

Note: Perform egg manipulation procedures in sterile conditions using a horizontal laminar flow hood and sterilized instruments and materials.

3.1) Remove the embryonic territory containing the somatopleura mesoderm at the level of somites 19-24 (ss19-24).

3.1.1) Remove the chicken egg from the incubator after 2.5 days of incubation.

3.1.2) With curved scissors, open a small hole in the shell. Insert a needle and aspirate 2mL of albumin with a 10mL syringe to lower albumin volume inside the egg and prevent damage of the embryo (located below the marked region of the shell). Discard the aspirated albumin.

3.1.3) Cut a circular hole (up to two-thirds of the top surface area) in the marked region of the shell using curved scissors.

3.1.4) Cut the vitelline membrane externally to the extraembryonic vessels while holding the embryo with thin forceps.

3.1.5) Under a stereomicroscope, place the embryo in a 100mm Petri dish with a black base containing 10mL of cold PBS.

Note: Use a stereomicroscope from this point forward for progressive magnification of microsurgery procedures.

3.1.6) Use four thin insect pins to hold the embryo to the bottom of the plate. Place the pins in the extraembryonic region forming a square shape.

3.1.7) Perform two cuts between the somites 19 and 24 transversely to the embryo axis and crossing all embryo territory, using wecker eye scissors.

3.1.8) Release the embryo section, ss19-24, by cutting marginal embryonic edges.

3.1.9) Aspirate the ss19-24 tissues and transfer to a glass dish three-quarters filled with cold PBS using a 2 mL sterile Pasteur pipette.

3.2) Isolate the lateral mesoderm from somatopleura region (ss19-24) by enzymatic digestion with pancreatin (8mg/mL; 1:3 dilution 25mg/mL with cold PBS).

3.2.1) With the help of spatula and thin forceps, transfer the ss19-24 tissues to a glass dish three-quarters filled with cold pancreatin solution.

3.2.2) Incubate for 30min on ice for enzymatic digestion.

3.2.3) Under the stereomicroscope, isolate the mesoderm from the surrounding tissues using two microscalpels in a holder.

Note: Keep all surfaces and solutions cold during this procedure. Change to a new cold pancreatin solution if taking a long time to dissect the tissues (>10min). As an illumination source, use LED lights incorporated in the stereomicroscope or in the optic, considering the limited heat load.

3.2.4) During mesoderm isolation, first remove the ectoderm at the surface followed by careful detachment of the ventrally located splancnopleura tissues.

3.2.5) Release the right lateral mesoderm of the somatopleura by cutting it in a parallel motion to the neural tube.

3.2.6) Repeat the mesoderm separation of the left side of the embryo.

Note: Make slow microscalpel movements during this procedure. The exposed extra-cellular matrix proteins stick to tissues and instruments, preventing fluid movements.

3.2.7) With the help of spatula and thin forceps transfer the isolated mesoderm to a glass dish three-quarters filled with cold FBS.

3.3) Keep the glass dish with the isolated tissues on ice during the preparation of *in vitro* assay.

4. *In vitro* organotypic assay: heterospecific association of quail 3/4PP endoderm and chicken somatopleura mesoderm

4.1) Prepare the culture medium with RPMI-1640 medium supplemented with 10% FBS and 1% Pen/Strep (Le Douarin and Jotereau, 1975; Neves *et al*., 2012).

4.2) Place a metal grid in a 35mm Petri dish with 5mL of culture medium.

Note: Remove the excess of liquid to level the medium surface with the top of the grid.

4.3) With the help of thin forceps, dip a membrane filter into the culture medium and then place it on the top of the grid to have one surface in contact with air.

Note: One-quarter of the membrane area (with 13mm diameter) is adequate for the tissue association.

4.4) Under the stereomicroscope, associate the isolated tissues on the top of the membrane filter. First transfer the 3/4PP endoderm (step 2) from the glass dish by gentle sliding with the help of a transplantation spoon (or spatula) and thin forceps. Repeat this procedure for the isolated mesoderm (step 3).

Note: With the help of a microscalpel, mix the tissues to maximize its association.

4.5) Carefully place the associated tissues in a humidified incubator at 37°C with 5% CO_2 for 48h. Cultured tissues can be grafted onto the chorioallantoic membrane (CAM).

Note: Ectopic organ formation in the CAM was previously detailed (Figueiredo and Neves, 2018).

V.5 Results

The protocol details a method to isolate avian embryonic tissues to be used in several cellular and developmental biology technical approaches.

This method was previously employed to study epithelial-mesenchymal interaction during early stages of thymus formation (Neves *et al.*, 2012). Herein, new results are showed in Figure 1 and Figure 2, using similar approaches.

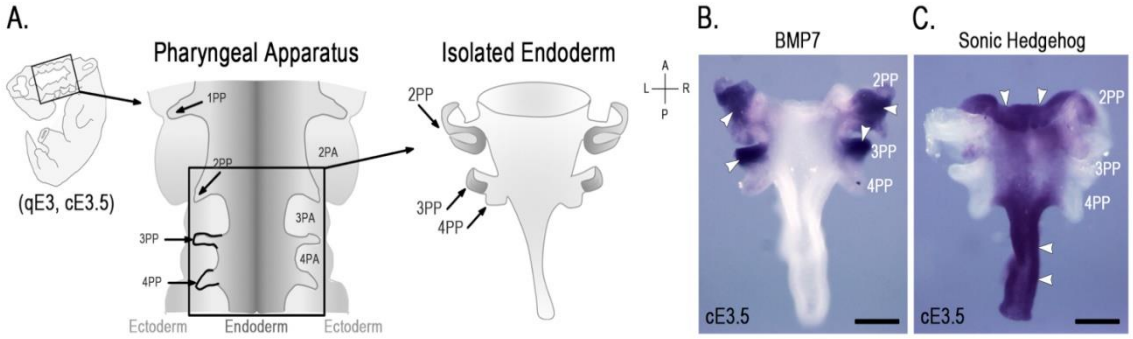

Figure 1. Representative results of gene-expression study of three-dimensionally preserved pharyngeal endoderm containing the presumptive territory of the thymus rudiment. Schematic representation of the pharyngeal apparatus and isolated endoderm containing the 2PP, 3PP and 4PP (at cE3.5 or qE3) (A). Whole-mount *in situ* hybridization with BMP7 (B) and Sonic Hedgehog (C) of isolated endoderm at cE3.5. Strong hybridization signals of *BMP7* and *Sonic Hedgehog* pointed by white arrowheads in endoderm of the 2PP and 3PP (B) and central pharynx (C), respectively. A, anterior; cE, chicken embryonic day; D, dorsal; L, left; P, posterior; PP, pharyngeal pouch; qE, quail embryonic day; R, right. Scale bars, 50μm.

Figure 1 is a schematic drawing of the endoderm isolated from the pharynx at qE3 (and cE3.5) (Fig. 1A) and the *in situ* expression of two endoderm-related genes, *Sonic Hedgehog* (Jerome and Papaioannou, 2001; Nie *et al.*, 2011) and *BMP7* (Zou *et al.*, 2006) in the isolated tissue. The whole-mount *in situ* hybridization procedures were performed as previously described (Neves *et al.*, 2012; Figueiredo *et al.*, 2016). The expression of *BMP7* was detected in the endoderm of the 2PP and 3PP and excluded from the central pharynx and 4PP (probe was kindly provided by Elisabeth Dupin) (Fig. 1B). Conversely, *Sonic Hedgehog* was detected in the endoderm of the central pharynx and excluded from the pouches (Fig. 1C) (Figueiredo *et al.*, 2016).

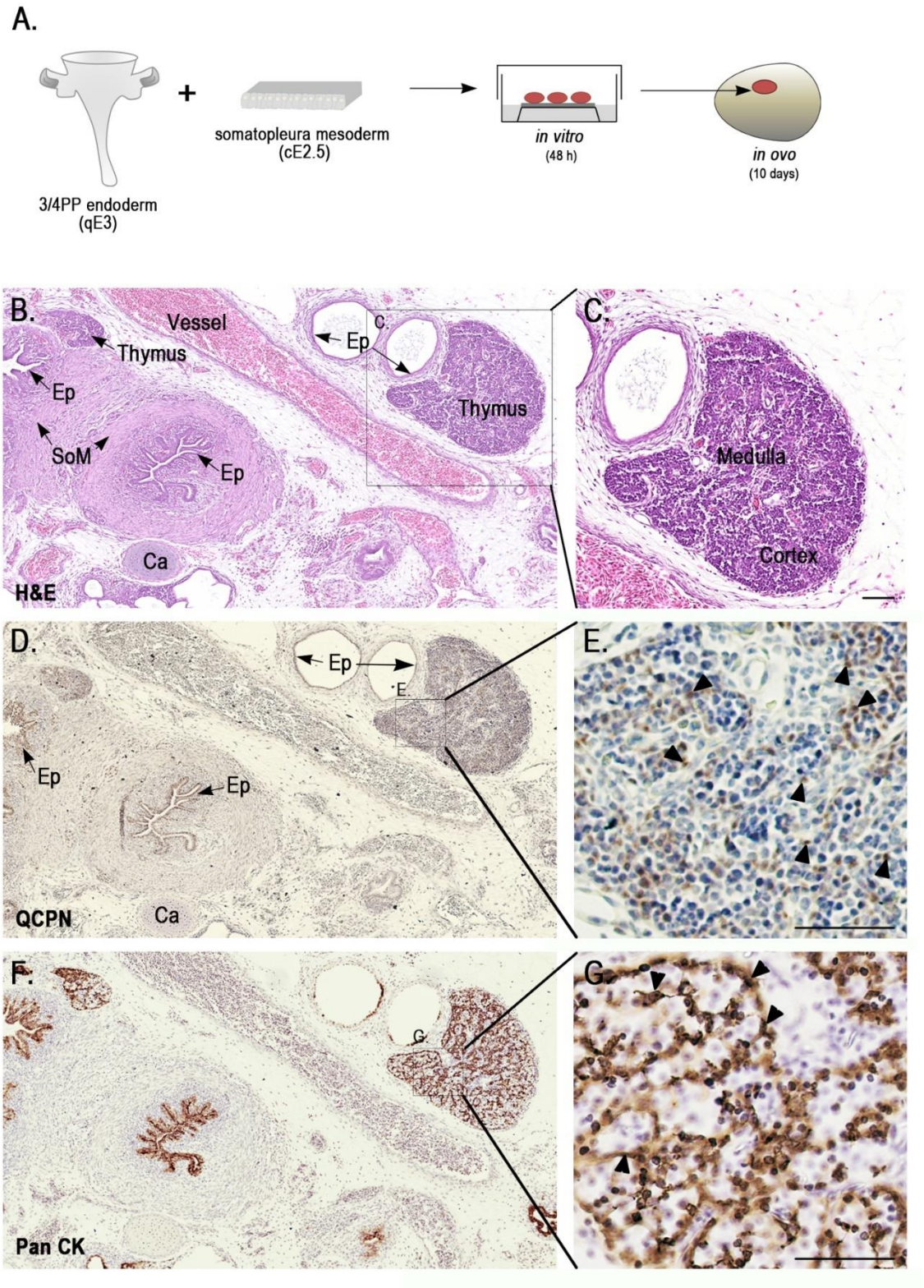

Figure 2. Representative results of *ex vivo* formation of chimeric organs. Schematic representation of the experimental approach used to develop quail-chicken chimeric thymi (A). Briefly, the isolated quail 3/4PP endoderm (qE3) was associated *in vitro* with chicken somatopleura mesoderm (cE2.5) for 48h. The 48h-cultured tissues were then grafted onto the CAM (cE8) and allowed to develop *in ovo* for further 10 days. Serial sections of CAM-derived explants (B-G) were analysed by conventional histology (B and C) and immunohistochemistry (D-G). In B and C (higher magnification of B), the slide was stained with H&E.

In D and E (higher magnification of D), the slide was immunodetected with QCPN antibody and counterstained with Gill's hematoxylin. In F and G (higher magnification of F), the slide was immunodetected with anti-Pan CK antibody and counterstained with Gill's hematoxylin. Black arrow heads point to strong brown immunostaining of QCPN (E) and Pan CK (G). See Table of Materials for image acquisition details. Ca, cartilage; Ep, epithelium; PP, pharyngeal pouch; SoM, smooth muscle. Scale bars: 50μm.

Figure 2 depicts the experimental design used to develop *ex vivo* quail-chicken chimeric organs. The heterospecific association of tissues were grown *in vitro* for 48h followed by *in ovo* development for 10 days (Fig. 2A). Thymi formed in CAM-derived explants were identified by conventional histology. The thymus presented normal morphological features with well-developed medulla and cortex compartments (Fig. 2B and C). Serial sections of the explants were further treated for immunocytochemistry (Fig. 2D-G), as described (Neves *et al.*, 2012; Figueiredo *et al.*, 2016). The QCPN-MAb Quail perinuclear (Fig. 2D and E) and anti-pan cytokeratin (CK) (Fig. 2F and G) antibodies were used as markers for quail (species-specific) and epithelial cells, respectively. The chimeric thymus showed $QCPN^{+}$ thymic epithelial cells (Fig. 2D and E), a reticular architecture (Fig. 2F and G), and colonization by lymphoid cells ($QCPN^{-}$) of donor origin (chicken).

V.6 Discussion

The embryonic tissue isolation procedure detailed here was improved from previous techniques to produce quail-chicken chimeric embryos in different biological contexts (Le Douarin and Jotereau, 1975; Takahashi, Bontoux and Le Douarin, 1991; Neves *et al.*, 2012).

This approach is suitable to isolate pure embryonic tissues without requiring genetic manipulation or the use of tissue-specific markers, which are often undetermined, limiting the use of genetically modified animal models. It can be used to study epithelial-mesenchymal interactions during development, with the ability to isolate pure tissues being the limiting factor. For instance, as development progresses, tissues become thicker, more compact and attach to other neighbouring tissues such that their separation is more difficult. This isolation procedure is, therefore, unsuitable for later stages of development, namely late-organogenesis.

This method is unique to study gene-expression in 3D-preserved embryonic tissues. To ensure the 3D-integrity of the isolated tissues, instruments, materials and solutions should be kept at low temperatures throughout the process.

The tissue microdissection procedure is also a critical step that relies, not only on the careful establishment of the experimental conditions (like temperature and duration of enzymatic digestion, as exemplified in Table 1), but also on the time-consuming hands-on training. This procedure requires patience and practice. If the operator loses the references of the region to be dissected, decreasing the stereoscope magnification (20x) will provide an overall observation that will help the next move decision.

The 48h *in vitro* step was established to promote the cellular interactions between distinct embryonic tissues, while the *in ovo* tissue grown in the CAM supports the long-term development and chimeric organ formation of the heterospecific association of tissues (Neves *et al.*, 2012). The *in vitro* tissues associations may overcome some limitations of *in vivo* manipulations. For instance, local administration of drugs or growth-factors (using beads) in regions of the embryo otherwise inaccessible *in vivo*, can be easily performed using this *in vitro* approach. This has previously shown to mimic local tissue interactions during organ formation in the pharyngeal region (Neves *et al.*, 2012).

Harvesting explants growing in CAM (Neves *et al.*, 2012; Figueiredo *et al.*, 2016; Figueiredo and Neves, 2018) is less time-consuming and is a simple method to track explants when compared to methods of collecting tissues grafted onto the body wall of chimeric embryos (Le Douarin and Jotereau, 1975). In addition, CAM can be transplanted with cells and tissues from other non-avian species, and it has been successfully used in several experimental contexts, from development to cancer (Davey and Tickle, 2007; Nowak-Sliwinska, Segura and Iruela-Arispe, 2014). For example, the CAM assay was previously applied in mice-into-chicken xenografts studies (Uematsu *et al.*, 2014) and is frequently used to test the invasive capacity of human tumours cells (Nowak-Sliwinska, Segura and Iruela-Arispe, 2014).

Recently, an elegant study with human-into-chicken xenograft has validated the chicken embryo as a model to test and explore early human development (Martyn *et al.*, 2018)Marty. In the future, it will be interesting to explore the methodology herein described using interspecies association of tissues, which may provide additional approaches to the mouse and human developmental studies.

CHAPTER VI

Genetic approach to modulate Notch Signalling in early thymus and parathyroid glands development.

In this Chapter, the main objective was to perform tissue-specific genetic manipulation of Notch signalling, particularly in the 3/4PP endoderm.

Ongoing Work

CHAPTER VI - GENETIC APPROACH TO MODULATE NOTCH SIGNALLING IN EARLY THYMUS AND PARATHYROID GLANDS DEVELOPMENT.

VI.1 Brief Introduction

In Chapter IV, we show for the first time that Notch signalling is involved in the specification of thymus and parathyroid glands. The block of Notch in pharyngeal explants using pharmacologic inhibitors reduced *Foxn1*/thymus-fated and *Gcm2*/*Pth*/parathyroid-fated domains in the 3/4PP endoderm, and further compromised the development of the parathyroid glands. However, since Notch signalling was inhibited in a pharyngeal explant containing all three tissue compartments – endoderm, mesenchyme, and ectoderm –, the contribution of each tissue to the endodermal outcomes we have observed remains unknown.

Many studies have shown the importance of epithelial-mesenchymal interactions in the early development of the 3/4PP endoderm (Le Douarin, 1967; Le Douarin and Jotereau, 1975; Le Douarin, Dieterlen-Lièvre and Oliver, 1984; Grevellec and Tucker, 2010; Neves *et al.*, 2012), and of the surrounding NCCs in the rudiments' separation and migration processes (Griffith *et al.*, 2009; Chen *et al.*, 2010; Foster *et al.*, 2010). In gut development, endodermal-mesenchymal interactions are necessary for the specification of the gut epithelia, and the mesenchyme is required for its growth and morphogenesis (reviewed in (Roberts, 2000; Zorn and Wells, 2009; Chin *et al.*, 2016)). Similar phenomenon may occur with the pharyngeal endoderm and surrounding mesenchyme. Interestingly, in zebrafish, mesodermal Fgf8 was shown to be responsible for guiding pouch epithelial outpocketing in the pharyngeal region (Choe and Crump, 2014). Notch signalling-related molecules are differently expressed in the 3/4PP endoderm and mesenchyme compartments at early stages of T/PT development. Interestingly, we have observed several Notch-target genes expressed mainly in the endodermal compartment (Fig. 2 E-F and Fig. S5C and E in Chapter IV) (Figueiredo, 2011; Figueiredo *et al.*, 2016), suggesting that Notch signal activation in the endoderm may be responsible for its role in the development of these organs. Moreover, communication between the endoderm and the mesenchyme might be occurring through Notch signalling at this point.

Combining the advantages of the quail-chick developmental model and the capacity to isolate three-dimensionally-preserved endoderm containing the prospective thymus/parathyroid rudiment, we aimed to modulate Notch signalling activity in the 3/4PP endoderm during thymus and parathyroids formation. We designed an approach to genetically modify isolated quail 3/4PP endoderm so that it would constitutively express the dominant-negative form of the Notch co-activator MAML1 (DNMAML1; loss-of-function) (Weng *et al.*, 2003; Maillard *et al.*, 2004), or the intracellular domain of Notch1 (ICN1; gain-of-function) (Weinmaster, 1997), using a transposon mediated gene transfer technique combined with the Tet-Off inducible system (Fig. 1) (Watanabe *et al.*, 2007). One of the advantages of this approach is to allow the genetic modification of tissues with no known markers. The sequences of *DNMAML1* and *ICN1* had been previously cloned into the pT2K-BI-TREeGFP vector from the Tet-inducible system, generating pT2K-DNMAML1eGFP and pT2K-ICN1eGFP vectors (Figueiredo, 2011). The constructs' functionality had been evaluated through the electroporation of the chicken neural tube and the subsequent analysis of the *Hes5-1* expression (Figueiredo, 2011), as it was shown to be a direct target of Notch in the neural tube (Lütolf *et al.*, 2002; Vilas-Boas *et al.*, 2011). A new DNMAML1 construct was generated during this thesis to potentially improve DNMAML1 protein stability and nuclear translocation, and its functionality was also validated in the neural tube of chicken embryos.

Our initial goal was to use the Tet-On system (Fig. 6A in Chapter I) to induce the modulation of Notch (loss- and gain-of-function) in specific developmental time-windows (by Dox administration), which would be particularly relevant for studying the role of Notch in later stages of organogenesis. However, after several unsuccessful attempts to work with the Tet-On system (given by Yoshiko Takahashi), we have confirmed (through several experiments described in Appendix III) that we were, instead, in the presence of the transactivator vector of the Tet-Off system. We, therefore, continued our work using the latter (Fig. 1).

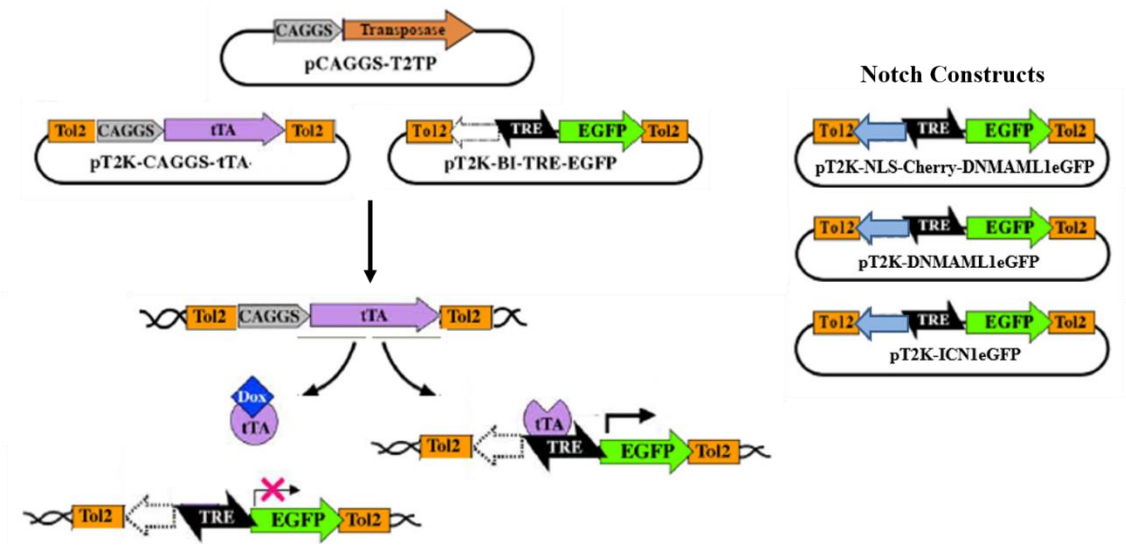

Figure 1. Tol2-mediated gene transfer system and tetracycline-dependent conditional expression combined system – Tet-Off System. Transient activity of transposase (pCAGGS-T2TP) will induce the transposon construct containing either TRE-eGFP (pT2K-BI-TREeGFP) or tTA (pT2K-CAGGS-tTA) to be integrated into the host genome. Upon integration, the Tet-Off system constitutively activates TRE-driven genes transcription (in the absence of Dox), which is inactivated by the addition of Dox. To modulate Notch signalling, Notch constructs were generated to induce loss- and gain-of-function of Notch. Dox, Doxycycline. Adapted from Watanabe *et al*., 2007.

To evaluate the genetic modulation of Notch signalling in the prospective thymus/parathyroid rudiments, we associated the genetically modified endoderm with chick mesenchyme *in vitro* for 48h (detailed in Chapter V), without Dox (Tet-Off system). The transcripts levels of *GFP*, vector-specific *DNMAML1*/NLS-*DNMAML1* and *ICN1* sequences, Notch target *Hes5.1*, and thymic (*Foxn1*) and parathyroid glands (*Gcm2*) markers, were analysed on the 48h-cultured tissues. Our results showed no clear effects of the Notch signalling modulation, regardless of the proven functionality of the Notch constructs in other biological contexts (detailed below). The inconclusive results revealed the need to optimize the experimental procedures.

After achieving the optimal experimental conditions, it is our goal to graft the organotypic culture onto the CAM of a chicken embryo at E8 and allow its further development *in ovo* for 10 days (detailed in Chapter III and VI). During this period, Dox administration at specific time-point will prevent the genetic modulation of Notch signalling during the late-stages of thymus and parathyroid organogenesis.

VI.2 Results/Discussion

To genetically modulate Notch activity in the isolated quail 3/4PP endoderm, we started by producing a new vector, pT2K-NLS-Cherry-DNMAML1eGFP (loss-of-function condition) (detailed in Section II.1.12.12). Considering the small size of DNMAML1 sequence (205bp), this new vector was generated to improve DNMAML1's protein stability and nuclear translocation (thus becoming more competitive against the endogenous MAML1), by fusing its DNA sequence to mCherry-nuclear localization signal (*CherryNLS*) sequence. To validate the construct's functionality, the neural tube of cE2 embryos was electroporated *in ovo* (see details Section II.2.3.1.1) with the pT2K-CAGGS-tTA and pT2K-NLS-Cherry-DNMAML1eGFP vectors, and *Hes5.1* expression analysed 24h post-electroporation (Fig. 2).

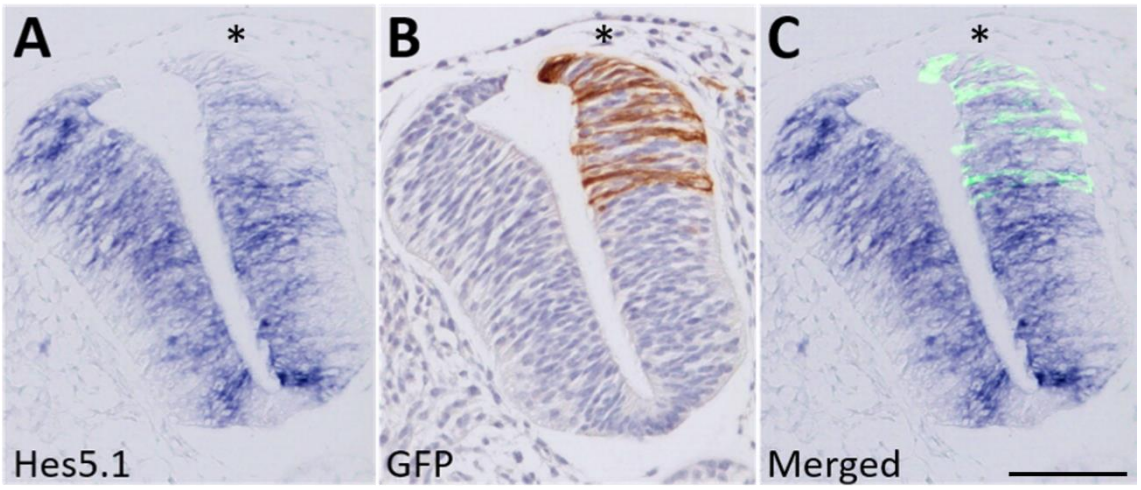

Figure 2. Functional analysis of pT2K-NLS-Cherry-DNMAML1eGFP vector. The neural tube of E2 chicken embryos was *in ovo* electroporated with the pT2k-CAGGS-tTA and pT2K-NLS-Cherry-DNMAML1eGFP vectors. 24h-post electroporated embryos were collected, whole-mount *in situ* hybridized for *Hes5.1* gene and sectioned (A). GFP^+ cells were detected by immunochemistry with anti-GFP antibody in post-whole mount *in situ* hybridization sections where *Hes5.1* expression was detected in the neural tube (B). Electroporated side (asterisk). E-embryonic day. Scale 100µm.

Hes5.1 expression (Fig. 2A and C) was lost in GFP^+ cells (Fig. 2B and C) of the electroporated side of the neural tube, confirming the construct's ability to downregulate Notch activity. Neural tube electroporation with the pT2K-BI-TREeGFP (control condition) showed no changes in *Hes5.1* expression in *GFP^+* cells (data not shown).

Considering the complexity of the Tet-Off system of vectors, the establishment of the electroporation conditions of isolated endoderm was performed with a single pCAGGS backbone vector, which contains a strong and ubiquitous promoter. Notch signalling modulation was executed with the pCAGGS-NLS-Cherry-DNMAML1-GFP vector (details of the construction in Section II.1.12.12), given that Notch loss-of-function condition allows a clearer analysis of the results, when compared with the gain-of-function condition (ICN1). Quail 3/4PP endoderm was isolated at E3 and different conditions – vector concentration and number of electric pulses and voltage – were tested (data not shown). After establishing the electroporation conditions (indicated in Section II.2.1.3), the electroporated endoderm was co-cultured with chicken somatopleural mesoderm (cE2.5) *in vitro* for 48h, and the expression of *GFP*, vector-derived NLS-DNMAML1 sequences, and *Hes5.1* was analysed in the harvested tissues. Notch target *Hes5.1* was shown to be one of the most responsive targets upon Notch inhibition at these stages (Figueiredo, 2011).

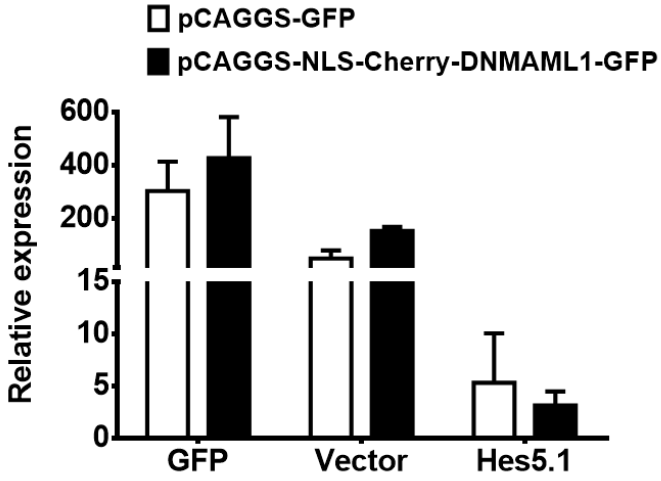

Figure 3. **Notch signalling transient modulation in the 3/4PP endoderm at early-stages of thymus and parathyroid formation.** Isolated quail 3/4PP endoderm (E3) was electroporated with pCAGGS-STOP-IRES-GFP (control condition), or with pCAGGS-NLS-Cherry-DNMAML1-GFP (Notch loss-of-function condition). The electroporated endoderm was then associated with chick somatopleural mesenchyme (at E2.5) *in vitro* for 48h and the expression levels of *GFP*, vector-derived *NLS-DNMAML1* sequences, and Notch target gene *Hes5.1* were examined by qRT-PCR. Expression of each transcript was measured as a ratio against the mean of *Actb* and *Hprt* transcript expression levels and expressed in arbitrary units.

The Notch loss-of-function condition (pCAGGS-NLS-Cherry-DNMAML1-GFP) showed high levels of *GFP* expression, similar to control condition (pCAGGS-GFP) (Fig. 3). As expected, a slight decrease in *Hes5.1* expression was observed in the experimental condition, when compared to control (Fig. 3).

We then proceeded to modulate Notch activity in the 3/4PP endoderm (prospective thymus/parathyroids rudiments), using the Tet-Off system of vectors, with the established electroporation conditions. These experiments were performed without the transposase plasmid, using only the transient effect of the vectors, due to the short period of culture. To study the loss-of-function of Notch signalling, the isolated 3/4PP endoderm at qE3 was electroporated with either the pT2K-NLS-Cherry-DNMAML1eGFP construct, or the previously generated vector, pT2K-DNMAML1eGFP. In parallel, to study the activation of Notch signalling, gain-of-function assays were performed with the pT2K-ICN1eGFP vector. The pT2K-BI-TREeGFP vector was used as a control condition. Similar co-culture experiments were performed, and 48h-cultured explants were analysed for the expression of *GFP*, vector specific sequences containing *DNMAML1* or *ICN1*, and Notch-target gene, *Hes5.1*.

We observed high expression levels of *GFP*, *DNMAML1* and *ICN1* transcripts for each corresponding condition (Fig. 4). Unexpectedly, a mild increase of *Hes5.1* was observed in both loss-of-function conditions, when compared to control (Fig. 4). In the case of Notch gain-of-function, a slight increase of *Hes5.1* was also observed (Fig. 5). These odd results suggest that electroporation procedures were not adequate to our system. This may reflect a stress response of the electroporated tissues, as Notch has been shown to be activated in several cellular stress conditions, such as oxidative stress, hypoxia, endoplasmic reticulum stress, and nutrient deprivation, in several developmental contexts (Mutoh *et al.*, 2012; Boopathy *et al.*, 2013; Caliceti *et al.*, 2014; Izrailit *et al.*, 2017).

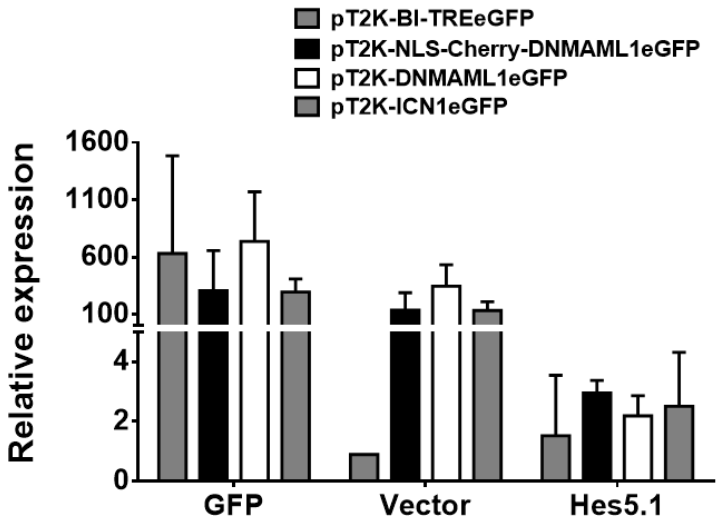

Figure 4. Genetic modulation of Notch signalling in the 3/4PP endoderm at early-stages of thymus and parathyroid formation. Isolated quail 3/4PP endoderm (at E3) was electroporated with pT2K-CAGGS-tTA and either pT2K-BI-TREeGFP (control condition), pT2K-NLS-Cherry-DNMAML1eGFP (loss-of-function), pT2K-DNMAML1eGFP (loss-of-function), or pT2K-ICN1eGFP (gain-of-function). The electroporated endoderm was then associated with chick somatopleural mesenchyme (E2.5) *in vitro* for 48h and gene expression levels examined by RT-PCR. *GFP*, vector-derived *DNMAML1* or *ICN1* sequences, and Notch target gene *Hes5.1* expression levels in 48h-cultured heterospecific associated tissues. Expression of each transcript was measured as a ratio against the mean of *Actb* and *Hprt* transcript expression levels and expressed in arbitrary units.

Furthermore, the 48h-cultured explants were analysed for the expression of thymic and parathyroid epithelial markers, *Foxn1* and *Gcm2*, respectively. Interestingly, the slight increase in Notch activity was accompanied by a tendency of augmentation in *Foxn1* and *Gcm2* expression (Fig. 5). Since our previous data showed a decrease in the expression of these markers when Notch signalling was pharmacologically inhibited in the pharyngeal region (Chapter IV and (Figueiredo *et al.*, 2016)), these results are consistent with a robust network between Notch activity and the expression of *Foxn1* and *Gcm2* at these stages of development.

In conclusion, these results revealed the need to optimize this experimental procedure to clarify the tissue-specific role of Notch in T/PT early development.

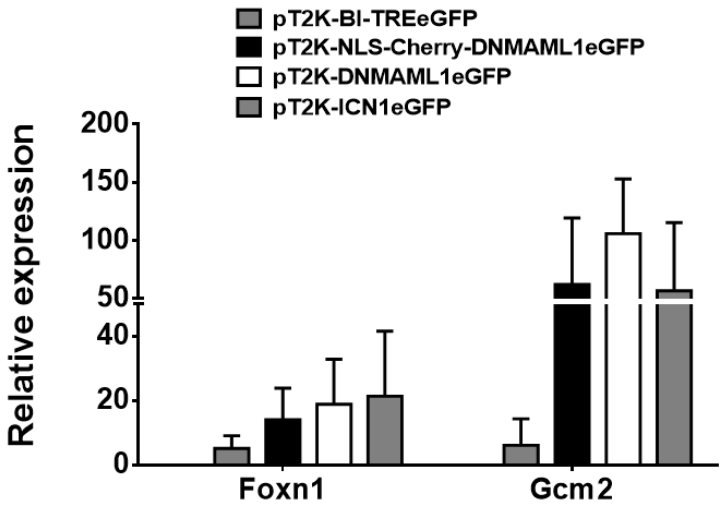

Figure 5. **Analysis of thymus and parathyroid glands markers after genetic modulation of Notch signalling in the 3/4PP endoderm at early-stages of thymus and parathyroids development.** Isolated quail 3/4PP endoderm (at E3) was electroporated with pT2K-CAGGS-tTA and either pT2K-BI-TREeGFP (control condition), pT2K-NLS-Cherry-DNMAML1eGFP, pT2K-DNMAML1eGFP, or pT2K-ICN1eGFP. The electroporated endoderm was then associated with chick somatopleural mesenchyme (at E2.5) *in vitro* for 48h and gene expression levels examined by RT-PCR. Lineage-specific genes, *Foxn1* (thymus marker) and *Gcm2* (parathyroids marker) expression levels in 48h-cultured heterospecific associated tissues. Expression of each transcript was measured as a ratio against the mean of *Actb* and *Hprt* transcript expression levels and expressed in arbitrary units.

CHAPTER VII

General Discussion and Future perspectives

CHAPTER VII - GENERAL DISCUSSION AND FUTURE PERSPECTIVES

VII.1 Summary of findings

Although major advances have been made in the understanding of T-cell differentiation – likely due to its potential applicability in medicine –, parts of thymus organogenesis's "black box" remain undecipherable. Recent studies have deepened our knowledge on the molecular and cellular mechanisms that control the different steps of thymus organogenesis, but there are still several missing pieces. Some of them are related to the stages where the thymus shares its primordium with the parathyroid glands. The patterning and morphogenetic events, as well as the underlying molecular mechanisms, during these early stages of thymus/parathyroids (T/PT) development remain, for the most part, poorly defined. Many genetically modified mouse models have been useful to clarify the role of several transcription factors and signalling pathways at these stages of development. However, it is sometimes difficult to pinpoint the requirement of key players in an exact cell type, as many of them are found in multiple cell types and are likely to be involved in essential interactions that influence cell fate decisions and organogenesis. Another limitation is the lack of specific genetic markers of the prospective domains of thymus and parathyroid glands before their specification, that would allow the modulation of pathways and transcription factors in these domains. This discovery would help to identify the molecular mechanisms responsible for the specification of these organs, which is another major missing piece.

The work conducted and detailed in this thesis aimed to determine the role of Notch signalling in the early stages of thymus and parathyroid glands development, as well as its possible interaction with another major signalling pathway, Hedgehog (Hh), using the avian model. Through *in vitro*, *in vivo* and *in ovo* approaches, including the two-step approach detailed in Chapter III, this work exposed a so far unreported role of Notch signalling in the thymus/parathyroids common primordium development and in parathyroid glands formation. The absence of Notch signalling during T/PT common primordium development downregulates *Foxn1* and *Gcm2*, both *in vitro* and *in vivo*, showing that Notch is required for their expression at these early stages. Among the Notch targets analysed, *Hey1* and *Gata3* (especially) are most likely to be involved in the regulation of *Foxn1* and *Gcm2* expression. The reduction of thymus- and parathyroids-

specific markers in the common primordium revealed different outcomes regarding subsequent organ development. *Foxn1* expression was able to recover and thymus formation was not significantly impaired, whereas the parathyroid glands never fully recovered, producing smaller glands and in reduced numbers. The data suggest that although Notch signals are required for the normal expression of *Foxn1* and *Gcm2* at these early stages of development, they are only crucial for the subsequent formation of the parathyroids. In addition, Hedgehog was found to act upstream of Notch at these stages. Hh regulates the median domains of the pouch endoderm, which seem to be more Hh-responsive than the pouch tips, namely the dorsal tip where the thymus is formed. Hh positively regulates the *Gata3*/*Gcm2*/parathyroid-fated domain and *Lfng* at the median/posterior territory of the developing 3/4PP endoderm. The latter was shown to be involved in the definition of the dorsal/posterior boundary of the *Foxn1*$^{+}$/thymic rudiment.

To evaluate whether the observed Notch effects were exclusively dependent on the endodermal Notch signals, we designed a genetic approach to modulate the Notch pathway in the 3rd and 4th pharyngeal pouches (3/4PP) endoderm. The block or constitutive activation of Notch signalling with the *Tol2*-mediated gene transfer and tetracycline-dependent conditional expression systems resulted in inconclusive results. Under the tested conditions, this approach was unable to modulate Notch, suggesting the need to optimize the electroporation or the overall conditions of the assay.

VII.2 Where does Notch fit in the cascades that regulate thymus and parathyroid glands early development?

To our knowledge, this thesis represents the first report of Notch signalling requirement for *Foxn1* and *Gcm2* expression at early stages of thymus and parathyroid development. Moreover, the 48h *in vitro* inhibition of Notch impaired subsequent parathyroid formation, both in number and size. Thus, additionally to its role in T/PT common primordium development, Notch signalling at that specific and short time-window is also crucial for parathyroids formation. However, it remains unclear where Notch is positioned within the known cascades that regulate T/PT development.

While a Hoxa3-Pax1-Gcm2 pathway has been previously proposed (Su *et al.*, 2001), strong evidence suggests that *Foxn1* could be placed next to *Gcm2*. In *Hoxa3*$^{-/-}$ mice *Gcm2* is expressed at very low levels, *Foxn1* expression suffers a delay, and ultimately the parathyroids do not form and the thymus suffers apoptosis (Chojnowski *et al.*, 2014). *Pax1*$^{-/-}$ mice start expressing *Gcm2* and *Foxn1*, but their expression decreases, resulting in hypoplastic organs (Wallin *et al.*, 1996; Su *et al.*, 2001). Also, Pax1/9 were recently shown to be required for *Foxn1* initiation, in a gene dose-dependent manner (Kelly, 2012). These phenotypes resemble, to some extent, what is observed when Notch signalling is pharmacologically inhibited *in vitro* between qE3-qE5, with a significant reduction of *Pax1*, *Gcm2*, and *Foxn1*, as well as hypoplastic parathyroids. The presence of a normal thymus can be related to the transient – rather than permanent – nature of Notch inhibition in this assay, or even to asynchronous responses to Notch from each pouch domain (further explored below). Worth noting, *Hoxa3*$^{-/-}$ mice also show downregulation of *Tbx1* and *Bmp4* in the endoderm (Chojnowski *et al.*, 2014), which are known to be involved in the development of the parathyroids and the thymus, respectively (Ivins *et al.*, 2005; Neves *et al.*, 2012; Swann *et al.*, 2017). This suggests that Hoxa3 may be acting upstream of *Tbx1* and *Bmp4*, and further supports the resulting impairment of *Gcm2* and *Foxn1* expression. The preliminary data provided in Chapter III also show a reduction of *Tbx1*, *Bmp4*, and *Six1* (which is placed under *Hoxa3* regulation) when Notch signalling is inhibited *in vitro* in the pharyngeal region between qE3-qE5. Overall, our results suggest that the Notch pathway may act in parallel with *Hoxa3* or under its regulation, above *Pax1* (and potentially *Tbx1*, *Bmp4*, and *Six1*). To clarify where Notch signalling stands, further analyses of the expression of Notch-related proteins in the

presumptive territories of T/PT in *Hoxa3*$^{-/-}$ mice, as well as of the expression patterns of *Pax1*, *Tbx1*, *Bmp4*, and *Six1* in chicken embryos injected *in ovo* with the Notch inhibitor LY-411.575 (Ly) could be performed.

In addition, *in situ* analysis of the *in vitro* explants grown in the presence of Notch signalling inhibitors could, in theory, add relevant positional information to the changes in expression levels detected by qRT-PCR. The analysis of sections of those explants could clarify the reductions of gene expression, as well as the potential changes in their domains of expression. However, the fact that tissues lose their 3D structure in culture makes an accurate evaluation of changes in 3/4PP expression domains very challenging. While the endodermal tissues are easily distinguished from the mesodermal and ectodermal tissues that comprise the explant, only a small percentage of the endoderm corresponds to the 3/4PP. Furthermore, potential changes in the pouches' expression domains are even harder to evaluate when sections of each explant may display the pouch endoderm in distinct orientations.

As previously mentioned, the fact that Notch signalling was modulated only through a short period of time might be insufficient to promote irreversible effects in thymus development as those seen for the parathyroid glands. It is possible that the thymus is less dependent on Notch effects than the parathyroids, meaning that other pathways could be crucial at this point to allow the later recovery of *Foxn1* expression. On the other hand, we cannot exclude the possibility of Notch signalling being crucial in early thymus development at a different (and possibly later) time-window. Once the parathyroids and thymic domains are established, the respective upregulation of *Gcm2* and *Foxn1* expression is essential for the subsequent organ differentiation (Nowell *et al.*, 2011; Manley, 2015). Since the *in vitro* assay of Notch signalling inhibition comprises the qE3-qE5 stages, and *Gcm2* and *Foxn1* expression is established at qE3 and qE4, respectively, it is possible that this 24h difference may have some impact on the reversibility of outcomes. It would be interesting to see what happens to thymus organogenesis in the chorioallantoic membrane (CAM) when this *in vitro* assay is performed for a day longer, or initiated at qE4, when *Foxn1* is established.

VII.3 *Gata3* is differently regulated in the common primordium

The expression of *Gata3* in the 3rd PP endoderm has been shown to be very dynamic between the presumptive domains of the parathyroids and thymus in the mouse model (Grigorieva and Mirczuk, 2010; Wei and Condie, 2011). Later in development, *Gata3* is known to be crucial for parathyroids function and proliferation (Grigorieva and Mirczuk, 2010), as well as for T-cell development (Hoflinger *et al.*, 2004; Fang *et al.*, 2007). We also found a dynamic *Gata3* expression in the avian model. At cE3.5/qE3, *Gata3* is expressed throughout the anterior domain and tips of the 3rd PP at early stages of development, with stronger hybridization signals appearing in the parathyroids domain by qE4. One day later (qE5), *Gata3* expression is observed in both developing parathyroid glands and thymus. Data from both mouse and avian models point to spatially and temporally distinct roles of *Gata3* in T/PT development.

Our work also suggests that *Gata3* expression is differently regulated in the pouch endoderm. *Gata3* at the tips (ventral and dorsal) of the pouch seems to be less responsive to Shh signals and more responsive to Notch signals, in opposition to the more median/anterior pouch domain. Hh inhibition resulted in a greater reduction of *Gata3* signals in the median area of the anterior pouch than in the pouch tips. This downregulation was accompanied with an almost complete absence of *Gcm2* expression, supporting the Gata3-Gcm2 pathway (Grigorieva and Mirczuk, 2010). Analysing *Gata3* expression in chicken embryos at earlier stages of development, such as cE3, through *in situ* hybridization (whole-mount and in sections), would help to clarify whether *Gata3* is indeed expressed in the presumptive domain of the parathyroid glands before *Gcm2* expression. On the other hand, *Gata3* expression in the pouch tips is regulated by Notch signalling in a Hh-independent way. When Notch signalling was blocked, *Gata3* was strongly reduced in the tips, compared with the median/anterior domain of the pouch. Overall, the data highlighted that Hh may be regulating *Gata3* in the median/anterior domain independently of Notch. In eye development, Hh was also shown to regulate *Hes1* in a Notch-independent manner (Wall *et al.*, 2009). To clarify these interactions, we could perform *in vivo* assays where Shh-beads would be placed in the pharyngeal region at the level of the 3/4PP and a Notch inhibitor would be injected in that same area. If Shh failed to induce *Gata3* expression in the presence of a Notch inhibitor, it would indicate that *Gata3* regulation in the median/anterior domain also depends on active Notch signalling.

One of the first genes distinctly expressed in the presumptive thymic domain in the mouse, even before *Gata3*, is *Isl1* (Wei and Condie, 2011). As *Isl1* was shown to directly induce *Gata3* expression in the digestive tract (Li *et al.*, 2014), it is possible that it is regulating *Gata3* in the thymic domain. To understand whether Notch signalling is modulating *Gata3* through *Isl1* we could analyse *Isl1* expression in pharyngeal regions grown *in vitro* in the presence of Notch inhibitors (by qRT-PCR). A reduction in *Isl1* levels would suggest that *Gata3* expression in this domain is controlled by Isl1, which in turn would be regulated – directly or not – by Notch signalling. And since different factors/pathways can regulate the processes of initiation and maintenance of *Gata3* expression, Isl1 and Notch signalling could be exclusively involved in either process or collaborating in one or both. Lastly, the fact that *Gata3* expression did not mirrored *Foxn1* expansion to the posterior domain of the pouch in the absence of Hh signals suggests that *Gata3* is not involved in the definition of the posterior border of the thymic domain, nor in *Foxn1* regulation. It would be interesting to see if *Isl1* would show the same "behaviour".

An additional analysis of the expression levels and domains of other early markers of the pouch (of one or both organ domains), such as *Nkx2.5*, *Nkx2.6*, and *Foxg1*, in the absence of Notch or Hh activity could also shed light on their underlying roles.

VII.4 The "no-fate" domain

In avian, while the 3/4PP endoderm gives rise to the thymus and parathyroid glands, only about half of the pouch endoderm tissue (the anterior/median region and the dorsal pouch) comes to express the organs' specific markers and will become part of these organs (Fig. 3B in Chapter I). The other half (mainly the median/posterior portion of the pouch) expresses neither of these markers and will not give rise to any organ, which may explain the apparent disregard for this region and its potential relevance. Besides this thesis, only one study suggested a potential role for the posterior domain of the pouch (Gardiner *et al.*, 2012). The authors showed that FGF-related molecules, including *Fgf8*, are expressed in a small posterior region of the 3rd PP in mouse embryos at mE10.5, when *Gcm2* and *Bmp4* are being expressed in the parathyroids and thymic domains, respectively, but *Foxn1* is not yet present. The work suggested that FGF signalling in that region regulated the boundaries of the other domains (Gardiner *et al.*, 2012).

Interestingly, and distinct from avian, when *Gcm2* and *Foxn1* are both being expressed in mouse embryos, only a temporary small central region composed of anterior and posterior cells (which express neither marker) is present between the two domains (Gordon *et al.*, 2001; Gordon and Manley, 2011; Bain *et al.*, 2016). These spatial differences between the pouch domains of mouse and avian (Fig. 3A and B in Chapter I) may be related to other structural features within the endodermal pouch that distinguish them. Compared with mammals, the positions of the T/PT domains in the common primordium of avian embryos are inverted along the dorsal-ventral axis (Fig. 3A and B in Chapter I). This may explain the distinct final anatomical positions these organs occupy in the two groups of vertebrates. While the thymus migrates caudally and ventrally to the chest in mammals, it moves to an anterior and dorsal (lateral) position in the neck of avian embryos (Fig. 2A in Chapter I). Parathyroid glands locate ventrally near the thyroid in mammals and avian, with the exception of the inferior parathyroids in humans, which are located caudally near the thymus (Fig. 2A in Chapter I) (Neves *et al.*, 2012).

Despite these differences, our results using the avian model also suggest that the posterior domain may act as a regulatory region to the other domains, namely defining the posterior boundary of the dorsal thymic domain. In addition, this regulation seems to involve both Notch and Hh signals. We have shown that *Fgf8* and *Lfng* are being expressed specifically in this pouch domain. Hh signalling inhibition led to a reduction of *Fgf8* expression (*in vitro*), the abrogation of *Lfng* expression (*in vivo*), and an expansion of the *Foxn1* domain to the posterior domain of the pouch (*in vivo*). These results suggest a Shh-Fgf8-Lfng cascade, where Shh coming from the central pharynx sends signals to the median/posterior pouch domain to express *Fgf8* and *Lfng*, which in turn define the posterior limit of the *Foxn1*$^{+}$ domain. This potential pathway is supported by data from other developmental contexts, where Shh was reported to positively regulate *Fgf8* expression (Aoto *et al.*, 2002) and *Lfng* was shown to respond to Fgf8 signals (Shifley *et al.*, 2008). Also, the fact that there is evidence of *Fgf8* expression in the posterior domain of the pouch and of the involvement of this domain in boundary definition both in mammals and in avian (through this work) further strengthens these conclusions. However, the expansion of *Foxn1* expression exclusively to the posterior domain of the pouch differs from what Moore-Scott & Manley observed in the *Shh*$^{-/-}$ mouse mutant, where *Foxn1* was said to expand throughout the pouch endoderm and to the central pharyngeal endoderm (Moore-Scott and Manley, 2005). Again, these

differences may be associated with the inverted positions of the T/PT domains in the pouch, and other inherited differences yet to be discovered. Further studies comparing avian and mouse models are crucial to clarify and understand these differences between the two groups of vertebrates.

During our work, expression of the *Delta1* ligand was observed in the median region of both the anterior and posterior pouch domain, while the dorsal domain of the pouch – the region of the presumptive thymus – does not seem to strongly express either *Delta1*, *Jagged1*, or *Jagged2* ligands (Fig. 5K and L of Chapter IV and data not shown). Considering that Notch-Delta alone is known to allow only two cell states, "sender" or "receiver" (Boareto *et al.*, 2015), it is possible that the posterior boundary of the thymic domain may be defined through the amount of Notch receptors versus Delta1 ligands between the dorsal and the posterior domains. In this scenario, the dorsal domain would be in a "receiver" state and the posterior domain in a "sender" state. While the standard view of Lfng functioning is based on Lfng-induced changes in Notch receptors, making them more prone to bind to Delta than to Jagged, a recent study showed that Lfng in ligand-expressing cells increases Notch activation in neighbouring cells, due to its ability to promote the localization of Delta1 ligand at the cell surface (Kadur *et al.*, 2018). Lfng in the median/posterior domain of the pouch may increase the availability of Delta1 on the surface of the posterior cells, activating Notch signalling in the boundary with the dorsal domain. The block of Hh signalling, and the subsequent loss of *Lfng* expression, may reduce the level of Delta1 ligands in the membrane of the posterior cells, preventing the activation of Notch signalling in the boundary and allowing the expansion of the *Foxn1*$^{+}$ domain. On the other hand, while interactions between receptors and ligands of the Notch pathway within the same cell are mainly considered to promote Notch cis-inhibition, recent evidence highlighted that cis-activation also occurs between Notch1 and Delta1 (Nandagopal, Santat and Elowitz, 2019). Thus, we could also postulate that this Lfng-dependent higher availability of Delta1 on the surface of posterior cells could, instead, lead to Delta1-Notch1 cis-activation in this region, promoting the expression of specific factors that regulate the dorsal/posterior boundary. Without Hh signals and *Lfng*, Delta1-Notch1 cis-activation may be reduced or absent in the posterior domain, changing the Notch landscape, and allowing the expansion of the thymic domain to the posterior region.

Post-translational modifications and changes in the trafficking of Notch ligands (as hypothesized above) may affect Notch activation without reflecting major changes in the transcripts and protein levels of Notch-related molecules, making the assessment of Notch changes even more complex (Bray, 2006; Kadur *et al.*, 2018). To better understand the potential Notch mechanism behind the posterior boundary definition in our model we could perform immunohistochemistry to analyse the presence and location of Delta1, Notch1, and ICN1 protein in tissue sections of the pharyngeal region of avian embryos during these stages of development and after *in vivo* exposure to Cyc-beads. The analysis of *Delta1* mRNA levels through qRT-PCR in avian pharyngeal regions grown in the presence of Hh inhibitors could also add relevant information to this issue.

Another unanswered question is how Notch signalling regulates these Notch-related molecules in the "no fate" domain. To clarify this, quantitative and spatial changes of *Lfng* and *Delta1* expression could be analysed through qRT-PCR and *in situ* hybridization in experiments where Notch is inhibited *in vitro* and *in vivo*. Again, protein analysis through immunohistochemistry would add another level of understanding in this context. Furthermore, and as proposed for *Gata3* in the previous section, *in vivo* experiments with simultaneous implantation of Shh-beads and injection of Ly in chicken embryos could clarify whether Hh is regulating *Lfng* expression in a Notch-independent manner. Furthermore, data from this and previous work in our lab (Figueiredo, 2011) showed that *Hes6.1* is also expressed in this territory. While our qRT-PCR data suggest that its expression levels are not altered when Notch is inhibited, *in situ* analysis of *Hes6.1* expression domain in the 3/4PP of chicken embryos after *in vivo* Ly injection could confirm whether there are spatial changes. Nevertheless, several studies suggest that *Hes6.1* is an "atypical" Notch target, being differently regulated in distinct regions of the chicken embryo, and sequestering other Hes proteins to suppress their own transcriptional repressive activity, leading to an increase in their expression (Vilas-Boas and Henrique, 2010). Our work suggests that this Notch target is regulated independently of Hh signalling in our model, as the *in vitro* and *in vivo* inhibition of Hh signalling resulted in no changes in *Hes6.1* expression.

Although it is unclear what happens to the "no fate" domain further in development in the avian model, it likely suffers apoptosis as in the mouse model (Gardiner *et al.*, 2012). Our observation that *Fgf8* expression – shown to regulate

proliferation in the foregut endoderm (Park *et al.*, 2006) – is reduced over time in the posterior domain of the 3/4PP endoderm in the avian also supports this hypothesis.

VII.5 Regulation of the anterior boundary of the thymic domain

The anterior boundary of the *Foxn1*$^{+}$ domain was unchanged when Hh signalling was inhibited, even though *Gcm2* expression in the anterior/median domain was lost. This may be due to the early specification of the parathyroids fate, accompanied by the definition of its boundary. The parathyroids domain is specified before, and regardless of, *Gcm2* expression (Liu, Yu and Manley, 2007), which may mean that the fate becomes "blocked" early on and prevents the expansion of *Foxn1* expression to that region.

Tbx1, known to be restricted to the parathyroid glands domain within the pharyngeal endoderm at these stages (Blackburn and Manley, 2004), to be expressed in the *Gcm2* null mutant (Liu, Yu and Manley, 2007), and to supress *Foxn1* expression (Reeh *et al.*, 2014; Bain *et al.*, 2016), could be a potential candidate for the prevention of *Foxn1* expansion. Since a Shh-Tbx1-Gcm2 pathway has been proposed, with *Tbx1* being positively regulated by Shh signalling in the pharyngeal region of mouse and chicken embryos (Garg *et al.*, 2001; Yamagishi *et al.*, 2003; Bain *et al.*, 2016), we would expect *Tbx1* transcripts to be reduced in the presence of pharmacological Hh inhibitors. Our preliminary qRT-PCR data from Chapter III show that *Tbx1* expression was not significantly changed in organotypic cultures grown with Cyc. However, this assay does not allow us to assess gene expression changes specifically in the pouch endoderm for genes that are also highly expressed in the other tissues, as it is the case of *Tbx1* in the surrounding mesenchyme. Thus, the potential changes in *Tbx1* expression within the pouch endoderm may be masked by its strong expression in the surrounding mesenchyme. Performing additional *in vitro* assays to increase the number of samples and the robustness of these qRT-PCR results, along with *in situ* hybridization and/or immunohistochemistry for Tbx1 in sections of chicken embryos exposed to Cyc-beads could clarify Tbx1 changes in our model.

Another potential candidate for the anterior boundary definition is Jagged1. *Jagged1* was found to be expressed in the anterior domain of the 3rd PP endoderm at cE3 and cE3.5 (Fig. 5L and Suppl. Fig. 5A in Chapter IV), and to become restricted to the

parathyroids domain later in development (data not shown). As *Jagged1* expression remained unchanged in the absence of Hh signalling, it may be defining the parathyroid glands territory independently of Hh and the Gata3-Gcm2 cascade. The fact that *Jagged1* expression is not altered when Hh is inhibited, but *Gata3* is, also supports the existence of distinct mechanisms through which Hh signalling regulates Notch-related molecules in the same domain of the pouch. Jagged1 may be an early player that defines the parathyroid glands domain, while Hh may induce the cascade of the parathyroid program (through the Notch target *Gata3*). Considering that Notch signalling inhibition also affected *Gcm2* expression and impaired organ formation, it would be interesting to investigate whether *Jagged1* changes its levels or patterns of expression when Notch signalling is blocked.

Worth noting, the preliminary results of Chapter III show also a significant decrease in *Bmp4* expression in the pharyngeal region after the pharmacological block of Hh signalling, which could seem to go against the reported expansion of the *Bmp4*$^{+}$ and *Foxn1*$^{+}$ domains in *Shh*$^{-/-}$ mice (Moore-Scott and Manley, 2005). However, as previously mentioned, this type of assay does not allow an evaluation of tissue-specific expression within the pharyngeal explant. Since *Bmp4* expression in the pharyngeal region is not restricted to the pouch endoderm (Patel *et al.*, 2006; Neves *et al.*, 2012; Bain *et al.*, 2016), we cannot draw conclusions about where this expression decrease takes place. Moreover, several studies in gut development (which has several similarities with our system) have shown that Hh signals in the epithelium regulate *Bmp4* expression in the surrounding mesenchyme (reviewed in Roberts, 2000; Chin *et al.*, 2016), suggesting that it may also be the case in the pharyngeal region. Again, further analysis of sections of chicken embryos exposed to Cyc-beads using *in situ* hybridization and/or immunohistochemistry for Bmp4 would help us understand where and in what way Hh signalling regulates *Bmp4* expression.

VII.6 The role of Notch in the pharyngeal endoderm

Our work revealed that Notch is involved in thymus and parathyroid glands early development. However, it remains unclear which tissue is the main driver of those Notch effects. The differential expression of Notch targets in distinct domains of the pouches suggests that the endoderm is where Notch activation is exerting its major influence. Our

strategy to modulate Notch specifically in the 3/4PP endoderm showed several limitations and was unable to modulate Notch signalling.

Although the experimental conditions used for the electroporation of the isolated 3/4PP endoderm were selected (among the many tested during this thesis) due to their results in terms of tissue integrity and subsequent *GFP* expression in culture, they may be suboptimal for the modulation of Notch signalling in these tissues. Additional tests of different electroporation conditions could be conducted to see if we can still use this approach to clarify the tissue-specific role of Notch in T/PT early development.

However, it is important to consider that the isolated 3/4PP endoderm contained, in fact, not only the 3/4PP from each side, but also the central endoderm (pharynx), which is the largest area of the isolated tissue (Fig. 1A in Chapter V). Thus, one can admit that the probability of transfecting the endoderm of the 3/4PP is much lower than that of transfecting the pharynx. Moreover, it is impossible to control the number of vectors that reaches each cell, and the fact that the transient system we used is composed of two large vectors (over 8Kb) may decrease even more the probability of successfully transfecting the cells of the 3/4PP endoderm with both vectors. These particularities may be partially responsible for the strong limitations found using this method.

In future experiments, we could isolate and electroporate only the specific endoderm of the 3/4PP, without the central endoderm. However, both the integrity and development of this small and fragile structure may be impaired without its central core. In case the 3/4PP endoderm alone would develop normally, and our approach would still not work, the use of RNA interference (RNAi) (Das *et al.*, 2006) or morpholinos (Norris and Streit, 2014) against the ICN1, MAML1, or other Notch-related proteins to impair Notch activation could be considered. If electroporation itself turned out to be an aggressive method to this small tissue, an adaptation of the lipofection technique could also be considered.

A less “clean” approach would be *in vivo* gene editing directed to the 3/4PP endoderm region. The classic *in vivo* electroporation is not a viable choice in this case, as the pharyngeal region is too close to the heart and the electric pulse in that area greatly reduces the viability of the embryos (less than 10% of viability; unpublished data from our group). Magnetofection (magnetic transfection) and sonoporation (ultrasound induced transfection) have been shown to be efficient *in vivo* (Scherer *et al.*, 2002; Ohta

et al., 2003). The main advantage would be their non-invasiveness, as surface magnets or ultrasound are used to deliver the DNA into targeted cells. The obvious main disadvantage of these *in vivo* methods would be the off-target effects. It would require a thorough *in situ* analysis of the number of endodermal and off-target cells electroporated, and the respective phenotypes, to make any reasonable causal associations.

Another possible approach would be the generation of transgenic mouse embryos that would have Notch signalling constitutively activated or blocked specifically in the endoderm of the 3/4PP. However, and as previously mentioned, so far, no specific marker of the 3/4PP endoderm has been identified. The discovery of such marker would revolutionize this type of studies. Currently, at best, one could use genes that are expressed in the presumptive domain of the thymus before the onset of *Foxn1* expression (currently, no gene is known to fit these parameters for the parathyroids). *Nkx2.5* and *Isl1* were shown to be expressed in this domain at mE9.5 and mE10.5, and *Nkx2.6* at mE10.5 (Wei and Condie, 2011). Thus, these genes could potentially work as thymic domain-specific genes at these stages, prior to *Foxn1* expression. However, they all seem to be expressed in the developing heart during this time-window, suggesting that Notch modulation in the heart could severely impair embryo survival. Nevertheless, for this to work, the transgenes would have to be activated at these specific stages of embryonic development, which is not feasible in mammalian embryos. On the other hand, the use of transgenic chicken embryos would allow *in ovo* injection of compounds to activate the inducible transgene at specific stages.

Recently, the development of transgenic chickens has become a reality thanks to transcription activator-like effector nuclease (TALEN)-mediated gene targeting (Park *et al.*, 2014; Taylor *et al.*, 2017) and the revolutionary clustered regularly interspaced short palindromic repeats (CRISPR)/CRISPR-associated 9 (Cas9) system (Dimitrov *et al.*, 2016; Oishi *et al.*, 2016; Antonova *et al.*, 2018). Interestingly, CRISPR/Cas9 mediated knockout has also been shown *in vivo* in chicken somatic cells, combined with *in ovo* electroporation (Véron *et al.*, 2015). These tools will be fundamental in future studies, allowing the combination of modern genetic techniques with the classical techniques in the avian embryo to provide insights into biological processes and their significance. Hopefully, both TALEN and CRISPR/Cas9 methods will soon be used at a large scale to generate specific genome-edited avian lines, which will have a great impact in basic and applied biomedical research.

VII.7 Conclusions

The data presented in this thesis describe for the first time the involvement of Notch in the early stages of thymus and parathyroid glands development. In addition, Hedgehog signalling was found to be acting upstream of the Notch pathway at these stages. The work also provided new data regarding potential players and potential interactions in this context. I hope this work contributes to the knowledge of normal thymus and parathyroid organogenesis, crucial for understanding the events responsible for the maintenance of healthy glands function later in life, or for repairing their function in disease.

REFERENCES

Abramson, J. and Anderson, G. (2017) 'Thymic Epithelial Cells', *Annual Review of Immunology*, 35(1), pp. 85–118. doi: 10.1146/annurev-immunol-051116-052320.

Abu-Issa, R. *et al.* (2002) 'Fgf8 is required for pharyngeal arch and cardiovascular development in the mouse.', *Development (Cambridge, England)*, 129(19), pp. 4613–4625.

Akiyama, Y. *et al.* (1996) 'The gcm-motif: a novel DNA-binding motif conserved in Drosophila and mammals.', *Proceedings of the National Academy of Sciences of the United States of America*, 93(25), pp. 14912–14916. doi: 10.1073/pnas.93.25.14912.

Del Álamo, D., Rouault, H. and Schweisguth, F. (2011) 'Mechanism and significance of cis-inhibition in notch signalling', *Current Biology*. doi: 10.1016/j.cub.2010.10.034.

Alexander, T., Nolte, C. and Krumlauf, R. (2009) 'Hox Genes and Segmentation of the Hindbrain and Axial Skeleton', *Annual Review of Cell and Developmental Biology*, 25, pp. 431–56. doi: 10.1146/annurev.cellbio.042308.113423.

Alfaro, A. C. *et al.* (2014) 'Ptch2 mediates the Shh response in Ptch1-/- cells', *Development*, 141(17), pp. 3331–3339. doi: 10.1242/dev.110056.

Alves, N. L. *et al.* (2009) 'Thymic epithelial cells: the multi-tasking framework of the T cell "cradle".', *Trends in Immunology*, 30(10), pp. 468–474. Available at: http://www.ncbi.nlm.nih.gov/pubmed/19781995.

Andersen, P. *et al.* (2012) 'Non-Canonical Notch Signaling: Emerging Role and Mechanism', *Trends Cell Biology*, 22(5), pp. 257–265. doi: 10.1016/j.tcb.2012.02.003.

Anderson, G. *et al.* (2006) 'Establishment and functioning of intrathymic microenvironments', *Immunological Reviews*, 209, pp. 10–27. doi: 10.1111/j.0105-2896.2006.00347.x.

Anderson, G., Lane, P. J. L. and Jenkinson, E. J. (2007) 'Generating intrathymic microenvironments to establish T-cell tolerance', *Nature reviews. Immunology*, 7(12), pp. 954–63. doi: 10.1038/nri2187.

Andersson, E. R., Sandberg, R. and Lendahl, U. (2011) 'Notch signaling: simplicity in design, versatility in function', *Development*, 138(17), pp. 3593–3612. doi: 10.1242/dev.063610.

Antonova, E. *et al.* (2018) 'Successful CRISPR/Cas9 mediated homologous recombination in a chicken cell line', *F1000Research*, 7(0), p. 238. doi: 10.12688/f1000research.13457.1.

Aoto, K. *et al.* (2002) 'Mouse GLI3 regulates Fgf8 expression and apoptosis in the developing neural tube, face, and limb bud', *Developmental Biology*, 251(2), pp. 320–332. doi: 10.1006/dbio.2002.0811.

Arnold, J. S. *et al.* (2006) 'Inactivation of Tbx1 in the pharyngeal endoderm results in 22q11DS malformations', *Development*, 133(5), pp. 977–987. doi: 10.1242/dev.02264.

Arrangoiz, R. *et al.* (2017) 'Parathyroid Embryology, Anatomy, and Pathophysiology of Primary Hyperparathyroidism', *International Journal of Otolaryngology and Head & Neck Surgery*, 06(04), pp. 39–58. doi: 10.4236/ijohns.2017.64007.

Auerbach, R. (1960) 'Morphogenetic interactions in the development of the mouse thymus

gland', *Dev. Biol.*, 2, pp. 271–284. Available at: http://dx.doi.org/10.1016/0012-1606(60)90009-9.

Aulehla, A. and Johnson, R. L. (1999) 'Dynamic expression of lunatic fringe suggests a link between notch signaling and an autonomous cellular oscillator driving somite segmentation', *Developmental Biology*. doi: 10.1006/dbio.1998.9164.

Auricchio, L. *et al.* (2005) 'Nail Dystrophy Associated With a Heterozygous Mutation of the Nude/SCID Human FOXN1 (WHN) Gene', *Archives of dermatology*, 141(5), pp. 647–648.

Bain, V. E. *et al.* (2016) *Tissue-specific roles for Sonic hedgehog signaling in establishing thymus and parathyroid organ fate*, *Development*. doi: 10.1242/dev.141903.

Balciunaite, G. *et al.* (2002) 'Wnt glycoproteins regulate the expression of FoxN1, the gene defective in nude mice.', *Nature immunology*, 3(11), pp. 1102–8. doi: 10.1038/ni850.

Baldini, A. (2005) 'Dissecting contiguous gene defects: TBX1', *Current Opinion in Genetics and Development*, pp. 279–284. doi: 10.1016/j.gde.2005.03.001.

Blackburn, C. C. *et al.* (1996) 'The nu gene acts cell-autonomously and is required for differentiation of thymic epithelial progenitors.', *Proceedings of the National Academy of Sciences of the United States of America*. National Acad Sciences, 93(12), pp. 5742–5746. Available at: http://www.pubmedcentral.nih.gov/articlerender.fcgi?artid=39131&tool=pmcentrez&rendertype=abstract.

Blackburn, C. C. and Manley, N. R. (2004) 'Developing a new paradigm for thymus organogenesis.', *Nature Reviews Immunology*. Nature Publishing Group, 4(4), pp. 278–289. Available at: http://hdl.handle.net/1842/706.

Blentic, A., Gale, E. and Maden, M. (2003) 'Retinoic acid signalling centres in the avian embryo identified by sites of expression of synthesising and catabolising enzymes', *Developmental Dynamics*, 227(1), pp. 114–127. doi: 10.1002/dvdy.10292.

Bleul, C. C. *et al.* (2006) 'Formation of a functional thymus initiated by a postnatal epithelial progenitor cell.', *Nature*. Nature Publishing Group, 441(7096), pp. 992–996. Available at: http://www.ncbi.nlm.nih.gov/pubmed/16791198.

Bleul, C. C. and Boehm, T. (2005) 'BMP signaling is required for normal thymus development.', *Journal of immunology (Baltimore, Md. : 1950)*, 175(8), pp. 5213–21. Available at: http://www.ncbi.nlm.nih.gov/pubmed/16210626.

Boareto, M. *et al.* (2015) 'Jagged-Delta asymmetry in Notch signaling can give rise to a Sender/Receiver hybrid phenotype.', *Proceedings of the National Academy of Sciences of the United States of America*, 112(5), pp. E402-9. doi: 10.1073/pnas.1416287112.

Bockman, D. E. and Kirby, M. L. (1984) 'Dependence of thymus development on derivatives of the neural crest.', *Science*, 223(4635), pp. 498–500. doi: 10.1126/science.6606851.

Boehm, T. *et al.* (2012) 'Evolution of vertebrate immunity.', *Current biology : CB*. Elsevier, 22(17), pp. R722-32. doi: 10.1016/j.cub.2012.07.003.

Bonini, N. M., Leiserson, W. M. and Benzer, S. (1993) 'The eyes absent gene: Genetic control of cell survival and differentiation in the developing Drosophila eye', *Cell*, 72(3), pp. 379–395. doi: 10.1016/0092-8674(93)90115-7.

Boopathy, A. V *et al.* (2013) 'Oxidative stress-induced Notch1 signaling promotes cardiogenic gene expression in mesenchymal stem cells', *Stem Cell Research & Therapy*. doi: 10.1186/scrt190.

Bourikas, D. and Stoeckli, E. T. (2003) 'New tools for gene manipulation in chicken embryos.', *Oligonucleotides*, 13(5), pp. 411–419. Available at: http://www.ncbi.nlm.nih.gov/pubmed/15000832.

Bray, S. (1998) 'Notch signalling in Drosophila: Three ways to use a pathway', *Seminars in Cell and Developmental Biology*, 9(6), pp. 591–597. doi: 10.1006/scdb.1998.0262.

Bray, S. (2006) 'Notch signalling: a simple pathway becomes complex.', *Nature reviews. Molecular cell biology*, 7(September), pp. 678–689. doi: 10.1038/nrm2009.

Bray, S. and Bernard, F. (2010) 'Notch targets and their regulation.', *Current topics in developmental biology*, 92(10), pp. 253–75. doi: 10.1016/S0070-2153(10)92008-5.

Brennan, D. *et al.* (2012) 'Noncanonical Hedgehog Signaling', *Vitamins & Hormones*, 88, pp. 55–72. doi: 10.1016/B978-0-12-394622-5.00003-1.Noncanonical.

Bronner-Fraser, M. (2008) 'Avian Embryology', *Academic Press*, pp. 20–24.

van Bueren, K. L. *et al.* (2010) 'Hes1 expression is reduced in Tbx1 null cells and is required for the development of structures affected in 22q11 deletion syndrome', *Developmental Biology*. Elsevier Inc., 340(2), pp. 369–380. doi: 10.1016/j.ydbio.2010.01.020.

Caliceti, C. *et al.* (2014) 'ROS, Notch, and Wnt signaling pathways: Crosstalk between three major regulators of cardiovascular biology', *BioMed Research International*. doi: 10.1155/2014/318714.

Carpenter, A. C. and Bosselut, R. (2010) 'Decision checkpoints in the thymus', *Nature Immunology*, 11(8), pp. 666–673. doi: 10.1038/ni.1887.

Carrieri, F. A. and Dale, J. K. (2017) 'Turn It Down a Notch', *Frontiers in Cell and Developmental Biology*, 4(January), pp. 1–9. doi: 10.3389/fcell.2016.00151.

de Celis, J. F. (2013) 'Understanding the determinants of notch interactions with its ligands.', *Science signaling*, 6(276), p. pe19. doi: 10.1126/scisignal.2004079.

Chen, H. *et al.* (2013) 'An Update on the Structure of the Parathyroid Gland', 5, pp. 1–9.

Chen, J. K. *et al.* (2002) 'Inhibition of Hedgehog signaling by direct binding of cyclopamine to Smoothened', *Genes and Development*. doi: 10.1101/gad.1025302.

Chen, L. *et al.* (2010) 'Mouse and zebrafish Hoxa3 orthologues have nonequivalent in vivo protein function.', *Proceedings of the National Academy of Sciences of the United States of America*, 107(23), pp. 10555–10560. doi: 10.1073/pnas.1005129107.

Chin, A. M. *et al.* (2016) 'Morphogenesis and maturation of the embryonic and postnatal intestine', *Seminars in Cell and Developmental Biology*. Elsevier Ltd, pp. 1–13. doi: 10.1016/j.semcdb.2017.01.011.

Chinn, I. K. *et al.* (2012) 'Changes in primary lymphoid organs with aging', *Seminars in Immunology*. doi: 10.1016/j.smim.2012.04.005.

Choe, C. P. and Crump, J. G. (2014) 'Tbx1 controls the morphogenesis of pharyngeal pouch

epithelia through mesodermal Wnt11r and Fgf8a.', *Development (Cambridge, England)*, 141(18), pp. 3583–93. doi: 10.1242/dev.111740.

Chojnowski, J. L. *et al.* (2014) 'Multiple roles for HOXA3 in regulating thymus and parathyroid differentiation and morphogenesis in mouse.', *Development (Cambridge, England)*, 141, pp. 3697–708. doi: 10.1242/dev.110833.

Chojnowski, J. L. *et al.* (2016) 'Temporal and spatial requirements for Hoxa3 in mouse embryonic development', *Developmental Biology*. Elsevier, 415(1), pp. 33–45. doi: 10.1016/j.ydbio.2016.05.010.

Christakis, I. A. and Palazzo, F. F. (2014) 'Parathyroid Glands: Homeostasis, Disease and Indications For Surgical Treatment', in *Parathyroid Glands: Regulation, Role in Human Disease and Indications for Surgery*, pp. 35–56.

Chuong, C. M. *et al.* (2005) 'Engineering Stem Cells into Organs: Topobiological Transformations Demonstrated by Beak, Feather, and Other Ectodermal Organ Morphogenesis', *Current Topics in Developmental Biology*. doi: 10.1016/S0070-2153(05)72005-6.

Cosgrove, D. *et al.* (1992) 'The thymic compartment responsible for positive selection of CD4+ T cells.', *International Immunology*, 4(6), pp. 707–710. Available at: http://www.ncbi.nlm.nih.gov/entrez/query.fcgi?cmd=Retrieve&db=PubMed&dopt=Citation&list_uids=1352128.

Creuzet, S. *et al.* (2002) 'Negative effect of Hox gene expression on the development of the neural crest-derived facial skeleton', *Development*, 129(18), pp. 4301–4313.

Crossley, P. H. and Martin, G. R. (1995) 'The mouse Fgf8 gene encodes a family of polypeptides and is expressed in regions that direct outgrowth and patterning in the developing embryo.', *Development (Cambridge, England)*, 121(2), pp. 439–451.

D'Souza, B., Meloty-Kapella, L. and Weinmaster, G. (2010) 'Canonical and non-canonical Notch ligands.', *Current topics in developmental biology*, 92(10), pp. 73–129. doi: 10.1016/S0070-2153(10)92003-6.

Dahl, E., Koseki, H. and Balling, R. (1997) 'Pax genes and organogenesis.', *BioEssays : news and reviews in molecular, cellular and developmental biology*, 19(9), pp. 755–765. doi: 10.1002/bies.950190905.

Darnell, D. K. *et al.* (2014) 'Developmental expression of chicken FOXN1 and putative target genes during feather development', *International Journal of Developmental Biology*. doi: 10.1387/ijdb.130023sy.

Das, R. M. *et al.* (2006) 'A robust system for RNA interference in the chicken using a modified microRNA operon', *Developmental Biology*, 294(2), pp. 554–563. doi: 10.1016/j.ydbio.2006.02.020.

Davey, M. G. and Tickle, C. (2007) 'The chicken as a model for embryonic development', *Cytogenetic and Genome Research*. doi: 10.1159/000103184.

Dieterlen-Lièvre, F. and Le Douarin, N. M. (2004) 'From the hemangioblast to self-tolerance: a series of innovations gained from studies on the avian embryo.', *Mechanisms of development*, 121(9), pp. 1117–28. doi: 10.1016/j.mod.2004.06.008.

Dietrich, S. and Gruss, P. (1995) 'Undulated phenotypes suggest a role of Pax-1 for the development of vertebral and extravertebral structures', *Developmental Biology*. doi:

10.1006/dbio.1995.1047.

Diman, N. Y. S. G. *et al.* (2011) 'A retinoic acid responsive Hoxa3 transgene expressed in embryonic pharyngeal endoderm, cardiac neural crest and a subdomain of the second heart field', *PLoS ONE*, 6(11), pp. 1–11. doi: 10.1371/journal.pone.0027624.

Dimitrov, L. *et al.* (2016) 'Germline gene editing in chickens by efficient crispr-mediated homologous recombination in primordial germ cells', *PLoS ONE*, 11(4). doi: 10.1371/journal.pone.0154303.

Dooley, J. *et al.* (2007) 'FGFR2IIIb signaling regulates thymic epithelial differentiation', *Developmental Dynamics*, 236(12), pp. 3459–3471. doi: 10.1002/dvdy.21364.

Dorey, K. and Amaya, E. (2010) 'FGF signalling: diverse roles during early vertebrate embryogenesis.', *Development (Cambridge, England)*, 137(22), pp. 3731–42. doi: 10.1242/dev.037689.

Dorsch, M. *et al.* (2002) 'Ectopic expression of Delta4 impairs hematopoietic development and leads to lymphoproliferative disease.', *Blood*.

Le Douarin, N. (1967) 'Détermination précoce des ébauches de la thyroïde et du thymus chez l'embryon de Poulet.', *C.R. Acad. Sci.*, 264, pp. 940–942.

Le Douarin, N. (1973) 'A biological cell labeling technique and its use in experimental embryology', *Developmental Biology*, 30(1), pp. 217–222. doi: 10.1016/0012-1606(73)90061-4.

Le Douarin, N. (2005) 'The Nogent Institute--50 years of embryology.', *The International journal of developmental biology*, 49(2–3), pp. 85–103. doi: 10.1387/ijdb.041952nl.

Le Douarin, N. M., Bussonnet, C. and Chaumont, F. (1968) 'Etude des capacités de différenciation et du rôle morphogène de l'endoderme pharyngien chez l'embryon d'Oiseau.', *Ann. Embryol. Morph.*, 1, pp. 29–40.

Le Douarin, N. M. and Dieterlen-Lièvre, F. (2013) 'How studies on the avian embryo have opened new avenues in the understanding of development: A view about the neural and hematopoietic systems', *Development Growth and Differentiation*, 55(1), pp. 1–14. doi: 10.1111/dgd.12015.

Le Douarin, N. M., Dieterlen-Lièvre, F. and Oliver, P. D. (1984) 'Ontogeny of primary lymphoid organs and lymphoid stem cells', *American Journal of Anatomy*, 170(3), pp. 261–299. doi: 10.1002/aja.1001700305.

Le Douarin, N. M. and Jotereau, F. V (1975) 'Tracing of cells of the avian thymus through embryonic life in interspecific chimeras.', *The Journal of Experimental Medicine*. The Rockefeller University Press, 142(1), pp. 17–40. doi: 10.1084/jem.142.1.17.

Le Douarin, N. M. and Teillet, M. a (1973) 'The migration of neural crest cells to the wall of the digestive tract in avian embryo.', *Journal of embryology and experimental morphology*, 30(1), pp. 31–48.

Dupé, V. *et al.* (1999) 'Key roles of retinoic acid receptors alpha and beta in the patterning of the caudal hindbrain, pharyngeal arches and otocyst in the mouse.', *Development (Cambridge, England)*, 126, pp. 5051–5059.

Etchevers, H. C. *et al.* (2001) 'The cephalic neural crest provides pericytes and smooth muscle cells to all blood vessels of the face and forebrain.', *Development (Cambridge, England)*. doi: 10.7554/elife.10036.016.

van Ewijk, W. *et al.* (2000) 'Stepwise development of thymic microenvironments in vivo is regulated by thymocyte subsets.', *Development (Cambridge, England)*, 127(8), pp. 1583–91. Available at: http://www.ncbi.nlm.nih.gov/pubmed/10725235.

van Ewijk, W., Shores, E. W. and Singer, A. (1994) 'Crosstalk in the mouse thymus', *Trends in Immunology*, 15(5), pp. 214–217. doi: 10.1016/1471490694900663.

Fang, T. C. *et al.* (2007) 'Notch Directly Regulates Gata3 Expression during T Helper 2 Cell Differentiation', *Immunity*, 27(1), pp. 100–110. doi: 10.1016/j.immuni.2007.04.018.

Farley, A. M. *et al.* (2013) 'Dynamics of thymus organogenesis and colonization in early human development.', *Development (Cambridge, England)*, 140(9), pp. 2015–26. doi: 10.1242/dev.087320.

Figueiredo, M. (2011) *The Role of Notch Signaling in Thymic Epithelium Development*. Faculdade de Ciências da Universidade de Lisboa.

Figueiredo, M. *et al.* (2016) 'Notch and Hedgehog in the thymus/parathyroid common primordium: Crosstalk in organ formation.', *Developmental biology*, 418(2), pp. 268–282. doi: 10.1016/j.ydbio.2016.08.012.

Figueiredo, M. and Neves, H. (2018) 'Two-step Approach to Explore Early-and Late-stages of Organ Formation in the Avian Model: The Thymus and Parathyroid Glands Organogenesis Paradigm', *Journal of Visualized Experiments*, (136), p. e57114. doi: 10.3791/57114.

Fior, R. and Henrique, D. (2005) 'A novel hes5/hes6 circuitry of negative regulation controls Notch activity during neurogenesis.', *Developmental biology*, 281(2), pp. 318–33. doi: 10.1016/j.ydbio.2005.03.017.

Fior, R. and Henrique, D. (2009) '"Notch-Off": a perspective on the termination of Notch signalling.', *The International journal of developmental biology*, 53(8–10), pp. 1379–84. doi: 10.1387/ijdb.072309rf.

Flanagan, S. P. (1966) '"Nude", a new hairless gene with pleiotropic effects in the mouse.', *Genetical research*, 8(3), pp. 295–309. doi: 10.1017/S0016672300010168.

Foster, K. *et al.* (2008) 'Contribution of Neural Crest-Derived Cells in the Embryonic and Adult Thymus', *The Journal of Immunology*, 180(5), pp. 3183–3189. doi: 10.4049/jimmunol.180.5.3183.

Foster, K. E. *et al.* (2010) 'EphB-ephrin-B2 interactions are required for thymus migration during organogenesis.', *Proceedings of the National Academy of Sciences of the United States of America*, 107(30), pp. 13414–9. doi: 10.1073/pnas.1003747107.

Frank, D. U. *et al.* (2002) 'An Fgf8 mouse mutant phenocopies human 22q11 deletion syndrome.', *Development (Cambridge, England)*, 129(19), pp. 4591–603. Available at: http://www.pubmedcentral.nih.gov/articlerender.fcgi?artid=1876665&tool=pmcentrez&rendertype=abstract.

von Freeden-Jeffry, U. *et al.* (1995) 'Lymphopenia in interleukin (IL)-7 gene-deleted mice identifies IL-7 as a nonredundant cytokine', *J Exp Med*, 181(4), pp. 1519–1526. doi: 10.1084/jem.181.4.1519.

Fryer, C. J. *et al.* (2002) 'Mastermind mediates chromatin-specific transcription and turnover of the Notch enhancer complex.', *Genes & Development*. Cold Spring Harbor Laboratory Press, 16(11), pp. 1397–1411. Available at:

http://www.pubmedcentral.nih.gov/articlerender.fcgi?artid=186317&tool=pmcentrez&rendertype=abstract.

Gardiner, J. R. *et al.* (2012) 'Localised inhibition of FGF signalling in the third pharyngeal pouch is required for normal thymus and parathyroid organogenesis.', *Development (Cambridge, England)*, 139(18), pp. 3456–66. doi: 10.1242/dev.079400.

Garg, V. *et al.* (2001) 'Tbx1, a DiGeorge syndrome candidate gene, is regulated by sonic hedgehog during pharyngeal arch development.', *Developmental biology*, 235(1), pp. 62–73. doi: 10.1006/dbio.2001.0283.

Gordon, J. *et al.* (2001) 'Gcm2 and Foxn1 mark early parathyroid- and thymus-specific domains in the developing third pharyngeal pouch.', *Mechanisms of Development*, 103(1–2), pp. 141–143. Available at: http://www.ncbi.nlm.nih.gov/pubmed/11335122.

Gordon, J. *et al.* (2004) 'Functional evidence for a single endodermal origin for the thymic epithelium.', *Nature immunology*, 5(5), pp. 546–553. doi: 10.1038/ni1064.

Gordon, J. *et al.* (2010) 'Evidence for an early role for BMP4 signaling in thymus and parathyroid morphogenesis.', *Developmental Biology*. Elsevier Inc., 339(1), pp. 141–154. doi: 10.1016/j.ydbio.2009.12.026.Evidence.

Gordon, J. and Manley, N. R. (2011) 'Mechanisms of thymus organogenesis and morphogenesis', *Development*, 138(18), pp. 3865–3878. doi: 10.1242/dev.059998.

Gotter, J. *et al.* (2004) 'Medullary epithelial cells of the human thymus express a highly diverse selection of tissue-specific genes colocalized in chromosomal clusters.', *The Journal of Experimental Medicine*. The Rockefeller University Press, 199(2), pp. 155–166. Available at: http://www.ncbi.nlm.nih.gov/pubmed/14734521.

Graham, A., Okabe, M. and Quinlan, R. (2005) 'The role of the endoderm in the development and evolution of the pharyngeal arches.', *Journal of anatomy*, 207(5), pp. 479–487. doi: 10.1111/j.1469-7580.2005.00472.x.

Grevellec, A., Graham, A. and Tucker, A. S. (2011) 'Shh signalling restricts the expression of Gcm2 and controls the position of the developing parathyroids.', *Developmental biology*. Elsevier B.V., 353(2), pp. 194–205. doi: 10.1016/j.ydbio.2011.02.012.

Grevellec, A. and Tucker, A. S. (2010) 'The pharyngeal pouches and clefts: Development, evolution, structure and derivatives.', *Seminars in cell & developmental biology*. Elsevier Ltd, 21(3), pp. 325–32. doi: 10.1016/j.semcdb.2010.01.022.

Griffith, A. V *et al.* (2009) 'Increased thymus- and decreased parathyroid-fated organ domains in Splotch mutant embryos', 327(1), pp. 216–227. doi: 10.1016/j.ydbio.2008.12.019.Increased.

Grigorieva, I. and Mirczuk, S. (2010) 'Gata3-deficient mice develop parathyroid abnormalities due to dysregulation of the parathyroid-specific transcription factor Gcm2', *The Journal of clinical …*, 120(6). doi: 10.1172/JCI42021.2144.

Groth, C. *et al.* (2010) 'Pharmacological analysis of Drosophila melanogaster gamma-secretase with respect to differential proteolysis of Notch and APP.', *Molecular pharmacology*. doi: 10.1124/mol.109.062471.

Günther, T. *et al.* (2000) 'Genetic ablation of parathyroid glands reveals another source of parathyroid hormone.', *Nature*, 406(6792), pp. 199–203. Available at: http://www.ncbi.nlm.nih.gov/pubmed/10910362.

Guo, C. *et al.* (2011) 'A Tbx1-Six1/Eya1-Fgf8 genetic pathway controls mammalian cardiovascular and craniofacial morphogenesis', *Journal of Clinical Investigation*, 121(4), pp. 1585–1595. doi: 10.1172/JCI44630.

Haines, N. and Irvine, K. D. (2003) 'Glycosylation regulates Notch signalling', *Nature Reviews Molecular Cell Biology*, 4(10), pp. 786–797. doi: 10.1038/nrm1228.

Hamburger, V. and Hamilton, H. L. (1951) 'A series of normal stages in the development of the chick embryo', *Journal of morphology*, 88(1), pp. 49–92. Available at: http://homepage.univie.ac.at/~metschb9/Hamburger51_ChickStages.pdf (Accessed: 2 November 2011).

Han, S. iee, Tsunekage, Y. and Kataoka, K. (2015) 'Gata3 cooperates with Gcm2 and MafB to activate parathyroid hormone gene expression by interacting with SP1', *Molecular and Cellular Endocrinology*. doi: 10.1016/j.mce.2015.04.018.

Haworth, K. E. *et al.* (2007) 'Sonic hedgehog in the pharyngeal endoderm controls arch pattern via regulation of Fgf8 in head ectoderm', *Developmental Biology*. doi: 10.1016/j.ydbio.2006.11.009.

Heitzler, P. (2010) *Biodiversity and noncanonical Notch signaling., Current topics in developmental biology*. Elsevier Inc. doi: 10.1016/S0070-2153(10)92014-0.

Henrique, D. *et al.* (1995) 'Expression of a delta homologue in prospective neurons in the chick', *Nature*. doi: 10.1038/375787a0.

Henrique, D. and Schweisguth, F. (2019) 'Mechanisms of notch signaling: A simple logic deployed in time and space', *Development (Cambridge)*, 146(3). doi: 10.1242/dev.172148.

Hettige, N. C. and Ernst, C. (2019) 'FOXG1 Dose in Brain Development', *Frontiers in Pediatrics*, 7(November), pp. 1–12. doi: 10.3389/fped.2019.00482.

Hetzer-Egger, C. *et al.* (2002) 'Thymopoiesis requires Pax9 function in thymic epithelial cells.', *European journal of immunology*, 32(4), pp. 1175–81. doi: 10.1002/1521-4141(200204)32:4<1175::AID-IMMU1175>3.0.CO;2-U.

Hicks, C. *et al.* (2000) 'Fringe differentially modulates Jagged1 and Delta1 signalling through Notch1 and Notch2', *Nature Cell Biology*. doi: 10.1038/35019553.

Hoflinger, S. *et al.* (2004) 'Analysis of notch1 function by in vitro T cell differentiation of pax5 mutant lymphoid progenitors', *Journal of immunology (Baltimore, Md : 1950)*, 173(6), pp. 3935–3944. doi: 10.4049/jimmunol.173.6.3935.

Hooper, J. E. and Scott, M. P. (2005) 'Communicating with hedgehogs', *Nature Reviews Molecular Cell Biology*, 6(4), pp. 306–317. doi: 10.1038/nrm1612.

Hori, K., Sen, A. and Artavanis-Tsakonas, S. (2013) 'Notch signaling at a glance.', *Journal of cell science*, 126(Pt 10), pp. 2135–40. doi: 10.1242/jcs.127308.

Hu, B. *et al.* (2010) 'Control of hair follicle cell fate by underlying mesenchyme through a CSL-Wnt5a-FoxN1 regulatory axis.', *Genes & development*, 24(14), pp. 1519–32. doi: 10.1101/gad.1886910.

Huangfu, D. *et al.* (2003) 'Hedgehog signalling in the mouse requires intraflagellar transport proteins', *Nature*, 426(6962), pp. 83–87. doi: 10.1038/nature02061.

Hurlbut, G. D. *et al.* (2007) 'Crossing paths with Notch in the hyper-network', *Current Opinion in Cell Biology*, 19(2), pp. 166–175. doi: 10.1016/j.ceb.2007.02.012.

Ishida, K. and Mitsui, T. (2016) 'Generation of bioengineered feather buds on a reconstructed chick skin from dissociated epithelial and mesenchymal cells', *Development Growth and Differentiation*. doi: 10.1111/dgd.12275.

Itoi, M. *et al.* (2001) 'Two distinct steps of immigration of hematopoietic progenitors into the early thymus anlage.', *International immunology*, 13(9), pp. 1203–1211. doi: 10.1093/intimm/13.9.1203.

Ivins, S. *et al.* (2005) 'Microarray analysis detects differentially expressed genes in the pharyngeal region of mice lacking Tbx1', *Developmental Biology*, 285(2), pp. 554–569. doi: 10.1016/j.ydbio.2005.06.026.

Izrailit, J. *et al.* (2017) 'Cellular stress induces TRB3/USP9x-dependent Notch activation in cancer', *Oncogene*. doi: 10.1038/onc.2016.276.

Jackson, A. *et al.* (2014) 'Endoderm-specific deletion of Tbx1 reveals an FGF-independent role for Tbx1 in pharyngeal apparatus morphogenesis', *Developmental Dynamics*, 243(9), pp. 1143–1151. doi: 10.1002/dvdy.24147.

Jaleco, a C. *et al.* (2001) 'Differential effects of Notch ligands Delta-1 and Jagged-1 in human lymphoid differentiation.', *The Journal of experimental medicine*, 194(7), pp. 991–1002. Available at: http://www.pubmedcentral.nih.gov/articlerender.fcgi?artid=2193482&tool=pmcentrez&rendertype=abstract.

Jenkinson, W. E., Jenkinson, E. J. and Anderson, G. (2003) 'Differential requirement for mesenchyme in the proliferation and maturation of thymic epithelial progenitors.', *The Journal of experimental medicine*, 198(2), pp. 325–32. doi: 10.1084/jem.20022135.

Jerome, L. A. and Papaioannou, V. E. (2001) 'DiGeorge syndrome phenotype in mice mutant for the T-box gene, Tbx1.', *Nature genetics*, 27(3), pp. 286–91. doi: 10.1038/85845.

Jiang, R. *et al.* (1998) 'Defects in limb, craniofacial, and thymic development in Jagged2 mutant mice', *Genes and Development*, 12(7), pp. 1046–1057. doi: 10.1101/gad.12.7.1046.

Johansson, E. *et al.* (2015) 'Revising the embryonic origin of thyroid C cells in mice and humans', *Development*, 142(20), pp. 3519–3528. doi: 10.1242/dev.126581.

Kadur, P. *et al.* (2018) 'Radical and lunatic fringes modulate notch ligands to support mammalian intestinal homeostasis', *eLife*, pp. 1–20. doi: https://doi.org/10.7554/eLife.35710.

Kageyama, R. *et al.* (2008) 'Dynamic Notch signaling in neural progenitor cells and a revised view of lateral inhibition', *Nature Neuroscience*, pp. 1247–1251. doi: 10.1038/nn.2208.

Kageyama, R. *et al.* (2010) *Ultradian oscillations in Notch signaling regulate dynamic biological events.*, *Current topics in developmental biology*. Elsevier Inc. doi: 10.1016/S0070-2153(10)92010-3.

Kameda, Y. *et al.* (2013) 'Hes1 is required for the development of pharyngeal organs and survival of neural crest-derived mesenchymal cells in pharyngeal arches.', *Cell and tissue research*, 353(1), pp. 9–25. doi: 10.1007/s00441-013-1649-z.

Kelly, M. (2012) *Molecular Regulation of Thymic Epithelial Lineage Specification*. University of

Edinburgh. Available at: http://hdl.handle.net/1842/10433.

Kiernan, A. E. (2013) 'Notch signaling during cell fate determination in the inner ear', *Seminars in Cell & Developmental Biology*. doi: 10.1016/j.semcdb.2013.04.002.

Kim, T.-H. *et al.* (2011) 'Endodermal Hedgehog signals modulate Notch pathway activity in the developing digestive tract mesenchyme.', *Development (Cambridge, England)*, 138(15), pp. 3225–33. doi: 10.1242/dev.066233.

Kirkpatrick, J. A. J. and DiGeorge, A. M. (1968) 'Congenital absence of the thymus', *Am J Roentgenol Radium Ther Nucl Med*, 103, pp. 32–7.

Klein, L. *et al.* (2014) 'Positive and negative selection of the T cell repertoire: what thymocytes see and don't see', *Nature reviews. Immunology*, 14(6), pp. 377–91. doi: 10.1038/nri3667.

Klug, D. B. *et al.* (1998) 'Interdependence of cortical thymic epithelial cell differentiation and T-lineage commitment.', *Proceedings of the National Academy of Sciences of the United States of America*. The National Academy of Sciences, 95(20), pp. 11822–11827. Available at: http://www.pubmedcentral.nih.gov/articlerender.fcgi?artid=21724&tool=pmcentrez&rendertype=abstract.

Knoblich, J. A. (2008) 'Mechanisms of Asymmetric Stem Cell Division', *Cell*, pp. 583–597. doi: 10.1016/j.cell.2008.02.007.

Kobayashi, T. and Kageyama, R. (2014) *Expression dynamics and functions of hes factors in development and diseases*. 1st edn, *Current Topics in Developmental Biology*. 1st edn. Elsevier Inc. doi: 10.1016/B978-0-12-405943-6.00007-5.

Kong, J. H. *et al.* (2015) 'Notch Activity Modulates the Responsiveness of Neural Progenitors to Sonic Hedgehog Signaling', *Developmental Cell*. The Authors, 33(4), pp. 373–387. doi: 10.1016/j.devcel.2015.03.005.

Kopan, R. and Ilagan, M. X. G. (2009) 'The Canonical Notch Signaling Pathway: Unfolding the Activation Mechanism', *Cell*, 137(2), pp. 216–233. doi: 10.1016/j.cell.2009.03.045.The.

Kopinke, D. *et al.* (2006) 'Retinoic acid is required for endodermal pouch morphogenesis and not for pharyngeal endoderm specification', *Developmental Dynamics*, 235(10), pp. 2695–2709. doi: 10.1002/dvdy.20905.

Kovall, R. a and Blacklow, S. C. (2010) *Mechanistic insights into Notch receptor signaling from structural and biochemical studies.*, *Current topics in developmental biology*. Elsevier Inc. doi: 10.1016/S0070-2153(10)92002-4.

Krispin, S., Nitzan, E. and Kalcheim, C. (2010) 'The dorsal neural tube: A dynamic setting for cell fate decisions', *Developmental Neurobiology*, 70(12), pp. 796–812. doi: 10.1002/dneu.20826.

Krstic, R. V. (1991) *Human Microscopic Anatomy: An Atlas for Students of Medicine and Biology*. Springer Science & Business Media.

Krumlauf, R. (1994) 'Hox genes in vertebrate development', *Cell*, 78(2), pp. 191–201. doi: 10.1016/0092-8674(94)90290-9.

Kulessa, H., Turk, G. and Hogan, B. L. M. (2000) 'Inhibition of Bmp signaling affects growth and differentiation in the anagen hair follicle', *EMBO Journal*, 19(24), pp. 6664–6674. doi: 10.1093/emboj/19.24.6664.

Lai, E. C. (2004) ‘Notch signaling: control of cell communication and cell fate.’, *Development (Cambridge, England)*, 131(5), pp. 965–73. doi: 10.1242/dev.01074.

Lawson, N. D., Vogel, A. M. and Weinstein, B. M. (2002) ‘Sonic hedgehog and vascular endothelial growth factor act upstream of the Notch pathway during arterial endothelial differentiation’, *Developmental Cell*, 3(1), pp. 127–136. doi: 10.1016/S1534-5807(02)00198-3.

LeBon, L. *et al.* (2014) ‘Fringe proteins modulate Notch-ligand cis and trans interactions to specify signaling states’, *eLife*, 3, p. e02950. doi: 10.7554/eLife.02950.

Lee, R. T. H., Zhao, Z. and Ingham, P. W. (2016) ‘Hedgehog signalling’, *Development*, 143(3), pp. 367–372. doi: 10.1242/dev.120154.

Leimeister, C. *et al.* (2000) ‘Oscillating expression of c-Hey2 in the presomitic mesoderm suggests that the segmentation clock may use combinatorial signaling through multiple interacting bHLH factors’, *Developmental Biology*. doi: 10.1006/dbio.2000.9884.

Lewis, J. (1998) ‘Notch signalling and the control of cell fate choices in vertebrates.’, *Seminars in cell developmental biology*, 9(6), pp. 583–589. Available at: http://www.ncbi.nlm.nih.gov/pubmed/9892564.

Li, X. *et al.* (2003) ‘Eya protein phosphatase activity regulates Six1-Dach-Eya transcriptional effects in mammalian organogenesis.’, *Nature*, 426(6964), pp. 247–254. doi: 10.1038/nature02283.

Li, Y. *et al.* (2012) ‘Genome-Wide Analysis of N1ICD/RBPJ Targets In Vivo Reveals Direct Transcriptional Regulation of Wnt, SHH, and Hippo Pathway Effectors by Notch1’, *Stem Cells*, (207), pp. 741–752. doi: 10.1002/stem.2011.

Li, Y. *et al.* (2014) ‘LIM homeodomain transcription factor Isl1 directs normal pyloric development by targeting Gata3’, *BMC Biology*, 12, pp. 1–15. doi: 10.1186/1741-7007-12-25.

Liao, B. K. and Oates, A. C. (2017) ‘Delta-Notch signalling in segmentation’, *Arthropod Structure and Development*. Elsevier Ltd, 46(3), pp. 429–447. doi: 10.1016/j.asd.2016.11.007.

Liao, J. *et al.* (2008) ‘Identification of downstream genetic pathways of Tbx1 in the second heart field’, *Developmental Biology*. doi: 10.1016/j.ydbio.2008.01.037.

Le Lièvre, C. S. and Le Douarin, N. M. (1975) ‘Mesenchymal derivatives of the neural crest: analysis of chimaeric quail and chick embryos.’, *Journal of embryology and experimental morphology*, 34(1), pp. 125–154. Available at: http://www.ncbi.nlm.nih.gov/pubmed/1185098.

Lilleväli, K. *et al.* (2007) ‘Comparative analysis of Gata3 Gata2 expression during chicken inner ear development’, *Developmental Dynamics*. doi: 10.1002/dvdy.21011.

Lillie, F. R. (1952) *Development of the chick : an introduction to embryology.* 3rd edn. Edited by H. L. Hamilton. New York, NY: Holt.

Lin, T. L. and Matsui, W. (2012) ‘Hedgehog pathway as a drug target: Smoothened inhibitors in development’, *OncoTargets and Therapy*, 5, pp. 47–58. doi: 10.2147/OTT.S21957.

Lind, E. F. *et al.* (2001) ‘Mapping Precursor Movement through the Postnatal Thymus Reveals Specific Microenvironments Supporting Defined Stages of Early Lymphoid Development’, *The Journal of Experimental Medicine*, 194(2), pp. 127–134. doi: 10.1084/jem.194.2.127.

Lindsay, E. a *et al.* (2001) ‘Tbx1 haploinsufficieny in the DiGeorge syndrome region causes aortic

arch defects in mice.', *Nature*, 410(6824), pp. 97–101. doi: 10.1038/35065105.

Liu, Z., Yu, S. and Manley, N. R. (2007) 'Gcm2 is required for the differentiation and survival of parathyroid precursor cells in the parathyroid/thymus primordia.', *Developmental Biology*, 305(1), pp. 333–346. Available at: http://www.pubmedcentral.nih.gov/articlerender.fcgi?artid=1931567&tool=pmcentrez&rendertype=abstract.

Lütolf, S. *et al.* (2002) 'Notch1 is required for neuronal and glial differentiation in the cerebellum.', *Development Cambridge England*, 129(2), pp. 373–85. Available at: http://www.ncbi.nlm.nih.gov/pubmed/11807030.

Lynch, H. E. *et al.* (2009) 'Thymic involution and immune reconstitution', 30(7), pp. 366–373. doi: 10.1016/j.it.2009.04.003.Thymic.

Macatee, T., Hammond, B. and Arenkiel, B. (2003) 'Ablation of specific expression domains reveals discrete functions of ectoderm-and endoderm-derived FGF8 during cardiovascular and pharyngeal development', …, 130(25), pp. 6361–6374. doi: 10.1242/dev.00850.Ablation.

Maeda, Y. and Noda, M. (2003) 'Coordinated development of embryonic long bone on chorioallantoic membrane in ovo prevents perichondrium-derived suppressive signals against cartilage growth', *Bone*. doi: 10.1016/S8756-3282(02)00917-1.

Maillard, I. *et al.* (2004) 'Mastermind critically regulates Notch-mediated lymphoid cell fate decisions.', *Blood*, 104(6), pp. 1696–1702. doi: 10.1182/blood-2004-02-0514.

Maillard, I., Fang, T. and Pear, W. S. (2005) 'Regulation of lymphoid development, differentiation, and function by the Notch pathway.', *Annual review of immunology*, 23, pp. 945–74. doi: 10.1146/annurev.immunol.23.021704.115747.

Manderfield, L. J. *et al.* (2012) 'Notch activation of Jagged1 contributes to the assembly of the arterial wall', *Circulation*. doi: 10.1161/CIRCULATIONAHA.111.047159.

Manley, N. R. *et al.* (2004) 'Abnormalities of caudal pharyngeal pouch development in Pbx1 knockout mice mimic loss of Hox3 paralogs', *Developmental Biology*, 276(2), pp. 301–312. doi: 10.1016/j.ydbio.2004.08.030.

Manley, N. R. *et al.* (2011) 'Structure and function of the thymic microenvironment', *Frontiers in Bioscience*, 16(1), pp. 2461–2477. doi: 10.2741/3866.

Manley, N. R. (2015) 'Embryology of the parathyroid Glands', pp. 11–19. doi: 10.1007/978-88-470-5376-2.

Manley, N. R. and Capecchi, M. R. (1995) 'The role of Hoxa-3 in mouse thymus and thyroid development.', *Development (Cambridge, England)*, 121(7), pp. 1989–2003. Available at: http://www.ncbi.nlm.nih.gov/pubmed/7635047.

Manley, N. R. and Capecchi, M. R. (1998) 'Hox group 3 paralogs regulate the development and migration of the thymus, thyroid, and parathyroid glands.', *Developmental biology*, 195(1), pp. 1–15. doi: 10.1006/dbio.1997.8827.

Manley, N. R. and Condie, B. G. (2010) *Transcriptional regulation of thymus organogenesis and thymic epithelial cell differentiation*. 1st edn, *Progress in Molecular Biology and Translational Science*. 1st edn. Elsevier Inc. doi: 10.1016/S1877-1173(10)92005-X.

Maret, A. *et al.* (2008) 'Analysis of the GCM2 gene in isolated hypoparathyroidism: A molecular

and biochemical study', *Journal of Clinical Endocrinology and Metabolism*, 93(4), pp. 1426–1432. doi: 10.1210/jc.2007-1783.

Marigo, V *et al.* (1996) 'Conservation in hedgehog signaling: induction of a chicken patched homolog by Sonic hedgehog in the developing limb.', *Development (Cambridge, England)*. doi: 10.1038/nature06718.

Marigo, Valeria *et al.* (1996) 'Sonic hedgehog differentially regulates expression of GLI and GLI3 during limb development', *Developmental Biology*. doi: 10.1006/dbio.1996.0300.

Martyn, I. *et al.* (2018) 'Self-organization of a human organizer by combined Wnt and Nodal signaling', *Nature*. Springer US, 558(7708), pp. 132–135. doi: 10.1038/s41586-018-0150-y.

McGlinn, E. *et al.* (2005) 'Pax9 and Jagged1 act downstream of Gli3 in vertebrate limb development', *Mechanisms of Development*, 122(11), pp. 1218–1233. doi: 10.1016/j.mod.2005.06.012.

Merkenschlager, M. *et al.* (1997) 'How many thymocytes audition for selection?', *The Journal of experimental medicine*, 186, pp. 1149–58. doi: 10.1084/jem.186.7.1149.

Meyers, E. N., Lewandoski, M. and Martin, G. R. (1998) 'An Fgf8 mutant allelic series generated by Cre- and Flp-mediated recombination.', *Nature genetics*, 18(2), pp. 136–41. doi: 10.1038/ng0298-136.

Miller, J. (2011) 'The golden anniversary of the thymus', *Nature Reviews Immunology*. Available at: http://www.nature.com/nri/journal/vaop/ncurrent/full/nri2993.html (Accessed: 21 October 2013).

Miller, J. F. (1961) 'Immunological function of the thymus.', *Lance*, 2(7205), pp. 748–749.

Modarai, B., Sawyer, A. and Ellis, H. (2004) 'The glands of Owen', *J R Soc Med*, 97(10), pp. 494–495. doi: 10.1258/jrsm.97.10.494.

Moore-Scott, B. a and Manley, N. R. (2005) 'Differential expression of Sonic hedgehog along the anterior-posterior axis regulates patterning of pharyngeal pouch endoderm and pharyngeal endoderm-derived organs.', *Developmental biology*, 278(2), pp. 323–35. doi: 10.1016/j.ydbio.2004.10.027.

Moura, R. S. *et al.* (2011) 'FGF signaling pathway in the developing chick lung: Expression and inhibition studies', *PLoS ONE*. doi: 10.1371/journal.pone.0017660.

Muller, S. M. *et al.* (2008) 'Neural Crest Origin of Perivascular Mesenchyme in the Adult Thymus', *The Journal of Immunology*, 180(8), pp. 5344–5351. doi: 10.4049/jimmunol.180.8.5344.

Musse, A. A., Meloty-Kapella, L. and Weinmaster, G. (2012) 'Notch ligand endocytosis: Mechanistic basis of signaling activity', *Seminars in Cell and Developmental Biology*, pp. 429–436. doi: 10.1016/j.semcdb.2012.01.011.

Mutoh, T. *et al.* (2012) 'Oxygen levels epigenetically regulate fate switching of neural precursor cells via hypoxia-inducible factor 1α-Notch signal interaction in the developing brain', *Stem Cells*. doi: 10.1002/stem.1019.

Myat, A. *et al.* (1996) 'A chick homologue of Serrate and its relationship with Notch and Delta homologues during central neurogenesis', *Developmental Biology*. doi: 10.1006/dbio.1996.0069.

Naiche, L. A. *et al.* (2005) 'T-Box Genes in Vertebrate Development', *Annual Review of Genetics*, 39, pp. 219–39. doi: 10.1146/.

Naito, T. *et al.* (2011) 'Transcriptional control of T-cell development', *International Immunology*. doi: 10.1093/intimm/dxr078.

Nakamura, H. *et al.* (2004) 'Gain- and loss-of-function in chick embryos by electroporation.', *Mechanisms of development*, 121(9), pp. 1137–43. doi: 10.1016/j.mod.2004.05.013.

Nakamura, H. and Funahashi, J. (2013) 'Electroporation: Past, present and future', *Development, Growth & Differentiation*, 55(1), pp. 15–19. doi: 10.1111/dgd.12012.

Nandagopal, N., Santat, L. A. and Elowitz, M. B. (2019) 'Cis-activation in the Notch signaling pathway', *eLife*, 8. doi: 10.7554/elife.37880.

National Research Council. (2000) 'Recent Advances in Developmental Biology', in *Scientific Frontiers in Developmental Toxicology and Risk Assessment*. Washington, DC: The National Academies Press., pp. 108–150. doi: doi: 10.17226/9871.

Nehls, M. *et al.* (1994) 'New member of the winged-helix protein family disrupted in mouse and rat nude mutations', *Nature*, 372(6501), pp. 103–107. doi: 10.1038/372103a0.

Nehls, M. *et al.* (1996) 'Two genetically separable steps in the differentiation of thymic epithelium.', *Science (New York, N.Y.)*, 272(5263), pp. 886–9. doi: 10.1126/science.272.5263.886.

Neubüser, a, Koseki, H. and Balling, R. (1995) 'Characterization and developmental expression of Pax9, a paired-box-containing gene related to Pax1.', *Developmental biology*, pp. 701–716. doi: 10.1006/dbio.1995.1248.

Neves, H. *et al.* (2012) 'Modulation of Bmp4 signalling in the epithelial-mesenchymal interactions that take place in early thymus and parathyroid development in avian embryos.', *Developmental biology*, 361(2), pp. 208–219. doi: 10.1016/j.ydbio.2011.10.022.

Neves, H. and Zilhão, R. (2014) 'Development of Parathyroid Glands and C-Cells', in Ashford, M. (ed.) *Parathyroid Glands: Regulation, Role in Human Disease and Indications for Surgery*. Nova Science, pp. 1–34. Available at: https://www.novapublishers.com/catalog/product_info.php?products_id=48022.

Nie, X. *et al.* (2011) 'Inactivation of Bmp4 from the Tbx1 expression domain causes abnormal pharyngeal arch artery and cardiac outflow tract remodeling', *Cells Tissues Organs*, 193(6), pp. 393–403. doi: 10.1159/000321170.

Niederreither, K. *et al.* (2003) 'The regional pattern of retinoic acid synthesis by RALDH2 is essential for the development of posterior pharyngeal arches and the enteric nervous system.', *Development (Cambridge, England)*, 130(11), pp. 2525–2534. doi: 10.1242/dev.00463.

Norris, A. and Streit, A. (2014) 'Morpholinos: Studying gene function in the chick', *Methods*, 66(3), pp. 454–465. doi: 10.1016/j.ymeth.2013.10.009.

Nowak-Sliwinska, P., Segura, T. and Iruela-Arispe, M. L. (2014) 'The chicken chorioallantoic membrane model in biology, medicine and bioengineering', *Angiogenesis*, 17(4), pp. 779–804. doi: 10.1007/s10456-014-9440-7.

Nowell, C. S. *et al.* (2011) 'Foxn1 regulates lineage progression in cortical and medullary thymic epithelial cells but is dispensable for medullary sublineage divergence.', *PLoS genetics*, 7(11), p.

e1002348. doi: 10.1371/journal.pgen.1002348.

Nowell, C. S., Farley, A. M. and Blackburn, C. C. (2007) 'Thymus organogenesis and development of the thymic stroma.', *Methods in molecular biology (Clifton, N.J.)*, 380(1), pp. 125–62. Available at: http://www.ncbi.nlm.nih.gov/pubmed/17876091.

O'Neill, K. *et al.* (2013) *Thymus and Parathyroid Organogenesis*. Fourth Edi, *Principles of Tissue Engineering: Fourth Edition*. Fourth Edi. Elsevier. doi: 10.1016/B978-0-12-398358-9.00043-4.

Ohki, H. *et al.* (1987) 'Tolerance induced by thymic epithelial grafts in birds.', *Science (New York, N.Y.)*, 237(4818), pp. 1032–5. doi: 10.1126/science.3616623.

Ohnemus, S. *et al.* (2002) 'Aortic arch and pharyngeal phenotype in the absence of BMP-dependent neural crest in the mouse.', *Mechanisms of development*, 119(2), pp. 127–35. Available at: http://www.ncbi.nlm.nih.gov/pubmed/12464426.

Ohta, S. *et al.* (2003) 'Microbubble-Enhanced Sonoporation: Efficient Gene Transduction Technique for Chick Embryos', *Genesis*, 37(2), pp. 91–101. doi: 10.1002/gene.10232.

Oishi, I. *et al.* (2016) 'Targeted mutagenesis in chicken using CRISPR/Cas9 system', *Scientific Reports*. Nature Publishing Group, 6(April), pp. 1–10. doi: 10.1038/srep23980.

Okabe, M. and Graham, A. (2004) 'The origin of the parathyroid gland.', *Proceedings of the National Academy of Sciences of the United States of America*, 101(51), pp. 17716–9. doi: 10.1073/pnas.0406116101.

Outram, S. V. *et al.* (2009) 'Indian hedgehog (Ihh) both promotes and restricts thymocyte differentiation', *Blood*. doi: 10.1182/blood-2008-03-144840.

Palmeirim, I. *et al.* (1997) 'Avian hairy Gene Expression Identifies a Molecular Clock Linked to Vertebrate Segmentation and Somitogenesis', *Cell*, 91(5), pp. 639–648. doi: 10.1016/S0092-8674(00)80451-1.

Park, E. J. *et al.* (2006) 'Required, tissue-specific roles for Fgf8 in outflow tract formation and remodeling', *Development*, 133(12), pp. 2419–2433. doi: 10.1242/dev.02367.

Park, T. S. *et al.* (2014) 'Targeted gene knockout in chickens mediated by TALENs.', *Proceedings of the National Academy of Sciences of the United States of America*, 111(35), pp. 1–6. doi: 10.1073/pnas.1410555111.

Patel, S. R. *et al.* (2006) 'Bmp4 and Noggin expression during early thymus and parathyroid organogenesis.', *Gene expression patterns GEP*, 6(8), pp. 794–799. Available at: http://www.ncbi.nlm.nih.gov/pubmed/16517216.

Peters, H. *et al.* (1998) 'Pax9-deficient mice lack pharyngeal pouch derivatives and teeth and exhibit craniofacial and limb abnormalities', *Genes and Development*, 12(17), pp. 2735–2747. doi: 10.1101/gad.12.17.2735.

Peters, H. *et al.* (1999) 'Pax1 and Pax9 synergistically regulate vertebral column development.', *Development (Cambridge, England)*, 126(23), pp. 5399–5408.

Petrie, H. T. (2003) 'Cell migration and the control of post-natal T-cell lymphopoiesis in the thymus', *Nature Reviews Immunology*, 3(11), pp. 859–866. doi: 10.1038/nri1223.

Petrie, H. T. and Zúñiga-Pflücker, J. C. (2007) 'Zoned Out: Functional Mapping of Stromal

Signaling Microenvironments in the Thymus', *Annual Review of Immunology*, 25(1), pp. 649–679. doi: 10.1146/annurev.immunol.23.021704.115715.

Pinheiro, P. (2011) *A Novel Parathyroid Protein in Chicken : Origin , Expression and Function*. Instituto de Ciências Biomédicas Abel Salazar - Universidade do Porto. Available at: http://hdl.handle.net/1842/10433.

Potts, J. T. (2005) 'Parathyroid hormone: past and present.', *The Journal of endocrinology*, 187(3), pp. 311–25. doi: 10.1677/joe.1.06057.

Pui, J. C. *et al.* (1999) 'Notch1 expression in early lymphopoiesis influences B versus T lineage determination', *Immunity*. doi: 10.1016/S1074-7613(00)80105-3.

Quaranta, R. *et al.* (2018) 'Revised roles of ISL1 in a hES cell-based model of human heart chamber specification', *eLife*. doi: 10.7554/eLife.31706.

Quinlan, R. *et al.* (2002) 'Deficits in the posterior pharyngeal endoderm in the absence of retinoids', *Developmental Dynamics*, 225(1), pp. 54–60. doi: 10.1002/dvdy.10137.

Radtke, F. *et al.* (1999) 'Deficient T cell fate specification in mice with an induced inactivation of Notch1', *Immunity*, 10(5), pp. 547–558. doi: 10.1016/S1074-7613(00)80054-0.

Radtke, F., Fasnacht, N. and Macdonald, H. R. (2010) 'Notch signaling in the immune system.', *Immunity*. Elsevier Inc., 32(1), pp. 14–27. doi: 10.1016/j.immuni.2010.01.004.

Rahnama, F. *et al.* (2006) 'Inhibition of GLI1 gene activation by Patched1.', *The Biochemical journal*, 394(Pt 1), pp. 19–26. doi: 10.1042/BJ20050941.

Reeh, K. a G. *et al.* (2014) 'Ectopic TBX1 suppresses thymic epithelial cell differentiation and proliferation during thymus organogenesis.', *Development (Cambridge, England)*, 141(15), pp. 2950–8. doi: 10.1242/dev.111641.

Reifers, F. *et al.* (2000) 'Induction and differentiation of the zebrafish heart requires fibroblast growth factor 8 (fgf8/acerebellar)', *Development*.

Revest, J. M. *et al.* (2001) 'Development of the thymus requires signaling through the fibroblast growth factor receptor R2-IIIb.', *Journal of immunology (Baltimore, Md. : 1950)*, 167(4), pp. 1954–1961. doi: 10.4049/jimmunol.167.4.1954.

Riddle, R. D. *et al.* (1993) 'Sonic hedgehog mediates the polarizing activity of the ZPA', *Cell*. doi: 10.1016/0092-8674(93)90626-2.

Roberts, C. *et al.* (2005) 'Retinoic acid down-regulates Tbx1 expression in vivo and in vitro', *Developmental Dynamics*, 232(4), pp. 928–938. doi: 10.1002/dvdy.20268.

Roberts, D. J. (2000) 'Molecular mechanisms of development of the gastrointestinal tract.', *Developmental dynamics : an official publication of the American Association of Anatomists*, 219(2), pp. 109–120. doi: 10.1002/1097-0177(2000)9999:9999<::AID-DVDY1047>3.0.CO;2-6.

Robey, E. *et al.* (1996) 'An activated form of Notch influences the choice between CD4 and CD8 T cell lineages', *Cell*. doi: 10.1016/S0092-8674(00)81368-9.

Rodewald, H.-R. (2008) 'Thymus organogenesis.', *Annual review of immunology*, 26, pp. 355–88. doi: 10.1146/annurev.immunol.26.021607.090408.

Rothenaigner, I. *et al.* (2011) 'Clonal analysis by distinct viral vectors identifies bona fide neural

stem cells in the adult zebrafish telencephalon and characterizes their division properties and fate', *Development*, 138(8), pp. 1459–1469. doi: 10.1242/dev.058156.

Ruiz i Altaba, A. (1997) 'Catching a Gli-mpse of hedgehog', *Cell*, pp. 193–196. doi: 10.1016/S0092-8674(00)80325-6.

Sato, Y. *et al.* (2007) 'Stable integration and conditional expression of electroporated transgenes in chicken embryos.', *Developmental biology*, 305(2), pp. 616–24. doi: 10.1016/j.ydbio.2007.01.043.

Scherer, F. *et al.* (2002) 'Magnetofection: Enhancing and targeting gene delivery by magnetic force in vitro and in vivo', *Gene Therapy*, 9(2), pp. 102–109. doi: 10.1038/sj/gt/3301624.

Seefeldt, B. *et al.* (2008) 'Fluorescent proteins for single-molecule fluorescence applications', *Journal of Biophotonics*. doi: 10.1002/jbio.200710024.

Serikaku, M. A. and O'Tousa, J. E. (1994) 'sine oculis is a homeobox gene required for Drosophila visual system development', *Genetics*, 138(4), pp. 1137–1150.

Shah, D. K. *et al.* (2004) 'Reduced thymocyte development in sonic hedgehog knockout embryos', *Journal of immunology (Baltimore, Md : 1950)*, 172(4), pp. 2296–2306. doi: 10.4049/jimmunol.172.4.2296.

Shah, D. K. and Zuniga-Pflucker, J. C. (2014) 'An Overview of the Intrathymic Intricacies of T Cell Development', *The Journal of Immunology*, 192(9), pp. 4017–4023. doi: 10.4049/jimmunol.1302259.

Shida, H. *et al.* (2015) 'Otic placode cell specification and proliferation are regulated by Notch signaling in avian development', *Developmental Dynamics*, p. n/a-n/a. doi: 10.1002/dvdy.24291.

Shifley, E. T. *et al.* (2008) 'Oscillatory lunatic fringe activity is crucial for segmentation of the anterior but not posterior skeleton', *Development*, 135(5), pp. 899–908. doi: 10.1242/dev.006742.

Shimojo, H., Ohtsuka, T. and Kageyama, R. (2011) 'Dynamic expression of Notch signaling genes in neural stem/ progenitor cells', *Frontiers in Neuroscience*. doi: 10.3389/fnins.2011.00078.

Singh, B. N. *et al.* (2011) 'Hedgehog signaling antagonist GDC-0449 (Vismodegib) inhibits pancreatic cancer stem cell characteristics: Molecular mechanisms', *PLoS ONE*, 6(11). doi: 10.1371/journal.pone.0027306.

Soza-Ried, C. *et al.* (2008) 'Maintenance of Thymic Epithelial Phenotype Requires Extrinsic Signals in Mouse and Zebrafish', *The Journal of Immunology*, 181(8), pp. 5272–5277. doi: 10.4049/jimmunol.181.8.5272.

Sprinzak, D. *et al.* (2010) 'Cis-interactions between Notch and Delta generate mutually exclusive signalling states', *Nature*. doi: 10.1038/nature08959.

Stanley, P. and Okajima, T. (2010) 'Roles of glycosylation in Notch signaling.', *Current topics in developmental biology*, 92(10), pp. 131–64. doi: 10.1016/S0070-2153(10)92004-8.

Stasiulewicz, M. *et al.* (2015) 'A conserved role for Notch in priming the cellular response to Shh through ciliary localisation of the key Shh transducer, Smoothened.', *Development (Cambridge, England)*, 142(13), pp. 2291–2303. doi: 10.1242/dev.125237.

Steinmann, G. G., Klaus, B. and Müller-Hermelink, H. K. (1985) 'The involution of the ageing

human thymic epithelium is independent of puberty. A morphometric study.', *Scandinavian journal of immunology*, 22(5), pp. 563–75. Available at: http://www.ncbi.nlm.nih.gov/pubmed/4081647.

Stern, C. D. (2004) 'The chick embryo--past, present and future as a model system in developmental biology.', *Mechanisms of development*, 121(9), pp. 1011–3. doi: 10.1016/j.mod.2004.06.009.

Stern, C. D. (2005) 'The chick: A great model system becomes even greater', *Developmental Cell*, 8(1), pp. 9–17. doi: 10.1016/j.devcel.2004.11.018.

Su, D. *et al.* (2001) 'Hoxa3 and pax1 regulate epithelial cell death and proliferation during thymus and parathyroid organogenesis.', *Developmental biology*, 236(2), pp. 316–29. doi: 10.1006/dbio.2001.0342.

Subhan, F. *et al.* (2013) 'Epidermal growth factor-like domain 8 inhibits the survival and proliferation of mouse thymocytes', *International Journal of Molecular Medicine*. doi: 10.3892/ijmm.2013.1448.

Swann, J. B. *et al.* (2017) 'Cooperative interaction of BMP signalling and Foxn1 gene dosage determines the size of the functionally active thymic epithelial compartment', *Scientific Reports*. Springer US, 7(1), p. 8492. doi: 10.1038/s41598-017-09213-1.

Takahama, Y. (2006) 'Journey through the thymus: stromal guides for T-cell development and selection.', *Nature reviews. Immunology*, 6(2), pp. 127–35. doi: 10.1038/nri1781.

Takahashi, Y., Bontoux, M. and Le Douarin, N. M. (1991) 'Epithelio--mesenchymal interactions are critical for Quox 7 expression and membrane bone differentiation in the neural crest derived mandibular mesenchyme', *Embo J*, 10(9), pp. 2387–2393.

Taylor, L. *et al.* (2017) 'Efficient TALEN-mediated gene targeting of chicken primordial germ cells', *Development*, 144(5), pp. 928–934. doi: 10.1242/dev.145367.

Tomita, K. *et al.* (1999) 'The bHLH gene Hes1 is essential for expansion of early T cell precursors', *Genes and Development*. doi: 10.1101/gad.13.9.1203.

Tsai, P. T., Lee, R. A. and Wu, H. (2003) 'BMP4 acts upstream of FGF in modulating thymic stroma and regulating thymopoiesis', *Blood*, 102(12), pp. 3947–3953. doi: 10.1182/blood-2003-05-1657.

Uematsu, E. *et al.* (2014) 'Use of in ovo chorioallantoic membrane engraftment to culture testes from neonatal mice', *Comparative Medicine*.

Varjosalo, M. and Taipale, J. (2008) 'Hedgehog: Functions and mechanisms', *Genes and Development*, 22(18), pp. 2454–2472. doi: 10.1101/gad.1693608.

Véron, N. *et al.* (2015) 'CRISPR mediated somatic cell genome engineering in the chicken', *Developmental Biology*. Elsevier, 407(1), pp. 68–74. doi: 10.1016/j.ydbio.2015.08.007.

Vilas-Boas, F. *et al.* (2011) *A novel reporter of notch signalling indicates regulated and random notch activation during Vertebrate neurogenesis.*, *BMC biology*. doi: 10.1186/1741-7007-9-58.

Vilas-Boas, F. and Henrique, D. (2010) 'HES6-1 and HES6-2 Function through Different Mechanisms during Neuronal Differentiation', *PLoS ONE*. Edited by E. Giniger. Public Library of Science, 5(12), p. 15. Available at: http://www.pubmedcentral.nih.gov/articlerender.fcgi?artid=2996300&tool=pmcentrez&rendert

ype=abstract.

Vitelli, F. *et al.* (2002) 'Tbx1 mutation causes multiple cardiovascular defects and disrupts neural crest and cranial nerve migratory pathways.', *Human molecular genetics*, 11(8), pp. 915–22. Available at: http://www.ncbi.nlm.nih.gov/pubmed/11971873.

Vroegindeweij, E. *et al.* (2010) 'Thymic cysts originate from Foxn1 positive thymic medullary epithelium', *Molecular Immunology*, 47(5), pp. 1106–1113. doi: 10.1016/j.molimm.2009.10.034.

Wall, D. S. *et al.* (2009) 'Progenitor cell proliferation in the retina is dependent on Notch-independent Sonic hedgehog/Hes1 activity', *Journal of Cell Biology*, 184(1), pp. 101–112. doi: 10.1083/jcb.200805155.

Wallin, J. *et al.* (1996) 'Pax1 is expressed during development of the thymus epithelium and is required for normal T-cell maturation', *Development*, 122(1), pp. 23–30. Available at: http://www.ncbi.nlm.nih.gov/pubmed/8565834.

Wang, R. N. *et al.* (2014) 'Bone Morphogenetic Protein (BMP) signaling in development and human diseases', *Genes & Diseases*, 1(1), pp. 87–105. doi: 10.1016/j.gendis.2014.07.005.

Washburn, T. *et al.* (1997) 'Notch activity influences the alphabeta versus gammadelta T cell lineage decision.', *Cell*.

Watanabe, T. *et al.* (2007) 'Tet-on inducible system combined with in ovo electroporation dissects multiple roles of genes in somitogenesis of chicken embryos.', *Developmental biology*, 305(2), pp. 625–36. doi: 10.1016/j.ydbio.2007.01.042.

Wei, Q. and Condie, B. G. (2011) 'A focused in situ hybridization screen identifies candidate transcriptional regulators of thymic epithelial cell development and function', *PLoS ONE*, 6(11). doi: 10.1371/journal.pone.0026795.

Weinmaster, G. (1997) 'The ins and outs of Notch signaling', *Molecular and Cellular Neuroscience*, pp. 91–102. Available at: http://www.sciencedirect.com/science?_ob=MImg&_imagekey=B6WNB-45TKY22-10-1&_cdi=6958&_user=582538&_orig=search&_coverDate=12/31/1997&_sk=999909997&view=c&wchp=dGLbVlz-zSkzS&md5=6b574c877351a088df392de8e087f6b2&ie=/sdarticle.pdf.

Wendling, O. *et al.* (2000) 'Retinoid signaling is essential for patterning the endoderm of the third and fourth pharyngeal arches', *Development*, 127(8), pp. 1553–1562. Available at: papers://a160a322-7748-499f-b1e5-c793de7b7813/Paper/p397.

Weng, A. P. *et al.* (2003) 'Growth Suppression of Pre-T Acute Lymphoblastic Leukemia Cells by Inhibition of Notch Signaling Growth Suppression of Pre-T Acute Lymphoblastic Leukemia Cells by Inhibition of Notch Signaling', *Molecular and cellular biology*, 23(2), pp. 655–664. doi: 10.1128/MCB.23.2.655.

Wolfe, M. S. (2012) ??'-Secretase inhibitors and modulators for Alzheimer's disease', *Journal of Neurochemistry*, 120(SUPPL. 1), pp. 89–98. doi: 10.1111/j.1471-4159.2011.07501.x.

Xie, G. *et al.* (2013) 'Cross-talk between Notch and Hedgehog regulates hepatic stellate cell fate in mice', *Hepatology*, 58(5), pp. 1801–1813. doi: 10.1002/hep.26511.

Xu, H., Cerrato, F. and Baldini, A. (2005) 'Timed mutation and cell-fate mapping reveal reiterated roles of Tbx1 during embryogenesis, and a crucial function during segmentation of the pharyngeal system via regulation of endoderm expansion.', *Development (Cambridge, England)*, 132(19), pp. 4387–4395. doi: 10.1242/dev.02018.

Xu, P.-X. *et al.* (2002) 'Eya1 is required for the morphogenesis of mammalian thymus, parathyroid and thyroid.', *Development (Cambridge, England)*, 129(13), pp. 3033–44. Available at: http://www.ncbi.nlm.nih.gov/pubmed/12070080.

Yamagishi, H. *et al.* (2003) 'Tbx1 is regulated by tissue-specific forkhead proteins through a common Sonic hedgehog-responsive enhancer', *Genes and Development*, 17(2), pp. 269–281. doi: 10.1101/gad.1048903.

Yang, L.-T. (2005) 'Fringe Glycosyltransferases Differentially Modulate Notch1 Proteolysis Induced by Delta1 and Jagged1', *Molecular Biology of the Cell*, 16(2), pp. 927–942. doi: 10.1091/mbc.E04-07-0614.

Zamisch, M. *et al.* (2005) 'Ontogeny and regulation of IL-7-expressing thymic epithelial cells.', *Journal of immunology (Baltimore, Md. : 1950)*, 174(1), pp. 60–7. doi: 10.4049/jimmunol.174.1.60.

Zenatti, P. P. *et al.* (2011) 'Oncogenic IL7R gain-of-function mutations in childhood T-cell acute lymphoblastic leukemia', *Nature Genetics*. doi: 10.1038/ng.924.

Zhang, Z. *et al.* (2005) 'Tbx1 expression in pharyngeal epithelia is necessary for pharyngeal arch artery development.', *Development (Cambridge, England)*, 132(23), pp. 5307–5315. doi: 10.1242/dev.02086.

Zhang, Z., Huynh, T. and Baldini, A. (2006) 'Mesodermal expression of Tbx1 is necessary and sufficient for pharyngeal arch and cardiac outflow tract development', *Development*, 133(18), pp. 3587–3595. doi: 10.1242/dev.02539.

Zheng, Y. H. *et al.* (2013) 'Notch γ-secretase inhibitor dibenzazepine attenuates angiotensin II-induced abdominal aortic aneurysm in ApoE knockout mice by multiple mechanisms', *PLoS ONE*. doi: 10.1371/journal.pone.0083310.

Zhulyn, O. *et al.* (2015) 'Ptch2 shares overlapping functions with Ptch1 in Smo regulation and limb development', *Developmental Biology*, 397(2), pp. 191–202. doi: 10.1016/j.ydbio.2014.10.023.

Zorn, A. M. and Wells, J. M. (2009) 'Vertebrate endoderm development and organ formation.', *Annual review of cell and developmental biology*, 25, pp. 221–51. doi: 10.1146/annurev.cellbio.042308.113344.

Zou, D. *et al.* (2006) 'Patterning of the third pharyngeal pouch into thymus/parathyroid by Six and Eya1.', *Developmental biology*, 293(2), pp. 499–512. doi: 10.1016/j.ydbio.2005.12.015.

APPENDIX I

Table of Materials of Chapter III

Name	Company	Catalogue Number	Comments
Chicken fertilized eggs (*Gallus gallus*)	Pintobar, Portugal		Poultry farm
Quail fertilized eggs (*Coturnix coturnix*)	Interaves, Portugal		Bird farm
15mL PP centrifuge tubes	Corning	430052	
50mL PP centrifuge tubes	Corning	430290	
60x20mm pyrex dishes	Duran group	21 755 41	
100x20 mm pyrex dishes	Duran group	21 755 48	
Polycarbonate Membrane Insert	Corning	3412	24mm transwell with 0.4mm Pore Polycarbonate Membrane Insert
Membrane filter	Millipore	DTTP01300	0.6mm Isopore membrane filter
6-well culture plates	Nunc, Thermo Fisher Scientific	140675	
Petri dish, 35x10mm	Sigma-Aldrich	P5112	
Pyrex bowls			From supermarket
Transfer pipettes	Samco Scientific, Thermo Fisher Scientific	2041S	2mL plastic pipet
Glass Pasteur pipette	Normax	5426015	
Whatman qualitative filter paper	Sigma-Aldrich	WHA1001090	Filter paper
Clear plastic tape			From supermarket
Cytokeratin (pan; acidic and basic, type I and II cytokeratins), clone Lu-5	BMA Biomedicals	T-1302	
Cyclopamine hydrate	Sigma-Aldrich	C4116	Pharmacological inhibitor of Hh signalling
Fetal Bovine Serum	Invitrogen, Thermo Fisher Scientific		Standart FBS
Paraformaldehyde	Sigma-Aldrich	P6148	
Penicillin-Streptomycin	Invitrogen, Thermo Fisher Scientific	15140-122	
Phosphate-Buffered Saline (PBS)	GIBCO, Thermo Fisher Scientific	10010023	
QCPN antibody	Developmental Studies Hybridoma Bank	QCPN	
RPMI 1640 Medium, GlutaMAX Supplement	GIBCO, Thermo Fisher Scientific	61870010	
Bluesil RTV141A/B Silicone Elastomer 1.1Kg Kit	ELKEM/Silmid	RH141001KG	To prepare the back base for petri dish

Stemolecule LY411575	Stemgent	04-0054	Pharmacological inhibitor of Notch signalling
TRIzol Reagent	Invitrogen, Thermo Fisher Scientific	15596026	Reagent for total RNA isolation
Dumont #5 Forceps	Fine Science Tools	11251-30	Thin forceps
Extra fine Bonn scissors, curved	Fine Science Tools	14085-08	Curved scissors
Insect pins	Fine Science Tools	26001-30	
Micro spatula	Fine Science Tools	10087-12	Transplantation spoon
Minutien Pins	Fine Science Tools	26002-20	Microscalpel
Moria Nickel Plated Pin Holder	Fine Science Tools	26016-12	Holder
Moria Perforated Spoon	Fine Science Tools	10370-17	Skimmer
Wecker Eye Scissor	Fine Science Tools	15010-11	
Camera	Leica Microsystems	MC170 HD	
Stereoscope	Leica Microsystems	Leica M80	
Microscope	Leica Microsystems	DM2500	

APPENDIX II

Table of Materials of Chapter V

Name	Company	Catalog Number	Comments
Chicken fertilized eggs (*Gallus gallus*)	Pintobar, Portugal		Poultry farm
Quail fertilized eggs (*Coturnix coturnix*)	Interaves, Portugal		Bird farm
15mL PP centrifuge tubes	Corning	430052	
50mL PP centrifuge tubes	Corning	430290	
60x20mm pyrex dishes	Duran group	21 755 41	
100x20mm pyrex dishes	Duran group	21 755 48	
Metal grid	Goodfellows		fine meshed stainless steel grid
Membrane filter	Millipore	DTTP01300	0.6mm Isopore membrane filter
Petri dish, 35x10mm	Sigma-Aldrich	P5112	
60x30mm pyrex bowls (small size)			from supermarket
100x50mm pyrex bowls (large size)			from supermarket
Transfer pipettes	Samco Scientific, Thermo Fisher Scientific	2041S	2mL plastic pipet
Glass pasteur pipette	Normax	5426015	
Clear plastic tape			from supermarket
Cytokeratin (pan; acidic and basic, type I and II cytokeratins), clone Lu-5	BMA Biomedicals	T-1302	
Fetal Bovine Serum	Invitrogen, Thermo Fisher Scientific		Standart FBS
Pancreatin	Sigma-Aldrich	P-3292	Prepare a 25mg/mL solution according to manufacturer's instructions; centrifuge and filter prior to aliquote and store at -20ºC. Aliquots can be kept frozen for several years.
Paraformaldehyde	Sigma-Aldrich	P6148	
Penicillin-Streptomycin	Invitrogen, Thermo Fisher Scientific	15140-122	
Phosphate-Buffered Saline (PBS)	GIBCO, Thermo Fisher Scientific	10010023	
QCPN antibody	Developmental Studies Hybridoma Bank	QCPN	
RPMI 1640 Medium, GlutaMAX Supplement	GIBCO, Thermo Fisher Scientific	61870010	
Bluesil RTV141A/B Silicone Elastomer 1.1Kg Kit	ELKEM/Silmid	RH141001KG	To prepare the back base for petri dish

Dumont #5 Forceps	Fine Science Tools	11251-30	Thin forceps
Extra fine Bonn scissors, curved	Fine Science Tools	14085-08	Curved scissors
Insect pins	Fine Science Tools	26001-30	0.3mm stainless steel pin
Micro spatula	Fine Science Tools	10087-12	Transplantation spoon
Minutien Pins	Fine Science Tools	26002-20	0.2mm stainless steel microscalpel
Minutien Pins	Fine Science Tools	26002-10	0.1mm stainless steel microscalpel
Moria Nickel Plated Pin Holder	Fine Science Tools	26016-12	Nickel plated pin holder
Moria Perforated Spoon	Fine Science Tools	10370-17	Skimmer
Wecker Eye Scissor	Fine Science Tools	15010-11	
Camera	Leica Microsystems	MC170 HD	
Microscope	Leica Microsystems	DM2500	
NanoZoomer S360 Digital slide scanner	Hamamatsu Photonics	C13220-01	
Stereoscope	Leica Microsystems	Leica M80	

APPENDIX III

Our initial objective was to genetically modulate Notch signalling in the pharyngeal endoderm through the Tet-On system, so Notch could be modulated in specific developmental time-windows, and for as long as desired, through the addition of Dox. Comparing to the Tet-Off, the Tet-On system would potentially be a simpler and safer method to modulate Notch signalling in the endoderm exclusively at later stages of development (during the *in ovo* organ formation experiments in the CAM) as it would only require Dox administration at those specific stages. After receiving the Tet-On system from Yoshiko Takahashi (Sato *et al.*, 2007), we made several attempts to work with the system of vectors, with no success, and two main experiments confirmed that we were in fact working with the Tet-Off system.

Functional assay by transfection of the cell line HEK-293T (in collaboration with Sofia Santos).

The Human Embryonic Kidney (HEK) 293T cell line (kindly provided by João Barata (Zenatti *et al.*, 2011)) was transfected with pCAGGS-T2TP, pT2K-BI-TREeGFP, and pT2K-CAGGS-rtTA-M2 – either the vector originally received from Yoshiko Takahashi as a retrotransactivator or a pT2K-CAGGS-rtTA-M2 kindly given by Domingos Henrique. The transfected cells were grown for a week with no Dox (control condition) or with Dox (2µg/mL) being added to the culture medium at day 0 and every 48h (experimental condition). After 48h of transfection, cells transfected with Takahashi's vector and grown in the presence of Dox showed no GFP expression (Fig. 1A). Conversely, almost 50% of GFP^+ cells with high intensity of fluorescence were observed in the absence of Dox (Fig. 1A). The retrotransactivator vector received from Domingos Henrique, on the other hand, behaved as expected: GFP expression was only upregulated in the presence of Dox (Fig. 1A). These results showed that the pT2K-CAGGS-rtTA-M2 received from Takahashi behaved as a pT2K-CAGGS-tTA (transactivator, Tet-Off system).

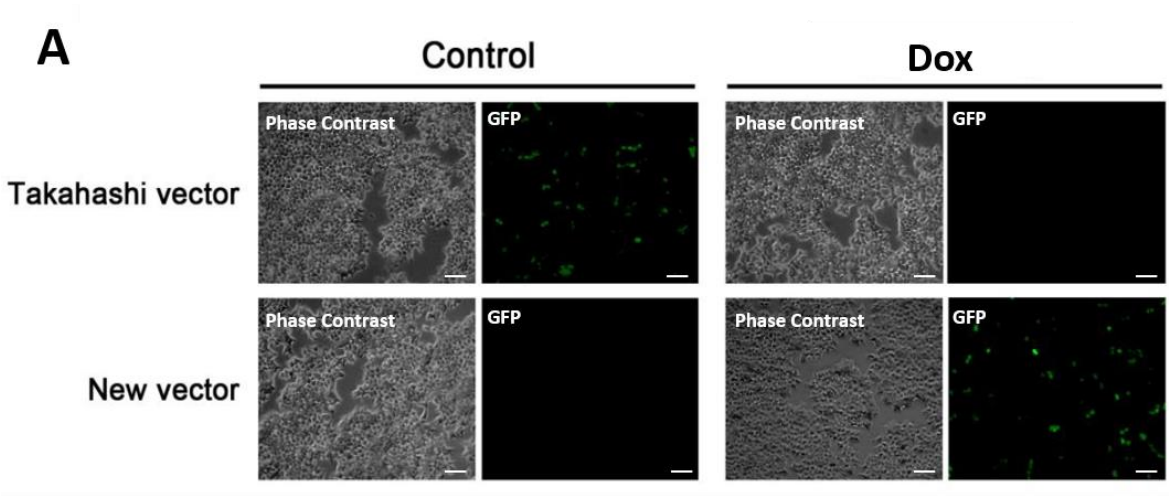

B

rtTA sequence

ATGTCTAGATTAGATAAAAGTAAAGTGATTAACAGCGCATTAGAGCTGCTTAATGAGGTCGGAATCGAAGGTTTAACAACCCGTAAACTCGCCCA
GAAGCTTGGTGTAGAGCAGCCTACACTGTATTGGCATGTAAAAAATAAGCGGGCTTTGCTCGACGCCTTAGCCATTGAGATGTTAGATAGGCACC
ATACTCACTTTTGCCCTTTAAAAGGGGAAAGCTGGCAAGATTTTTTACGCAATAACGCTAAAAGTTTTAGATGTGCTTTACTAAGTCATCGCAATGG
AGCAAAAGTACATTCAGATACACGGCCTACAGAAAAACAGTATGAAACTCTCGAAAATCAATTAGCCTTTTTATGCCAACAAGGTTTTTCACTAGA
GAACGCGTTATATGCACTCAGCGCTGTGGGGCATTTTACTTTAGGTTGCGTATTGGAAGATCAAGAGCATCAAGTCGCTAAAGAAGAAAGGGAAA
CACCTACTACTGATAGTATGCCGCCATTATTACGACAAGCTATCGAATTATTTGATCACCAAGGTGCAGAGCCAGCCTTCTTATTCGGCCTTGAATT
GATCATATGCGGATTAGAAAAACAACTTAAATGTGAAAGTGGGTCCGCGTACAGCCGCGCGCGTACGAAAAACAATTACGGGTCTACCATCGAG
GGCCTGCTCGATCTCCCGGACGACGACGCCCCCGAAGAGGCGGGGCTGGCGGCTCCGCGCCTGTCCTTTCTCCCCGCGGGACACACGCGCAGAC
TGTCGACGGCCCCCCCGACCGATGTCAGCCTGGGGGACGAGCTCCACTTAGACGGCGAGGACGTGGCGATGGCGCATGCCGACGCGCTAGACG
ATTTCGATCTGGACATGTTGGGGGACGGGGATTCCCCGGGTCCGGGATTTACCCCCCACGACTCCGCCCCCTACGGCGCTCTGGATATGGCCGAC
TTCGAGTTTGAGCAGATGTTTACCGATGCCCTTGGAATTGACGAGTACGGTGGGTAG (**Primers**; **HindIII site**)

tTA sequence

ATGTCTAGATTAGATAAAAGTAAAGTGATTAACAGCGCATTAGAGCTGCTTAATGAGGTCGGAATCGAAGGTTTAACAACCCGTAAACTCGCCCA
GAAGCTAGGTGTAGAGCAGCCTACATTGTATTGGCATGTAAAAAATAAGCGGGCTTTGCTCGACGCCTTAGCCATTGAGATGTTAGATAGGCACC
ATACTCACTTTTGCCCTTTAGAAGGGGAAAGCTGGCAAGATTTTTTACGTAATAACGCTAAAAGTTTTAGATGTGCTTTACTAAGTCATCGCGATGG
AGCAAAAGTACATTTAGGTACACGGCCTACAGAAAAACAGTATGAAACTCTCGAAAATCAATTAGCCTTTTTATGCCAACAAGGTTTTTCACTAGA
GAATGCATTATATGCACTCAGCGCTGTGGGGCATTTTACTTTAGGTTGCGTATTGGAAGATCAAGAGCATCAAGTCGCTAAAGAAGAAAGGGAAA
CACCTACTACTGATAGTATGCCGCCATTATTACGACAAGCTATCGAATTATTTGATCACCAAGGTGCAGAGCCAGCCTTCTTATTCGGCCTTGAATT
GATCATATGCGGATTAGAAAAACAACTTAAATGTGAAAGTGGGTCCGCGTACAGCCGCGCGCGTACGAAAAACAATTACGGGTCTACCATCGAG
GGCCTGCTCGATCTCCCGGACGACGACGCCCCCGAAGAGGCGGGGCTGGCGGCTCCGCGCCTGTCCTTTCTCCCCGCGGGACACACGCGCAGAC
TGTCGACGGCCCCCCCGACCGATGTCAGCCTGGGGGACGAGCTCCACTTAGACGGCGAGGACGTGGCGATGGCGCATGCCGACGCGCTAGACG
ATTTCGATCTGGACATGTTGGGGGACGGGGATTCCCCGGGTCCGGGATTTACCCCCCACGACTCCGCCCCCTACGGCGCTCTGGATATGGCCGAC
TTCGAGTTTGAGCAGATGTTTACCGATGCCCTTGGAATTGACGAGTACGGTGGGTAG (**Primers**; **SnaBI site**)

Figure 1. Analysis of the pT2K-CAGGS-TA-M2 received from Takahashi. HEK-293T cell line transfection assay with the *Tol2*-mediated gene transfer and tetracycline-dependent conditional expression system of vectors (A). Fluorescence microscopy analysis of HEK-293T cell line 48h after transfection with pCAGGS-T2TP, pT2K-BI-TREeGFP, and pT2K-CAGGS-rtTA-M2 from Takahashi or from Domingos Henrique, with or without Dox administration. Retrotransactivator (rtTA) and transactivator (tTA) gene sequences (B). Enzymatic restriction sites (blue) in the rtTA and tTA genes and primers which sequences are common in both genes (red). Scale bars, 100µm.

Analysis of pT2K-CAGGS-rtTA-M2 (Takahashi's vector) by enzymatic restriction (in collaboration with Joana Silva).

The retrotransactivator (tTA) and transactivator (tTA) sequences are too similar to be distinguished by a simple enzymatic restriction analysis of the full vectors (Fig. 1B). A sequence analysis allowed us to identify distinct restriction enzyme sites between them: rtTA contains a HindIII restriction site, while tTA has a SnaBI restriction site (Fig. 1B). Thus, to confirm that we were, in fact, working with the transactivator, instead of the retrotransactivator, we analysed the enzymatic restriction pattern of a PCR-amplified region of the "rtTA" sequence in the Takahashi's vector pT2K-CAGGS-rtTA-M2. PCR was performed in the Takahashi's vector, using primers which sequences are common between rtTA and tTA genes and which amplify a fragment that contains the region of the restriction sites above mentioned (Fig. 1B). The PCR product was incubated with either HindIII or SnaBI. The amplified fragment from Takahashi's vector was digested by SnaBI, instead of HindIII, showing a restriction pattern specific of the tTA sequence. Together, these findings confirmed that the so called retrotransactivator vector received from Takahashi was, in fact, pT2K-CAGGS-tTA (transactivator, Tet-Off system).

APPENDIX IV

Developmental Biology 418 (2016) 268–282

Contents lists available at ScienceDirect

Developmental Biology

journal homepage: www.elsevier.com/locate/developmentalbiology

Original research article

Notch and Hedgehog in the thymus/parathyroid common primordium: Crosstalk in organ formation

Marta Figueiredo [a,b,1], Joana Clara Silva [a,1,2], Ana Sofia Santos [a,3], Vitor Proa [a], Isabel Alcobia [a,b], Rita Zilhão [c], António Cidadão [a], Hélia Neves [a,b,*]

[a] Instituto de Histologia e Biologia do Desenvolvimento, Faculdade de Medicina da Universidade de Lisboa, Edifício Egas Moniz, Piso 3, Ala C, Av. Prof. Egas Moniz, 1649-028 Lisboa, Portugal
[b] Instituto de Medicina Molecular, Faculdade de Medicina da Universidade de Lisboa, Av. Prof. Egas Moniz, 1649-028 Lisboa, Portugal
[c] Departamento de Biologia Vegetal, Faculdade de Ciências da Universidade de Lisboa, Campo Grande C2, 1749-016 Lisboa, Portugal

ARTICLE INFO

Article history:
Received 6 October 2015
Received in revised form
12 August 2016
Accepted 13 August 2016
Available online 18 August 2016

Keywords:
Notch
Hedgehog
Thymus/parathyroids common primordium
Pharyngeal pouches
Avian

ABSTRACT

The avian thymus and parathyroids (T/PT) common primordium derives from the endoderm of the third and fourth pharyngeal pouches (3/4PP). The molecular mechanisms that govern T/PT development are not fully understood. Here we study the effects of Notch and Hedgehog (Hh) signalling modulation during common primordium development using *in vitro*, *in vivo* and *in ovo* approaches. The impairment of Notch activity reduced Foxn1/thymus-fated and Gcm2/Pth/parathyroid-fated domains in the 3/4PP and further compromised the development of the parathyroid glands. When Hh signalling was abolished, we observed a reduction in the *Gata3*/*Gcm2*- and *Lfng*-expression domains at the median/anterior and median/posterior territories of the pouches, respectively. In contrast, the *Foxn1* expression-domain at the dorsal tip of the pouches expanded ventrally into the *Lfng*-expression domain. This study offers novel evidence on the role of Notch signalling in T/PT common primordium development, in an Hh-dependent manner.

1. Introduction

The parathyroid glands and the thymus are organs with distinct functions, carried out mainly by epithelial cells which have a common embryological origin, that is, the endoderm of the pharyngeal pouches (PP). The epithelia of these organs in the avian model originate from the third and fourth PP (3/4PP) endoderm. It is worth noting, that in mammals the thymic epithelium derives from the 3PP endoderm (Farley et al., 2013; Gordon et al., 2001) and in mouse and human the epithelium of parathyroids derives from the 3PP and 3/4PP, respectively. The main function of the parathyroid endocrine epithelium is to secrete a peptidic hormone, the parathyroid hormone (Pth), essential for the regulation of calcium and phosphate homeostasis (Potts, 2005). In the thymus, the epithelial cells establish complex interactions with the developing lymphocytes to produce self-restricted and self-tolerant T-cells, which generate central immune tolerance.

Parathyroid and thymic organogenesis starts with the budding off and outgrowth of rudiments from pouches of the foregut endoderm (Manley and Condie, 2010), accompanied by the lining of neural crest-derived connective tissues (Grevellec and Tucker, 2010). These early steps involve pouch patterning and the establishment of a common primordium (Manley and Condie, 2010) in which the distinct parathyroid and thymic prospective domains, can be distinguished by the expression of the organ-specific genes, Gcm2 (Glial cells missing 2) and Foxn1, respectively.

In avian embryos, *Gcm2* transcripts were first detected by RT-PCR in isolated quail (q) endoderm at embryonic day (E) 2.5 (25–30 somite-stage) (Neves et al., 2012). However, *in situ* expression of *Gcm2* has only been observed in the anterior domain of the 3PP and 4PP at Hamburger and Hamilton Stage 18 (HH18) and HH22, respectively (Okabe and Graham, 2004). This temporal sequence of *Gcm2* expression follows the chronological formation of the pouches. As development proceeds, Pth is upregulated in the developing glands. In avian, *Pth* expression was first observed *in situ* at chicken (c) E5.5 (HH28) (Grevellec et al., 2011). In Gcm2

* Corresponding author at: Instituto de Histologia e Biologia do Desenvolvimento, Faculdade de Medicina da Universidade de Lisboa, Edifício Egas Moniz, Piso 3, Ala C, Av. Prof. Egas Moniz, 1649-028 Lisboa, Portugal.
E-mail addresses: martafigueiredo@medicina.ulisboa.pt (M. Figueiredo), j.clarasilva@dundee.ac.uk (J.C. Silva), assantos@hikma.com (A.S. Santos), vitorproa@medicina.ulisboa.pt (V. Proa), halcobia@medicina.ulisboa.pt (I. Alcobia), rmzilhao@fc.ul.pt (R. Zilhão), a.cidadao@campus.ul.pt (A. Cidadão), helia.neves@campus.ul.pt, hneves@medicina.ulisboa.pt (H. Neves).
[1] Co-authors, these authors contributed equally to this work.
[2] Present Address: JKD College of Life Sciences, University of Dundee, Dow Street, DD1 5EH, Dundee, UK.
[3] Present Address: Hikma Farmacêutica (Portugal), S.A., Sintra, Portugal.

http://dx.doi.org/10.1016/j.ydbio.2016.08.012
0012-1606/

homozygous null mutant mice, the expression of *Pth* is not initiated and no parathyroid glands are formed (Günther et al., 2000; Liu et al., 2007).

The transcription factor of the winged helix/forkhead class, Foxn1, is the earliest known marker of the thymic rudiment. *Foxn1* transcripts were detected in isolated quail endoderm 24 h after *Gcm2* expression. At cE4.5, *Foxn1* expression was observed *in situ* in the dorsal tip of the 3/4PP and transcription endures until birth (Neves et al., 2012). The gene is mutated in the nude mouse strain, which displays abnormal hair growth and failure of thymus development, leading to immunodeficiency (Nehls et al., 1996; Blackburn et al., 1996; Bleul et al., 2006).

As in other developmental processes, the activation of the correct transcriptional programs during parathyroid (Neves and Zilhão, 2014) and thymic (Manley and Condie, 2010) organogenesis depends on the crosstalk of several signalling pathways which respond to extracellular signals.

Notch signalling is a major pathway during development that acts in a juxtacrine fashion and is responsible for cell-fate decisions (Lewis, 1998; Lai, 2004). In the last fifteen years, several reports have shown that Notch is fundamental during epithelial-lymphoid cell interactions at late-stages of thymus formation (Rodewald, 2008). Notably, perinatal mutant mice with loss of Notch ligand Jag2 exhibit aberrant thymic morphology with smaller medullar compartments (Jiang et al., 1998). Notch activity is also required for the commitment of lymphoid progenitor cells to the T-cell lineage (Pui et al., 1999; Radtke et al., 1999), in a ligand dependent manner (Jaleco et al., 2001; Dorsch et al., 2002). Whilst largely unknown, there is some evidence for the role of Notch signalling in the early-development of these organs. In mice, the loss of Notch-target Hes1 promotes a spectrum of malformations of pharyngeal endoderm-derived organs, including parathyroid glands aplasia/hypoplasia (Kameda et al., 2013) and abnormal thymic formation (Tomita et al., 1999; van Bueren et al., 2010; Kameda et al., 2013).

Paracrine Hedgehog (Hh) signalling is also involved in craniofacial and neck morphogenesis (Grevellec and Tucker, 2010), and regulates T/PT common primordium development (Moore-Scott and Manley, 2005). In Sonic Hh (Shh) homozygous null mutants the rudiment boundaries are compromised, displaying an expanded domain of the prospective thymic territory at the expense of the Gcm2/parathyroid-fated domain (Moore-Scott and Manley, 2005). This mutant fails to form parathyroid glands (Moore-Scott and Manley, 2005) and displays functional defects in the thymus (Shah et al., 2004). At later stages of development, Shh and Indian Hh, other Hh signalling molecule, are known to regulate thymocyte differentiation after thymic epithelium colonization by lymphoid progenitor cells (Outram et al., 2009).

Hh and Notch pathways interact in multiple biological scenarios (McGlinn et al., 2005; Lawson et al., 2002; Stasiulewicz et al., 2015). In distinct developmental contexts, Notch signalling is known to control morphological boundary formation by the mechanism of lateral inhibition (Lewis, 1998; Lai, 2004; Kiernan, 2013). In light of this evidence, we hypothesized that similar mechanisms could operate in the development of T/PT common primordium. In order to test this hypothesis, Notch and Hh signals were inhibited *in vitro* and *in vivo* in the presumptive territories of thymus and parathyroids by ectopic administration of the respective pharmacological inhibitors. Briefly, our results show a positive regulatory effect of Notch signalling in T/PT common primordium development and parathyroid gland formation. Hh positively regulates the Gata3/Gcm2/parathyroid-fated domain. Furthermore, Hh establishes the dorsal/posterior boundary of Foxn1/thymic rudiment by positively regulating Lfng/Notch signals at the posterior/median territory of the developing 3/4PP endoderm.

2. Materials and methods

2.1. Embryo preparation

Fertilised Japanese quail (*Coturnix coturnix japonica*) and chicken (*Gallus gallus*) eggs were incubated at 38 °C in a humidified incubator. Chicken Embryos were staged according to Hamburger and Hamilton (Hamburger and Hamilton, 1951). Quail (q) embryos were dissected at embryonic day (E) 3 and E4 for *in vitro* development studies and whole-mount *in situ* hybridisation (WM-ISH) procedures. Chicken (c) embryos were used at E2.5 (HH17) and E3.5 (HH21) for *in vivo* assays and at E8 for *in ovo* organ formation assays. Chicken pharyngeal endoderm was isolated at E3.5 and E4.5 (HH24-25) and used for WM-ISH, as previously described (Neves et al., 2012).

2.2. In vitro organotypic assay

The third and fourth pharyngeal arches region (3/4PAR) was dissected from qE3 on PBS (3/4PAR-0 h), and kept on ice until culture. The 3/4PAR included the 3/4PP and foregut endoderm and the ventral mesenchymal- and ectodermal-neighbouring cells. The dorsal structures like notochord, somites and neural tube were removed (Fig. 1A–F). Explants were then placed on a 24 mm Transwell® with 0.4 μm Pore Polycarbonate Membrane Insert (Corning Product #3412). Seven explants per well were placed with the ventral side up and the dorsal side in contact with the membrane (Fig. 1G). The tissues were grown partially immersed in culture medium, RPMI-1640 Medium (Sigma) supplemented with 10% FBS (Invitrogen), 1 × Pen/Strep (Invitrogen) in a humidified incubator at 37 °C with 5% CO_2, for 48 h (3/4PAR-48 h).

For Notch signalling inhibition assays, culture medium was supplemented with LY-411.575 (Ly, Stemgent - Stemolecule™) at 50 nM (Ly-50), 100 nM (Ly-100) or 200 nM (Ly-200) or with Dibenzazepine (DBZ, Selleckchem) at 5 μM (DBZ-5), 10 μM (DBZ-10) or 15 μM (DBZ-15) (experimental conditions). For Hh signalling inhibition assays, culture medium was supplemented with 20 μM of Cyclopamine (Cyc, Sigma) or with 10 μM of Vismodegib (Vis, Selleckchem) (experimental conditions). In parallel, explants were grown with culture medium supplemented with the drug solvent, DMSO, at similar concentrations as the ones present in the medium of experimental conditions [Control-50 (Ly) – 0.0005% DMSO; Control-100 (Ly) – 0.001% DMSO; Control-200 (Ly) – 0.002% DMSO; Control-5 (DBZ) – 0.05%; Control-10 (DBZ) – 0.10%; Control-15 (DBZ) – 0.15%; Control (Cyc) – 0.16%; Control (Vis) – 0.2%] (control conditions).

Following the incubation period, cultured explants were either used for RNA isolation (see Quantitative real time RT-PCR section) or grafted onto chorioallantoic membrane (CAM) at cE8.

2.3. In ovo organ formation assay

The 3/4PAR explants grown *in vitro* for 48 h were grafted onto CAM of chicken embryos at cE8 (Fig. 1G). Transplanted tissues were allowed to further develop *in ovo* for 10 days in a humidified incubator at 38 °C, as previously described (Neves et al., 2012). For Notch inhibition assays, the 3/4PAR-48 h explants derived from Ly-200 (3/4PAR Ly-200) were grafted and developed in CAM (Graft-Ly) (experimental condition). For the control conditions, 3/4PAR-48 h explants derived from Control-200 (3/4PAR Control-200) were grafted and developed in CAM (Graft-Control). For both conditions, transplanted tissues were allowed to further develop *in ovo* for 3 and 10 days in a humidified incubator at 38 °C. Survival and organ formation were evaluated in CAM-derived explants grown *in ovo* for 10 days.

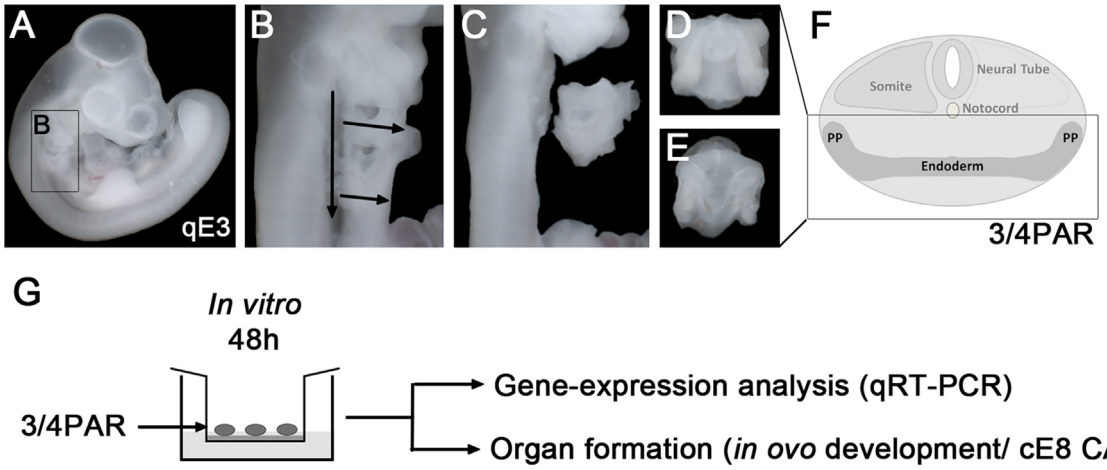

Fig. 1. Schematic representation of *in vitro* and *in ovo* experimental design. Sequential mechanical isolation steps of the 3/4PAR (A–C). Ventral (D) and Dorsal (E) views of the isolated 3/4PAR. Schematic representations of the transversal section of the embryo at the region of interest (F) and of the experimental design (G). PAR, pharyngeal arch region.

2.4. In vivo assays

For *in vivo* Notch inhibition assays, 20–40 µL of 5 µM, 10 µM or 20 µM of Ly were injected on the right side of the embryo near the region of the heart and pharyngeal arches, after local removal of extra-embryonic membranes, at cE2.5 and cE3.5. In parallel, control embryos were injected with 20–40 µl of DMSO at a similar concentration as the one present in the medium of experimental conditions (0.05%, 0.1% and 0.2%, respectively). Chicken embryos were allowed to develop *in ovo* for 20–24 h in a humidified incubator at 38 °C.

For *in vivo* Hh inhibition assays, heparin acrylic beads (Sigma) were rinsed in PBS and soaked overnight at 4 °C in a solution of 6 mM of Cyc or in PBS. Cyc- and PBS-beads were inserted in the embryo pharynx lumen through the second cleft and placed at the level of the 3/4PP, after local removal of extra-embryonic membranes, at cE2.5 and qE3 (Cyc and Control-PBS, respectively). In order to increase Hh inhibition effects, multiple beads were placed per embryo. Quail embryos were allowed to develop for 20–24 h in 30 mm petri-dishes containing 2 mL of PBS in a humidified incubator with 5% CO_2 at 37°C. Chicken embryos were allowed to develop *in ovo* for 20–24 h in a humidified incubator at 38 °C.

2.5. Quantitative real time RT-PCR

Total RNA from the samples was extracted using a combination of TRIzol reagent (Invitrogen) and RNeasy Mini Kit (QIAGEN) according to the manufacturer's instructions. RNA samples were obtained from freshly isolated 3/4PAR from qE3 (3/4PAR-0 h) and from 3/4PAR grown *in vitro* for 48 h (3/4PAR-48 h). Triplicates of 7 explants per sample were analysed for each condition. After DNAse treatment for 15 min, first-strand cDNA synthesis was performed in a total volume of 20 µL, by reverse transcription of 300 ng of total RNA using the SuperScript™ III Reverse Transcriptase kit and Oligo $(dT)_{12–18}$ Primer (Invitrogen), according to the manufacturer's instructions. All steps of RNA extraction and cDNA synthesis were performed in a vertical laminar flow hood to avoid contamination. Concentration and purity of both the RNA and cDNA samples were determined using a NanoDrop® ND-1000 Spectrophotometer (Thermo Scientific).

To exclude the amplification of genomic DNA, primers were designed to span introns near the 3′poly-A tail using Primer3 software (Table 1). Quantitative RT-PCR (qRT-PCR) assays were run in a ViiA7™ Fast Real-Time PCR System (Applied Biosystems) in MicroAmp® Optical 384-Well Reaction Plate (Applied Biosystems). Reactions were performed in a final volume of 10 µL using 5 µL of Power SYBR® Green PCR Master Mix (Applied Biosystems), 0.4 µM final concentration of primers and 1 µL (up to 1 µg) of cDNA. Thermocycling conditions were as follows: an initial denaturation at 50 °C for 20 s and 95 °C for 10 min, followed by 40 cycles at 95 °C for 15 s and at 60 °C for 1 min. To confirm primer specificity, a melting curve was generated at the end of each experiment. Relative quantification of gene expression was determined by the ΔΔCt method (Livak and Schmittgen, 2001) using β-actin (*Actb*)

Table 1
List of primers used in qRT-PCR assays.

Primer	Forward primer (5′-3′)	Reverse primer (5′-3′)	Product size (bp)
ACTB	TGGCACCTAGCACAATGAAA	GCCAGGATAGAGCCTCCAAT	82
HPRT	ACGCCCTCGACTACAATGAA	CAACTGTGCTTTCATGCTTTG	98
Foxn1	CGACATCGATGCTCTGAATC	AGGCTGTCATCCTTCAGCTC	81
Gcm2	TCAGAATTCCCAGAAAAAGAGA	GAGGGCAGATTTTGCATGTT	93
PTH	CTGATGGAAGACCAATGATGAA	AAGCCAGTCCTGTCTCTCCA	98
Gata3	CTGTAATGCCTGTGGGCTCT	CATTTTTCGGTTTCTGGTCTG	94
Pax1	GGGAAGTCACGGACAGAAAA	GGATCGAGAGTCCGTGGAT	81
Fgf8	GCATGAACAAGAAGGGGAAA	AGCGCCGTGTAGTTGTTCTC	97
Hey1	ACCGTGGATCACCTGAAGAT	CGGTAGTCCATAGCCAAAGC	80
Hes5.1	CCGACATCCTGGAGATGACT	AGGCATACCCTTCGCAGTAA	99
Hes6.1	GGAGGTGCTGGAGCTGAC	GCATGCACTGGATGTAGCC	122
Patched1	GGAAGCCACTGAGAATCCTG	TGCAATCTGGGACTTGACTG	81
Shh	CGGCTTCGACTGGGTCTACT	ATTTCGCTGCCACTGAGTTT	80
Gli1	AAGGATGACGGCAAGCTG	GTCACTGCTGCACGATGACT	86
Gli3	TGGAATGCTTCCAAGACTGA	CTGCAGCTGCTGTTTGATTG	96

and Hypoxanthine-guanine phosphoribosyltransferase (*Hprt*) as endogenous genes. Three technical replicates were used for each condition.

2.6. In situ hybridisation and immunohistochemistry

Quail and chicken embryos, *in vitro* explants and CAM-derived explants were fixed overnight in 4% paraformaldehyde/PBS at 4 °C. Samples were then processed for whole-mount *in situ* hybridisation, immunohistochemistry and immunofluorescence.

Whole-mount preparations were hybridised with *Delta1* (Henrique et al., 1995), *Fgf8* (Crossley et al., 1996), *Foxn1* (Neves et al., 2012), *Gata3* (Lilleväli et al., 2007), *Gcm2* (Neves et al., 2012), *Gli1* (Marigo et al., 1996a), *Gli3* (Marigo et al., 1996a), *Hey1* (Leimeister et al., 2000), *Jag1* (Myat et al., 1996), *Lfng* (Aulehla and Johnson, 1999), *Notch1* (Myat et al., 1996), *Shh* (Riddle et al., 1993), *Patched1* (Marigo et al., 1996b) and *Pax1* (Wallin et al., 1996) probes as previously described (Etchevers et al., 2001; Henrique et al., 1995). Paraffin sections of CAM-derived explants grown for 3 days were *in situ* hybridised with *Foxn1* and *Hes5.1* (Fior and Henrique, 2005).

Paraffin sections of explants developed *in ovo* for 10 days were analysed by haematoxylin-eosin staining (H&E) to determine the number, size and morphology of thymic lobes and parathyroid glands formed. Sections of CAM-explants were further treated for immunocytochemistry with the anti-pan [Lu-5] Cytokeratin antibody (Pan CK) (Abcam; for labelling epithelial cells).

2.7. Microscopy

H&E and immunohistochemistry images were collected using Software Leica Firewire and Leica DM2500 microscope with Leica DFC420 camera. WM-ISH pictures were taken under a Leica Z6 APO equipped with a Leica DFC490 camera.

2.8. Statistical analysis

Means and standard deviations were determined with Microsoft Excel/GraphPad Prism® (version 6.01) software. Two-tailed Student's *t*-tests and Mann-Whitney non-parametric tests were used for the analysis of *in vitro* and *in ovo* assays, respectively. Results were considered significantly different when the *P* value was less than 0.05 ($P < 0.05$).

3. Results

3.1. Notch-target genes Hey1, Hes5.1 and Gata3 are involved in the 3rd and 4th pharyngeal pouches endoderm development

To investigate the role of Notch signalling during the development of thymus and parathyroids (T/PT) common primordium we analysed the expression of Notch-target genes, *Hey1*, *Hes5.1*, *Hes6.1* and *Gata3* (Fang et al., 2007; Naito et al., 2011), within the presumptive territories of these organs (3/4PAR) (Fig. 2).

Notch-target gene expression was evaluated during normal development of the 3/4PAR. qE3 3/4PAR was isolated (3/4PAR-0 h) and grown *in vitro* for 48 h (3/4PAR-48 h) (Fig. 2A). As depicted in Fig. 2B, high levels of *Hey1* and *Gata3* transcripts were detected in freshly isolated tissues and significantly decreased after 48 h of culture. A similar trend was observed in the lowly-expressed transcripts, *Hes5.1* and *Hes6.1*. The reduction of *Hey1* and *Gata3* transcript levels was further supported by *in vivo* gene-expression evaluation at similar developmental time-windows, *i.e.* qE3 and qE4. *Hey1* transcripts were broadly detected along the endoderm, mesenchyme and ectoderm of the 3/4PAR (Fig. 2C and D) whereas *Gata3* expression was restricted to the endoderm of the pouches. At qE3, the strongest *Gata3* hybridisation signals were observed in the tips and anterior domain of the 3PP endoderm (Fig. 2E), the T/PT common primordium territory. After 24 h of development, *Gata3*-expression domain was confined to a more median/anterior position (Fig. 2F), at the parathyroid rudiment territory (Neves et al., 2012). *Gata3* expression was maintained later in the developing parathyroids (Suppl. Fig. 1A). Interestingly, Gata3 has been previously shown to be involved in parathyroid formation (Grigorieva et al., 2010).

Notch signalling was then modulated during common primordium formation (Fig. 2A and G–L). 3/4PAR was grown *in vitro* in the presence of three doses of the Notch inhibitor LY-411.575 (Ly), at 50 nM, 100 nM and 200 nM (Fig. 2G). A strong and significant reduction of *Hey1* (67%, 77% and 74%) and *Hes5.1* expression (98%, 74% and 92%) was observed in the pharyngeal tissues treated with Ly (Ly-50, Ly-100 and Ly-200, respectively), when compared to control conditions. *Gata3* transcript levels were also diminished (45%, 31% and 29% in Ly-50, Ly-100 and Ly-200, respectively) while no changes were observed for *Hes6.1* expression in either condition. This Notch-target gene belongs to the Hes6 family previously reported to be transcriptionally repressed by Hes5 genes (Fior and Henrique, 2005).

To validate the specificity of Notch signalling inhibition effects, similar *in vitro* assays were performed using three doses (5 μM, 10 μM and 15 μM) of a different Notch inhibitor, Dibenzazepine (DBZ) (Fig. 2H). As expected, a strong decrease of *Hey1* (72%, 71% and 66%) and *Hes5.1* (93%, 93% and 98%) transcript levels was accompanied with a less impressive reduction in *Gata3* expression (46%, 38% and 26%) in explants cultured with increasing doses of DBZ. Likewise, the expression levels of *Hes6.1* in DBZ-treated explants were similar to control conditions.

The capacity to inhibit Notch was further confirmed by an *in vivo* approach with the injection of Ly (5–20 μM) on the right side of the pharyngeal region of developing embryos. Ly administration was performed at cE2.5, the developmental stage prior to the formation of T/PT common primordium and to the *in situ* detection of *Gcm2* (Okabe and Graham, 2004). Injected embryos were allowed to develop for 20–24 h and then *in situ* analysed for *Hey1* and *Gata3* expression (Fig. 2I–L). These genes were selected because of their high expression during *in vitro* development (Fig. 2B). Chicken embryos were used in these experiments as some of the probes were inefficient for WM-ISH in quail embryos. In Ly-injected embryos, *Hey1* expression was abolished in all tissues of the pharyngeal region (Fig. 2J, n = 3/3), while *Gata3* expression was downregulated in the dorsal/tip and anterior domains of common primordium (Fig. 2L, n = 9/11).

Taken together, our data show that Notch-target genes *Hey1* and *Gata3* may act as positive mediators of Notch activity during the development of the T/PT common primordium.

3.2. Notch signalling inhibition promotes the reduction of Foxn1 and Gcm2/Pth expression in the endoderm of the 3rd and 4th pharyngeal pouches

To investigate the effects of Notch signalling inhibition during common primordium stages, we analysed the transcript levels of the T- and PT-related markers, *Foxn1* (Neves et al., 2012) and *Gcm2/Pth* (Neves et al., 2012; Grevellec et al., 2011) genes, respectively (Fig. 3). The expression analysis was expanded to transcription factors known to be involved in the morphogenesis of the pouches and formation of these organs, the *Pax1* and *Fgf8* genes (Dietrich and Gruss, 1995; Wallin et al., 1996; Su et al., 2001; Guo et al., 2011; Frank et al., 2002). *In vitro* and *in vivo* assays were performed as described in the previous section (schematic representation, Fig. 3A).

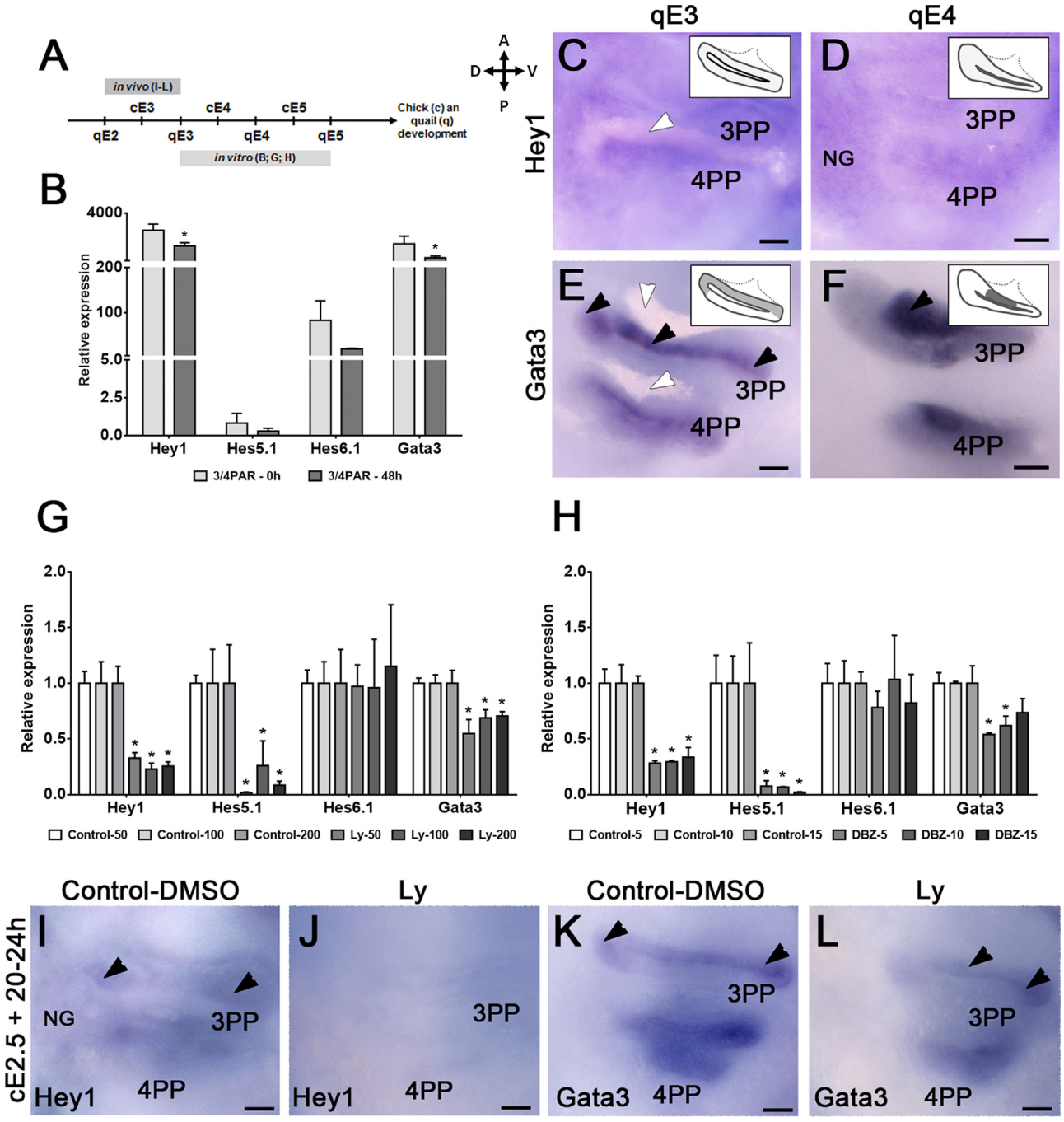

Fig. 2. Notch-target genes are involved in T/PT common primordium formation. Timeline of *in vitro* and *in vivo* assays in chicken and quail development (A). *In vitro* (B) and *in vivo* (C–F) expression of Notch-target genes in the 3/4PAR. Isolated 3/4PAR at qE3 was grown *in vitro* for 48 h. The expression levels of Notch-target genes of freshly isolated (3/4PAR-0 h) and cultured (3/4PAR-48 h) tissues were examined by qRT-PCR (B). In parallel, the expression of *Hey1* (C and D) and *Gata3* (E and F) was observed in the endoderm of the 3/4PP at qE3 (C and E, respectively) and qE4 (D and F, respectively) by WM-ISH. Schematic drawings in the top/right panels depict the gene-expression domains in the 3PP, the well-defined pouch. *In vitro* (G and H) and *in vivo* (I–L) expression of Notch-target genes in the 3/4PAR with Notch signalling inhibition. Isolated 3/4PAR at qE3 was grown *in vitro* for 48 h with three doses of Ly, 50 nM (Ly-50), 100 nM (Ly-100) and 200 nM (Ly-200) (G) or three doses of DBZ, 5μM (DBZ-5), 10 μM (DBZ-10) and 15 μM (DBZ-15) (H). The expression levels of Notch-target genes were measured in the cultured tissues by qRT-PCR (each transcript in control = 1). For the purpose of Notch signalling inhibition *in vivo*, the right side of cE2.5 embryos were injected in the pharyngeal region with either DMSO (I and K) or Ly (J and L) and allowed to develop *in ovo* for 20–24 h. The expression of Notch-target genes, *Hey1* (I and J) and *Gata3* (K and L) was detected by WM-ISH. For qRT-PCR, expression of each transcript was measured as a ratio against the mean of the *Actb* and *Hprt* transcript expression levels and expressed in arbitrary units. Black arrowheads point to the strong hybridisation signals in the 3PP endoderm and white arrowheads point to the pharyngeal arches. A, anterior; cE, chicken embryonic day; D, dorsal; DBZ, Dibenzazepine; Ly, LY-411.575; NG, nodose ganglion; P, posterior; PP, pharyngeal pouch; qE, quail embryonic day; V, ventral. Scale bars, 50 μm.

We began by examining the *in vitro* development of pharyngeal tissues (Fig. 3B). Predictably, *Foxn1* transcripts were almost undetectable in 3/4PAR-0 h but increased 35-fold during 48 h culture, confirming thymic epithelium specification during this developmental time-window (Neves et al., 2012). Conversely, the transcription factor *Gcm2* was already strongly expressed in freshly isolated tissues and increased 4-fold in 3/4PAR-48 h. In parallel, we observed a striking augmentation of *Pth* expression (986-fold), an indication of parathyroid epithelium differentiation (Günther et al., 2000). Minor changes were globally detected in the expression of *Pax1*, while *Fgf8* transcripts were significantly reduced. A similar trend was observed in the gene expression

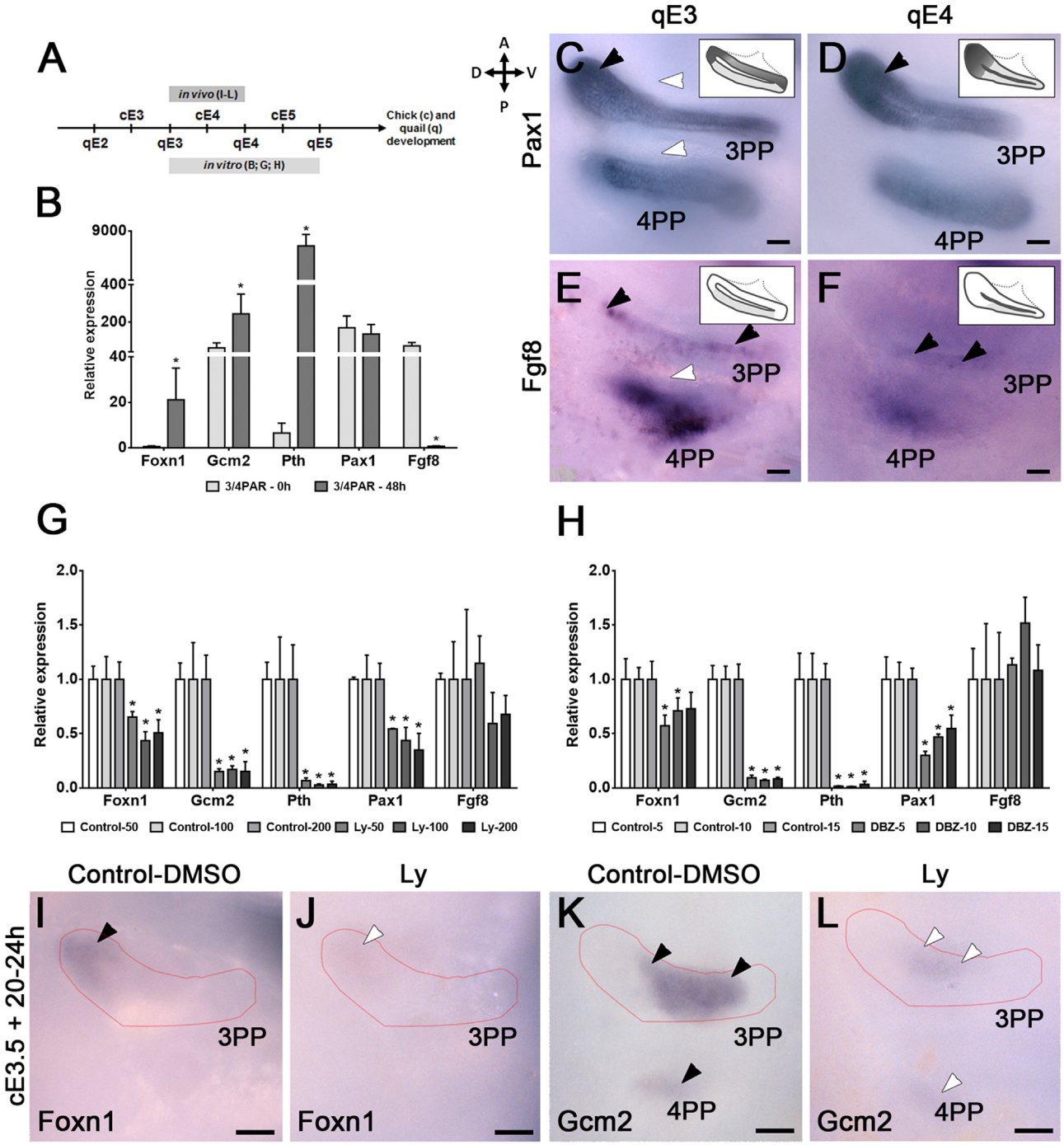

Fig. 3. The effects of Notch signalling modulation during T/PT common primordium formation. Timeline of *in vitro* and *in vivo* assays in chicken and quail development (A). *In vitro* (B) and *in vivo* (C–F) expression of thymic, parathyroid and PP endodermal markers in the 3/4PAR. The 3/4PAR at qE3 was mechanically isolated and grown *in vitro* for 48 h. Gene-expression levels of freshly isolated (3/4PAR-0 h) and cultured (3/4PAR-48 h) tissues were examined by qRT-PCR (B). In parallel, *Pax1* (C and D) and *Fgf8* (E and F) expression was detected by WM-ISH in the developing endoderm of the 3/4PP at qE3 (C and E) and qE4 (D and F). Schematic drawings in the top/right panels depict the gene-expression domains in the 3PP, the well-defined pouch. *In vitro* (G and H) and *in vivo* (I–L) expression of thymic, parathyroid and PP endodermal markers in the 3/4PAR with Notch signalling inhibition. Isolated 3/4PAR at qE3 was grown *in vitro* for 48 h with three doses of Ly, 50 nM (Ly-50), 100 nM (Ly-100) and 200 nM (Ly-200) (G) or three doses of DBZ, 5 μM (DBZ-5), 10 μM (DBZ-10) and 15 μM (DBZ-15) (H). For Notch signalling *in vivo* assay, the expression of *Foxn1* (I and J) and *Gcm2* (K and L) was observed by WM-ISH in the 3/4PAR of cE3.5 embryos developed for 20–24 h after Ly (J and L) or DMSO (I and K) injection. For qRT-PCR, expression of each transcript was measured as a ratio against the mean of *Actb* and *Hprt* transcript expression levels and expressed in arbitrary units. The faint red line delimits the 3PP endoderm. Black arrowheads point to the strong hybridisation signals and white arrowheads point to pharyngeal arches (C and E) or to weak/absent hybridisation signals in the 3/4PP endoderm (J and L). A, anterior; cE, chicken embryonic day; D, dorsal; DBZ, Dibenzazepine; Ly, LY-411.575; P, posterior; PAR, pharyngeal arch region; PP, pharyngeal pouch; qE, quail embryonic day; V, ventral. Scale bars, 50 μm.

patterns of *Pax1* and *Fgf8 in situ* at similar developmental time-windows (qE3 and qE4; Fig. 3C–F). High levels of *Pax1* expression were observed in the 3/4PP endoderm. The stronger hybridisation signals were confined to the dorsal tip of the pouches (Fig. 3C and D), the presumptive territory of the thymic rudiment (Neves et al., 2012). The expression of *Pax1* was maintained in the thymic epithelium at later stages of development (Suppl. Fig. 1C), as has been observed in mice (Wallin et al., 1996). Faint hybridisation signals of

Fgf8 were observed in the posterior/median domain of the 3/4PP endoderm at qE3 (Fig. 3E) and almost disappeared at qE4 (Fig. 3F). In short, our *in vitro* system reproduced the normal dynamic of *Foxn1*, *Gcm2*, *Pth*, *Pax1* and *Fgf8* expression in the developing endoderm of the 3/4PP. The *in situ* study also confirmed the restricted expression of *Pax1* and *Fgf8* in the endodermal pouch compartment at these stages of development.

To analyse the effects of Notch inhibition, pharyngeal tissues were treated with Ly (Fig. 3G), as described above. When compared to control conditions, a significant reduction of *Foxn1* expression was observed in Ly-derived explants (35%, 56% and 49% in Ly-50, Ly-100 and Ly-200, respectively), suggesting that the abolishment of Notch activity compromises thymic epithelium specification. A significant decrease of *Pax1* expression (46%, 55% and 65%) was also consistently observed with increasing doses of Ly. In addition, Ly-treated tissues showed a reduction of *Gcm2* transcript levels (around 80%), alongside the almost total lack of *Pth* expression (more than 90% reduction), revealing the requirement of Notch signalling activity in the early-stages of parathyroid epithelium differentiation. No significant changes in *Fgf8* expression levels were detected during *in vitro* development.

Similar results were obtained when Notch signalling was abrogated using DBZ (Fig. 3H). *Foxn1*, *Gcm2*, *Pth* and *Pax1* transcript levels were significantly reduced in DBZ-treated explants. The expression levels of *Fgf8* were similar in the DBZ and control conditions.

The *in vivo* results (Fig. 3A and I–L) supported the *in vitro* effects, as described above. Ly was injected in the 3/4PAR at cE3.5, the corresponding stage to qE3, and allowed to develop for further 20–24 h. As previously reported (Neves et al., 2012), *Foxn1*- and *Gcm2*-expression domains were localized in the dorsal-tip (n=4/4; Fig. 3I) and median/anterior (n=5/5; Fig. 3K) region of the 3/4PP, respectively, in control embryos (Control-DMSO). The expression of *Foxn1* (n=4/4; Fig. 3J) and *Gcm2* (n=5/5; Fig. 3L) was strongly diminished in the pouches of Ly-injected embryos. The decrease of *Gcm2* expression was only observed in embryos injected with the highest concentration of Ly (20 μM), whereas *Foxn1* expression was reduced even with the lowest dose (5 μM). Concordantly, only transcripts of *Gcm2*, and not *Foxn1*, were clearly detected in freshly isolated tissues at qE3 (Fig. 3B), the developmental stage similar to the moment of embryo injection.

These data provide evidence that Notch signalling has positive regulatory effects during the development of the T/PT common primordium.

3.3. Notch signalling inhibition during early-development of the 3rd and 4th pharyngeal arch region impairs the subsequent formation of parathyroid glands

We then asked if Notch signalling was required at the T/PT common primordium stage for the respective organ formation. To address this question, Ly-treated tissues were grafted onto CAM and allowed to develop *in ovo* for 10 days (Fig. 4A).

We have previously used *in ovo* assays to evaluate the capacity of explants to form organs when grafted onto CAM (Neves et al., 2012). Distinct pharyngeal derived organs displaying normal tissue-tissue interactions were formed in CAM-derived DMSO-free explants (3/4PAR-48 h) (Suppl. Fig. 1D–J). These organs were, however, anatomically displaced due to physical constrains during the ectopic growth in CAM. Briefly, chimeric thymus was formed as a result of quail thymic epithelial colonization by lymphoid progenitor cells of donor origin (chicken) (Suppl. Fig. 1F). Thymic lobes showed normal morphological characteristics with discrete cortical and medullary compartments (Suppl. Fig. 1E). Only one third of the lobes were formed per explant (4, n=6), compared with the usual bilateral segmentation of up to 7 thymic lobes per embryo. Regarding the parathyroid glands, each explant showed similar size and number of organs formed (1.7, n=6) when compared to normal embryogenesis (2 parathyroids per embryo). The glands showed normal morphological features with parenchymal cells arranged in clusters, encircled by numerous capillaries and surrounded by a dense and irregular connective tissue capsule (Suppl. Fig. 1H and I).

The ability of the pharyngeal tissues treated with Ly (3/4PAR Ly-200) to form organs when grafted onto CAM was then assessed (Graft-Ly) (Fig. 4B–M). The number of thymic lobes formed in Graft-Ly was slightly higher than in control conditions, but with similar sizes (Fig. 4B) and normal morphology (Fig. 4D and F). These results demonstrated that absence of Notch signals at the common primordium stage was not sufficient to block thymus formation. Moreover, the subsequent development of the thymic rudiment may have been caused, at least partly, by the reactivation of Notch activity in the drug-free CAM environment. When Ly-derived explants were analysed 3 days post-grafting onto CAM strong *Hes5.1* expression was observed, confirming the reactivation of Notch signalling (Fig. 4H, n=3/4). Likewise, *Foxn1* expression was detected in thymic rudiments derived from Graft-Ly (Fig. 4H′) and Graft-Control (Fig. 4G′, n=3/3). Altogether, the data indicate that early-absence of Notch signalling may delay thymic epithelium specification from the T/PT common primordium without blocking it. To further explore the role of Notch signalling at later stages of thymus development, explants were grown in CAM with daily administration of 200 nM of Ly. Under these conditions, Notch signalling blocking was not achieved, as assessed by Notch-target gene-expression analysis (data not shown). This was probably due to the inaccessibility and/or inappropriate concentration of Ly. The number, size and morphology of the thymuses formed were similar in CAM-derived explants irrespectively of *in ovo* daily administration of Notch inhibitor (data not shown).

The capacity of *in vitro* Ly-treated pharyngeal tissues to form parathyroids was then evaluated (Fig. 4I–M). We observed both fewer and significantly small sized parathyroid glands in Graft-Ly explants (40% less than control) (Fig. 4I). These glands also showed poorly developed parenchymal cells clusters (Fig. 4K and M). These results demonstrate that Notch signalling inhibition at the T/PT common primordium stage is sufficient to prevent normal parathyroid epithelium differentiation and to irreversibly compromise long-term organ formation.

Having shown parathyroids aplasia/hypoplasia in cultured explants deprived of Notch signals, we asked if Notch regulates cell-proliferation and/or cell-death during common primordium stages. 3/4PAR grown *in vitro* with 200 nM of Ly was fixed and analysed *in situ*. Apoptotic and mitotic cells were identified by the presence of Casp3 (Suppl. Fig. 2A and B) and Phos-H3 (Suppl. Fig. 2C and D), at 24 h and 48 h of development, respectively. The number of Casp3$^+$ E-Cad$^+$ cells was similar in 24 h-cultured tissues, regardless of the drug treatment (1133 ± 431 and 958 ± 183 apoptotic cells/mm^2 of endodermal tissue in Control- and Ly-derived explants, respectively) (Suppl. Fig. 2A and B). When tissues were analysed after 48 h in culture, no differences were observed in the number of Phos-H3 positive nuclei in experimental and control conditions (229 ± 40 and 250 ± 53 mitoses/mm^2 of endodermal tissue in Control- and Ly-derived explants, respectively). Moreover, almost no apoptotic features, characterized by pyknosis, were observed with DAPI staining (Suppl. Fig. 2C and D). Accordingly, similar survival rates were observed in CAM-derived explants [75% (n=6/8) in Graft-Control and 88% (n=8/9) in Graft-Ly], suggesting no involvement of Notch signalling in proliferation/cell death during 3/4PP endoderm development.

Altogether the results indicate that blocking Notch signalling activity during the common primordium stage impairs parathyroid gland formation, possibly by preventing normal epithelium

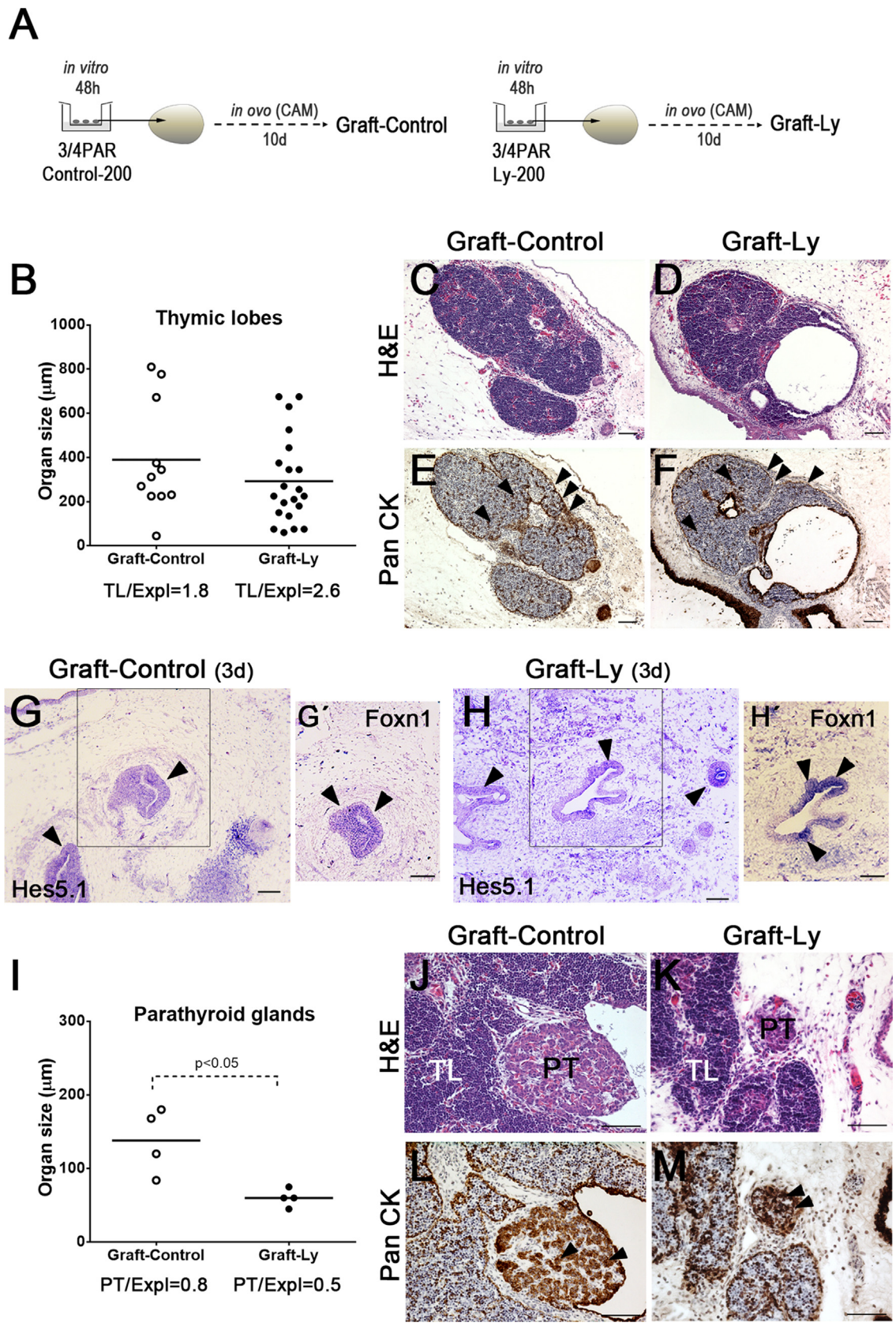

Fig. 4. The effect of early-Notch signalling inhibition in the subsequent formation of the thymus and parathyroid glands. Schematic representation of the 3/4PAR grown *in vitro* for 48 h in the absence (3/4PAR Control-200) or presence of 200 nM of Ly (3/4PAR Ly-200) and then grafted onto CAM of a cE8 embryo. Explants were allowed to develop *in ovo* for 10 days: Graft-Control, explants grown *in vitro* with DMSO; Graft-Ly, explants grown *in vitro* with Ly (A). The size of thymic lobes (B) and parathyroid glands (I) formed in CAM-derived explants. Serial sections of Graft-Control (C and E; J and L) and Graft-Ly (D and F; K and M) slides were H&E stained (C, D, J and K) and immunodetected with anti-Pan CK antibody and counterstained with Gill's hematoxylin (E, F, L and M). The expression of *Hes5.1* (G and H) and *Foxn1* (G′ and H′) was detected by ISH in serial sections of 3d Graft-Control (G and G′) and Graft-Ly (H and H′) slides. Black arrowheads point to immunoreactive positive cells (E, F, L and M) and to strong hybridisation signals in the endoderm (G–H′). CAM, chorioallantoic membrane; Expl, explants; PAR, pharyngeal arch region; PT, parathyroid glands; TL, thymic lobe; 10 d, ten days; 3 d, three days. Scale bars, 50 μm.

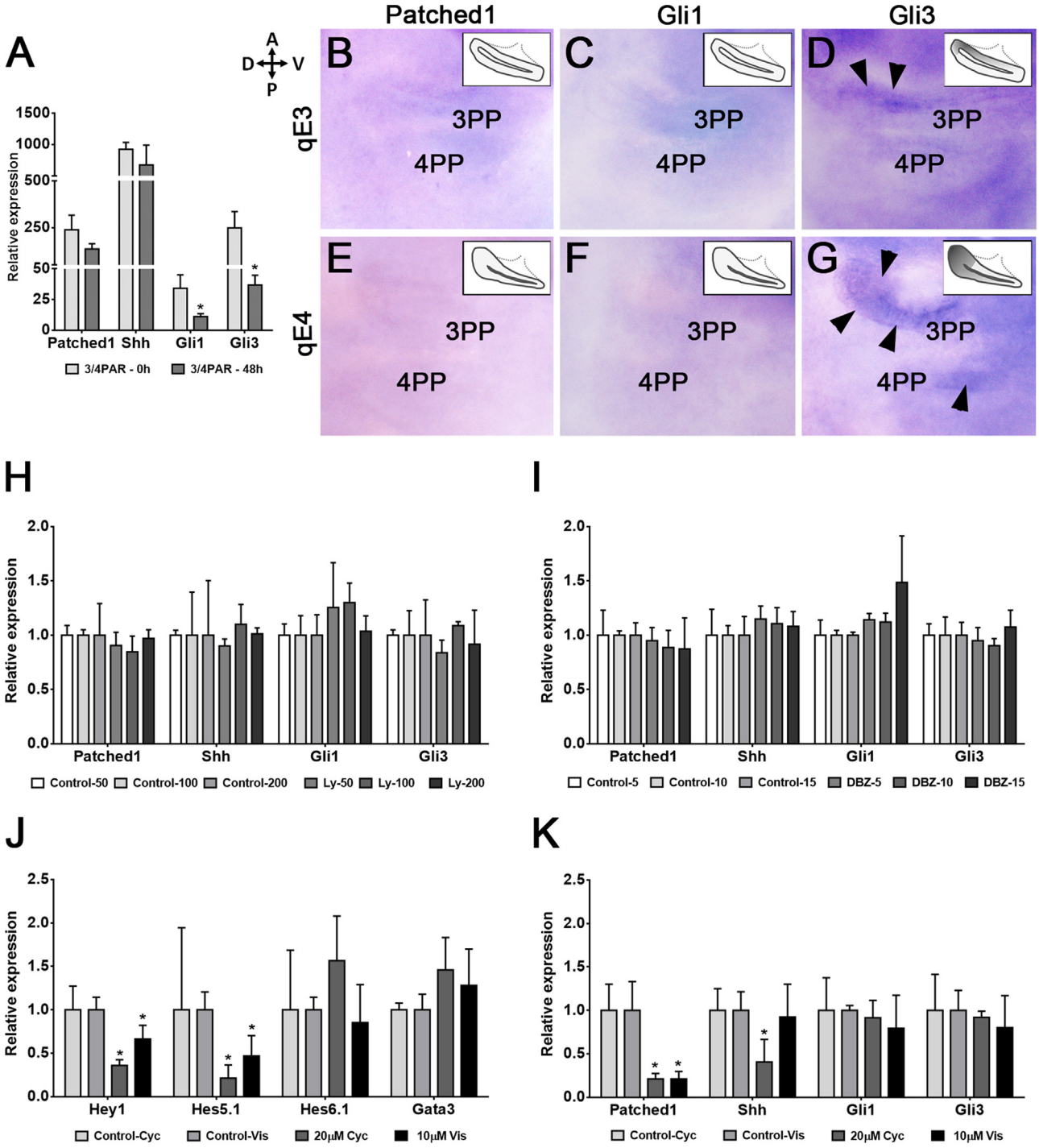

Fig. 5. Crosstalk of Notch and Hh signalling pathways during T/PT common primordium formation. *In vitro* (A) and *in vivo* (B–G) expression of Hh-related genes in the 3/4PAR. The 3/4PAR at qE3 was mechanically isolated and grown *in vitro* for 48 h. Gene-expression levels of freshly isolated (3/4PAR-0 h) and cultured (3/4PAR-48 h) tissues were examined by qRT-PCR (A). In parallel, *Patched1* (B and E), *Gli1* (C and F) and *Gli3* (D and G) expression was observed in the developing endoderm of the 3/4PP at qE3 (B–D) and qE4 (E–G). Schematic drawings in the top/right panels depict the gene-expression domains in the 3PP, the well-defined pouch. Notch (H and I) and Hh (J and K) inhibition *in vitro* assays. Expression levels of Hh-related (H, I and K) and Notch-related (J) genes in 3/4PAR grown *in vitro* for 48 h in the presence of Ly (H), DBZ (I), Cyc and Vis (J and K) were examined by qRT-PCR. Expression of each transcript was measured as a ratio against the mean of the *Actb* and *Hprt* transcript expression levels and expressed in arbitrary units (each transcript in control=1). Black arrowheads point to the hybridisation signals in the 3/4PP endoderm (D and G). A, anterior; Cyc, Cyclopamine; D, dorsal; DBZ, Dibenzazepine; Ly, LY-411.575; P, posterior; PAR, pharyngeal arch region; PP, pharyngeal pouch; qE, quail embryonic day; V, ventral; Vis, Vismodegib. Scale bars, 50 μm.

differentiation, without affecting thymus development.

3.4. Hedgehog modulates Notch signalling in the developing endoderm of the 3rd and 4th pharyngeal pouches

Given the role of Notch as a modulator of Hh signalling in the dorso-ventral patterning of the neural tube (Stasiulewicz et al., 2015), we further investigated if Hh signalling could be modulated by Notch during T/PT common primordium formation.

We started by studying the expression of distinct Hh-related genes in pharyngeal tissues (Fig. 5A–G). The expression of *Patched1* (Hh receptor), *Shh* (Hh ligand), *Gli1* and *Gli3* (Hh-target genes) was

analysed during *in vitro* (Fig. 5A) and *in vivo* (Fig. 5B–G) development, as described above. *Shh* was the most highly expressed Hh-related gene in the developing 3/4PAR (Fig. 5A). Its expression was confined to the endodermal territory of the central pharynx, excluding the 3/4PP (data not shown). The transcript levels of *Patched1* were maintained during 48 h of culture and its hybridisation signals were faint in all pharyngeal tissues (Fig. 5B and E). Interestingly, *Gli1* and *Gli3* transcripts were significantly reduced during *in vitro* development. The *in situ* analysis of these genes revealed hybridisation signals of *Gli1* (Fig. 5C and F) and *Gli3* (Fig. 5D and G) along the endoderm, mesenchyme and ectoderm of the 3/4PAR. However, *Gli3* expression was more evident in the anterior/dorsal tip- (Fig. 5D) and posterior/dorsal tip-domains (Fig. 5G) of the 3PP endoderm, at qE3 and qE4, respectively.

Having demonstrated which genes are involved in the activation of Hh in the 3/4PAR, we asked if blocking Notch activity could interfere with Hh signalling. The expression of Hh-related genes was quantified in 3/4PAR grown *in vitro* for 48 h in the presence of either Notch inhibitor. When compared to control conditions, no differences were observed in the transcript levels of the four genes in Ly- or DBZ-treated tissues (Fig. 5H and I). These *in vitro* effects were confirmed by a Hh-related gene-expression analysis of embryos that had Notch signals blocked at similar developmental-time windows. No obvious changes in *Patched1*, *Gli1* and *Gli3* expression were observed in Ly-injected embryos, when compared to control embryos (Suppl. Fig. 3).

To clarify the interactions between the Notch and Hh pathways, we then questioned if Hh activity could modulate Notch signalling during common primordium formation. Pharyngeal tissues were treated with Cyclopamine (Cyc), a well-described teratogen known to inhibit Hh signal transduction by binding to the heptahelical bundle of Smoothened (Chen et al., 2002). In parallel, another Hh inhibitor Vismodegib (Vis) was used to validate the *in vitro* Hh inhibitory effects. The expression of Notch-target genes was then analysed in explants grown in the presence of these inhibitors to evaluate the capacity of Hh activity to modulate Notch during common primordium formation (Fig. 5J and K). Explants grown in the presence of Cyc or Vis showed a significant reduction of *Hey1* (63% and 29%, respectively) and *Hes5.1* (79% and 60%, respectively) transcript levels, suggesting Notch signalling modulation by Hh during this developmental time-window. Concordantly, no changes were observed in the expression of *Hes6.1* and *Gata3*.

The block of Hh signalling was confirmed by the strong reduction of *Patched1* expression (80%) in tissues grown with either Hh inhibitor (Fig. 5K), as previously described (Grevellec et al., 2011; Cordero et al., 2004). A significant reduction of *Shh* transcripts was also detected in Cyc-treated explants, as has been reported in other developmental contexts (Cordero et al., 2004). The expression levels of *Gli1* and *Gli3* were unchanged in both experimental conditions.

Finally, functional readouts of *in vitro* Hh inhibition with Cyc were evaluated (Suppl. Fig. 4). Consistent with results reported in the $Shh^{-/-}$ mice phenotype (Moore-Scott and Manley, 2005), a significant increase in *Foxn1* expression was accompanied with a reduction of the parathyroid-markers, *Gcm2* and *Pth*, in Cyc-treated explants (Suppl. Fig. 4A). The moderate reduction of *Gcm2* transcripts, in contrast with its absence in the mutant mice, is in accordance with a less responsive *Gcm2*-expression domain to Hh at these stages of development (Grevellec et al., 2011). Moreover, pharyngeal tissues with compromised Hh activity showed massive apoptosis, disruption of epithelial integrity (Suppl. Fig. 4B′ and C′) and low survival rates when grafted onto the CAM, resulting in thymic hypoplasia and abnormal parathyroid formation (Suppl. Fig. 4E–I′). The results are consistent with previous reports describing the role of Hh in the formation of pharyngeal endoderm-derived organs (Moore-Scott and Manley, 2005; Grevellec et al., 2011; Shah et al., 2004; Outram et al., 2009).

Together, the data suggest a fine-tuning modulation of Notch and Hh pathways during T/PT common primordium formation. Importantly, Hh signalling may regulate Notch activity during this developmental time-window.

3.5. Hedgehog modulates Notch signalling in distinct domains of the developing endoderm of the 3rd and 4th pharyngeal pouches

As shown above, Hh regulates the expression of Notch-target genes in cultured tissues. We therefore carried out *in vivo* modulation of Hh activity during the development of T/PT common primordium. Beads soaked with Cyc (6 mM) were placed in the lumen of the pharynx through the second cleft and sited near the 3/4PP at cE2.5 and qE3. After 20–24 h of development, embryos were fixed and analysed by WM-ISH for Notch-target genes and organ epithelial markers (Fig. 6).

Embryos developed with low Hh activity in the pharyngeal region showed a reduction in *Gata3* expression in the anterior/median territory of the 3PP endoderm (Fig. 6E, n=4/5), when compared with control embryos (Fig. 6A, n=5/5). In the same pouch region, we observed the loss of *Gcm2* expression (Fig. 6F, n=4/5), an expected result considering that $Shh^{-/-}$ mice have no *Gcm2* expression in the presumptive territory of the parathyroids (Moore-Scott and Manley, 2005). These results suggested that Hh activity positively regulates Gata3/Notch signals in the Gcm2/parathyroid-fated domain of the 3/4PP endoderm. However, embryos with Cyc-soaked beads (Cyc-beads) showed the maintenance of *Gata3* expression in the dorsal tip of the 3PP, the presumptive thymic domain (Fig. 6E). At later stages, low Hh activity in the pharyngeal region led to a decrease of *Gata3* expression in the 4PP endoderm of qE3 (a similar stage to cE3.5, Fig. 6J) embryos (Fig. 6G, n=3/3). This effect recapitulates the one observed in the 3PP at an earlier stage of development (cE2.5). This dynamic spatial and temporal action of Hh signalling has already been described for the modulation of *Gcm2* expression during PP development (Grevellec et al., 2011).

To further investigate downstream targets of Hh signalling in the presumptive thymic rudiment, we screened for the expression of other Notch-related genes in 3/4PP endoderm. Several genes were studied and their expression patterns were unaltered or inconsistently modified when Hh signalling was impaired (Suppl. Fig. 5A–F). Only *Lfng*, a Notch modulator, showed robust modified expression in these conditions. *Lfng* is normally expressed in the posterior/median territory of the 3PP endoderm (Fig. 6D, n=4/4), the territory excluded from the T/PT common primordium, and in mesenchymal cells. In the absence of Hh signals, its expression was downregulated in the pouch and in some neighbouring cells (Fig. 6H, n=4/4). Lfng is known to inhibit Jag1-mediated signalling and to potentiate Notch1 activation via the Delta1 ligand (Hicks et al., 2000). In cE3, faint expression of *Notch1* (Fig. 6I) and *Delta1* (Fig. 6K) was observed in the endoderm and neighbouring cells of the 3PP. The expression of *Jag1* (Fig. 6L) appeared more restricted to the anterior/median domain of the 3PP. The data indicate a preferential activation of Notch via Lfng/Delta1 in the posterior/median domain of the pouches.

Having in mind that the posterior boundary of Foxn1/thymus-fated domain is the *Lfng*-expression domain, we questioned if the territory of the former could be altered when Hh signalling was abolished. When compared to controls (Fig. 6M, n=7/7), qE3 embryos with Cyc-beads presented an enlarged *Foxn1*-expression domain with stronger hybridisation signals (Fig. 6N, n=4/6). The expansion of the Foxn1/thymus-fated domain was from the dorsal tip to a more posterior/median region of the pouch. This territory partially overlapped with the *Lfng*-expression domain, which in turn was prevented in the absence of Hh. These results thus

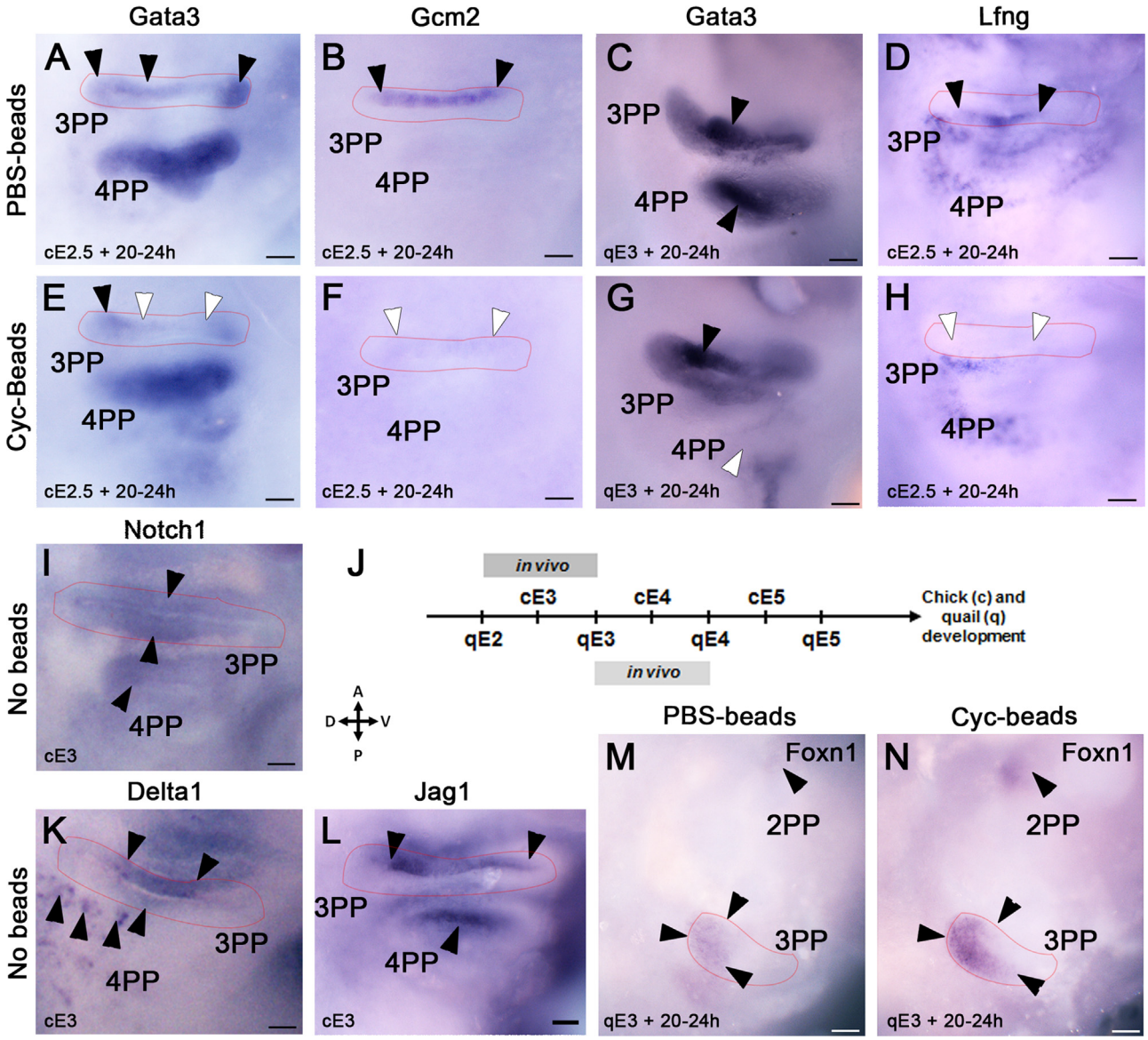

Fig. 6. The effect of *in vivo* Hh signalling inhibition during T/PT common primordium formation. PBS-beads (A-D and M) and Cyc-beads (E–H and N) were implanted in the pharyngeal region of cE2.5 (A, B, D–F and H) and qE3 (C, G, M and N) and embryos allowed to develop for 20–24 h. Expression of *Gata3* (A, C, E and G), *Gcm2* (B and F), *Lfng* (D and H) and *Foxn1* (M and N) was observed by WM-ISH. In parallel, the expression of *Notch1* (I), *Delta1* (K) and *Jag1* (L) was examined in the pharyngeal region of cE3. Timeline of *in vivo* assays in chicken and quail development (J). Faint red line delimits the 3PP endoderm. Black and white arrowheads point to strong and weak/absent hybridisation signals in the PP endoderm, respectively. A, anterior; cE, chicken embryonic day; Cyc, cyclopamine; D, dorsal; P, posterior; PP, pharyngeal pouch; qE, quail embryonic day; V, ventral. Scale bars, 50 μm.

suggest that Lfng/Notch activity defines the posterior boundary of the Foxn1/thymus-fated domain, in an Hh-dependent manner.

Notably, an enriched expression of *Foxn1* was observed in the 2PP endoderm (Fig. 6N), suggesting that Hh signalling prevents the Foxn1/thymus-fated domain in the most anterior pouches. Similar ectopic and abnormal *Gcm2* expression in the 2PP was previously reported as a result of Hh inhibition (Grevellec et al., 2011).

4. Discussion

In avians, as in mammals, the thymus and parathyroids epithelia derive from a common endodermal primordium of the pharyngeal pouches. This process involves the patterning of the pouches followed by rudiment specification. In this study, we propose that the temporal and spatial dynamics of the pharyngeal morphogenesis are regulated by Notch and Hh signals during the development of the T/PT common primordium and the formation of thymic and parathyroid rudiments.

4.1. Thymus and parathyroids common primordium

In avians, as opposed to mice, the thymus and parathyroid epithelia derive not from one (3PP) but from two sequentially developing pharyngeal pouches, the 3PP and 4PP. Consistent with the temporal gap of 12 h to 24 h between the formation of the two pouches, a delay in the expression of several transcriptional regulators known to be involved in PP patterning and early-formation of these organs has also been observed (Manley and Condie, 2010). For example, *Gcm2* expression in the anterior domain of the 3PP was first reported at HH18 (cE3; qE2.5), prior to the formation of the 4PP. Only at HH22 (cE4; qE3) was the expression of *Gcm2* observed in the 4PP (Okabe and Graham, 2004). To overcome this

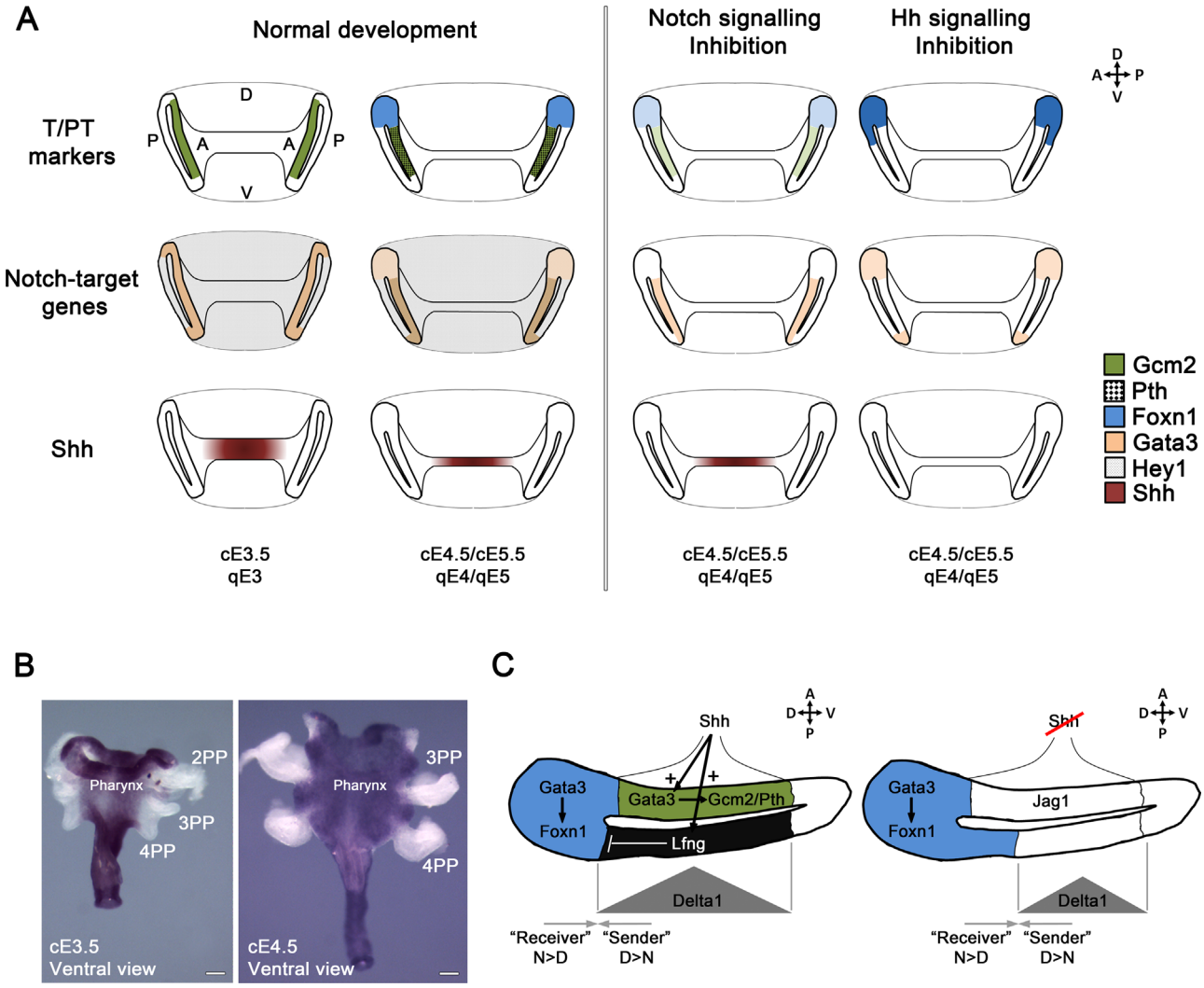

Fig. 7. Model of Hh and Notch signalling modulation during thymic and parathyroid rudiment formation. Schematic representation of the results obtained during *in vivo* and *in vitro* assays (A). Cross sections of the most ventral region of the embryo and expression of T/PT markers, Notch-target genes and Shh in 3PP endoderm during normal development and when Notch and Hh signalling is inhibited (A). Expression of *Shh* in isolated pharyngeal endoderm examined by WM-ISH at cE3.5 and cE4.5 (B). Schematic model of Notch and Hh signalling crosstalk during T/PT common primordium formation during normal development and in the absence of Hh signalling (C). In detail is depicted a proposed model for the lateral inhibition mechanism involved in the median/posterior thymic boundary definition. In this case, the relative levels of Notch and Delta determine the cell's signalling state. The cell with more Notch than Delta becomes a 'receiver' and cells with more Delta than Notch become 'sender' cells. In the absence of Hh, reduction of the Delta1 signalling gradient shifts the boundary to a more median position within the pouch. Arrows indicate putative signalling crosstalk (see Discussion for details). A, anterior; cE, chicken embryonic day; D, dorsal; D > N, Delta > Notch; N > D, Notch > Delta; P, posterior; PP, pharyngeal pouch; qE, quail embryonic day; V, ventral. Scale bars, 100 μm.

complexity we opted to perform the *in vitro* studies at qE3 stage when both pouches are already formed.

We observed a consistent impairment in the development of the T/PT common primordium when Notch signalling was *in vitro* and *in vivo* inhibited (schematic representation in Fig. 7A). The expression of thymic and parathyroid markers (*Foxn1* and *Gcm2/Pth*) was strikingly decreased. These effects were accompanied with the reduction of *Gata3*, suggesting that this Notch-target is a downstream mediator of Notch activity during common primordium development. In agreement, heterozygous mice mutants for Gata3 have smaller T/PT common primordium with fewer cells expressing *Gcm2* (Grigorieva et al., 2010).

When Hes1, another Notch-target, was deleted in neural crest cells, there was aplasia/hypoplasia of these organs, stressing the importance of driving specific Notch signals into distinct tissues during early stages of thymic and parathyroid formation (Kameda et al., 2013). We have previously developed an *in vitro* experimental system with the heterospecific association of quail and chicken tissues, which has allowed us to study epithelial-mesenchymal interactions during thymus and parathyroid organogenesis (Neves et al., 2012). Insufficient information on quail and chicken genetic sequences has been a limiting step for discriminating tissues of different origin by qRT-PCR assays. As a consequence, the complete distinction of the endodermal and mesenchymal specific functions during organ formation, particularly important in a cell-cell contact signalling activation like in the Notch pathway, could not be fully addressed in this study.

We identified a new domain in the 3PP at qE3 (cE3.5), excluded from the common primordium, in which the Notch-modulator *Lfng*, and also *Fgf8* were expressed. The reduction of *Lfng* and *Fgf8* (Suppl. Fig. 4A) in the absence of Hh suggests that this domain may be involved in the regulation of T/PT common primordium development, in an Hh-dependent manner. These data, though limited, suggests a putative Shh-Fgf8-Lfng network, involving distinct signalling centres located in the endoderm of the pharynx and within the pouches. In other biological contexts, Lfng is known to respond to Fgf8 signals (Shifley et al., 2008). On the other hand, Fgf8 has been shown to respond to Shh produced by

the pharyngeal endoderm during arch patterning (Haworth et al., 2007). And in the developing 3PP, a hyper-responsiveness to Fgf8 alters, at least in part, the initiation of parathyroid- and thymus-fated markers (Gardiner et al., 2012).

The endoderm of the pharynx is indeed the main source of Hh signals, via Shh secretion, during the development of the T/PT common primordium (Fig. 7B). The median/anterior and median/posterior territories of the developing pouches are closer to the source of Hh, as opposed to the tips, which will grow apart to more dorsal and ventral positions. At qE3, expression of various Notch-related genes is distributed along the pouches. The median/anterior region and tips of the pouch originate a *Gata3*-expression domain while the median/posterior territory gives rise to the *Lfng*-expression domain. The restricted median/anterior domain of *Gata3* also co-expresses *Gcm2*. As development proceeds, the *Gata3*/*Gcm2* domain starts to express *Pth* and becomes more restricted to a smaller central territory of the anterior/median region of the pouch (Fig. 7A), originating the parathyroid rudiment at qE4 (Neves et al., 2012).

When Hh signals were abolished in the pharynx, downregulation of *Gata3*/*Gcm2* and *Lfng* expression was observed, indicating that the median domains of the pouches are positively regulated by Hh signalling. In contrast, the expression of *Gata3* was maintained at the tips of the pouches, suggesting that there are Gata3/Notch signals in the common primordium that respond differently to Hh (schematic representations in Fig. 7C). It is therefore conceivable that during the specification of the rudiments, the parathyroid-fated domain is more sensitive to Hh signalling, while the thymus-fated domain is unresponsive to Hh.

Overtime, the source of Shh gets further away and overall the pouches become less sensitive to Hh. In fact, the upregulation of *Gcm2* was reported to correlate with the loss of Hh receptor *Patched1* during 3PP development in mice (Grevellec et al., 2011).

4.2. Parathyroid rudiment

The specification of the parathyroid rudiment is known to be dependent on *Gcm2* transcriptional activation. Deficiency of Gcm2 in mice leads to the absence of parathyroid glands without affecting thymus formation (Liu et al., 2007). Notch-target Gata3 (Fang et al., 2007; Naito et al., 2011) is one of the upstream regulators of Gcm2, as Gata3$^{-/-}$ mice showed no *Gcm2* expression and no gland formation (Grigorieva et al., 2010). In this investigation, the decreased expression of *Gata3* was accompanied by a sharp reduction of *Gcm2* in the absence of Notch, demonstrating a Notch signalling activation requirement, via Gata3, for parathyroid epithelium differentiation. Evidence supporting this hypothesis was the loss of *Pth* expression and abnormal parathyroid formation, when common primordium was grown in the absence of Notch activity. It has been recently shown in mice that Gata3 cooperates with Gcm2 to activate *Pth* expression (Han et al., 2015).

Apart from a possible role in epithelium differentiation, Gata3/Notch signals may also regulate cell survival in the parathyroid rudiment. The impairment of Gcm2/Gata3-Notch signals results in the reduced number and size of the parathyroids, in accordance with the mouse model where parathyroid precursors undergo rapid apoptosis in the absence of Gcm2 (Liu et al., 2007). Although no differences were detected in the number of proliferating or apoptotic cells in the developing pharyngeal endoderm treated with Ly, we cannot exclude the role of Notch in these biological processes. *In situ* analysis showed small clusters of apoptotic cells on the endoderm grown *in vitro* for 24 h (not shown). This suggests well-defined domains with a tight regulation of cell numbers that may correspond to organ rudiments, that is, the parathyroid glands. We also postulate that these untraced apoptotic events may occur even earlier during *in vitro* development.

During the course of our study we further attempted to identify the Notch ligands involved in PT rudiment formation. Only *Jag1* was confined to the median/anterior territory of the pouches at cE3, overlapping with the Gcm2/parathyroid-fated domain. The capacity of *Jag1*-expressing cells to define boundaries by lateral inhibition has been reported in other developmental processes (Kiernan, 2013). In this study, the *Jag1*-expression domain, as opposed to the Gata3/Gcm2/parathyroid-fated domain, was not altered when the pharyngeal source of Hh was abolished (Suppl. Fig. 5B), suggesting that Jag1 defines the boundary of the rudiment independent of Hh. It may be that parathyroid cell-fate specification, accompanied by the definition of the boundary of the rudiments, occurs earlier in development. In agreement with this, the location of the parathyroid dorsal boundary appears to be unchanged when Gcm2/Pth expression is lost.

Nevertheless, the theory that there is positive regulation of Hh in settling the Gata3/Gcm2/parathyroid-fated domain is supported by the abnormal morphology and size of the glands in the absence of Hh signalling.

4.3. Thymic rudiment

The individual thymic rudiment was previously identified by the *Foxn1*-expression domain in the dorsal tip of the pouches at qE4 (Neves et al., 2012). In this work we show that *Foxn1* expression was strongly reduced when Notch signalling was impaired. The early downregulation of *Foxn1* could however be reversed by subsequent restitution of Notch signalling activity in the thymic rudiment.

Notch signalling is known to play a unique function in the control of hair follicle differentiation by modulation of *Foxn1* (Hu et al., 2010). Although hair is an epidermal appendage that arose after the last shared common ancestor between mammals and birds, embryonic chicken feathers and nails also express *Foxn1*, demonstrating the conservation of these developmental processes during evolution (Darnell et al., 2014). In addition, nude mice (Foxn1$^{-/-}$) have two major defects, abnormal hair growth and defective development of the thymic epithelium (Nehls et al., 1996; Blackburn et al., 1996; Bleul et al., 2006), suggesting a common Notch-Foxn1 pathway in both developmental processes.

The Notch-target gene Gata3 may be one of the upstream regulators of Foxn1, since *Gata3* is expressed in the dorsal tip of the 3/4PP endoderm during T/PT common primordium formation. At this developmental stage, *Gata3* in the prospective thymic rudiment is modulated by Notch (schematic representation in Fig. 7C).

When Hh signalling was blocked, we observed an expansion of the Foxn1/thymus-fated domain to a more median/posterior region, at the expense of the loss of *Lfng*–expression domain (Fig. 7C). The capacity of the thymic rudiment to expand posteriorly suggests some degree of cell-fate plasticity of endodermal cells in the posterior/median domain of the pouch. Together with *Lfng*, the only Notch ligand faintly expressed in the median/posterior territory of the pouches was *Delta1*. Lfng typically enhances Notch activation by ligands belonging to the Delta family and reduces Notch activation by Jagged ligands (reviewed in Stanley and Okajima (2010)). This suggests that the posterior thymic boundary is determined by a lateral inhibition mechanism via Delta1. In the absence of Hh signals in the pharyngeal region, the disappearance of the *Lfng*-expression domain may result in reduced Delta1 activity and boundary displacement. Specifically, a reduction of the Delta1 signalling strength gradient may result in an augmentation of the posterior thymic rudiment territory. Here, we describe the previously unreported regulation of the posterior boundary of thymic rudiment by Notch signalling via Lfng, in an Hh-dependent

manner (Fig. 7C).

Another Notch-target gene, *Hey1,* was markedly reduced when Notch activity was blocked in the pharyngeal tissues. Although *Hey1* expression was not restricted to the endoderm of the pouches, our data suggest its involvement in the primordium development. In agreement, a recent report showed *Hey1* expression in the thymic epithelium of mice (Subhan et al., 2013).

The transcription factor Pax1, important for thymus (Dietrich and Gruss, 1995; Wallin et al., 1996) and parathyroid (Su et al., 2001) formation, was also downregulated when Notch signalling was inhibited, suggesting that Notch may act upstream of Pax1 during T/PT common primordium development. Taking into account that *Pax1* is expressed very early in pouch formation (not shown) and during thymic epithelium differentiation; it is therefore conceivable that distinct mechanisms may positively regulate Pax1, from pharyngeal pouch morphogenesis to thymus organogenesis. A biphasic role in these distinct windows of development was recently described for the activity of another transcription factor, the Tbx1 gene (Reeh et al., 2014).

In conclusion, our work shows that Notch signalling is crucial for T/PT common primordium development and parathyroid formation, in an Hh-dependent manner. Finally, we conclude that, despite the evolutionary distance, the regulatory mechanisms controlling the formation of these organs appear to be conserved in avians and mammals.

Conflicts of interest

The authors declare no conflict of interests.

Acknowledgments

The authors are grateful to Domingos Henrique, Joaquin Rodriguez Leon, Solveig Thorsteinsdottir and Kim Dale for reagents, to Sérgio Dias for helpful discussions and to Interaves Portugal for contributing with quail fertilised eggs. This work was supported by Fundação para a Ciência e para a Tecnologia (FCT), project PTDC/SAU-BID/115264/2009. M. Figueiredo received two research fellowships from FCT.

Appendix A. Supplementary material

Supplementary data associated with this article can be found in the online version at http://dx.doi.org/10.1016/j.ydbio.2016.08.012.

References

Aulehla, A., Johnson, R.L., 1999. Dynamic expression of lunatic fringe suggests a link between notch signaling and an autonomous cellular oscillator driving somite segmentation. Dev. Biol. 207, 49–61.

Blackburn, C.C., Augustine, C.L., Li, R., Harvey, R.P., Malin, M.A., Boyd, R.L., Miller, J.F., Morahan, G., 1996. The nu gene acts cell-autonomously and is required for differentiation of thymic epithelial progenitors. Proc. Natl. Acad. Sci. USA 93, 5742–5746.

Bleul, C.C., Corbeaux, T., Reuter, A., Fisch, P., Mönting, J.S., Boehm, T., 2006. Formation of a functional thymus initiated by a postnatal epithelial progenitor cell. Nature 441, 992–996.

Chen, J.K., Taipale, J., Cooper, M.K., Beachy, P.A., 2002. Inhibition of Hedgehog signaling by direct binding of cyclopamine to Smoothened. Genes Dev. 16, 2743–2748.

Cordero, D., Marcucio, R., Hu, D., Gaffield, W., Tapadia, M., Helms, J.A., 2004. Temporal perturbations in sonic hedgehog signaling elicit the spectrum of holoprosencephaly phenotypes. J. Clin. Investig. 114, 485–494.

Crossley, P.H., Minowada, G., MacArthur, C.A., Martin, G.R., 1996. Roles for FGF8 in the induction, initiation, and maintenance of chick limb development. Cell 84, 127–136.

Darnell, D.K., Zhang, L.S., Hannenhalli, S., Yaklichkin, S.Y., 2014. Developmental expression of chicken FOXN1 and putative target genes during feather development. Int. J. Dev. Biol. 58, 57–64. http://dx.doi.org/10.1387/ijdb.130023sy.

Dietrich, S., Gruss, P., 1995. Undulated phenotypes suggest a role of Pax-1 for the development of vertebral and extravertebral structures. Dev. Biol. 167, 529–548.

Dorsch, M., Zheng, G., Yowe, D., Rao, P., Wang, Y., Shen, Q., Murphy, C., Xiong, X., Shi, Q., Gutierrez-Ramos, J.C., Fraser, C., Villeval, J.L., 2002. Ectopic expression of Delta4 impairs hematopoietic development and leads to lymphoproliferative disease. Blood 100, 2046–2055.

Etchevers, H.C., Vincent, C., Le Douarin, N.M., Couly, G.F., 2001. The cephalic neural crest provides pericytes and smooth muscle cells to all blood vessels of the face and forebrain. Development 128, 1059–1168.

Fang, T.C., Yashiro-Ohtani, Y., Del Bianco, C., Knoblock, D.M., Blacklow, S.C., Pear, W. S., 2007. Notch directly regulates Gata3 expression during T helper 2 cell differentiation. Immunity 27, 100–110.

Farley, A.M., Morris, L.X., Vroegindeweij, E., Depreter, M.L., Vaidya, H., Stenhouse, F. H., Tomlinson, S.R., Anderson, R.A., Cupedo, T., Cornelissen, J.J., Blackburn, C.C., 2013. Dynamics of thymus organogenesis and colonization in early human development. Development 140, 2015–2026. http://dx.doi.org/10.1242/dev.087320.

Fior, R., Henrique, D., 2005. A novel hes5/hes6 circuitry of negative regulation controls Notch activity during neurogenesis. Dev. Biol. 281, 318–333.

Frank, D.U., Fotheringham, L.K., Brewer, J.A., Muglia, L.J., Tristani-Firouzi, M., Capecchi, M.R., Moon, A.M., 2002. An Fgf8 mouse mutant phenocopies human 22q11 deletion syndrome. Development 129, 4591–4603.

Gardiner, J.R., Jackson, A.L., Gordon, J., Lickert, H., Manley, N.R., Basson, M.A., 2012. Localised inhibition of FGF signalling in the third pharyngeal pouch is required for normal thymus and parathyroid organogenesis. Development 139, 3456–3466. http://dx.doi.org/10.1242/dev.079400.

Gordon, J., Bennett, A.R., Blackburn, C.C., Manley, N.R., 2001. Gcm2 and Foxn1 mark early parathyroid- and thymus-specific domains in the developing third pharyngeal pouch. Mech. Dev. 103, 141–143.

Grevellec, A., Tucker, A.S., 2010. The pharyngeal pouches and clefts: development, evolution, structure and derivatives. Semin. Cell Dev. Biol. 21, 325–332. http://dx.doi.org/10.1016/j.semcdb.2010.01.022.

Grevellec, A., Graham, A., Tucker, A.S., 2011. Shh signalling restricts the expression of Gcm2 and controls the position of the developing parathyroids. Dev. Biol. 353, 194–205. http://dx.doi.org/10.1016/j.ydbio.2011.02.012.

Grigorieva, I.V., Mirczuk, S., Gaynor, K.U., Nesbit, M.A., Grigorieva, E.F., Wei, Q., Ali, A., Fairclough, R.J., Stacey, J.M., Stechman, M.J., Mihai, R., Kurek, D., Fraser, W.D., Hough, T., Condie, B.G., Manley, N., Grosveld, F., Thakker, R.V., 2010. Gata3-deficient mice develop parathyroid abnormalities due to dysregulation of the parathyroid-specific transcription factor Gcm2. J. Clin. Investig. 120, 2144–2155. http://dx.doi.org/10.1172/JCI42021.

Günther, T., Chen, Z.F., Kim, J., Priemel, M., Rueger, J.M., Amling, M., Moseley, J.M., Martin, T.J., Anderson, D.J., Karsenty, G., 2000. Genetic ablation of parathyroid glands reveals another source of parathyroid hormone. Nature 406, 199–203.

Guo, C., Sun, Y., Zhou, B., Adam, R.M., Li, X., Pu, W.T., Morrow, B.E., Moon, A., Li, X., 2011. A Tbx1-Six1/Eya1-Fgf8 genetic pathway controls mammalian cardiovascular and craniofacial morphogenesis. J. Clin. Investig. 121, 1585–1595. http://dx.doi.org/10.1172/JCI44630.

Han, S.I., Tsunekage, Y., Kataoka, K., 2015. Gata3 cooperates with Gcm2 and MafB to activate parathyroid hormone gene expression by interacting with SP1. Mol. Cell. Endocrinol. 411, 113–120. http://dx.doi.org/10.1016/j.mce.2015.04.018.

Haworth, K.E., Wilson, J.M., Grevellec, A., Cobourne, M.T., Healy, C., Helms, J.A., Sharpe, P.T., Tucker, A.S., 2007. Sonic hedgehog in the pharyngeal endoderm controls arch pattern via regulation of Fgf8 in head ectoderm. Dev. Biol. 303, 244–258.

Henrique, D., Adam, J., Myat, A., Chitnis, A., Lewis, J., Ish-Horowicz, D., 1995. Expression of a Delta homologue in prospective neurons in the chick. Nature 375, 787–790.

Hicks, C., Johnston, S.H., diSibio, G., Collazo, A., Vogt, T.F., Weinmaster, G., 2000. Fringe differentially modulates Jagged1 and Delta1 signalling through Notch1 and Notch2. Nat. Cell Biol. 2, 515–520.

Hu, B., Lefort, K., Qiu, W., Nguyen, B.C., Rajaram, R.D., Castillo, E., He, F., Chen, Y., Angel, P., Brisken, C., Dotto, G.P., 2010. Control of hair follicle cell fate by underlying mesenchyme through a CSL-Wnt5a-FoxN1 regulatory axis. Genes Dev. 24, 1519–1532. http://dx.doi.org/10.1101/gad.1886910.

Jaleco, A.C., Neves, H., Hooijberg, E., Gameiro, P., Clode, N., Haury, M., Henrique, D., Parreira, L., 2001. Differential effects of Notch ligands Delta-1 and Jagged-1 in human lymphoid differentiation. J. Exp. Med. 194, 991–1002.

Jiang, R., Lan, Y., Chapman, H.D., Shawber, C., Norton, C.R., et al., 1998. Defects in limb, craniofacial, and thymic development in Jagged2 mutant mice. Genes Dev. 12, 1046–1057.

Kameda, Y., Saitoh, T., Nemoto, N., Katoh, T., Iseki, S., Fujimura, T., 2013. Hes1 is required for the development of pharyngeal organs and survival of neural crest-derived mesenchymal cells in pharyngeal arches. Cell Tissue Res 353, 9–25. http://dx.doi.org/10.1007/s00441-013-1649-z.

Kiernan, A.E., 2013. Notch signaling during cell fate determination in the inner ear. Semin. Cell Dev. Biol. 24, 470–479. http://dx.doi.org/10.1016/j.semcdb.2013.04.002.

Lai, E.C., 2004. Notch signaling: control of cell communication and cell fate. Development 131, 965–973.

Lawson, N.D., Vogel, A.M., Weinstein, B.M., 2002. sonic hedgehog and vascular endothelial growth factor act upstream of the Notch pathway during arterial endothelial differentiation. Dev. Cell 3, 127–136.

Leimeister, C., Dale, K., Fischer, A., Klamt, B., Hrabe de Angelis, M., Radtke, F., McGrew, M.J., Pourquié, O., Gessler, M., 2000. Oscillating expression of c-Hey2 in the presomitic mesoderm suggests that the segmentation clock may use combinatorial signalling through multiple interacting bHLH factors. Dev. Biol. 227, 91–103.

Lewis, J., 1998. Notch signalling and the control of cell fate choices in vertebrates. Semin. Cell Dev. Biol. 9, 583–589.

Lilleväli, K., Haugas, M., Pituello, F., Salminen, M., 2007. Comparative analysis of Gata3 and Gata2 expression during chicken inner ear development. Dev. Dyn. 236, 306–313.

Liu, Z., Yu, S., Manley, N.R., 2007. Gcm2 is required for the differentiation and survival of parathyroid precursor cells in the parathyroid/thymus primordia. Dev. Biol. 305, 333–346.

Livak, K.J., Schmittgen, T.D., 2001. Analysis of relative gene expression data using real-time quantitative PCR and the 2(-Delta Delta C(T)) method. Methods 25, 402–408.

Manley, N.R., Condie, B.G., 2010. Transcriptional regulation of thymus organogenesis and thymic epithelial cell differentiation. Prog. Mol. Biol. Transl. Sci. 92, 103–120. http://dx.doi.org/10.1016/S1877-1173(10)92005-X.

Marigo, V., Johnson, R.L., Vortkamp, A., Tabin, C.J., 1996a. Sonic hedgehog differentially regulates expression of GLI and GLI3 during limb development. Dev. Biol. 180, 273–283.

Marigo, V., Scott, M.P., Johnson, R.L., Goodrich, L.V., Tabin, C.J., 1996b. Conservation in hedgehog signaling: induction of a chicken patched homolog by Sonic hedgehog in the developing limb. Development 122, 1225–1233.

McGlinn, E., van Bueren, K.L., Fiorenza, S., Mo, R., Poh, A.M., Forrest, A., Soares, M.B., Bonaldo Mde, F., Grimmond, S., Hui, C.C., Wainwright, B., Wicking, C., 2005. Pax9 and Jagged1 act downstream of Gli3 in vertebrate limb development. Mech. Dev. 122, 1218–1233.

Moore-Scott, B.A., Manley, N.R., 2005. Differential expression of Sonic hedgehog along the anterior-posterior axis regulates patterning of pharyngeal pouch endoderm and pharyngeal endoderm-derived organs. Dev. Biol. 278, 323–335.

Myat, A., Henrique, D., Ish-Horowicz, D., Lewis, J., 1996. A chick homologue of Serrate and its relationship with Notch and Delta homologues during central neurogenesis. Dev. Biol. 174, 233–247.

Naito, T., Tanaka, H., Naoe, Y., Taniuchi, I., 2011. Transcriptional control of T-cell development. Int. Immunol. 23, 661–668. http://dx.doi.org/10.1093/intimm/dxr078.

Nehls, M., Kyewski, B., Messerle, M., Waldschütz, R., Schüddekopf, K., Smith, A.J., Boehm, T., 1996. Two genetically separable steps in the differentiation of thymic epithelium. Science 272, 886–889.

Neves, H., Zilhão, R., 2014. Development of parathyroid glands and C-Cells. In: Ashford, M. (Ed.), Parathyroid Glands: Regulation, Role in Human Disease and Indications for Surgery. Nova Science Publishers New York, United States of America, pp. 1–34.

Neves, H., Dupin, E., Parreira, L., Le Douarin, N.M., 2012. Modulation of Bmp4 signalling in the epithelial-mesenchymal interactions that take place in early thymus and parathyroid development in avian embryos. Dev. Biol. 361, 208–219. http://dx.doi.org/10.1016/j.ydbio.2011.10.022.

Okabe, M., Graham, A., 2004. The origin of the parathyroid gland. Proc. Natl. Acad. Sci. USA 101, 17716–17719.

Outram, S.V., Hager-Theodorides, A.L., Shah, D.K., Rowbotham, N.J., Drakopoulou, E., Ross, S.E., Lanske, B., Dessens, J.T., Crompton, T., 2009. Indian hedgehog (Ihh) both promotes and restricts thymocyte differentiation. Blood 113, 2217–2228. http://dx.doi.org/10.1182/blood-2008-03-144840.

Potts, J.T., 2005. Parathyroid hormone: past and present. J. Endocrinol. 187, 311–325.

Pui, J.C., Allman, D., Xu, L., DeRoco, S., Karnell, F.G., Bakkour, S., Lee, J.Y., Kadesch, T., Hardy, R.R., Aster, J.C., Pear, W.S., 1999. Notch1 expression in early lymphopoiesis influences B versus T lineage determination. Immunity 11, 299–308.

Radtke, F., Wilson, A., Stark, G., Bauer, M., van Meerwijk, J., MacDonald, H.R., Aguet, M., 1999. Deficient T cell fate specification in mice with an induced inactivation of Notch1. Immunity 10, 547–558.

Reeh, K.A., Cardenas, K.T., Bain, V.E., Liu, Z., Laurent, M., Manley, N.R., Richie, E.R., 2014. Ectopic TBX1 suppresses thymic epithelial cell differentiation and proliferation during thymus organogenesis. Development 141, 2950–2958. http://dx.doi.org/10.1242/dev.111641.

Riddle, R.D., Johnson, R.L., Laufer, E., Tabin, C., 1993. Sonic hedgehog mediates the polarizing activity of the ZPA. Cell 75, 1401–1416.

Rodewald, H.R., 2008. Thymus organogenesis. Annu Rev. Immunol. 26, 355–388.

Shah, D.K., Hager-Theodorides, A.L., Outram, S.V., Ross, S.E., Varas, A., Crompton, T., 2004. Reduced thymocyte development in sonic hedgehog knockout embryos. J. Immunol. 172, 2296–2306.

Shifley, E.T., Vanhorn, K.M., Perez-Balaguer, A., Franklin, J.D., Weinstein, M., Cole, S. E., 2008. Oscillatory lunatic fringe activity is crucial for segmentation of the anterior but not posterior skeleton. Development 135, 899–908. http://dx.doi.org/10.1242/dev.006742.

Stanley, P., Okajima, T., 2010. Roles of glycosylation in Notch signaling. Curr. Top. Dev. Biol. 92, 131–164. http://dx.doi.org/10.1016/S0070-2153(10)92004-8.

Stasiulewicz, M., Gray, S.D., Mastromina, I., Silva, J.C., Björklund, M., Seymour, P.A., Booth, D., Thompson, C., Green, R.J., Hall, E.A., Serup, P., Dale, J.K., 2015. A conserved role for Notch signaling in priming the cellular response to Shh through ciliary localisation of the key Shh transducer Smo. Development 142, 2291–2303. http://dx.doi.org/10.1242/dev.125237.

Su, D., Ellis, S., Napier, A., Lee, K., Manley, N.R., 2001. Hoxa3 and pax1 regulate epithelial cell death and proliferation during thymus and parathyroid organogenesis. Dev. Biol. 236, 316–329.

Subhan, F., Yoon, T.D., Choi, H.J., Muhammad, I., Lee, J., Hong, C., Oh, S.O., Baek, S.Y., Kim, B.S., Yoon, S., 2013. Epidermal growth factor-like domain 8 inhibits the survival and proliferation of mouse thymocytes. Int J. Mol. Med. 32, 952–958. http://dx.doi.org/10.3892/ijmm.2013.1448.

Tomita, K., Hattori, M., Nakamura, E., Nakanishi, S., Minato, N., Kageyama, R., 1999. The bHLH gene Hes1 is essential for expansion of early T cell precursors. Genes Dev. 13, 1203–1210.

van Bueren, K.L., Papangeli, I., Rochais, F., Pearce, K., Roberts, C., Calmont, A., Szumska, D., Kelly, R.G., Bhattacharya, S., Scambler, P.J., 2010. Hes1 expression is reduced in Tbx1 null cells and is required for the development of structures affected in 22q11 deletion syndrome. Dev. Biol. 340, 369–380. http://dx.doi.org/10.1016/j.ydbio.2010.01.020.

Wallin, J., Eibel, H., Neubüser, A., Wilting, J., Koseki, H., Balling, R., 1996. Pax1 is expressed during development of the thymus epithelium and is required for normal T-cell maturation. Development 122, 23–30.

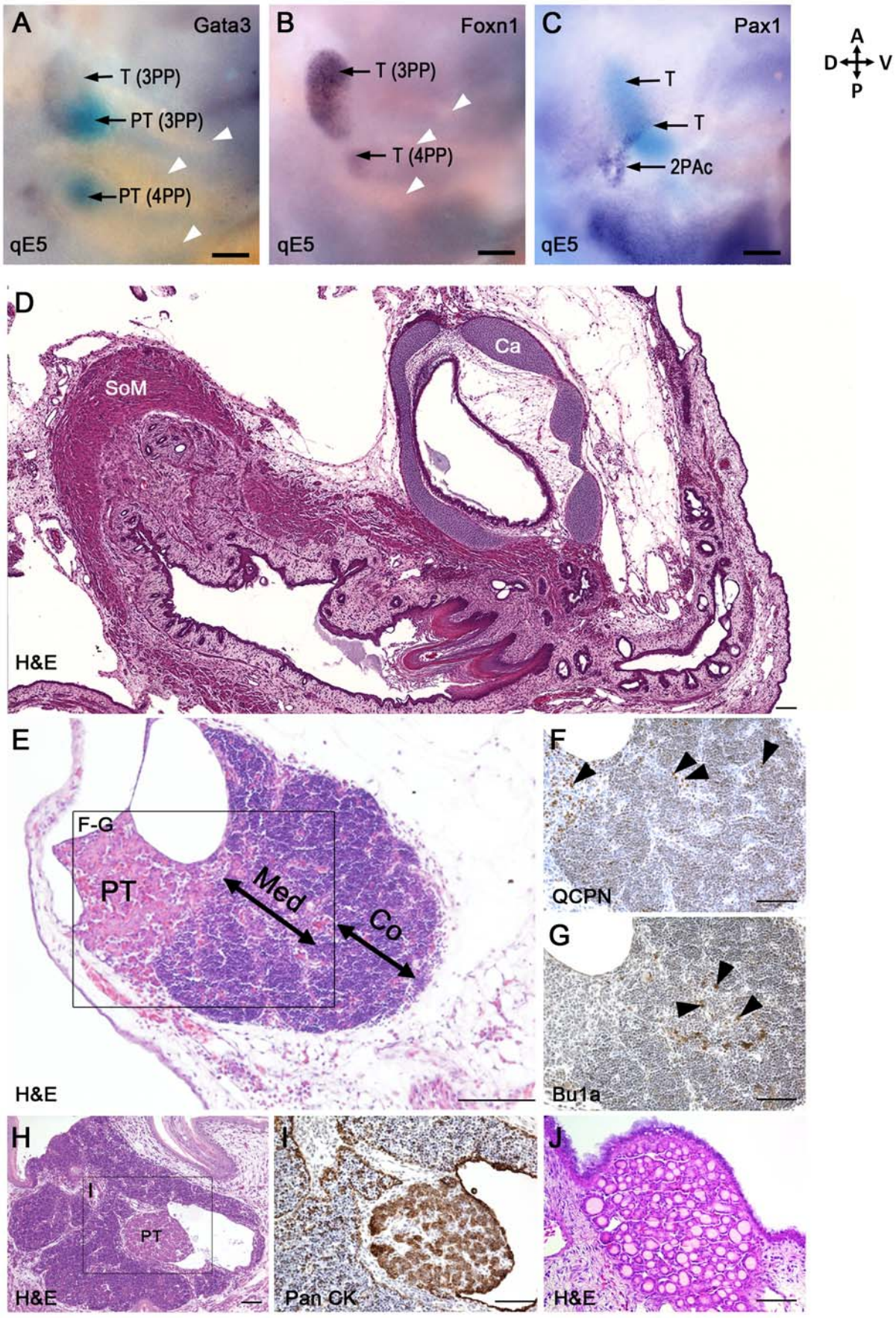
A
Gata3
T (3PP)
PT (3PP)
PT (4PP)
qE5
B
Foxn1
T (3PP)
T (4PP)
qE5
C
Pax1
T
T
2PAc
qE5
A
D
V
P
D
SoM
Ca
H&E
E
F-G
PT
Med
Co
H&E
F
QCPN
G
Bu1a
H
I
PT
H&E
I
Pan CK
J
H&E

Figure S1. Gene expression in the pharyngeal arch region and organ formation in CAM. Expression of *Gata3* (A), *Foxn1* (B) and *Pax1* (C) in quail embryos at E5 detected by WM-ISH. BM purple detection allowed discrimination between more internal (light blue) (parathyroid rudiment in A) and superficial (purple) hybridization signals (thymic rudiment in A). Formation of organs from explants grafted onto CAM and developed *in ovo* for 10 days (D-J). Sections of quail 3/4 PAR explants grown for 48h *in vitro* followed by 10 days *in ovo* development. Single (D and J) and serial sections (E-G and H-I) were processed for H&E staining (D, E, H and J) and immunodetected with anti-QCPN (Developmental Studies Hybridoma Bank; for labelling of quail cells) (F), anti-Bu1a (SouthernBiotech; for labelling B-cells) (G) and anti-Pan CK (I) antibodies counterstained with Gill's hematoxylin (blue staining). Transverse section of distinct "organ-like structures": respiratory mucosa involved by cartilage; gut mucosa, with single and stratified epithelium surrounded by arranged layers of smooth muscle (D). Transverse section of chimeric thymus, with clear discrimination between cortical and medullary compartments (E) and with quail-derived thymic epithelial cells ($QCPN^+$- brown staining) and lymphoid cells of host origin (F). Rare B-cell population in thymic medullary and cortical compartments (G). Transverse section of parathyroid gland (H), with parenchymal cells arranged in clusters (Pan CK^+- brown staining), encircled by capillaries and surrounded by a connective tissue capsule (I). Transverse section of thyroid gland with multiple follicles filled with luminal colloid (J). Black and white arrowheads indicate immunereactive positive cells and pharyngeal arches, respectively. A, anterior; Ca, cartilage; Co, cortex of the thymus; D, dorsal; Med, medulla of the thymus; P, posterior; PAc, pharyngeal arch closure; PT, parathyroid glands; qE, quail embryonic day; SoM, smooth muscle; T, thymus; V, ventral. Scale bars, 50µm (A-C) and 100µm (D-J).

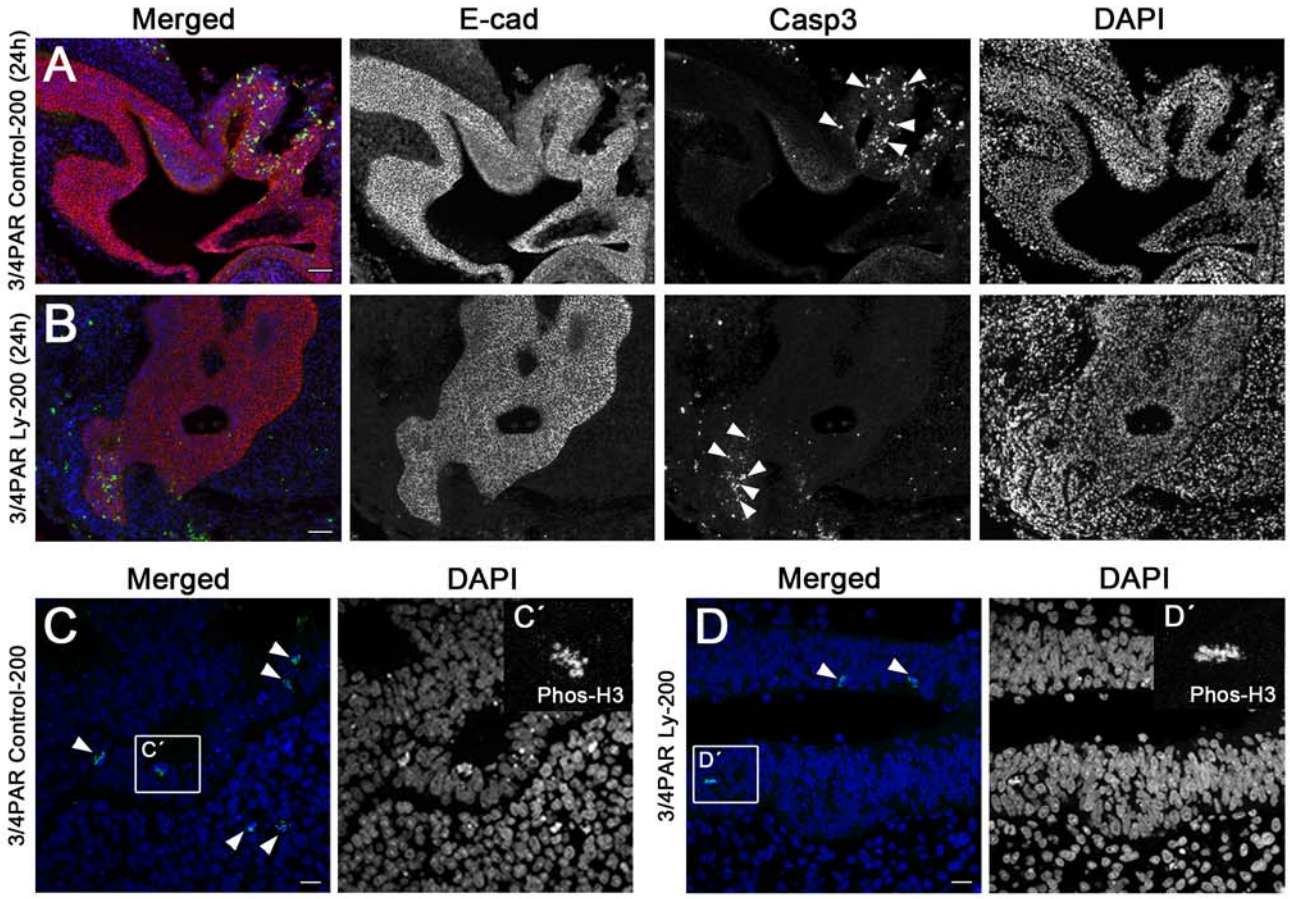

Figure S2. Proliferation and apoptosis of developing 3/4PAR in the absence of Notch signalling. Sections of 3/4PAR grown *in vitro* for 24h (A and B) and 48h (C and D) with DMSO (A and C) and Ly (B and D) were immunostained with anti-E-Cad/anti-Casp3 (A and B) and anti-Phospho-H3 (C and D) counterstained with DAPI. Detail of Phospho-H3 positive cells (C´ and D´). Paraffin sections of 24h-explants were treated for immunofluorescence with the anti-Caspase 3 (Casp3) antibody [anti-cleaved caspase-3 (Asp175) from Cell Signalling, for apoptotic cells] and anti-E-cadherin (E-cad) antibody (BD-610181 from BD Biosciences, for epithelial cells) and counterstained with DAPI, according to the manufacture instructions. Paraffin sections of 48h-explants were treated for immunofluorescence with the Anti-phospho-Histone H3 (Phos-H3) antibody (Anti-phospho-Histone H3 [pSer^{10}], H0412 from Sigma, for mitotic cells) and counterstained with DAPI, according to the manufacture instructions and as described (Neves et al., 2012). Three randomly distributed slides with eight pieces per slide were selected from each explant sample. Three explant samples were analysed per culture condition. In each sample image, a Z-pile of 7.6 µm (0.4µm sections) was collected using the Metamorph Software (Version 7.7.9.0) and Zeiss Axiovert 200M microscope with Roper Scientific HQ CoolSnap camera. Image J Software (version 1.49T) was used for apoptosis/µm^2 and mitoses/µm^2 counting. Immunofluorescence images were acquired with Zeiss LSM 510 META confocal microscope using LSM510 (version 4.0SP2) software. Scale bars, 50µm (A and B) and 10µm (C and D).

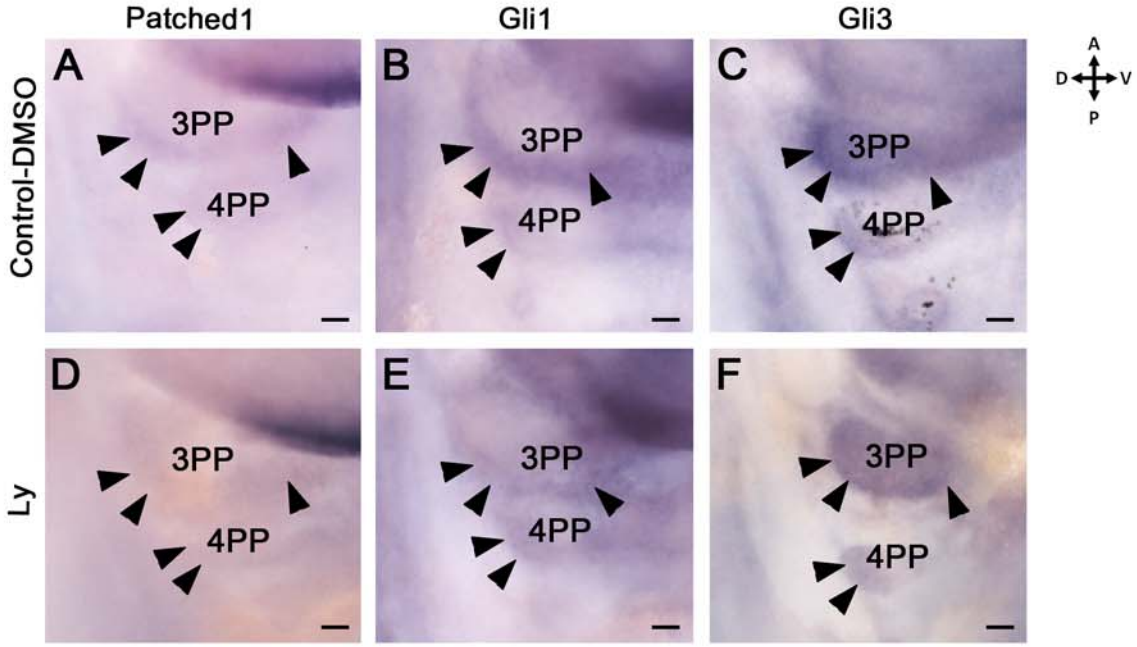

Figure S3. Modulation of Hh-related genes expression in the absence of Notch signalling during T/PT common primordium formation. Expression of *Patched1* (A and D), *Gli1* (B and E) and *Gli3* (C and F) detected by WM-ISH in the 3/4PAR of cE3.5 embryos developed for 20-24h after Ly (D-F) or DMSO (A-C) injection. Black arrowheads point to hybridization signals in the 3/4PP endoderm. A, anterior; D, dorsal; Ly, LY-411.575; P, posterior; PP, pharyngeal pouch; V, ventral. Scale bars, 50μm.

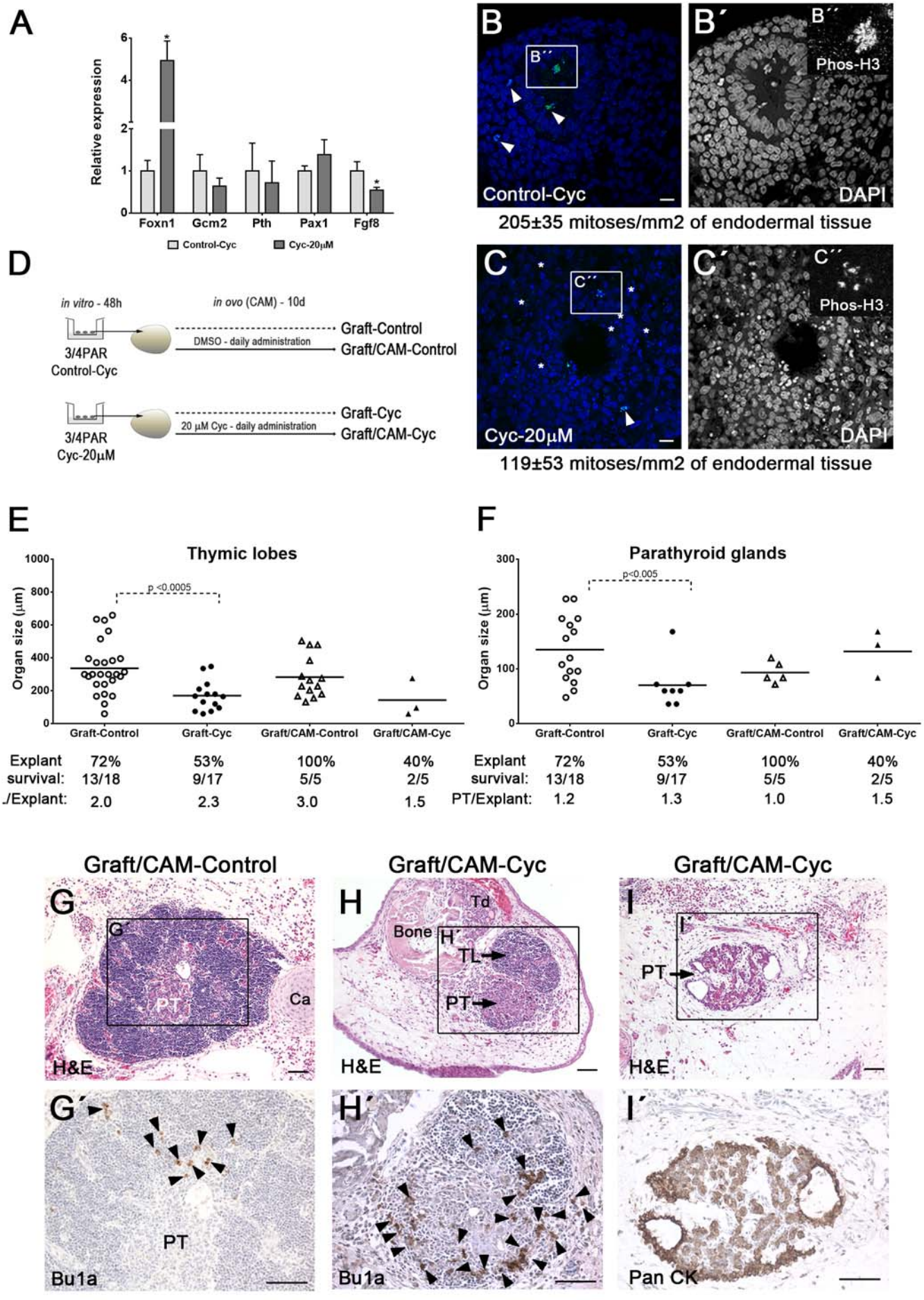
A
Relative expression
Foxn1
Gcm2
Pth
Pax1
Fgf8
Control-Cyc
Cyc-20μM
B
B´
B´´
Phos-H3
Control-Cyc
DAPI
205±35 mitoses/mm2 of endodermal tissue
C
C´
C´´
Phos-H3
Cyc-20μM
DAPI
119±53 mitoses/mm2 of endodermal tissue
D
in vitro - 48h
in ovo (CAM) - 10d
3/4PAR
Control-Cyc
Graft-Control
DMSO - daily administration
Graft/CAM-Control
3/4PAR
Cyc-20μM
Graft-Cyc
20 μM Cyc - daily administration
Graft/CAM-Cyc
E
Thymic lobes
Organ size (μm)
p<0.0005
Graft-Control
Graft-Cyc
Graft/CAM-Control
Graft/CAM-Cyc
Explant survival:
72%
13/18
53%
9/17
100%
5/5
40%
2/5
TL/Explant:
2.0
2.3
3.0
1.5
F
Parathyroid glands
Organ size (μm)
p<0.005
Graft-Control
Graft-Cyc
Graft/CAM-Control
Graft/CAM-Cyc
Explant survival:
72%
13/18
53%
9/17
100%
5/5
40%
2/5
PT/Explant:
1.2
1.3
1.0
1.5
Graft/CAM-Control
Graft/CAM-Cyc
Graft/CAM-Cyc
G
G´
PT
Ca
H&E
H
Td
Bone
H´
TL
PT
H&E
I
I´
PT
H&E
G´
PT
Bu1a
H´
Bu1a
I´
Pan CK

Figure S4. The effect of Hh signalling inhibition in the formation of the thymus and parathyroid glands. For Hh inhibition *in vitro* assay, pharyngeal tissues were grown with 20μM of Cyc and the expression levels of thymic, parathyroid and PP endoderm markers were assessed in cultured tissues by qRT-PCR (each transcript in control=1) (A). Sections of tissues cultured for 48h with DMSO (B and B´) and with 20μM Cyc (C and C´) were immunostained with anti-Phospho H3 antibody counterstained with DAPI. Detail of Phospho-H3 positive cells (B´´ and C´´). Schematic representation of the 3/4PAR grown *in vitro* for 48h in the absence (3/4PAR Control-Cyc) or presence of 20μM Cyc (3/4PAR Cyc-20μM) and further grafted onto CAM of a chicken embryo at E8. Explants were allowed to develop *in ovo* for further 10 days: Graft-Control, explants grown *in vitro* with DMSO; Graft-Cyc, explants grown *in vitro* with Cyc; Graft/CAM-Control, explants grown *in vitro* and *in ovo* with DMSO; Graft/CAM-Cyc, explants grown *in vitro* and *in ovo* with Cyc (D). The sizes of thymic lobes (E) and parathyroid glands (F) formed in CAM-derived explants. Serial sections of Graft/CAM-Control (G and G´) and Graft/CAM-Cyc (H and H´, I and I´) slides were H&E stained (G-I) and immunodetected with anti-Bu1a antibody (G´ and H´) and anti-Pan CK antibody (I´) counterstained with Gill's hematoxylin. Briefly, Graft/CAM-Cyc explants showed a reduction in the number and sizes of thymic lobes along with an augmentation of B-cells (H´). A slight increase in the number and size of parathyroid glands was observed. However, gland hyperplasia was due to expanded mesenchymal spaces along with abnormal epithelial morphology and irregular encapsulation (I´). Expression of each transcript was measured as a ratio against the *Actb* and *Hprt* transcripts mean and expressed in arbitrary units (each transcript in control=1). Ca, cartilage; CAM, chorioallantoic membrane; PAR, pharyngeal arch region; PT, parathyroid glands; TL, thymic lobes; 10d, ten days. White (B and C) and black (G´and H´) arrowheads point immunoreactive positive cells. White asterisks highlight some apoptotic cells (C). Black and white scale bars represent 50μm and 10μm, respectively.

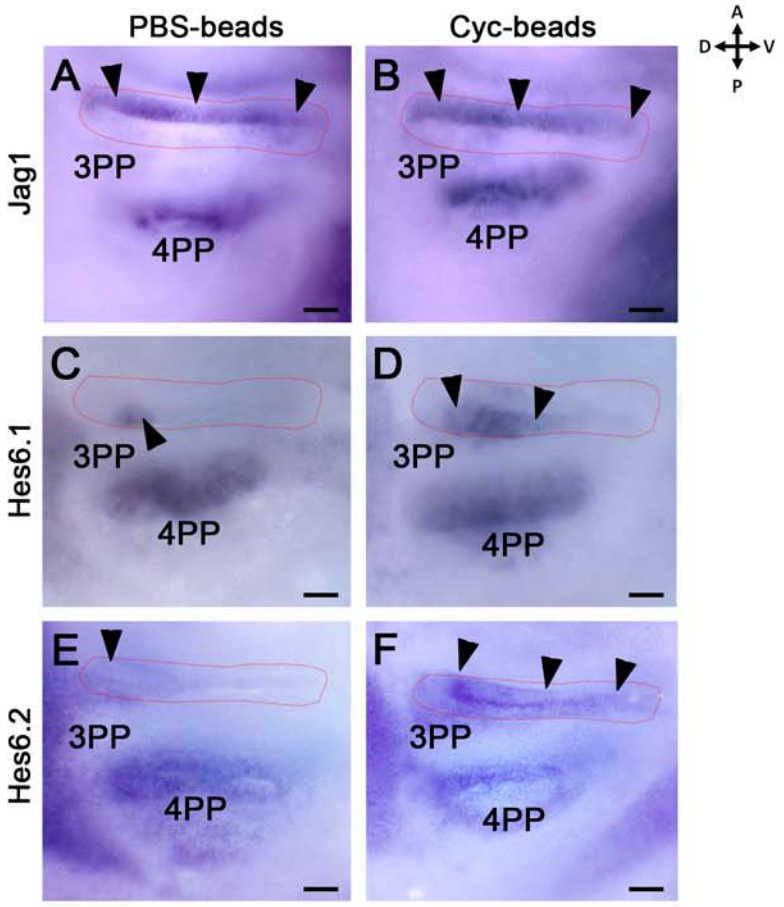

Figure S5. The effect of *in vivo* inhibition of Hh signalling during T/PT common primordium formation. PBS-beads (A, C and E) and Cyc-beads (B, D and F) were implanted in the pharyngeal region of cE2.5 and embryos allowed to develop for further 20-24h. Expression of *Jag1* (A and B), *Hes6.1* (C and D) and *Hes6.2* (E and F) was detected by WM-ISH. Faint red line delimits the 3PP endoderm. Black arrowheads point to strong hybridization signals. A, anterior; cE, chicken embryonic day; Cyc; cyclopamine; D, dorsal; P, posterior; PP, pharyngeal pouch; V, ventral. Scale bars, 50μm.

In Journal of Visualized Experiments 2018, 136, e57114
https://www.jove.com/video/57114/two-step-approach-to-explore-early-late-stages-organ-formation-avian

Two-step Approach to Explore Early- and Late-stages of Organ Formation in the Avian Model: The Thymus and Parathyroid Glands Organogenesis Paradigm.

Marta Figueiredo[1], Hélia Neves[1]

[1]Instituto de Histologia e Biologia do Desenvolvimento, Faculdade de Medicina da Universidade de Lisboa, Edifício Egas Moniz, Piso 3, Ala C, Av. Prof. Egas Moniz, 1649-028 Lisboa, Portugal

SUMMARY

This article provides an updated approach to the classical quail-chicken chimera system to study organ formation, by combining novel *in vitro* and *in ovo* experimental procedures.

ABSTRACT

The avian embryo, as an experimental model, has been of utmost importance for seminal discoveries in developmental biology. Among several approaches, the formation of quail-chicken chimeras and the use of the chorioallantoic membrane (CAM) to sustain the development of ectopic tissues date back to the last century. Nowadays, the combination of these classical techniques with recent *in vitro* methodologies offers novel prospects to further explore organ formation.

Here we describe a two step-approach to study early-and late-stages of organogenesis. Briefly, the embryonic region containing the presumptive territory of the organ is isolated from quail embryos and grown *in vitro* in an organotypic system (up to 48 h). Cultured tissues are subsequently grafted onto the CAM of a chicken embryo. After 10 days of *in ovo* development, fully formed organs are obtained from grafted tissues. This method also allows the modulation of signaling pathways by the regular administration of pharmacological agents and tissue genetic manipulation throughout in vitro and *in ovo* development steps. Additionally, developing tissues can be collected at any time-window to analyze their gene-expression profile (using quantitative PCR (qPCR), microarrays, etc.) and morphology (assessed with conventional histology and immunochemistry).

The described experimental procedure can be used as a tool to follow organ formation outside the avian embryo, from the early stages of organogenesis to fully formed and functional organs.

INTRODUCTION

Avian embryos have been widely used in seminal developmental biology studies. The main advantages of the avian model include the possibility to open the egg, the relatively easy access to the embryo, and the ability to perform micromanipulation. Some examples comprise the classic quail-chicken chimera system for studying cell fate[1], application of specific growth factors to the embryo[2], and the growth of ectopic cellular structures in the CAM[1, 3, 4].

To get new insights into distinct stages of organ formation, we have recently developed a method which combines grafting techniques with *in vitro* manipulation of embryonic tissues[5]. The two-step approach enables the discrimination and exploration of both early- and late-stages of organogenesis, which are often limited due to highly dynamic and complex tissue interactions[2]. Moreover, the lack of suitable tissue-specific markers frequently limits the use of genetically modified animal models[6]. This novel method of the two-step approach largely overcomes such limitations.

To study early-stages of organ formation, in the first step, the quail embryonic territory comprising the prospective organ rudiment is isolated and grown in an *in vitro* organotypic system for 48 h. During this period, pharmacological modulation of specific signalling pathways can be performed by adding drugs to the culture medium[5, 7]. Additionally, cultured tissues can be collected at any stage of *in vitro* growth and probed for gene-expression (using methods as qPCR, microarrays, etc.).

In the second step, 48 h-cultured tissues are then grafted onto the CAM of a chicken (c) embryo at embryonic day (E) 8 (Hamburger and Hamilton (HH)-stages 33–35)[8]. The CAM behaves as a vascular supplier of nutrients and allows gas exchanges[1, 3, 4] to grafted tissues enabling its development *in ovo* for longer periods of time. This experimental step is especially well suited to study late-stages of organogenesis, as fully formed organs can be obtained after 10 days of *in ovo* development[5, 9, 10, 11]. Morphological analysis is easily performed by conventional histology to confirm proper organ formation and donor origin of cells can be identified by immunohistochemistry using species-specific antibodies (*i.e*, MAb Quail PeriNuclear (QCPN)). During the CAM incubation period, grafts can also be grown in the presence of pharmacological agents and collected at any stage of development to evaluate the progression of organogenesis.

The two-step approach, described here in depth, has already been employed in Figueiredo *et al.*[5] to explore the avian parathyroid/thymus common primordium development. Accordingly, the inherent particularities of the embryonic territories and stages of development involved in the organogenesis of the thymus and parathyroid glands will be presented below.

The thymus and parathyroid glands epithelia, though functionally distinct, both derive from the endoderm of the pharyngeal pouches (PP)[12]. In avian, the epithelia of these organs originate from the third and fourth PP endoderm (3/4PP)[12], while in mammals the thymic epithelium derives from the 3PP and the epithelium of parathyroid glands derives from the 3PP and 3/4PP in mouse and human, respectively[13, 14].

One of the earliest stages in the formation of these organs is the emergence of discrete thymus and parathyroid domains in the common primordium. In chicken, these domains can be identified by *in situ* hybridization, with specific molecular markers, at E4.5[15]. As development proceeds, these organ rudiments individualize and separate from the pharynx, while a thin mesenchymal capsule, formed by neural crest-derived cells, surrounds them (at E5; HH-stage 27). Later on, the thymic epithelium is colonized by hematopoietic progenitor cells (at E6.5; HH-stage 30)[12].

As in classical quail-chicken studies[1, 12], the two-step approach is particularly useful to study the formation of hematopoietic/lymphoid organs, namely the thymus[5]. As the quail explant, with the organ rudiment, is grafted in the chicken embryo prior to hematopoietic progenitor cell colonization, a chimeric thymus is formed with chicken blood-borne progenitor cells infiltrating a quail thymic epithelial counterpart. This method is, therefore, a useful tool to explore the contribution of hematopoietic cells in the development of the avian hemato/lymphoid system.

PROTOCOL

All these experiments follow the animal care and ethical guidelines of the Centro Académico Médico de Lisboa.

1. Incubation of Fertilized Quail and Chicken Eggs

1.1) Incubate Japanese quail (*Coturnix coturnix japonica*) and chicken (*Gallus gallus*) fertilized eggs for 3 and 8 days, respectively.

1.1.1) Place the eggs with the air chamber (egg blunt end) facing up in a humidified incubator at 38 °C.

1.1.2) Use around 20 quail eggs and 40 chicken eggs to perform this experiment.

Note: These numbers should be doubled when establishing this procedure for the first time.

2. Isolation of Quail Embryonic Region Containing the Presumptive Territory of Thymic and Parathyroid Rudiments

Note: Perform egg manipulation procedures in sterile conditions using a horizontal laminar flow hood and sterilized instruments and materials.

2.1) Prepare a large borosilicate glass bowl about 3/4 filled with cold phosphate-buffered saline (PBS) solution.

2.2) Open a quail egg after 3 days of incubation by tapping the shell and cutting a circular opening on the opposite side of its blunt end with curved scissors. Carefully remove pieces of shell and transfer the embryo to the glass bowl filled with cold PBS.

2.3) Hold the quail (q) embryo at E3 (qE3) (the quail stage corresponding to the HH-stage 21 of the chicken) with the help of thin forceps. Make a cut into the vitelline membrane enveloping the yolk using curved scissors. Continue to cut around and externally to the circumference of extra-embryonic vessels.

2.4) Transfer the embryo to a small bowl about 3/4 filled with cold PBS with the help of thin forceps. Thoroughly wash the embryo from the remaining attached yolk.

2.5) Use a skimmer to transfer the embryo to a 100 mm glass Petri dish with black base (see **Table of Materials**) containing 10 mL of cold PBS.

2.6) Place the Petri dish under a stereomicroscope.

Note: From this point forward, perform the microsurgery procedures under a stereomicroscope for progressive magnification. As an illumination source, it is advised to use LED lights incorporated in the stereomicroscope or in the optic

fibers, considering the limited heat load.

2.7) Hold the embryo to the bottom of the plate with thin insect pins. Place four pins forming a square shape in the extra-embryonic region.

2.8) Remove the extraembryonic membranes of the cephalic region with the help of thin forceps and place a fifth pin there.

Note: If the embryo is correctly positioned, then the otic vesicle, the heart tube, and the 1st, 2nd, and 3rd pharyngeal arches (PAs) should be visible.

2.9) Dissect the embryonic region of interest, *i.e.*, the 3rd and 4th pharyngeal arch region (3/4PAR), using Wecker eye scissors.

2.9.1) Start cutting longitudinally and parallel to the embryo axis, between the somite/neural tube area and the PAs.

2.9.2) Remove the ventrally positioned heart tube by cutting it. Keeping the scissors in the same position, rotate the Petri dish to reposition the embryo according to the direction of the cut.

2.9.3) Cut between the 2nd and 3rd PAs and below the 4th PA.

2.9.4) Detach the remaining membranes from the 3/4PAR with the help of thin forceps.

2.10) Aspirate the isolated tissues (the 3/4PAR) and transfer them to a glass dish 3/4 filled with cold PBS using a 2 mL sterile plastic pipette.

Note: Hereafter, tissues can be grown *in vitro* up to 48 h or be immediately grafted onto the CAM of a chicken embryo at E8.

2.11) Keep the glass dish containing the isolated 3/4PAR on ice during the preparation of the *in vitro* assay.

3. *In Vitro* Organotypic Assay: Culture of the Embryonic Region Containing the Presumptive Territory of Thymic and Parathyroid Rudiments

3.1) Prepare the culture medium with RPMI-1640 Medium supplemented with 10% FBS and 1% penicillin/streptomycin.

Note: Soluble pharmacological reagents can be added to the medium (for example, LY-411.575 (Ly) and di-benzazepine or cyclopamine and vismodegib, to inhibit Notch and Hedgehog (Hh) signaling pathways, respectively. For this assay, use 50–200 nM of Ly or 5–15 µM of Di-benzazepine to inhibit Notch signaling in the 3/4PAR. Use 20 µM of cyclopamine or with 10 µM of vismodegib to inhibit Hh signaling in the 3/4PAR[5].

3.2) Prepare the *in vitro* culture of the 3/4PP explant in a 6-well plate.

3.2.1) Fill one well from the 6-well plate with 5 mL of culture medium. Place a 24 mm Polycarbonate Membrane Insert (see **Table of Materials**) on the well with the help of thin forceps.

3.2.2) Under the stereomicroscope, transfer the 3/4PAR explant from the glass dish to the membrane surface by gently sliding with the help of a transplantation spoon (or spatula) and thin forceps. Place the explants with the ventral side up and the dorsal side in contact with the membrane. Add up to seven explants per membrane insert. Proceed to step 3.4.

3.3) Alternatively, culture explants in floating membrane filters.

3.3.1) Prepare a 35 mm Petri dish with 5 mL of culture medium. With the help of thin forceps, float a membrane filter (see **Table of Materials**) and keep a dry surface in contact with air.

3.3.2) Under the stereomicroscope, transfer the 3/4PAR explant from the glass dish to the membrane filter by gentle sliding with the help of a transplantation

spoon (or spatula) and thin forceps. Place the explants with the ventral side up and the dorsal side in contact with the membrane. Add up to 8 explants per membrane filter.

3.4) Carefully place the explants prepared in steps 3.2 and 3.3 in a humidified incubator at 37 °C with 5% CO_2.

3.5) After a 48-h incubation period, remove the 6-well plate and the 35 mm Petri dish from the incubator.

3.5.1) Collect the cultured explants from the membrane insert of the 6-well plate.

3.5.1.1) Add PBS at room temperature (RT) to the membrane insert.

3.5.1.2) Detach the explants from the membrane by vigorous flushing using a 2 mL sterile plastic pipette.

3.5.1.3) With the help of the spatula and thin forceps, transfer the cultured explants to a glass dish 3/4 filled with PBS at RT.

3.5.2) Similarly, collect the cultured explants from the floating membrane filter in the 35 mm Petri dish.

3.5.2.1) Transfer the membrane filter with thin forceps to a new 35 mm Petri dish filled with PBS at RT.

3.5.2.2) Detach the explants from the membrane filter by vigorous pipetting using a 2 mL sterile plastic pipette.

3.5.2.3) With the help of thin forceps, discharge the explant-free membrane filter after confirming that no explants remained attached to it.

3.5.2.4) With a spatula and thin forceps, transfer the explants to a glass dish filled with PBS at RT.

3.6) Transfer the cultured explants with a spatula to 1 mL of a reagent for total RNA isolation and use for gene-expression studies.

CAUTION: Exposure to this reagent (see **Table of Materials**) can be a serious health hazard. Wear appropriate protective eyewear, clothing, and gloves. Follow the handling instructions and read the safety data sheets provided by the manufacturer.

3.7) Alternatively, graft the cultured tissues onto CAM of chicken embryos at E8. Follow to step 4.

4. Preparation of the CAM

4.1) Remove the chicken eggs with 8 days of embryonic development from the incubator.

Note: Eggs were incubated with air chamber facing upwards at 38 °C in a humidified incubator.

4.2) Cover the blunt end of the egg with clear plastic tape to prevent pieces of the shell from falling into the air chamber. Tap the shell and cut a circular opening in the egg with curved scissors. The air chamber should be visible.

4.3) Remove with caution the white membrane of the air chamber with thin forceps. CAM is then visible and accessible for ectopic tissue transplantation.

Note: Do not use PBS to hydrate the CAM, before or after transplantation, since PBS promotes sliding and misplacement of the explants. If the membrane dries out, discard the egg.

5. Grafting of Cultured Explants onto the CAM

5.1) Create small vascular lesions/wounds in the smaller vessels of the CAM with

a microscalpel in a holder.

Note: Use the tip of a Pasteur pipette to remove blood by capillarity in the case of excess bleeding.

5.2) Use a spatula and thin forceps to transfer the cultured explant to the wounded area of the CAM.

5.3) Cut a piece of a filter paper slightly larger than the explant and place it on the top of the explant.

Note: The filter paper helps tracking the explant location after its development in the CAM. Also, it allows daily drug delivery to the explant during *in ovo* development, if necessary (described in step 5.6).

5.4) Seal the egg window with clear plastic tape and identify it using a charcoal pencil.

Note: The plastic tape protects the embryo from dehydration during the incubation period.

5.5) Incubate the manipulated egg for 10 days in a humidified incubator at 38 °C. Follow to step 6.

5.6) Optional Step: Daily drug administration during incubation period

5.6.1) To access the filter, partially lift the plastic tape. Add 100 µL of drug solution, drop by drop, on top of the paper. Re-seal the window and place the egg back in the humidified incubator at 38 °C.

Note: For this assay, the dose of 20 µM of cyclopamine will inhibit Hh signaling during *in ovo* development[5].

6. Ectopic Organ Formation in the CAM After 10 Days of *In Ovo* Development

6.1) After 10 days of incubation, remove the egg from the incubator and carefully withdraw the plastic tape.

6.2) Cut the CAM around the filter region using curved scissors and transfer the CAM-derived explant with filter paper to a small glass bowl about 3/4 filled with cold PBS.

6.3) With the help of thin forceps transfer the CAM-derived explant to a 100 mm Petri dish with black base containing 10 mL of PBS. Gently remove the filter paper and the excess of membrane using Wecker eye scissors and thin forceps.

6.4) Transfer the CAM-explant to fixative solution (3.7% PFA in PBS) with a skimmer. Euthanize the chicken embryos without removing them from the egg by making a precise cut in the neck region of the embryo with the help of large scissors.

6.5) Assess the organ formation in paraffin sections of the CAM-derived explants by conventional histology and immunohistochemistry.

RESULTS

The above described protocol details a method that allows the investigation of both early- and late-stages of organogenesis, often limited by complex cellular and molecular interactions. This method was previously employed in Figueiredo *et al.*[5] to unravel the role of Notch and Hedgehog (Hh) signalling in avian thymus/parathyroid common primordium development.

Herein, new results are showed in **Figure 1** and **2**, using the same model of organogenesis. In **Figure 1A** is depicted the experimental design used to explore the early-stages of thymus and parathyroids formation. The quail embryonic

territory comprising the prospective organ rudiments (3/4PAR) was isolated and grown *in vitro* for 48h in a organotypic system.

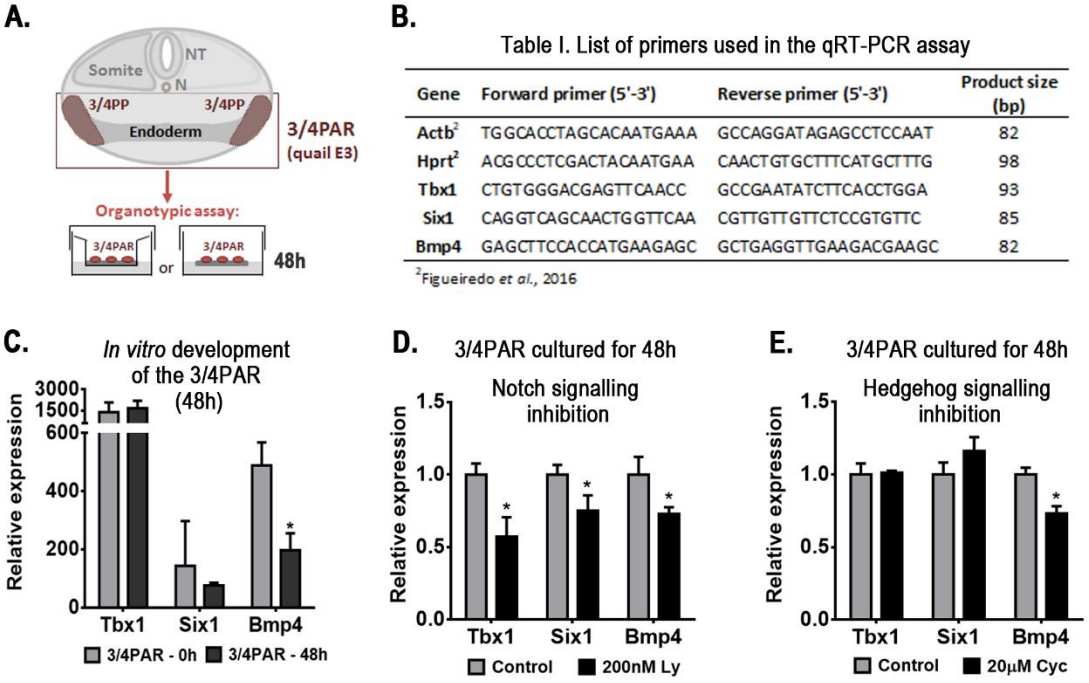

Figure 1. Representative results obtained with the organotypic culture assay: gene-expression analysis of the embryonic region containing the presumptive territories of the thymus and parathyroids (3/4PAR) developed *in vitro* for 48 h. Schematic representation of the transversal section of the embryo at the region of interest and the experimental design (A). Briefly, the 3/4PAR at qE3 was mechanically isolated and grown *in vitro* for 48 h. The expression of the 3/4PAR-related genes, Tbx1, Six1, and Bmp4, was examined by qRT-PCR using the primers in the table (B). The expression of Tbx1, Six1, and Bmp4 was analyzed in freshly isolated (3/4PAR-0 h) and cultured (3/4PAR-48 h) tissues (C). The expression of PAR-related genes was analyzed in tissues grown *in vitro* for 48 h in the presence of 200 nM Ly411575 (D) and 20 μM cyclopamine (E), which are pharmacological inhibitors of Notch and Hedgehog signaling pathways, respectively. Expression of each transcript was measured as a ratio against the mean of the β-actin and hypoxanthine-guaninephosphoribosyltransferase transcript expression levels and expressed in arbitrary units (each transcript in the control = 1). Means and standard deviations were determined with a software for biostatistics analysis and scientific graphic design. Error bars represent standard deviations of the mean. Two-tailed unpaired Student's *t*-test was used and results were considered significantly different when the *p*-value was less than 0.05 ($p < 0.05$). β-actin, Actb; cyclopamine, Cyc; Hypoxanthine-guaninephosphoribosyltransferase, Hprt; LY-411.575, Ly; N, Notocord; NT, Neural Tube; PAR, pharyngeal arch region; PP, pharyngeal pouch.

The expression of genes known to be involved in the formation of PAR structures (PAR-related genes), *i.e.*, Tbx1[16, 17], Six1[18], and Bmp4[15, 17], was evaluated during the normal development. Quantitative real time PCR (qRT-PCR) was performed as previously described[5] (primers are listed in **Figure 1B**). Transcripts of the three genes were detected in freshly isolated (3/4PAR-0 h) and in 48 h-cultured tissues (3/4PAR-48 h) (**Figure 1C**). Only Bmp4 expression levels were significantly decreased after 48 h of culture.

To evaluate the role of Notch and Hh signaling pathways in the early-stages of thymus and parathyroid development, pharmacological inhibitors were added to the culture medium during *in vitro* development. Inhibitor doses are described in Figueiredo *et al.*[5] The expression levels of the three genes analyzed were significantly reduced in the 3/4PAR grown in the presence of Notch inhibitor, when compared to control conditions (without drug) (**Figure 1D**). Conversely, only Bmp4 transcripts were significantly reduced in the 48 h-cultured tissues when Hg signaling was blocked (**Figure 1E**).

To study late-stages of thymus and parathyroid glands organogenesis, cultured tissues were then grafted onto CAMs and allowed to further develop for 10 days (see experimental design in **Figure 2A**).

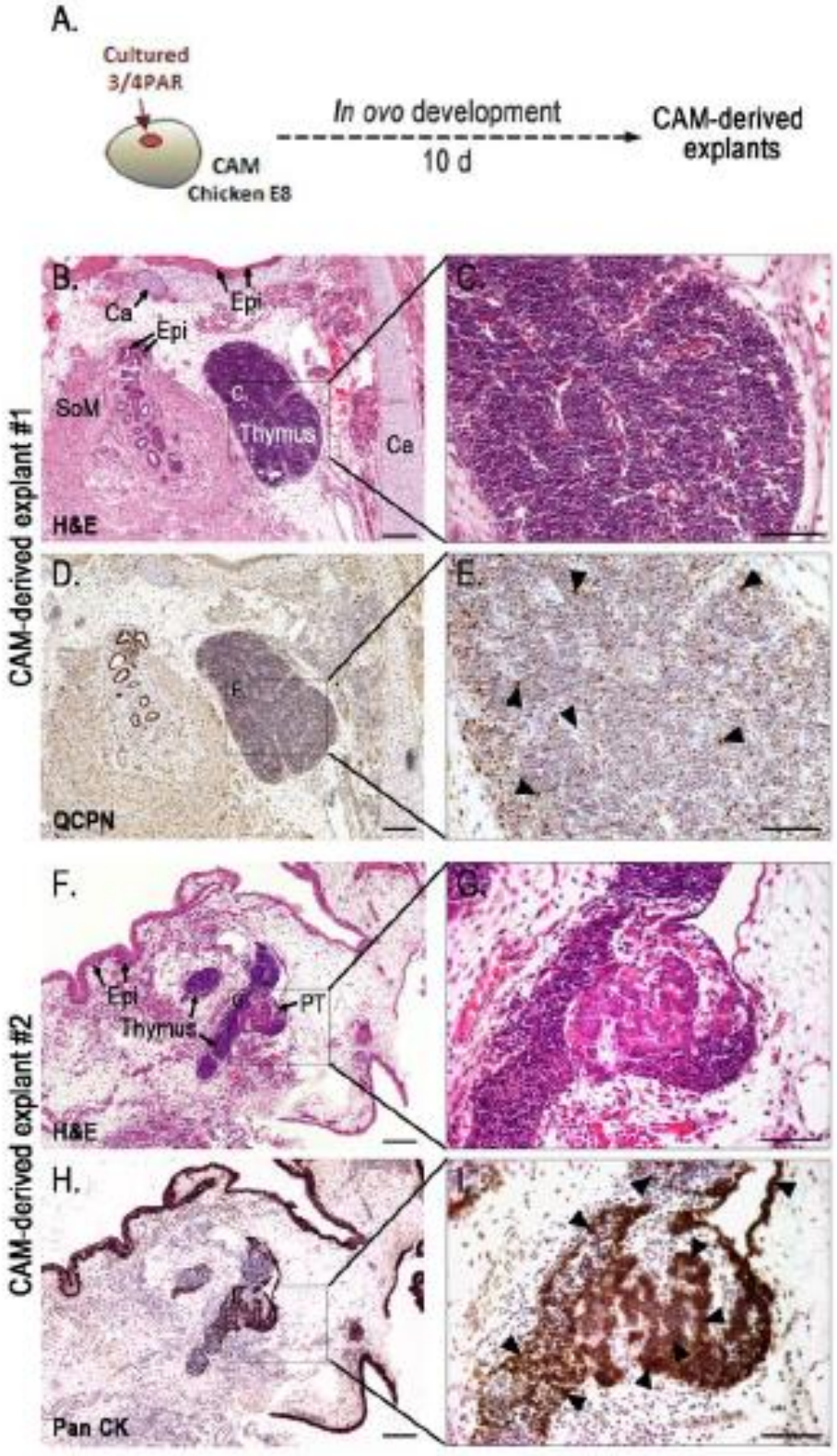

Figure 2. Representative results obtained with the *in ovo* assay: morphological analysis of the grafts grown for 10 days in the chorioallantoic membrane. Schematic representation of 48 h-cultured PAR grafted onto the CAM and developed for a further 10 days (**A**). Serial sections of CAM-derived explants (**B–I**) slides stained with H&E (**B**, **C**, **F**, and **G**) and immunodetected with QCPN (**D** and **E**) and anti-Pan CK (**H** and **I**) antibodies and counterstained with Gill's

hematoxylin. Black arrow heads indicate strong immunostaining for QCPN (**E**) and Pan CK (**I**). A transverse section of a chimeric thymus with lymphoid cells of host origin and quail-derived thymic epithelial cells with strong QCPN$^+$ signals (black arrowheads) (**E**). Strong pan-CK$^+$ signals (black arrowheads) in the epithelia of the thymus and parathyroid glands (**I**). Images were collected using imaging software and a microscope with a camera (see **Table of Materials**). Ca, cartilage; CAM, chorioallantoic membrane; Epi, epithelium; PAR, pharyngeal arch region; PT, parathyroid glands; SoM, smooth muscle; 10 d, ten days. Scale bars, 50 µm (**B**, **D**, **F**, and **H**) and 100 µm (**C**, **E**, **G**, and **I**).

Morphological analysis of organs developing on CAM-derived explants was performed by conventional histology and immunohistochemistry (**Figure 2B–I**), as previously described[5]. CAM-derived explants showed fully formed chimeric thymus (**Figure 2B–E**) with quail-derived (QCPN$^+$) thymic epithelium colonized by lymphoid progenitor cells of donor origin (chicken) (**Figures 2D, E**). Serial sections of CAM-derived explants further processed for immunocytochemistry with anti-pan cytokeratin (anti-pan CK) antibody (an epithelial cell marker), showed thymic and parathyroid epithelia with normal morphological features (**Figure 2H, I**). The thymic epithelial cells displayed a reticular architecture while parathyroid parenchymal cells were globular, arranged in clusters and encircled by numerous capillaries. Additionally, other PAR-derived structures from the respiratory apparatus could be observed in the grafts. Cartilage, respiratory epithelium, and smooth muscle associated to the mucosa were easily distinguished in **Figure 2B**.

DISCUSSION

A crucial aspect for the success of this method is the quality of both the chicken and quail eggs. Considering the long incubation periods, particularly during the *in ovo* assay, a good quality of chicken eggs improves viability rates (up to 90%) by the end of the procedure. To achieve this, test eggs from different suppliers. Incubate unmanipulated eggs for long periods (up to 16–17 days) and check their development. To be considered a good quality batch, more than 80% of the embryos should present normal development. It is also important to ensure that

each incubation step provides reproducible synchronous developmental stages to guarantee reliable and truly representative results at the end. Due to egg shell porosity, maintain a humidified atmosphere in the incubator for all egg incubation steps. To avoid environmental contamination, antibiotics can be added to the PBS solutions in the procedure (optional step).

This method starts by isolating quail organ rudiments and growing them in an organotypic system for 48 h. This first-step, already used to study thymus and parathyroid early-development[5], can also be applied to other organs if the assay limitations are taken into account. Small explants of organ rudiments (less than 3 mm) and short periods of *in vitro* incubation (up to 48 h) are advised to prevent inefficient diffusion of nutrients and drying of the tissues, which usually occurs when explants reach larger dimensions.

This method also allows the modulation of signaling pathways, which bypasses complex genetic manipulation by the use of soluble reagents, such as pharmacological inhibitors[5,7]. For this procedure, increasing doses of the drug should be tested to identify the physiological/toxic culture conditions. The inhibitory actions can be measured by gene expression analysis of the signaling pathway target-genes.

In step-two of this procedure, cultured tissues are grafted onto the CAM to study the late-stages of organ formation. The CAM assay has been used in other contexts of organogenesis like skeletal development and feather formation by direct grafting of the organ rudiments onto CAM[9, 10, 11]. Additionally, CAM engraftment was also successfully applied in mice-into-chicken xenografts to study testes maturation[19]. Although the CAM assay is a powerful research tool to study late-stages of organ formation, it is important to be aware of its limitations. One of the most critical steps of the protocol is the CAM preparation for grafting. It is important to target only the smaller vessels for vascular lesions. However, if only a few of those are lesioned, the subsequent angiogenic response may not be sufficient to promote invasion of grafted tissues by new vessels originating from the CAM. Consequently, the transplanted tissues will not have enough nutrients or gas exchanges to sustain growth. On the other hand, if the integrity of large vessels is compromised when preparing the wounded area, the embryo has to be discarded.

An important limitation of *in ovo* development using the CAM is the anatomical displacement of formed organs, due to three-dimensional constraint of growing explants. This often results in the incomplete separation of thymus and parathyroid glands (**Figure 2F–I**), and in inadequate thymic segmentation, with reduction of the normal number of organs formed[5].

Another constraint of the CAM system may be a sub-optimal accessibility of pharmacological reagents[5], even with daily drug administration, thus limiting the analysis of explant late-stage development. As an example, previous studies showed that cyclopamine successfully inhibit Hh signaling *in ovo*, while Notch signaling inhibitor, Ly411575, showed no inhibitory properties *in ovo*[5].

Beyond these limitations, this method provides important experimental approaches to investigate the early- and late-stages of organ formation using the avian model. In addition, developing tissues can be manipulated and harvested at any time-window of the *in vitro* and *in ovo* development making the method also suitable for longitudinal studies in organogenesis.

DISCLOSURES

The authors have nothing to disclose.

ACKNOWLEDGMENTS

The authors are grateful to António Cidadão, Isabel Alcobia, and Leonor Parreira for the critical reading of the manuscript, to Padma Akkapeddi for video narration, and to Vitor Proa from the Histology Service of the Instituto de Histologia e Biologia do Desenvolvimento, Faculdade de Medicina de Lisboa, Universidade de Lisboa, for technical support. We are particularly indebted to Paulo Caeiro and Hugo Silva from the Unidade de audiovisuais (Audiovisual Unit), Faculdade de Medicina de Lisboa, Universidade de Lisboa for their outstanding commitment to the production of this video. We acknowledge Leica Microsystems for kindly providing a stereoscope equipped with video system and to Interaves - Sociedade Agro-Pecuária, S.A for contributing with quail fertilized eggs. This

work was supported by Faculdade de Medicina de Lisboa, Universidade de Lisboa (FMUL).

MATERIALS

Name	Company	Catalogue Number	Comments
Chicken fertilized eggs (*Gallus gallus*)	Pintobar, Portugal		Poultry farm
Quail fertilized eggs (*Coturnix coturnix*)	Interaves, Portugal		Bird farm
15 mL PP centrifuge tubes	Corning	430052	
50 mL PP centrifuge tubes	Corning	430290	
60 x 20 mm pyrex dishes	Duran group	21 755 41	
100 x 20 mm pyrex dishes	Duran group	21 755 48	
Polycarbonate Membrane Insert	Corning	3412	24 mm transwell with 0.4 mm Pore Polycarbonate Membrane Insert
Membrane filter	Millipore	DTTP01300	0.6 mm Isopore membrane filter
6-well culture plates	Nunc, Thermo Fisher Scientific	140675	
Petri dish, 35 x 10 mm	Sigma-Aldrich	P5112	
Pyrex bowls			From supermarket
Transfer pipettes	Samco Scientific, Thermo Fisher Scientific	2041S	2 mL plastic pipet
Glass pasteur pipette	Normax	5426015	
Whatman qualitative filter paper	Sigma-Aldrich	WHA1001090	Filter paper
Clear plastic tape			From supermarket
Cytokeratin (pan; acidic and basic, type I and II cytokeratins), clone Lu-5	BMA Biomedicals	T-1302	
Cyclopamine hydrate	Sigma-Aldrich	C4116	Pharmacological inhibitor of Hh signalling
Fetal Bovine Serum	Invitrogen, Thermo Fisher Scientific		Standart FBS
Paraformaldehyde	Sigma-Aldrich	P6148	
Penicillin-Streptomycin	Invitrogen, Thermo Fisher Scientific	15140-122	
Phosphate-Buffered Saline (PBS)	GIBCO, Thermo Fisher Scientific	10010023	
QCPN antibody	Developmental Studies Hybridoma Bank	QCPN	

RPMI 1640 Medium, GlutaMAX Supplement	GIBCO, Thermo Fisher Scientific	61870010	
Bluesil RTV141A/B Silicone Elastomer 1.1Kg Kit	ELKEM/Silmid	RH141001KG	To prepare the back base for petri dish
Stemolecule LY411575	Stemgent	04-0054	Pharmacological inhibitor of Notch signalling
TRIzol Reagent	Invitrogen, Thermo Fisher Scientific	15596026	Reagent for total RNA isolation
Dumont #5 Forceps	Fine Science Tools	11251-30	Thin forceps
Extra fine Bonn scissors, curved	Fine Science Tools	14085-08	Curved scissors
Insect pins	Fine Science Tools	26001-30	
Micro spatula	Fine Science Tools	10087-12	Transplantation spoon
Minutien Pins	Fine Science Tools	26002-20	Microscalpel
Moria Nickel Plated Pin Holder	Fine Science Tools	26016-12	Holder
Moria Perforated Spoon	Fine Science Tools	10370-17	Skimmer
Wecker Eye Scissor	Fine Science Tools	15010-11	
Camera	Leica Microsystems	MC170 HD	
Stereoscope	Leica Microsystems	Leica M80	
Microscope	Leica Microsystems	DM2500	

REFERENCES

1. Le Douarin, N.M. The Nogent Institute–50 years of embryology*. Int J Dev Biol.* **49** (2-3), 85–103 (2005).

2. Chuong, C.M., Wu, P., Plikus, M., Jiang, T.X., Bruce Widelitz, R. Engineering stem cells into organs: topobiological transformations demonstrated by beak, feather, and other ectodermal organ morphogenesis. *Curr Top Dev Biol.* **72**, 237-274 (2006).

3. Davey, M.G., Tickle, C. The chicken as a model for embryonic development. *Cytogenet Genome Res.* **117** (1-4), 231-239 (2007).

4. Nowak-Sliwinska, P., Segura, T., Iruela-Arispe, M.L. The chicken chorioallantoic membrane model in biology, medicine and bioengineering. *Angiogenesis.* **17** (4), 779-804, doi: 10.1007/s10456-014-9440-7 (2014).

5. Figueiredo, M.*, Silva, J.C.*, *et al.* Notch and Hedgehog in the thymus/parathyroid common primordium: Crosstalk in organ formation. *Dev Biol*. **418** (2), 268–282, doi: 10.1016/j.ydbio.2016.08.012 (2016). *First co-authors

6. National Research Council. *Scientific Frontiers in Developmental Toxicology and Risk Assessment.* Chapter 6 - Recent Advances in Developmental Biology. Washington, DC: The National Academies Press, doi: 10.17226/9871 (2000).

7. Moura, R.S., Coutinho-Borges, J.P., Pacheco, A.P., Damota, P.O., Correia-Pinto, J. FGF signalling pathway in the developing chick lung: expression and inhibition studies. *PLoS One.* **6** (3), e17660, doi: 10.1371/journal.pone.0017660 (2011).

8. Hamburger, V., Hamilton, H. A series of normal stages in the development of the chick embryo. *J. Morphol.* **88**, 49–92 (1951).

9. Takahashi, Y., Bontoux, M., Le Douarin, N.M. Epithelio-mesenchymal interactions are critical for Quox 7 expression and membrane bone differentiation in the neural crest derived mandibular mesenchyme. *EMBO J.* **10** (9), 2387-2393 (1991).

10. Maeda, Y., Noda, M. Coordinated development of embryonic long bone on chorioallantoic membrane *in ovo* prevents perichondrium-derived suppressive signals against cartilage growth. *Bone.* **32** (1), 27-34 (2003).

11. Ishida, K., Mitsui, T. Generation of bioengineered feather buds on a reconstructed chick skin from dissociated epithelial and mesenchymal cells. *Dev Growth Differ.* **58** (3), 303-142016. doi: 10.1111/dgd.12275 (2016).

12. Le Douarin, N.M., Jotereau, F. Tracing of cells of the avian thymus trough embryonic life in interspecific chimeras. *J. Exp. Med.* **142**, 17-40 (1975).

13. Farley, A.M., *et al*. Dynamics of thymus organogenesis and colonization in early human development. *Development*. **140**, 2015-2026, doi: 10.1242/dev.087320 (2013).

14. Gordon, J., Bennett, A.R., Blackburn, C.C., Manley, N.R. Gcm2 and Foxn1 mark early parathyroid- and thymus-specific domains in the developing third pharyngeal pouch. *Mech Dev.* **103**, 141-143 (2001).

15. Neves, H., Dupin, E., Parreira, L., Le Douarin, N.M. Modulation of Bmp4 signalling in the epithelial–mesenchymal interactions that take place in early thymus and parathyroid development in avian embryos. *Dev Biol*. **361** (2), 208–219, doi: 10.1016/j.ydbio.2011.10.022 (2012).

16. Jerome, L.A., Papaioannou, V.E. DiGeorge syndrome phenotype in mice mutant for the T-box gene, Tbx1. *Nat Genet.* **27** (3), 286-291 (2001).

17. Nie, X., Brown, C.B., Wang, Q., Jiao, K. Inactivation of Bmp4 from the Tbx1 expression domain causes abnormal pharyngeal arch artery and cardiac outflow tract remodeling. *Cells Tissues Organs.* **193** (6), 393-403, doi: 10.1159/000321170 (2011).

18. Zou, D., Silvius, D., Davenport, J., Grifone, R., Maire, P., Xu, P.X. Patterning of the third pharyngeal pouch into thymus/parathyroid by Six and Eya1. *Dev Biol.* **293** (2), 499-512 (2006).

19. Uematsu, E., *et al*. Use of *in ovo* chorioallantoic membrane engraftment to culture testes from neonatal mice. *Comp Med.* **64** (4), 264-269 (2014).

In Journal of Visualized Experiments 2019, 144, e58965
https://www.jove.com/video/57114/two-step-approach-to-explore-early-late-stages-organ-formation-avian

Isolation of Embryonic Tissues and Formation of Quail-Chicken Chimeric Organs Using The Thymus Example.

Marta Figueiredo[1], Hélia Neves[1]

[1]Instituto de Histologia e Biologia do Desenvolvimento, Faculdade de Medicina da Universidade de Lisboa, Edifício Egas Moniz, Piso 3, Ala C, Av. Prof. Egas Moniz, 1649-028 Lisboa, Portugal

SUMMARY

This article provides a method to isolate pure embryonic tissues from quail and chicken embryos that can be combined to form ex vivo chimeric organs.

ABSTRACT

The capacity to isolate embryonic tissues was an essential step for establishing the quail-chicken chimera system, which in turn has provided undisputed contributions to unveiling key processes in developmental biology.

Herein is described an optimized method to isolate embryonic tissues from quail and chickens by microsurgery and enzymatic digestion while preserving its biological properties. After isolation, tissues from both species are associated in an *in vitro* organotypic assay for 48h. Quail and chicken tissues can be discriminated by distinct nuclear features and molecular markers allowing the study of the cellular cross-talk between heterospecific association of tissues. This

approach is, therefore, a useful tool for studying complex tissue interactions in developmental processes with highly dynamic spatial modifications, such as those occurring during pharyngeal morphogenesis and the formation of the foregut endoderm-derived organs. This experimental approach was first developed to study the epithelial-mesenchymal interactions during early-stages of thymus formation. In this, the endoderm-derived prospective thymic rudiment and mesoderm-derived mesenchyme were isolated from quail and chicken embryos, respectively.

The capacity of the associated tissues to generate organs can be further tested by grafting them onto the chorioallantoic membrane (CAM) of a chicken embryo. The CAM provides nutrients and allows gas exchanges to the explanted tissues. After 10 days of *in ovo* development, the chimeric organs can be analysed in the harvested explants by conventional morphological methods. This procedure also allows studying tissue-specific contributions during organ formation, from its initial development (*in vitro* development) to the final stages of organogenesis (*in ovo* development).

Finally, the improved isolation method also provides three-dimensionally (3D) preserved embryonic tissues, that can also be used for high-resolution topographical analysis of tissue-specific gene-expression patterns.

INTRODUCTION

In the early 1970s, an elegant quail-chicken chimera system was developed by Le Douarin, opening new avenues to understand the role of cell migration and cellular interactions during development[1,2]. The model was devised on the premise that cell exchange between the two species would not significantly disturb embryogenesis, later confirmed when used to study numerous developmental processes, including the formation of the nervous and the hematopoietic systems[1]. Taking the latter as an example, the cyclic waves of hematopoietic progenitors colonizing the thymic epithelial rudiment was first observed using the quail-chicken chimera system[3]. For that, the prospective

territory of the thymus, the endoderm of the third and fourth pharyngeal pouches (3/4PP), was mechanically and enzymatically isolated from quail (q) embryos at 15 to 30- somite stage [embryonic day (E) 1.5- E2.5]. These stages correspond to chicken Hamburger and Hamilton4 (HH) - stages 12-17. The isolation procedures started with the use of trypsin to enzymatically dissociate the endoderm from the attached mesenchyme. The isolated endoderm was grafted into the somatopleura region of a host chicken (c) embryo at E3-E3.5 (HH-stages 20-21). This heterologous mesenchyme was considered "permissive" to thymic epithelium development contributing also to the organ formation[3]. Afterward, successive waves of chicken host blood-borne progenitor cells infiltrated the quail donor thymic epithelial counterpart contributing to thymus formation in the host embryo[3].

More recently, a modified version of this approach was also proven to be important for studying epithelial-mesenchymal interactions during early stages of thymus formation[5]. In this respect, the tissues involved in the formation of the ectopic thymus in chimeric embryos[3] were isolated, both from donor and host embryos, and associated ex vivo. An improved protocol was used to isolate the quail 3/4PP endoderm (E2.5-E3) and the chicken somatopleura mesoderm (E2.5-E3). Briefly, embryonic tissues were isolated by microsurgery and subject to *in vitro* pancreatin digestion. Also, the conditions of enzymatic digestion, temperature and time of incubation were optimized according to tissue-type and developmental stage (**Table 1**).

Next, the isolated tissues were associated in an organotypic *in vitro* system for 48 h, as previously reported[5,6]. The *in vitro* association of tissues mimics the local cellular interactions in the embryo, overcoming some restrictions of the *in vivo* manipulation. This system is particularly useful to study cellular interactions in complex morphogenic events, such as the development of the pharyngeal apparatus.

The contribution of each tissue in thymus histogenesis, as well as the ability of the heterospecific association to generate a thymus can be further explored using the CAM methodology, previously detailed[5,7,8]. Succinctly, the cultured tissues were grafted onto the CAM of cE8 embryos and allowed to develop *in ovo* for 10

days. Then, thymus formation was evaluated by morphological analysis in the harvested explants. As in the classical quail-chicken studies[3], the quail thymic epithelium was colonized by hematopoietic progenitor cells (HPCs) derived from the chicken embryo, which was later shown to contribute to organ development[9,10]. The HPCs migrated from the embryo to the ectopic chimeric thymus through the highly vascularized CAM[5,7,8]. Quail derived thymic epithelium can be identified by immunohistochemistry using species-specific antibodies (i.e., QCPN- MAb Quail PeriNuclear), overcoming the need for tissue-specific molecular markers.

This experimental method, as the two-step approach reported in previous publication[8], allows the modulation of signalling pathways by regular administration of pharmacological agents during *in vitro* and *in ovo* development. Also, explants can be harvested at any time-point of the course of the experiment[8].

Lastly, the isolation protocol here detailed allows the preservation of the natural properties and 3D-architecture of embryonic tissues, particularly useful for detailing *in situ* gene-expression patterns of embryonic territories otherwise inaccessible by conventional methods. In addition, transcriptome analysis approaches, including RNA-seq or microarrays, can also be applied in isolated tissues without requiring genetic markers while providing a tissue-specific high throughput "omics" analysis.

PROTOCOL

All these experiments follow the animal care and ethical guidelines of the Centro Académico Médico de Lisboa.

1. Fertilized quail and chicken egg incubation

1.1) Place fertilized eggs of Japanese quail (*Coturnix coturnix japonica*) in a 38 °C humidified incubator for 3 days. Incubate the eggs (egg blunt end) facing up in the air chamber.

Note: The humidified environment is achieved by placing a water container at the bottom of the incubator.

1.2) Incubate fertilized eggs of chicken (*Gallus gallus*) for 2.5 days in a 38 °C humidified incubator. Incubate the eggs in a horizontal position and mark the upper side using a piece of charcoal to identify the embryo location.

Note: Start with 40 quail eggs and 60 chicken eggs when establishing this experiment.

2. Isolation of quail endoderm containing the prospective domain of the thymic rudiment

Note: Use a horizontal laminar flow hood and sterilized instruments and materials for egg manipulation procedures in sterile conditions.

2.1) Remove the embryonic region containing the presumptive territory of thymic rudiment, the pharyngeal arch region containing the 3rd and 4th arches (3/4PAR), as described[7,8].

2.1.1) Fill a large borosilicate glass bowl (100 mm x 50 mm; 100 cm^3) with 60 mL of cold phosphate-buffered saline solution (PBS).

2.1.2) With the help of curved scissors, tap and cut a circular hole in the shell of a quail egg that has been incubated for 3 days. Make the hole on the opposite side of the egg blunt and transfer the yolk (with the embryo) to the bowl with cold PBS.

2.1.3) Remove the embryo from the yolk by cutting the vitelline membrane externally to extra-embryonic vessels using curved scissors.

2.1.4) With the help of thin forceps, transfer the embryo to a small bowl (60 mm x 30 mm; 15 cm^3) filled with 10 mL of cold PBS.

2.1.5) With a skimmer, move the embryo to a 100 mm Petri dish with a black base (see **Table of Materials**) containing 10 mL of cold PBS and place it under a stereomicroscope.

2.1.6) Dissect the 3/4PAR, as previously described[8].

2.1.7) Aspirate the 3/4PAR and transfer to a glass dish three-quarters filled with cold PBS using a 2 mL sterile Pasteur pipette.

2.2) Isolate the endoderm containing the presumptive territory of thymic rudiment (the 3/4PP endoderm) by enzymatic digestion with pancreatin.

2.2.1) With the help of spatula and thin forceps, transfer the 3/4PAR to a glass dish three-quarters filled with cold pancreatin (8 mg/mL; 1:3 dilution 25 mg/mL with cold PBS).

2.2.2) Incubate for 1h on ice for enzymatic digestion.

Note: The time of enzymatic digestion depends of the stage of development (**Table 1**).

2.2.3) Place the glass dish under the stereomicroscope (40x-60x magnification) to isolate the endoderm from the 3/4PAR.

Note: Keep all surfaces and solutions cold during this procedure. Change to a new cold pancreatin solution if taking a long time to dissect the tissues (>15 min). As an illumination source, use LED lights incorporated in the stereomicroscope or in the optic fibres, considering the limited heat load.

2.2.4) To isolate the endoderm from the surrounding tissues use stainless steel microscalpels in pin holders.

Note: Use microscalpels with a diameter between 0.1 mm and 0.2 mm and nickel pin holders with a jaw opening diameter of 0 mm to 1 mm.

2.2.4.1) First remove the neural tube and mesoderm attached to the dorsal surface of the pharyngeal endoderm.

2.2.4.2) With the dorsal side up, carefully detach and remove the mesenchyme between the pharyngeal arches and expose the pharyngeal pouches. Perform this procedure on both sides of the 3/4PAR.

2.2.4.3) Remove the heart tube and the mesenchyme surrounding the anterior pouches.

2.2.4.4) With the ventral side up, cut the ectoderm of the 2nd and 3rd pharyngeal arches and carefully remove the mesenchyme attached to the pouches. Repeat this procedure on the other side of the 3/4PAR. At this stage the thyroid rudiment should be visible.

2.2.4.5) Remove any remaining mesenchymal cells attached to the pharyngeal endoderm with the two microscalpels.

2.2.4.6) Make a transversal cut between the 2nd and 3rd PP, dissociating the pharyngeal endoderm containing the 3rd and 4th pouches from the anterior part of the endoderm having the thyroid rudiment and 2nd pharyngeal pouch.

2.2.4.7) With the help of spatula and thin forceps, transfer the isolated 3/4PP endoderm to a glass dish three-quarters filled with 100% cold fetal bovine serum (FBS).

2.3) Keep the glass dish with the isolated tissues on ice during the preparation of *in vitro* assay. Alternatively, the isolated tissues can be three-dimensionally preserved and *in situ* analysed for gene-expression.

3. Isolation of chicken somatopleura mesoderm

Note: Perform egg manipulation procedures in sterile conditions using a horizontal laminar flow hood and sterilized instruments and materials.

3.1) Remove the embryonic territory containing the somatopleura mesoderm at the level of somites 19-24 (ss19-24).

3.1.1) Remove the chicken egg from the incubator after 2.5 days of incubation.

3.1.2) With curved scissors, open a small hole in the shell. Insert a needle and aspirate 2 mL of albumin with a 10 mL syringe to lower albumin volume inside the egg and prevent damage of the embryo (located below the marked region of the shell). Discard the aspirated albumin.

3.1.3) Cut a circular hole (up to two-thirds of the top surface area) in the marked region of the shell using curved scissors.

3.1.4) Cut the vitelline membrane externally to the extraembryonic vessels while holding the embryo with thin forceps.

3.1.5) Under a stereomicroscope, place the embryo in a 100 mm Petri dish with a black base containing 10 mL of cold PBS.

Note: Use a stereomicroscope from this point forward for progressive magnification of microsurgery procedures.

3.1.6) Use four thin insect pins to hold the embryo to the bottom of the plate. Place the pins in the extraembryonic region forming a square shape.

3.1.7) Perform two cuts between the somites 19 and 24 transversely to the embryo axis and crossing all embryo territory, using wecker eye scissors.

3.1.8) Release the embryo section, ss19-24, by cutting marginal embryonic edges.

3.1.9) Aspirate the ss19-24 tissues and transfer to a glass dish three-quarters filled with cold PBS using a 2 mL sterile Pasteur pipette.

3.2) Isolate the lateral mesoderm from somatopleura region (ss19-24) by enzymatic digestion with pancreatin (8 mg/mL; 1:3 dilution 25 mg/mL with cold PBS).

3.2.1) With the help of spatula and thin forceps, transfer the ss19-24 tissues to a glass dish three-quarters filled with cold pancreatin solution.

3.2.2) Incubate for 30 min on ice for enzymatic digestion.

3.2.3) Under the stereomicroscope, isolate the mesoderm from the surrounding tissues using two microscalpels in a holder.

Note: Keep all surfaces and solutions cold during this procedure. Change to a new cold pancreatin solution if taking a long time to dissect the tissues (>10 min). As an illumination source, use LED lights incorporated in the stereomicroscope or in the optic, considering the limited heat load.

3.2.4) During mesoderm isolation, first remove the ectoderm at the surface followed by careful detachment of the ventrally located splancnopleura tissues.

3.2.5) Release the right lateral mesoderm of the somatopleura by cutting it in a parallel motion to the neural tube.

3.2.6) Repeat the mesoderm separation of the left side of the embryo.

Note: Make slow microscalpel movements during this procedure. The exposed extra-cellular matrix proteins stick to tissues and instruments, preventing fluid movements.

3.2.7) With the help of spatula and thin forceps transfer the isolated mesoderm to a glass dish three-quarters filled with cold FBS.

3.3) Keep the glass dish with the isolated tissues on ice during the preparation of *in vitro* assay.

4. *In vitro* organotypic assay: heterospecific association of quail 3/4PP endoderm and chicken somatopleura mesoderm

4.1) Prepare the culture medium with RPMI-1640 medium supplemented with 10% FBS and 1% Pen/Strep[3,5].

4.2) Place a metal grid in a 35 mm Petri dish with 5 mL of culture medium.

Note: Remove the excess of liquid to level the medium surface with the top of the grid.

4.3) With the help of thin forceps, dip a membrane filter into the culture medium and then place it on the top of the grid to have one surface in contact with air.

Note: One-quarter of the membrane area (with 13 mm diameter) is adequate for the tissue association.

4.4) Under the stereomicroscope, associate the isolated tissues on the top of the membrane filter. First transfer the 3/4PP endoderm (step 2) from the glass dish by gentle sliding with the help of a transplantation spoon (or spatula) and thin forceps. Repeat this procedure for the isolated mesoderm (step 3).

Note: With the help of a microscalpel, mix the tissues to maximize its association.

4.5) Carefully place the associated tissues in a humidified incubator at 37 °C with 5% CO_2 for 48 h. Cultured tissues can be grafted onto the chorioallantoic membrane (CAM).

Note: Ectopic organ formation in the CAM was previously detailed[8].

RESULTS

The protocol details a method to isolate avian embryonic tissues to be used in several cellular and developmental biology technical approaches. This method was previously employed to study epithelial-mesenchymal interactions during early stages of thymus formation[5]. Herein, new results are shown in **Figure 1** and **Figure 2**, using similar approaches.

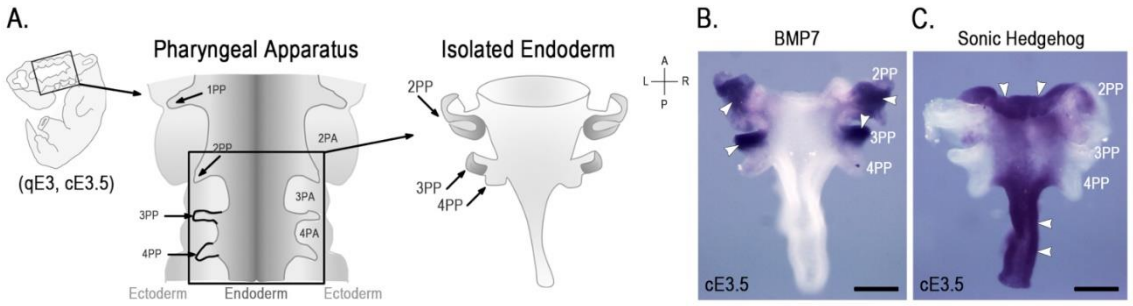

Figure 1. Representative results of gene-expression study of three-dimensionally preserved pharyngeal endoderm containing the presumptive territory of the thymus rudiment. Schematic representation of the pharyngeal apparatus and isolated endoderm containing the 2PP, 3PP and 4PP (at cE3.5 or qE3) (**A**). Whole-mount *in situ* hybridization with BMP7 (**B**) and Sonic Hedgehog (**C**) of isolated endoderm at cE3.5. Strong hybridization signals of *BMP7* and *Sonic Hedgehog* pointed by white arrowheads in endoderm of the 2PP and 3PP (**B**) and central pharynx (**C**), respectively. A, anterior; cE, chicken embryonic day; L, left; P, posterior; PP, pharyngeal pouch; qE, quail embryonic day; R, right. Scale bars, 50 µm.

Figure 1 is a schematic drawing of the endoderm isolated from the pharynx at qE3 (and cE3.5) (**Figure 1A**) and the *in situ* expression of two endoderm-related genes, sonic hedgehog[11,12] and BMP7[13] in the isolated tissue. The whole-mount *in situ* hybridization procedures were performed as previously described[5,7]. The expression of *BMP7* was detected in the endoderm of the 2PP and 3PP and excluded from the central pharynx and 4PP (probe was kindly provided by Elisabeth Dupin) (**Figure 1B**). Conversely, *Sonic Hedgehog* was detected in the endoderm of the central pharynx and excluded from the pouches[7] (**Figure 1C**).

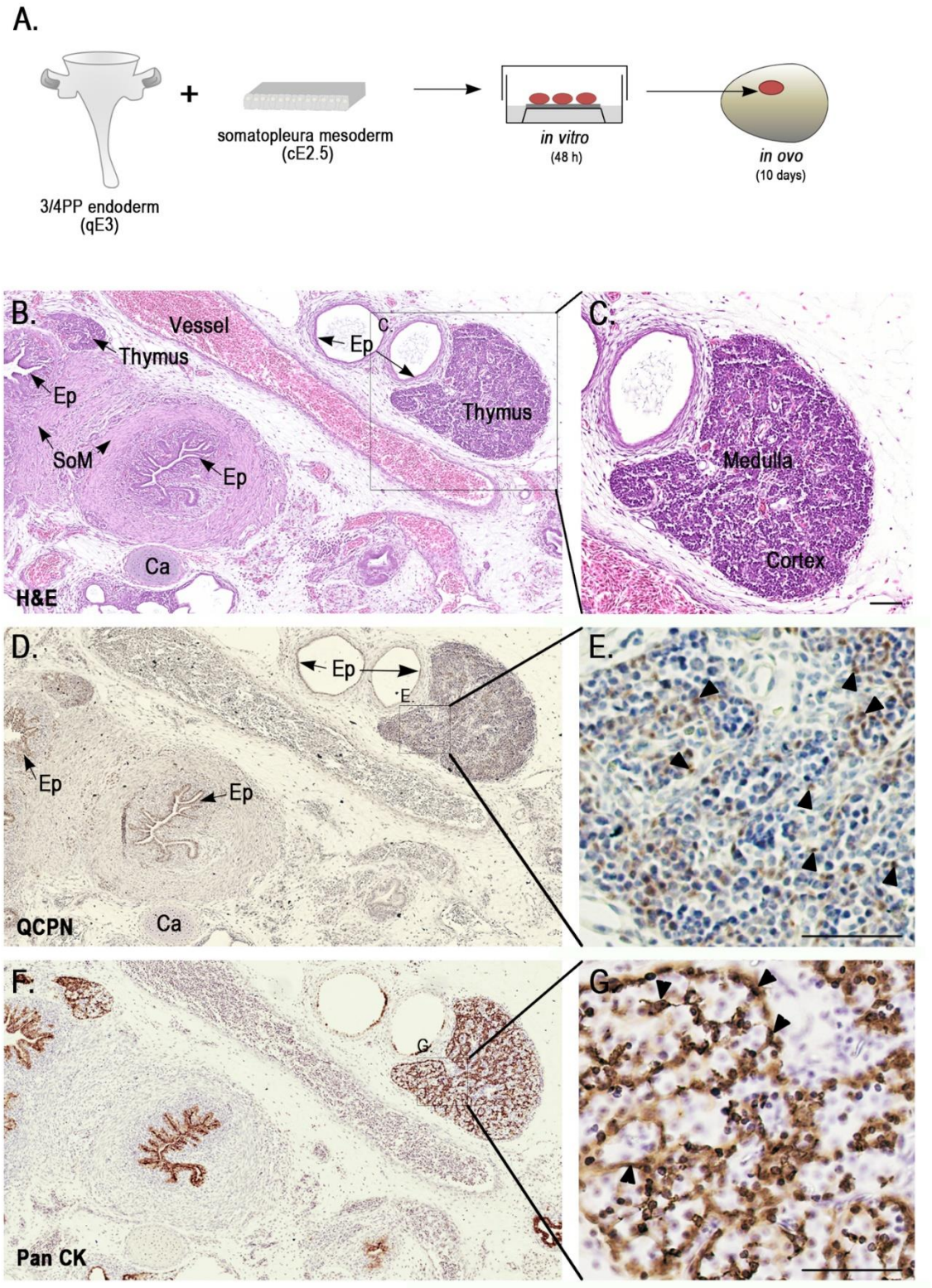

Figure 2. Representative results of *ex vivo* formation of chimeric organs. Schematic representation of the experimental approach used to develop quail-chicken chimeric thymi (**A**). Briefly, the isolated quail 3/4PP endoderm (qE3) was associated *in vitro* with chicken somatopleura mesoderm (cE2.5) for 48 h. The 48 h cultured tissues were then grafted onto the CAM (cE8) and allowed to develop *in ovo* for further 10 days. Serial sections of CAM-derived explants (**B-G**) were analyzed by conventional histology (**B** and **C**) and immunohistochemistry

(**D** to **G**). In **B** and **C** (higher magnification of **B**), the slide was stained with H&E. In **D** and **E** (higher magnification of **D**), the slide was immunodetected with QCPN antibody and counterstained with Gill's hematoxylin. In **F** and **G** (higher magnification of **F**), the slide was immunodetected with anti-Pan CK antibody and counterstained with Gill's hematoxylin. Black arrow heads point to strong brown immunostaining of QCPN (**E**) and Pan CK (**G**). See **Table of Materials** for image acquisition details. Ca, cartilage; Ep, epithelium; PP, pharyngeal pouch; SoM, smooth muscle. Scale bars: 50 µm.

Figure 2 depicts the experimental design used to develop ex vivo quail-chicken chimeric organs. The heterospecific association of tissues were grown *in vitro* for 48 h followed by *in ovo* development for 10 days (**Figure 2A**). Thymi formed in CAM-derived explants were identified by conventional histology. The thymus presented normal morphological features with well-developed medulla and cortex compartments (**Figure 2B, C**). Serial sections of the explants were further treated for immunocytochemistry (**Figure 2D**-G), as described[5,7]. The QCPN- MAb Quail perinuclear (**Figure 2D, E**) and anti-pan cytokeratin (CK) (**Figure 2F, G**) antibodies were used as markers for quail (species-specific) and epithelial cells, respectively. The chimeric thymus showed $QCPN^{+}$thymic epithelial cells (**Figure 2D, E**), a reticular architecture (**Figure 2F, G**), and colonization by lymphoid cells ($QCPN^{-}$) of donor origin (chicken).

Table 1. Conditions of enzymatic digestion during embryonic tissues isolation.

Isolated tissue	Stage of development	Concentration	Temperature	Incubation period
Pharynx endoderm	qE2-E2.5	8 mg/mL	On ice	45-60 min
	cE2.5-E3			
	qE3	8 mg/mL	On ice	60-90 min
	cE3.5			
	qE4	8 mg/mL	On ice	90 min
	cE4.5			
Somatopleura mesoderm	qE2-E2.5	8 mg/mL	On ice	30-50 min
	cE2.5-E3			

c, chicken; E, Embryonic day; q, quail.

DISCUSSION

The embryonic tissue isolation procedure detailed here was improved from previous techniques to produce quail-chicken chimeric embryos in different biological contexts[3,5,6].

This approach is suitable to isolate pure embryonic tissues without requiring genetic manipulation or the use of tissue-specific markers, which are often undetermined, limiting the use of genetically modified animal models. It can be used to study epithelial-mesenchymal interactions during development, with the ability to isolate pure tissues being the limiting factor. For instance, as development progresses, tissues become thicker, more compact and attach to other neighboring tissues such that their separation is more difficult. This isolation procedure is, therefore, unsuitable for later stages of development, namely late-organogenesis.

This method is unique to study gene-expression in 3D-preserved embryonic tissues. To ensure the 3D-integrity of the isolated tissues, instruments, materials and solutions should be kept at low temperatures throughout the process.

The tissue microdissection procedure is also a critical step that relies, not only on the careful establishment of the experimental conditions (like temperature and duration of enzymatic digestion, as exemplified in **Table 1**), but also on the time-consuming hands-on training. This procedure requires patience and practice. If the operator loses the references of the region to be dissected, decreasing the stereoscope magnification (20x) will provide an overall observation that will help the next move decision.

The 48 h *in vitro* step was established to promote the cellular interactions between distinct embryonic tissues, while the *in ovo* tissue grown in the CAM supports the long-term development and chimeric organ formation of the heterospecific association of tissues[5]. The *in vitro* tissues associations may overcome some limitations of *in vivo* manipulations. For instance, local administration of drugs or growth-factors (using beads) in regions of the embryo otherwise inaccessible *in vivo*, can be easily performed using this *in vitro*

approach. This has previously shown to mimic local tissue interactions during organ formation in the pharyngeal region[5].

Harvesting explants growing in CAM[5,7,8] is less time-consuming and is a simple method to track explants when compared to methods of collecting tissues grafted onto the body wall of chimeric embryos[3]. In addition, CAM can be transplanted with cells and tissues from other non-avian species, and it has been successfully used in several experimental contexts, from development to cancer[14,15]. For example, the CAM assay was previously applied in mice-into-chicken xenografts studies[16] and is frequently used to test the invasive capacity of human tumors cells[15].

Recently, an elegant study with human-into-chicken xenograft has validated the chicken embryo as a model to test and explore early human development[17]. In the future, it will be interesting to explore the methodology herein described using interspecies association of tissues, which may provide additional approaches to the mouse and human developmental studies.

DISCLOSURES

The authors have nothing to disclose.

ACKNOWLEDGMENTS

The authors are grateful to Isabel Alcobia for the critical reading of the manuscript, to Mário Henriques for video narration and to Vitor Proa from the Histology Service of the Instituto de Histologia e Biologia do Desenvolvimento, Faculdade de Medicina de Lisboa, Universidade de Lisboa, for technical support. We are particularly indebted to Paulo Caeiro and Hugo Silva from the Unidade de audiovisuais (Audiovisual Unit), Faculdade de Medicina de Lisboa, Universidade de Lisboa for their outstanding commitment to the production of this video. We acknowledge Leica Microsystems for kindly providing a stereoscope equipped with a video system and to Interaves - Sociedade Agro-Pecuária, S.A

for contributing with quail fertilized eggs. This work was supported by Faculdade de Medicina de Lisboa, Universidade de Lisboa (FMUL).

MATERIALS

Name	Company	Catalog Number	Comments
Chicken fertilized eggs (*Gallus gallus*)	Pintobar, Portugal		Poultry farm
Quail fertilized eggs (*Coturnix coturnix*)	Interaves, Portugal		Bird farm
15 mL PP centrifuge tubes	Corning	430052	
50 mL PP centrifuge tubes	Corning	430290	
60 x 20 mm pyrex dishes	Duran group	21 755 41	
100 x 20 mm pyrex dishes	Duran group	21 755 48	
Metal grid	Goodfellows		fine meshed stainless steel grid
Membrane filter	Millipore	DTTP01300	0.6 mm Isopore membrane filter
Petri dish, 35 x 10 mm	Sigma-Aldrich	P5112	
60 x 30 mm pyrex bowls (small size)			from supermarket
100 x 50 mm pyrex bowls (large size)			from supermarket
Transfer pipettes	Samco Scientific, Thermo Fisher Scientific	2041S	2 mL plastic pipet
Glass pasteur pipette	Normax	5426015	
Clear plastic tape			from supermarket
Cytokeratin (pan; acidic and basic, type I and II cytokeratins), clone Lu-5	BMA Biomedicals	T-1302	
Fetal Bovine Serum	Invitrogen, Thermo Fisher Scientific		Standart FBS
Pancreatin	Sigma-Aldrich	P-3292	Prepare a 25 mg/mL solution according to manufacturer's instructions; centrifuge and filter prior to aliquote and store at -20 ºC. Aliquots can be kept frozen for several years.
Paraformaldehyde	Sigma-Aldrich	P6148	
Penicillin-Streptomycin	Invitrogen, Thermo Fisher Scientific	15140-122	
Phosphate-Buffered Saline (PBS)	GIBCO, Thermo Fisher Scientific	10010023	

QCPN antibody	Developmental Studies Hybridoma Bank	QCPN	
RPMI 1640 Medium, GlutaMAX Supplement	GIBCO, Thermo Fisher Scientific	61870010	
Bluesil RTV141A/B Silicone Elastomer 1.1Kg Kit	ELKEM/Silmid	RH141001KG	To prepare the back base for petri dish
Dumont #5 Forceps	Fine Science Tools	11251-30	Thin forceps
Extra fine Bonn scissors, curved	Fine Science Tools	14085-08	Curved scissors
Insect pins	Fine Science Tools	26001-30	0.3 mm stainless steel pin
Micro spatula	Fine Science Tools	10087-12	Transplantation spoon
Minutien Pins	Fine Science Tools	26002-20	0.2 mm stainless steel microscalpel
Minutien Pins	Fine Science Tools	26002-10	0.1 mm stainless steel microscalpel
Moria Nickel Plated Pin Holder	Fine Science Tools	26016-12	Nickel plated pin holder
Moria Perforated Spoon	Fine Science Tools	10370-17	Skimmer
Wecker Eye Scissor	Fine Science Tools	15010-11	
Camera	Leica Microsystems	MC170 HD	
Microscope	Leica Microsystems	DM2500	
NanoZoomer S360 Digital slide scanner	Hamamatsu Photonics	C13220-01	
Stereoscope	Leica Microsystems	Leica M80	

REFERENCES

1. Le Douarin, N. The Nogent Institute--50 years of embryology. *The International Journal of Developmental Biology*. **49**, (2-3), 85-103 (2005).

2. Le Douarin, N. M., Teillet, M. A. The migration of neural crest cells to the wall of the digestive tract in avian embryo. *Journal of Embryology and Experimental Morphology*. **30**, (1), 31-48 (1973).

3. Le Douarin, N. M., Jotereau, F. V. Tracing of cells of the avian thymus through embryonic life in interspecific chimeras. *Journal of Experimental Medicine*. **142**, (1), 17-40 (1975).

4. Hamburger, V., Hamilton, H. L. A series of normal stages in the development of the chick embryo. 1951.*Developmental Dynamics*. **195**, (4), 231-272 (1992).

5. Neves, H., Dupin, E., Parreira, L., Le Douarin, N. M. Modulation of Bmp4 signalling in the epithelial-mesenchymal interactions that take place in early thymus and parathyroid development in avian embryos. *Developmental Biology*. **361**, (2), 208-219 (2012).

6. Takahashi, Y., Bontoux, M., Le Douarin, N. M. Epithelio--mesenchymal interactions are critical for Quox 7 expression and membrane bone differentiation in the neural crest derived mandibular mesenchyme. *Embo Journal*. **10**, (9), 2387-2393 (1991).

7. Figueiredo, M., *et al.* Notch and Hedgehog in the thymus/parathyroid common primordium: Crosstalk in organ formation. *Developmental Biology*. **418**, (2), 268-282 (2016).

8. Figueiredo, M., Neves, H. Two-step Approach to Explore Early-and Late-stages of Organ Formation in the Avian Model: The Thymus and Parathyroid Glands Organogenesis Paradigm Video Link. *Journal of Visualized Experiments*. (2018).

9. Nehls, M., *et al.* Two genetically separable steps in the differentiation of thymic epithelium. *Science (New York, N.Y.)*. **272**, (5263), 886-889 (1996).

10. Morahan, G., *et al.* The nu gene acts cell-autonomously and is required for differentiation of thymic epithelial progenitors. *Proceedings of the National Academy of Sciences of the United States of America*. **93**, (12), 5742-5746 (1996).

11. Jerome, L. A., Papaioannou, V. E. DiGeorge syndrome phenotype in mice mutant for the T-box gene, Tbx1.*Nature Genetics*. **27**, (3), 286-291 (2001).

12. Nie, X., Brown, C. B., Wang, Q., Jiao, K. Inactivation of Bmp4 from the Tbx1 expression domain causes abnormal pharyngeal arch artery and cardiac outflow tract remodeling. *Cells Tissues Organs*. **193**, (6), 393-403 (2011).

13. Zou, D., *et al.* Patterning of the third pharyngeal pouch into thymus/parathyroid by Six and Eya1.*Developmental Biology*. **293**, (2), 499-513 (2006).

14. Davey, M. G., Tickle, C. The chicken as a model for embryonic development. *Cytogenetic and Genome Research*. **117**, (1-4), 231-239 (2007).

15. Nowak-sliwinska, P., Segura, T., Iruela-arispe, M. L., Angeles, L. The chicken chorioallantoic membrane model in biology, medicine and bioengineering. *Angiogenesis*. **17**, (4), 779-804 (2014).

16. Uematsu, E., *et al.* Use of in ovo chorioallantoic membrane engraftment to culture testes from neonatal mice. *Comparative Medicine*. **64**, (4), 264-269 (2014).

17. Martyn, I., Kanno, T. Y., Ruzo, A., Siggia, E. D., Brivanlou, A. H. Self-organization of a human organizer by combined Wnt and Nodal signaling. *Nature*. **558**, (7708), 132-135 (2018).